

TECHNICAL REPORT STANDARD TITLE PAGE

1. Report No. TX-01 1784-3		2. Government Accession No.		3. Recipient's Catalog No.	
4. Title and Subtitle Impact of Load Plate on Response of Falling Weight Deflectometer				5. Report Date March 2004	
				6. Performing Organization Code	
7. Author(s) S. Rocha, S. Nazarian and V. Tandon				8. Performing Organization Report No. Research Report 1784-3	
9. Performing Organization Name and Address Center for Transportation Infrastructure Systems The University of Texas at El Paso El Paso, Texas 79968-0516				10. Work Unit No.	
				11. Contract or Grant No. Study No. 0-1784	
12. Sponsoring Agency Name and Address Texas Department of Transportation P.O. Box 5051 Austin, Texas 78763				13. Type of Report and Period Covered Final Report September 2001 – August 2002	
				14. Sponsoring Agency Code	
15. Supplementary Notes Research Performed in Cooperation with TxDOT and FHWA					
16. Abstract Currently, all TxDOT FWDs operate with a solid load plate. Several experimental and analytical studies have shown that such a configuration may result in a non-uniform load distribution under a rutted or weak flexible pavement. A split plate design that may improve the load distribution on rutted or weak pavements is currently available. A non-uniform load distribution may significantly affect the central deflection measured on a weaker pavement structure. Since more than 50% of Texas roadways are farm-to-market structures, this matter is of utmost importance. The behaviors of solid and split plates were thoroughly evaluated in this study. It seems that the FWDs equipped with split plates impart more uniform load to the pavement, and in general improve the performance of the FWD. However, the deflections measured with the two plates are different. As such, should TxDOT decide to utilize split load plates, a means of adjusting the deflections measured with the new configuration to those historically measured with the solid plate should be devised.					
17. Key Words Falling Weight Deflectometer, Loading Plate, Solid Plate, Split Plate, Load Cell			18. Distribution Statement No restrictions. This document is available to the public through the National Technical Information Service, 5285 Port Royal Road, Springfield, Virginia 22161		
19. Security Classif. (of this report) Unclassified		20. Security Classif. (of this page) Unclassified		21. No. of Pages 120	22. Price

Impact of Solid and Split Plates on Response of Falling Weight Deflectometer

by

**Sergio Rocha, BSEE
Soheil Nazarian, Ph.D., P.E.
and
Vivek Tandon, Ph.D., P.E.**

Research Project 1784-3

**Evaluate Reproducibility of TxDOT FWD Fleet
and Recommend Improvements to
FWD Calibration Procedure**

Conducted for

Texas Department of Transportation

**Center for Transportation Infrastructure Systems
The University of Texas at El Paso
El Paso, TX 79968-0516
Research Report 1784-3
March 2004**

The contents of this report reflect the view of the authors, who are responsible for the facts and the accuracy of the data presented herein. The contents do not necessarily reflect the official views or policies of the Texas Department of Transportation or the Federal Highway Administration. This report does not constitute a standard, specification, or regulation.

**NOT INTENDED FOR CONSTRUCTION, BIDDING,
OR PERMIT PURPOSES**

Sergio Rocha, BSEE
Soheil Nazarian, Ph.D., P.E. (69263)
Vivek Tandon, Ph.D., P.E. (88219)

Acknowledgements

The satisfactory progress of this project could not have happened without the help and input of many personnel of TxDOT. Andrew Wimsatt is the Project Director and Elias Rmeili is the Project Coordinator. Dar Hao Chen, Mike Murphy, Randy Beck and Carl Bertrand are the advisors to the project. The authors acknowledge Randy Beck and Carl Bertrand for their active participation in the progress of this project.

Abstract

Currently, all TxDOT FWDs operate with a solid load plate. Several experimental and analytical studies have shown that such a configuration may result in a non-uniform load distribution under a rutted or weak flexible pavement. The FWD vendor currently markets a split plate design that may improve the load distribution on rutted or weak pavements. A non-uniform load distribution may significantly affect the central deflection measured on a weaker pavement structure. Since more than 50% of Texas roadways are farm-to-market structures, this matter is of utmost importance.

The behaviors of solid and split plates were thoroughly evaluated in this study. It seems that the falling weight deflectometers equipped with split plates impart more uniform load to the pavement. The split plate in general improved the performance of the FWD. However, the deflections measured with the two plates are different. As such, should TxDOT decide to utilize split load plates, a means of adjusting the deflections measured with the new configuration to those historically measured with the solid plate should be devised.

Implementation Statement

The results from this study will provide the technical background necessary for TxDOT staff to draw conclusions whether it is appropriate to change the load plates of the FWD fleet from solid to split. In terms of operation, the split plates are desirable. However, a strategy for harmonizing the deflections historically collected with the solid plates with those measured with the split plates should be devised. This study has been purely technical in nature, a cost benefit analysis is recommended before TxDOT decides to install split plates on the FWD fleet.

Table of Contents

ACKNOWLEDGEMENTS.....	VII
ABSTRACT.....	IX
IMPLEMENTATION STATEMENT.....	XI
TABLE OF CONTENTS.....	XIII
LIST OF FIGURES.....	XV
LIST OF TABLES.....	XVII
CHAPTER 1.....	1
INTRODUCTION.....	1
PROBLEM STATEMENT.....	1
OBJECTIVE.....	1
ORGANIZATION.....	2
CHAPTER 2.....	3
REVIEW OF LITERATURE.....	3
CHAPTER 3.....	13
EVALUATION OF PLATES ON SOLID PAVEMENT.....	13
CHAPTER 4.....	23
EVALUATION OF PLATES ON NON-SOLID PAVEMENTS.....	23
CHAPTER 5.....	41
CLOSURE.....	41
SUMMARY.....	41
CONCLUSIONS.....	41
REFERENCES.....	43
APPENDIX A – COMPLETE LOAD AND DEFLECTION DATA FROM TTI TEST SITES.....	43
APPENDIX B – COMPLETE LOAD AND DEFLECTION DATA FROM UTEP TEST SLABS.....	43
APPENDIX C – COMPLETE LOAD PLATE MOTION DATA FROM UTEP TEST SLABS.....	43

List of Figures

Figure 2.1 – Typical Load Plates used under FWD Devices	3
Figure 2.2 – Distribution of pressure under Rigid and Segmented Plates	4
Figure 2.3 – Pavement profiles used by Bodappati et. al.....	5
Figure 2.4 – Pressure Distribution under FWD Plate Simulated by Finite Element Analysis	6
Figure 2.5 – Influence of Pad Stiffness on Pressure Distribution under Plate.....	10
Figure 2.6 – Influence of Pad Thickness on Pressure Distribution under Plate	10
Figure 2.7 – Influence of Base Layer Stiffness on Pressure Distribution under Plate.....	12
Figure 3.1 – Typical Load and Deflection Time Histories from Three Sites	13
Figure 3.2 – Comparison of Variations in Deflection with Load under Split Plate and Solid Plate at Three Sites.....	14
Figure 3.3 – Installation of Strain Gauges on Load Plate.....	15
Figure 3.4 – Typical Variations in Strain Time Histories along FWD Load Plate.....	16
Figure 3.5 – Variations in Strain Time Histories along FWD Load Plate (Brand New Load Plate Assembly)	16
Figure 3.6 – Variations in Strain Time Histories along FWD Load Plate (Split Plate Assembly)	17
Figure 3.7 – Comparison of Load Time Histories Reported by FWD from Three Different Load Plates.....	18
Figure 3.8 – Comparison of Deflection Time Histories Reported by FWD From Three Different Load Plates	19
Figure 3.9 – Typical Placement of Accelerometers on Load Plate.....	19
Figure 3.10 – Typical motion of Load Plate	20
Figure 4.1 – Layout of Concrete Slabs used for Evaluating Load Plates	22
Figure 4.2 – FWD Loading Assembly and Control Box on Undercarriage	23
Figure 4.3 – Typical Load and Deflection Time Histories Measured on Level Slab.	25
Figure 4.4 – Variations in Deflection with Load on Three Test Points Measured on Level Slab.....	26
Figure 4.5 – Variations in Contact Pressure on Three Test Points Measured on Level Slab.....	27
Figure 4.6 – Variation in Acceleration of the Plates on Three Test Points Measured on Level Slab.....	28
Figure 4.7 – Typical Load and Deflection Time Histories Measured on Inclined Slab	29

Figure 4.8 – Variation in Deflection with Load on Three Test Points Measured on Inclined Slab.....	30
Figure 4.9 – Variations in Contact Pressure on Three Test Points Measured on Inclined Slab.....	31
Figure 4.10 – Variations in Acceleration of the Plates on Three Test Points Measured on Inclined Slab.....	33
Figure 4.11 – Typical Load and Deflection Time Histories Measured on Rutted Slab.....	34
Figure 4.12 – Variation in Deflection with Load on Three Test Points Measured on Rutted Slab.....	35
Figure 4.13 – Variations in Contact Pressure on Three Test Points Measured on Rutted Slab.....	36
Figure 4.14 – Variations in Acceleration on Three Test Points Measured on Rutted Slab.....	37

List of Tables

Table 2.1 – Impact of Plate/Pavement Interaction on Surface Deflections	7
Table 2.2 – Influence of Plate Components on Stress Distribution.....	9
Table 2.3 – Influence of Plate Components on Stress Distribution.....	11
Table 3.1 – Layer Information of Selected Sites	12

Chapter 1

Introduction

Problem Statement

The falling weight deflectometer (FWD) device has been extensively used by the Texas Department of Transportation (TxDOT) to support routine pavement design, to select rehabilitation strategies, to route super-heavy loads, to load zone, and to support other pavement management activities. A FWD primarily measures the pavement deflection at seven to nine points due to an imparted load. The measured load and deflections along with pavement parameters are entered in a backcalculation program to obtain the stiffness profile of an existing pavement. These backcalculated moduli are then used to compute the strains at the interfaces of the pavement layers. The remaining life of the pavement is finally determined by using a semi-empirical relationship between the number of equivalent single axle loads applied to the pavement and the critical strains at the interfaces of the different pavement layers.

Currently, all TxDOT FWDs operate with a solid load plate. Several experimental and analytical studies have shown that such a configuration may result in a non-uniform load distribution under a rutted or weak flexible pavement. The FWD vendor currently offers a split plate design that may improve the load distribution on rutted or weak pavements. A non-uniform load distribution may significantly affect the central deflection measured on a weaker pavement structure. Since more than 50% of Texas roadways are farm-to-market structures, this matter is of utmost importance.

Objective

The primary objective of this report is to provide information about the response of pavement structures under solid and split plates. This was achieved by a thorough review of the literature, and a comprehensive small-scale and full-scale field tests. The results are reported herein.

Organization

The report consists of five chapters. A review of literature focusing on the distribution of pressure under split and solid plates from several experimental and numerical studies is included in Chapter 2. Chapter 3 contains the results from the instrumentation of the load plates of three FWDs to quantify their behaviors. Chapter 4 is dedicated to the results from comprehensive tests carried out to quantify the behaviors of these plates. Summary, conclusions and our recommendations are described in Chapter 5.

Chapter 2

Review of Literature

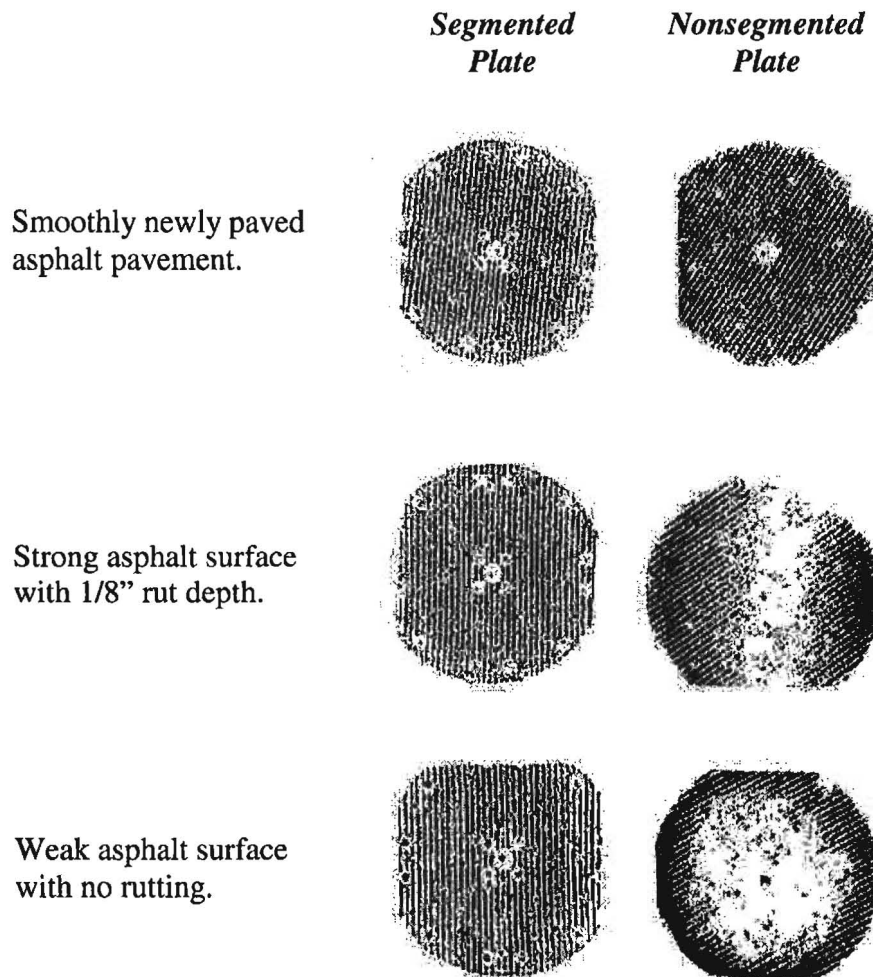
Typical solid (rigid) and split (segmented) load plates used with FWDs are shown in Figure 2.1. The load plate transfers the applied load to the pavement through a multi-layered plate. The solid plate typically consists of a steel plate connected to a Polyvinyl Chloride (PVC) plate. The split load cell on the other hand is made up of two metal plates in the shape of half-circles. These two plates are joined by a center piece through a hinge mechanism and rubber dampers. The hinge and damping elements allow the two half circles some flexibility to conform to non-uniform surfaces. The bottom of each plate has a ribbed neoprene isolation pad that is intended to equally distribute the pressure under the load plate.



Figure 2.1 – Typical Load Plates Used under FWD Devices

To evaluate the influence of two plate types Touma et al. (1991) performed a field study on three pavement sections consisting of a smooth, newly-paved, strong asphalt pavement, a strong asphalt pavement with a small rut, and a weak asphalt with no apparent rut. The results from field measurements are summarized in Figure 2.2. For the segmented plate, the stress distributions for all three pavements were reasonably uniform. The distribution of pressure was also reasonably uniform under the solid plate placed on the strong smooth pavement. However, for the other two pavement sections shown in Figure 2.2, the distributions of pressure on top of the pavement were non-uniform along the radius of the plate. This phenomenon negatively impacts the deflection of the sensor located in the center of the load plate (Sensor 1).

Note: The shape of the film imprints is not completely circular because the film is only 270mm (10 5/8 in) in width while the diameter of the load plate is 305mm (12 in).



**Figure 2.2 – Distribution of pressure Under Rigid and Segmented Plates
(from Touma et al., 1991)**

Touma et al. also suggested that to assume a uniform pressure distribution under the FWD plate for backcalculation of moduli may in some instances introduce unacceptable errors. They considered three contact stress distributions: uniform (full contact), partial edge distribution (rutting), and partial circumferential distribution (weak pavement). The measured deflections from each loading case were used to backcalculate layer moduli. The analysis indicated that when either of the two non-uniform conditions occurs (partial edge or partial circumferential), making the assumption that full contact was achieved may lead to significant errors in the backcalculated moduli.

Boddapati et al. (1994) used finite element modeling to simulate the distribution of pressure under pavements for a number of conditions. In that study, the composite loading plate of the FWD was assumed to consist of a steel plate over a PVC plate. The steel and PVC plates rested over a rubber pad. A three-layer flexible pavement section was used in that study as a standard cross-section (see Figure 2.3a). A rigid pavement consisting of a concrete layer over a subgrade was also studied. The load plate and the pavement were discretized for the purpose of the finite element simulation.

The pressure distributions under the loading plate at the pavement surface are graphically presented in Figure 2.4 for the flexible and rigid pavements. The horizontal line represents the uniform pressure distribution anticipated on the pavement. For the flexible pavement, some concentration of stress at the edges is apparent. Little stress is imparted to the pavement near the center of the plate. For the rigid pavement, the pressure is more or less constant except for the inner and outer one inch of the plate.

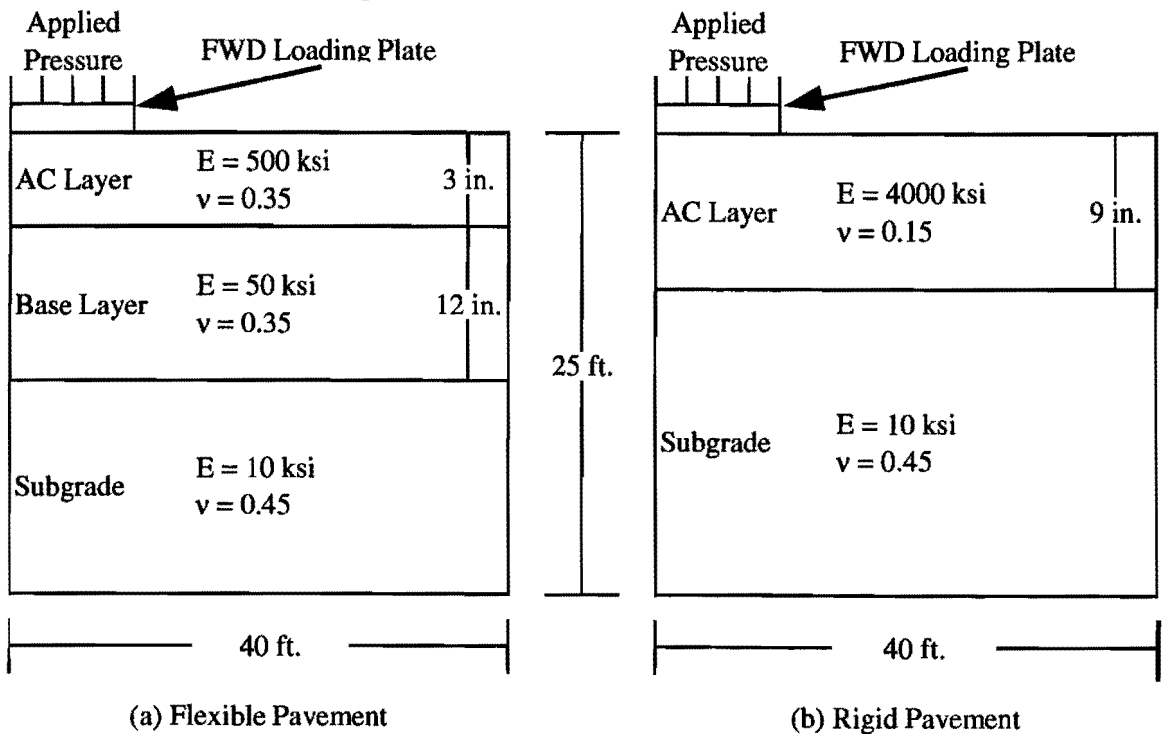


Figure 2.3 – Pavement Profiles Used by Boddapati et al. (1994)

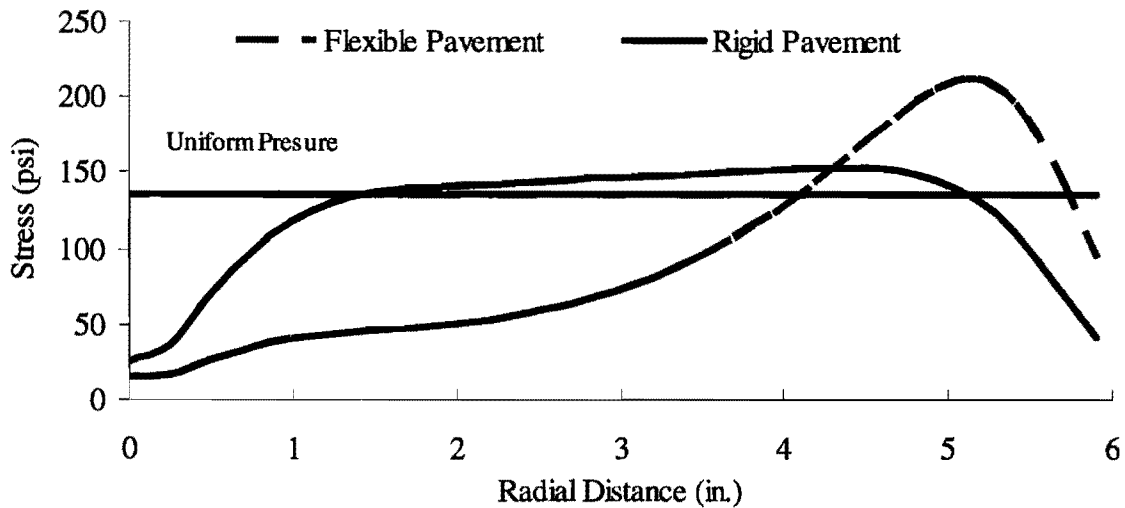


Figure 2.4 – Pressure Distribution under FWD Plate Simulated by Finite Element Analysis

To determine the energy concentration on the loaded area due to the FWD-pavement interaction, Boddapati et.al. (1994) introduced the stress recovery ratio, S_r parameter as:

$$S_r(\%) = \frac{P_i * 100}{P_u} \quad (2.1)$$

where p_u = stress assuming uniform stress distribution, p_i = average stress applied to the pavement. The closer the value of S_r is to unity, the more uniform the stress distribution will be. To determine p_u , the applied load was divided by the area of the plate, whereas, p_i was determined by calculating average stress obtained considering the FWD/pavement interaction. For the flexible pavement, the stress recovery ratio was about 70%. To the contrary, the rigid pavement recorded a S_r of 94%.

Since Boddapatti et.al. (1994) is very relevant to this project, we have summarized it here. The deflections calculated with the uniform pressure distribution and when the FWD-pavement interaction was considered on flexible and rigid pavements are compared in Table 2.1. For the flexible pavement, the difference in deflections is 6.3% for the first sensor and practically zero for the other sensors. For the rigid pavement, since the differences are less than 1%, the FWD-pavement interaction results in small variation in the outcome. As such, the interaction should not be of any concern.

The stiffness and thickness of each component of the FWD plate were also varied to determine their influences on the deflection basins. In addition, moduli and thicknesses of the pavement layers were varied to produce a realistic range of in-service pavement systems.

The influence of the FWD plate components is shown in Table 2.2. For the case of the standard plate, the difference between the central deflections obtained with the uniform distribution and when the plate-pavement interaction is considered, as indicated before, is 6.3%. By doubling

Table 2.1 - Impact of Plate/Pavement Interaction on Surface Deflections for Typical Flexible and Rigid Pavements

Type of Pavement	Model	Deflection (in mils) Measured at (in.)						
		0	12	24	36	48	60	72
Flexible	Uniform	34.3	21.4	13.6	9.3	6.5	4.6	3.5
	Simulated	32.1	21.4	13.6	9.3	6.5	4.6	3.5
	% Difference	6.3	0.1	0	0	0	0	0
Rigid	Uniform	10.4	9.4	8.2	6.7	5.4	4.3	3.3
	Simulated	10.3	9.4	8.2	6.7	5.4	4.3	3.3
	% Difference	0.4	0	0	0	0	0	0

Table 2.2 - Influence of Plate Components on Stress Distribution and Central Deflection of FWD

Parameter	Modulus of Plate Component (ksi)			Thickness of component (in.)			S _r (%)	Central* Deflection (mils)
	Steel	PVC	Pad	Steel	PVC	Pad		
Standard Plate	10000	1000	5	1	1	0.25	71	1.29 (6.3%)
Steel Plate Modulus	5000	1000	5	1	1	0.25	74	1.29 (6.1%)
	20000						68	1.27 (6.9%)
Steel Plate Thickness	10000	1000	5	0.5	1	0.25	80	1.31 (4.5%)
				1.5			65	1.27 (7.5%)
PVC Plate Modulus	10000	500	5	1	1	0.25	74	1.29 (6.0%)
		2000					68	1.27 (6.9%)
PVC Plate Thickness	10000	1000	5	1	0.5	0.25	75	1.30 (5.5%)
					1.5		68	1.27 (6.9%)
Pad Modulus	10000	1000	1	1	1	0.25	82	1.33 (3.1%)
			25				65	1.24 (9.8%)
Pad Thickness	10000	1000	5	1	1	0	57	1.16 (15.2%)
						0.125	69	1.26 (7.7%)
						0.375	74	1.30 (5.1%)

* Numbers in parentheses correspond to differences from a uniform load distribution

* S_r denotes stress recovery ratio as defined in equation 2.1.

and halving the stiffness of the plate, the differences in the central deflections vary between 6.1% and 6.9%, not much different from the 6.3% obtained for the standard plate. The impact of the stiffness of the plate on the overall FWD-pavement interaction is small. In practical terms, the user and manufacturer should not be much concerned with the actual stiffness of the steel plate. One can replace the steel plate with hardened steel or aluminum and still obtain similar results. However, irrespective of the type of metal used, the central deflection on the standard pavement would be different by about 6.5% relative to the case when a uniform stress distribution is considered.

The second parameter studied was the thickness of the steel plate. The plate thickness slightly influences the central deflection measured. As the thickness decreases to 0.5 in. (12.5 mm), the plate becomes more flexible thus it can better conform to the pavement surface. In this case, the difference in deflection is about 4.5% which is nearly 2% less than the 6.3% obtained for the standard plate. Thickening of the steel plate would naturally result in a more rigid plate system, which in turn results in a larger deviation (7.5%) in the values of central deflection between the cases when the plate/pavement interaction is and is not considered.

The PVC plate is placed to uniformly distribute the imparted load from the FWD loading plate more evenly. Once again the variation in the PVC plate stiffness or thickness has a small influence on pressure distribution along the interface and central deflections. The variation in the PVC plate stiffness from 500 ksi (3500 MPa) to 2,000 ksi (14000 MPa) resulted in differences of central deflections from 6% to 7%. The variation of PVC plate thickness from 0.5 in. (12.5 mm) to 1.5 in. (37.5 mm) causes a difference in deflections ranging from 5.5% to 7%.

The rubber (or neoprene) pad facilitates the distribution of the load to the pavement. To find the influence of the stiffness of the rubber pad on the overall distribution of the loads, two cases were studied. In one case, the stiffness of the pad varied from 1 ksi (7 MPa) to 25 ksi (175 MPa). In the other case, the thickness of the pad varied from 0 in. (no-pad) to 3/8 in. (9.5 mm). As illustrated in Figure 2.5, with the decrease in the modulus of the pad the stress distribution becomes more uniform. The stress recovery ratio increases from 65% to about 82%. The differences in deflections calculated by two approaches decrease from 10% to about 3% (see Table 2.2). This implies that the stiffness of the rubber pad is of significant importance and should not be ignored.

Unlike the pad stiffness, the variation in rubber pad thickness from 3/8 in. (9.5 mm) to about 1/8 in. (3 mm) has small influence on the pressure distribution and central deflections. The exclusion of the pad results in significant concentration of stress at the outer edge of the plate (see Figure 2.6). In addition, a low pressure zone is developed along the central part of the plate. This reduces the stress recovery to 57%. In this case, the central deflections calculated with and without the pad differ by 15% (see Table 2.2). When the pad was used, the variation in deflections is about 5% to 8%. Practically speaking, the pad should be periodically checked to ensure that its properties have not changed. In addition, to ensure uniform central deflection, the pad should be acquired from the same source.

So far the effects of different components of the FWD plate on the central deflection were investigated. The other parameters that play a role in the FWD-pavement interaction are the thickness and modulus of each layer. The impact of each of these parameters on the response of

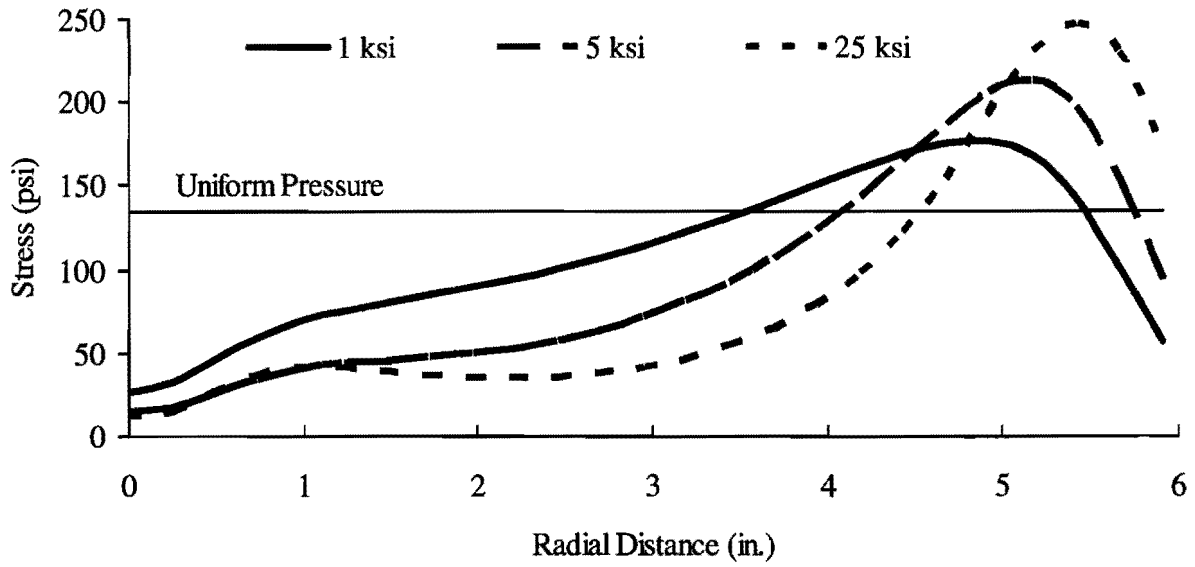


Figure 2.5 – Influence of Pad Stiffness on the Pressure Distribution under the Plate

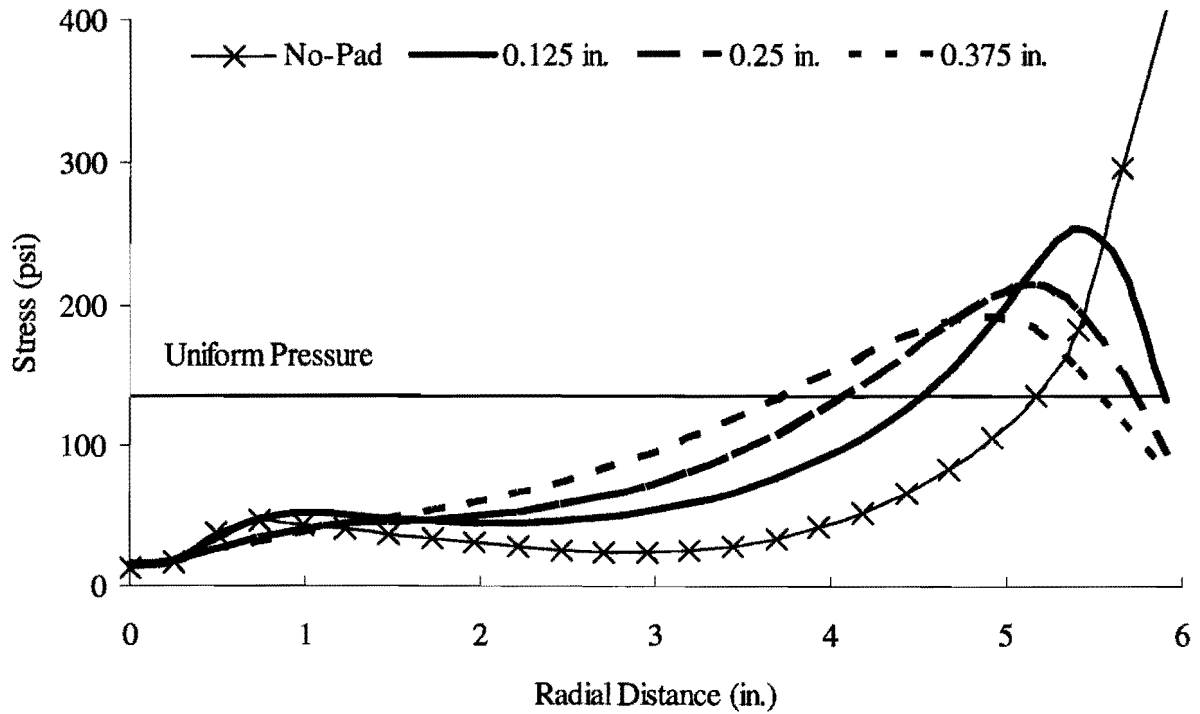


Figure 2.6 – Influence of Pad Thickness on the Pressure Distribution under the Plate

the pavement is presented in the following paragraph, utilizing a procedure similar to that followed for different plate components. The results of these sensitivity analyses are summarized in Table 2.3

The variation in the AC layer stiffness results in large variations in the deflection of the central sensors. The variation in deflection simulated with the uniform stress distribution and from the pressure obtained under the plate ranged from 9% to 4%, as the stiffness of the asphalt layer increased from 250 ksi (1750 MPa) to 1,000 ksi (7,000 MPa).

The thin asphalt layer (thickness of 1 in. or 25 mm) results in a low pressure zone along the central parts of the loading plate. As the thickness increases from 1 in. (25 mm) to 5 in. (125 mm), the stress distribution under the plate becomes more uniform. The stress recovery decreased from 74% to about 71%, as the thickness of the asphalt layer increased from 1 in. (25 mm) to 3 in. (75 mm). A S_r of about 79% is recorded with further increase in the asphalt layer thickness to 5 in. (125 mm). As shown in Table 2.3, the differences in deflections decreased from 12% to about 4%, with the change in thickness from 1 in. (25 mm) to 5 in. (125 mm). Therefore, the difference in deflections measured at the center of the plate is dependent on the AC layer thickness. The thicker the AC layer is, the less important the interaction will be.

The change in the base layer stiffness influences the pressure distribution under the plate. As shown in Figure 2.7, a base layer with a stiffness of 12.5 ksi (88 MPa) develops a non-contact zone along the central parts of the plate. This results in the concentration of the entire load along the outer edge. As the base layer stiffness increases to 200 ksi (1400 MPa), the stress distribution under the plate becomes more uniform. The S_r increases from 55% to about 84% with the increase in the base layer moduli from 12.5 ksi (88 MPa) to 50 ksi (350 MPa). Such large increase in the stress recovery with the increase in the base layer stiffness results in a difference in deflections ranging from 10% to about 3% (see Table 2.3).

Table 2.3 – Influence of Plate Components on Stress Distribution and Central Deflection of FWD

Parameter	Modulus (ksi)			Thickness (in.)			S_r (%)	Central Deflection (mils)
	AC	Base	Subgrade	AC	Base	Subgrade		
Standard Plate	500	50	10	3	12	285	71	1.28
AC Modulus	250	50	10	3	12	285	72	1.37
	1000						72	1.19
AC Thickness	500	50	10	1	12	287	74	1.57
				5		283	79	1.04
Base Modulus	500	12.5	10	3	12	285	55	2.12
		200					84	0.78
Base Thickness	500	50	10	3	6	291	66	1.63
					18	279	72	1.10
Subgrade Modulus	500	50	2.5	3	12	285	69	2.63
			40				73	0.70

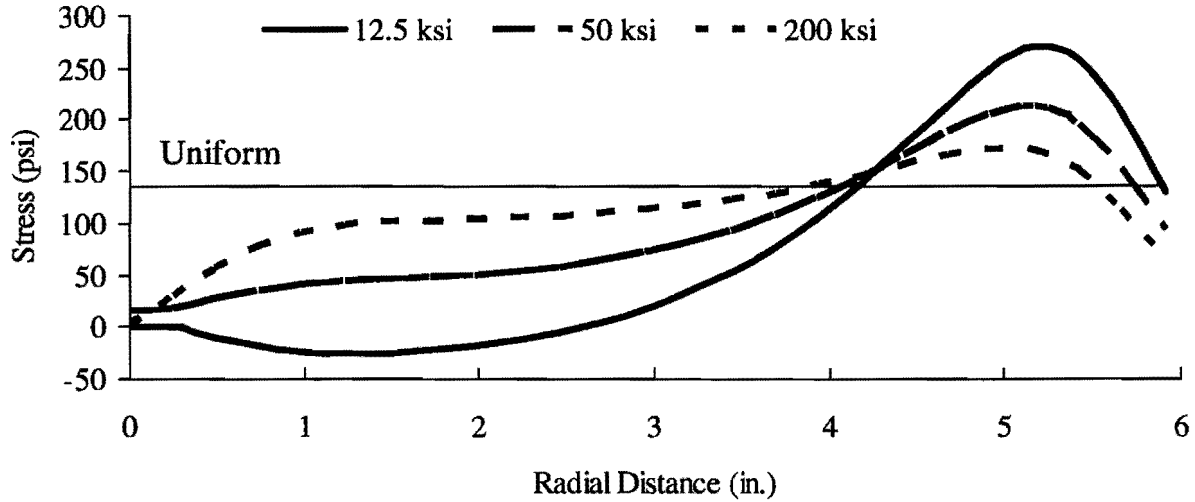


Figure 2.7 – Influence of Base Layer Stiffness on Pressure Distribution under Plate

On the other hand, the change in the base layer thickness exerts a small influence on the pressure distribution under the plate. The difference between deflections obtained from the two approaches is about 6.5% with the change in thickness from 6 in. (150 mm) to 12 in. (300 mm).

To determine the influence of the stiffness of the subgrade on the overall response of the pavement system, the stiffness of the subgrade varied from 2.5 ksi (17.5 MPa) to 40 ksi (280 MPa). The variations in the subgrade stiffness have some influence on the pressure distribution along the interface. The differences in the deflections obtained from the two approaches vary from 4% to 10%, as the stiffness of the subgrade increases from 2.5 ksi (17.5 MPa) to 40 ksi (280 MPa).

These two studies indicate that the components and the design of a load plate impact the results of the FWD system and should be considered to maintain an interchangeable and well-maintained fleet.

Chapter 3

Evaluation of Plates on Smooth and Level Pavement

The evaluation of the plates was carried out in two stages. Field tests were first carried out to quantify the differences in the actual conditions. The second stage consisted of devising and testing appropriate instrumentations.

Field Evaluation

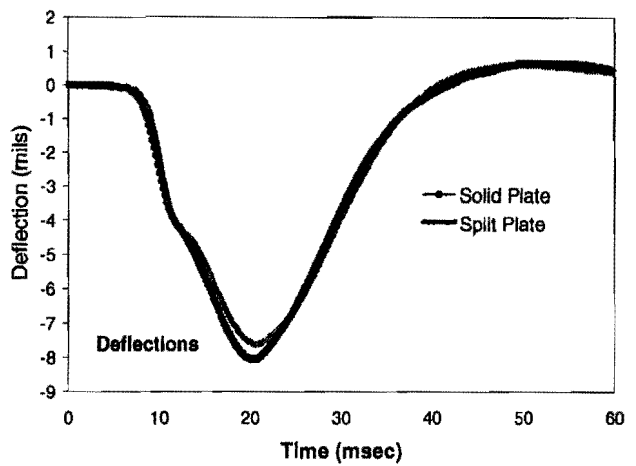
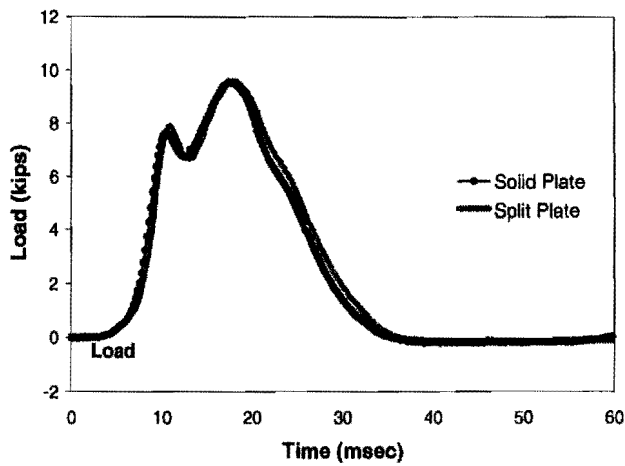
In conjunction with the field validation reported in Rocha et al. (2001 and 2002), a series of field test were carried out to determine the variation in load and deflection as a function of the overall stiffness of sites. Two flexible sites and one rigid site were tested. The layering at each site is summarized in Table 3.1. The sites are extensively described in Rocha et al. (2002).

Table 3.1– Layer Information of Selected Sites

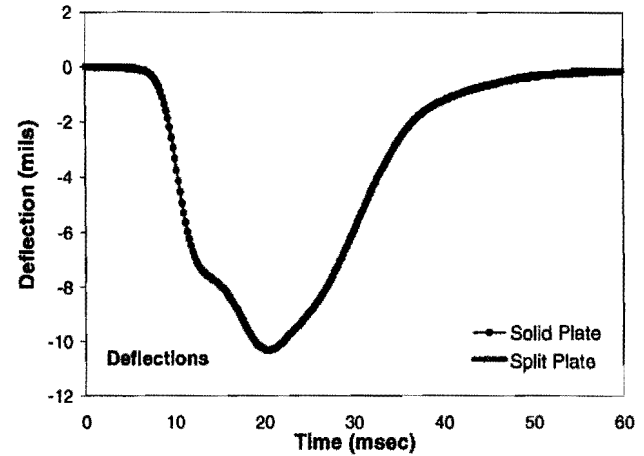
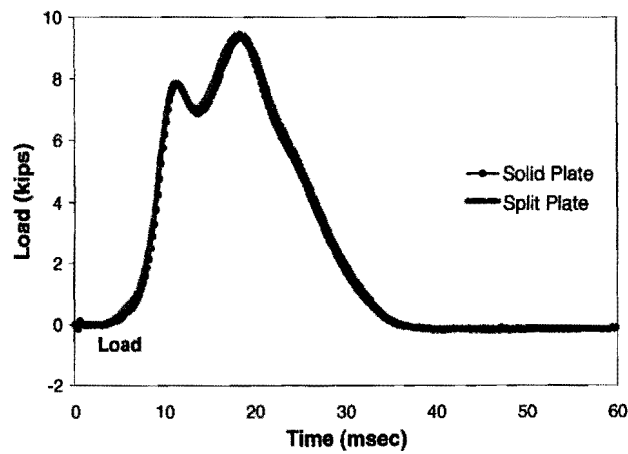
Site	Condition	Layer Information
1	Strong Flexible	5 in. (125 mm) ACP
		12 in. (300 mm) Stabilized Base
2	Weak Flexible	1.5 in. (37 mm) ACP
		10 in. (250 mm) Granular Base
3	Rigid	8 in. (200 mm) PCC

The three sites were tested back-to-back by the same FWD first with a solid plate and then with a split plate. Each site was tested three times. Each time, the FWD was situated at a precise location. The air and pavement temperature were measured. The FWD test was then carried out by applying two seating drops at a nominal load level of 12 kips (53 KN), followed by six drops at four nominal load levels of 6 kips (27 KN), 9 kips (40 KN), 12 kips (53 KN) and 15 kips (67 KN). At each load level, the peak loads and peak deflections were recorded for all drops and the load and deflection time histories were saved for drops 2, 4 and 6. The results are comprehensively provided in Appendix A and are summarized below.

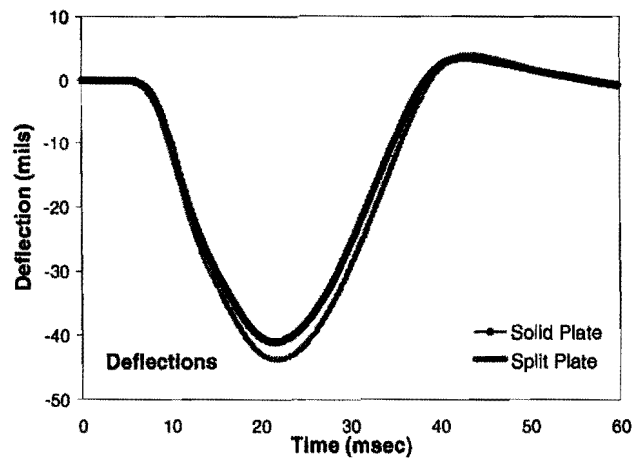
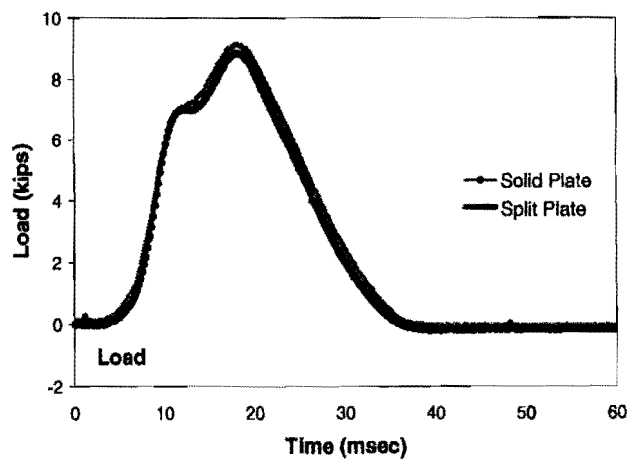
Typical load and deflection time histories from Drop Height 2 at the three sites are compared in Figure 3.1. In general, the load time histories from the solid and split plates are similar. The



a) Rigid Site



b) Strong Flexible Site



c) Weak Flexible Site

Figure 3.1 – Typical Load and Deflection Time Histories from Three Sites

stronger the pavement, the higher the peak load exerted to the pavement. The deflection time histories were somewhat different. As the pavement becomes stronger, the difference in the deflections measured with the two plates becomes smaller.

The variations in peak deflections as a function of measured peak loads are included in Figure 3.2. For the rigid site, as shown in Figure 3.2a, the FWD equipped with the solid plate measures deflections that are about 6% greater than the split plate for the same load. For a nominal load of about 6 kip (27 KN), the loads reported under the solid plate are slightly greater than those from the split plate. On the other hand for nominal loads of 12 kip (53 KN) and 15 kip (67 KN) the loads reported by the split plate are greater than those from the solid plate.

For the strong and the weak flexible sites, the loads recorded with the split plate are always greater than those from the rigid plate indicating perhaps that the plate is better conforming to the pavement as reported by Boddapatti et al. (1994).

This case study clearly demonstrated that by changing the plate, the load and deflections measured with the FWD will change slightly. Since this change is felt by the central geophone the most, it may have an impact in the backcalculated results. As such, an instrumentation plan was devised and carried out to quantify these differences.

Instrumentation

The load plate transfers the applied load to the pavement through a multi-layered plate. The solid plate typically consists of a 3/4-in. (19-mm) thick steel plate connected to a 7/8-in. (22-mm) thick PVC plate. A ribbed neoprene plate, glued to the PVC plate, is in contact with the pavement to provide a uniform load distribution. To study the characteristics of the load plate, it was instrumented with accelerometers and strain gauges.

Four strain gauges as shown in Figure 3.3 were placed along a radius of the plate to measure the strain experienced by the plate. The nominal locations of the strain gauges from the center of the plate were 3.9 in. (98 mm), 4.6 in. (118 mm), 5.4 in. (137 mm) and 6.1 in. (156 mm). Because of their small size (less than 1 in., 25 mm) and ease of installation, dynamic strain gauges are ideal for the type of instrumentation required for this project. The dynamic strain gauges are piezoelectric in nature. They incorporate quartz sensing elements and built-in microelectronic signal conditioning circuitry to generate an output signal that is proportional to dynamic strain influences. Since these sensors only respond to dynamic strains, they may be used to detect low-level dynamic strains that are superimposed on a large static load. The nominal sensitivity of the strain gauges used is 50 mV/ μ strain.

Typical response of the solid load plate on a concrete slab is shown in Figure 3.4. The highest strain is experienced by the strain gauge closest to the load. The strain decreases as the radial distance increases. Typically the strain measured by the first strain gauge was three to four times that of the fourth strain gauge. Similar results for testing on flexible pavement were obtained. While the strain patterns observed on both the load and strike plates were similar in shape, the amount of strain, particularly on the strike plate, was of such magnitude on the flexible surface that it only allowed us to measure strains at Drop Height 1. On all other heights, the strain signals exceeded the limits of the strain gauge.

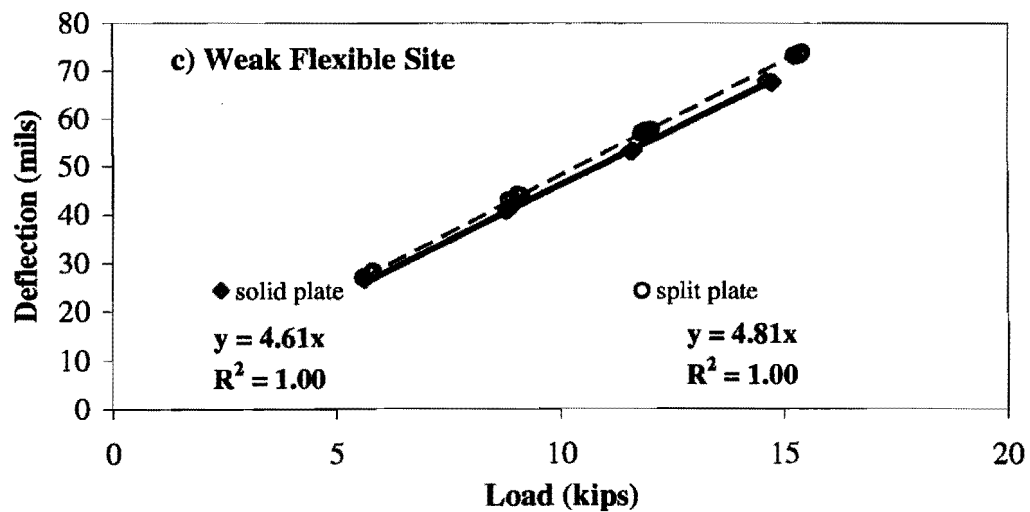
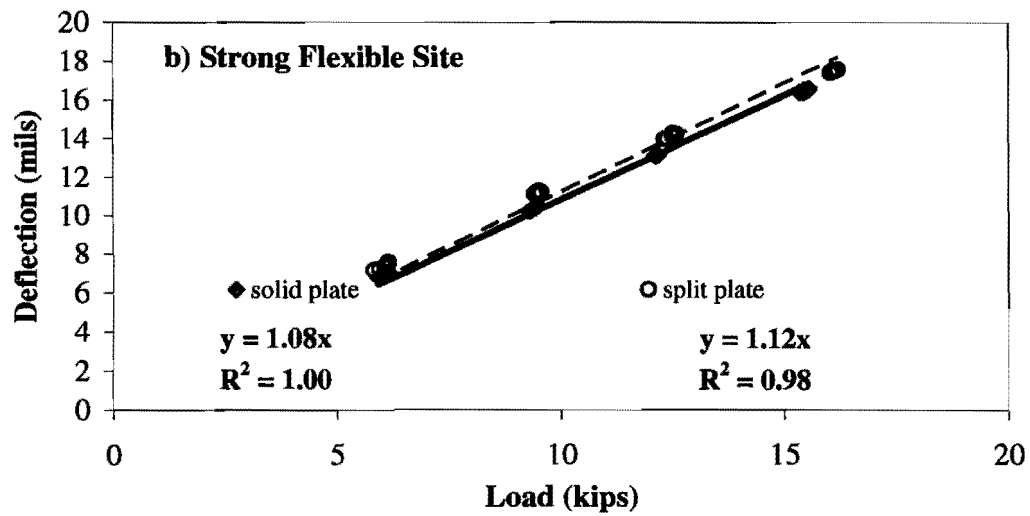
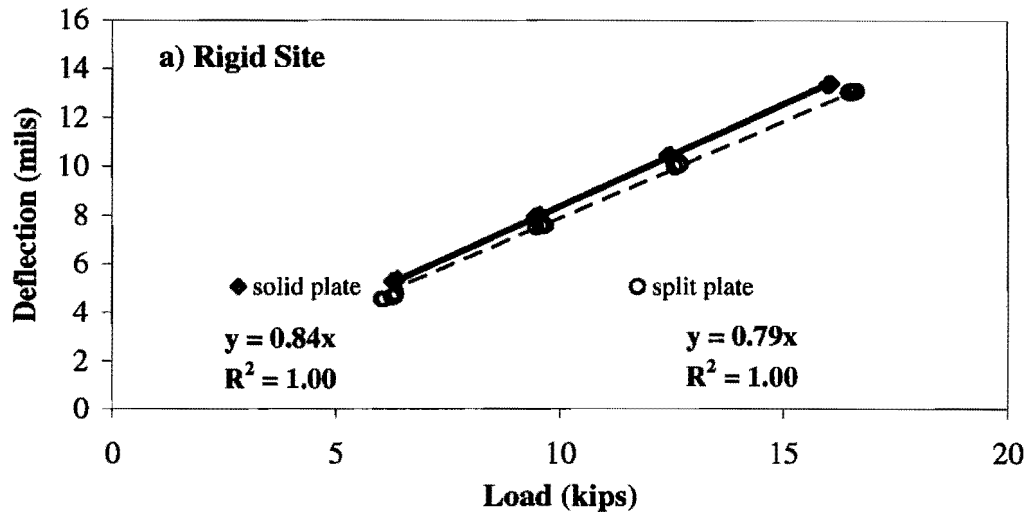


Figure 3.2 – Comparison of Variations in Deflection with Load under Split Plate and Solid Plate at Three Sites

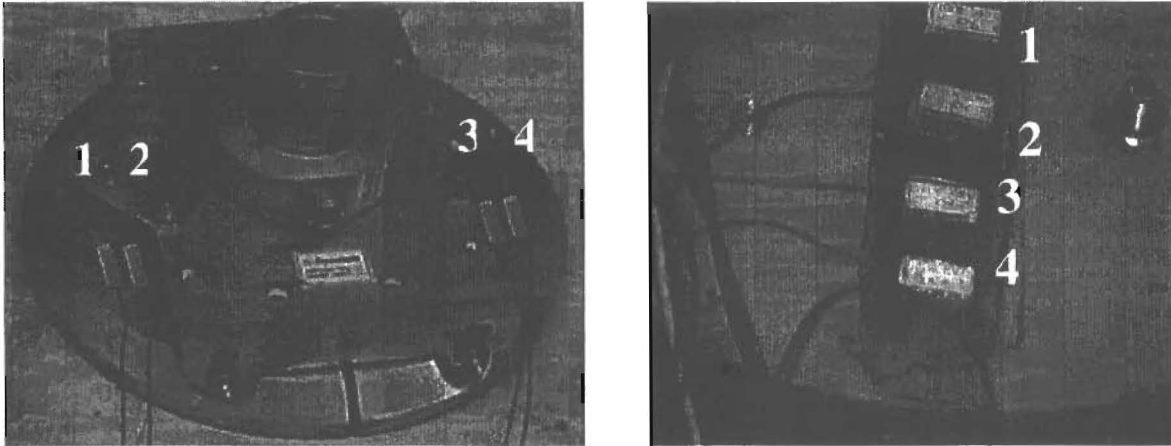


Figure 3.3 – Installation of Strain Gauges on Load Plate

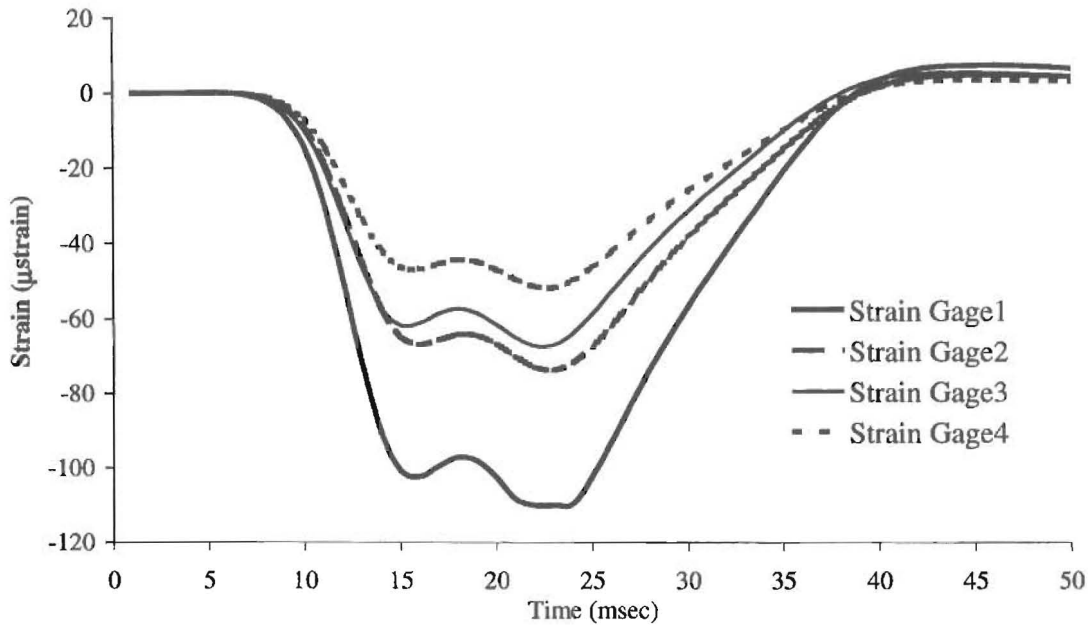


Figure 3.4 – Typical Variations in Strain Time Histories along FWD Load Plate

To investigate the impact of the condition of the load assembly on the response of the load cell, the old load plate assembly was replaced with a brand new one, without altering any other components. The distribution of strain along the new plate is shown in Figure 3.5. In this case, the strains are smaller than those shown in Figure 3.4. Strain Gauge 4, which is farthest from the load experiences negligible strain. A comparison of Figures 3.4 and 3.5 indicates that changing the load plate assembly also changes the load pulse shape. This was a surprising finding. However, a closer inspection of the old load assembly revealed that accumulation of dirt and lack of lubrication could be the reason for this phenomenon. When the old assembly was cleaned, lubricated and reinstalled, the load pulse shape was similar to the one obtained from the new one.

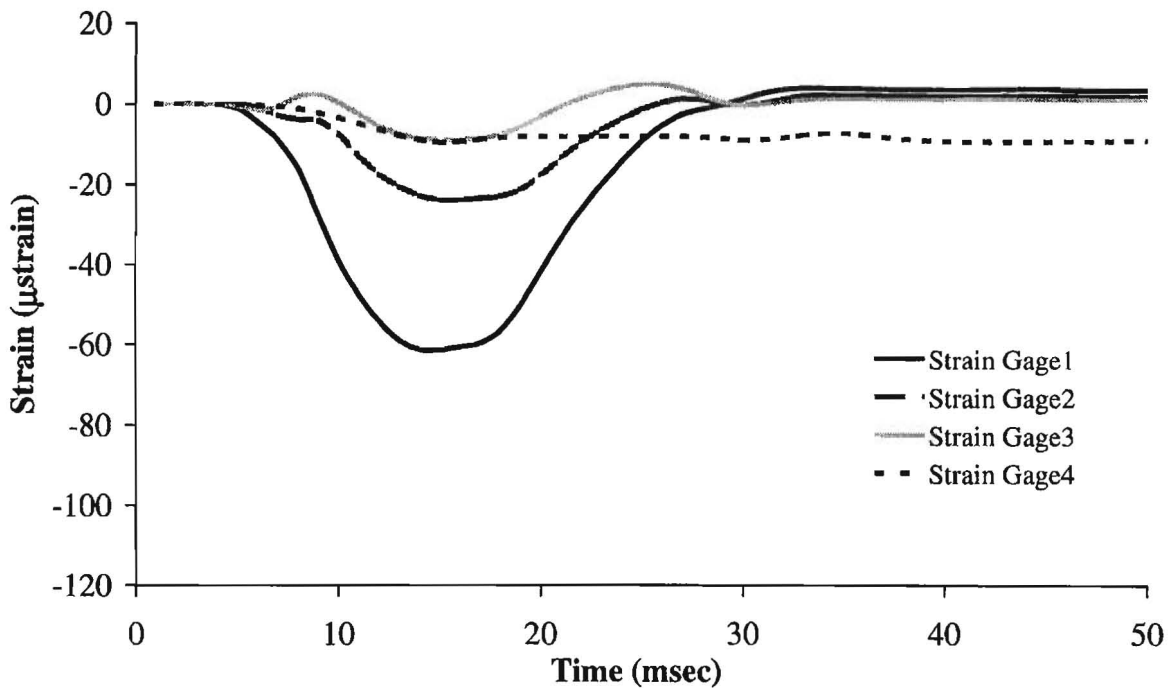


Figure 3.5 – Variations in Strain Time Histories along FWD Load Plate (Brand New Load Plate Assembly)

A split plate assembly was also mounted on the FWD (see Figure 3.3). Because of the shape of the plate, Strain Gauges 1 and 2 could not be placed on the load plate. The strain time histories for Gauges 3 and 4 using a split plate are shown in Figure 3.6. As seen in Figure 2.1, the load is transferred through an intermediate plate to the split load plate. In this case, the load plate experiences small strains, but in the opposite direction of those measured on the two solid plates.

The time histories measured at one point on the slab are compared in Figure 3.7 for the same drop height. The split plate and the new solid plate provide similar pulse shapes. However, the pulse shape from the original load plate was somewhat different. For the two solid plates, the load pulse shape and the responses from the strain gauges are quite similar. The measured peak loads reported by the FWD varied by about 3%.

Similarly, the time history deflections reported by the FWD (simultaneous with the loads shown in Figure 3.7) are demonstrated in Figure 3.8 for one sensor. In this case, the time histories are similar in shape; however, the differences in peak values are around 5%. Based on studies similar to this, one can conclude that the condition of the load plate assembly may impact the deflections measured with the FWD.

To monitor the motion of the load plate, three accelerometers were placed about 5.5 in. (140 mm) from the center of the plate along three locations (see Figure 3.9). Tandon (1990) describe the conceptual design of such accelerometers. In principle, an accelerometer transmits output voltage that is proportional to the acceleration of the mass it is attached to. Once again, the calibration of accelerometers is discussed in Tandon and Nazarian (2000). To obtain displacement, the response

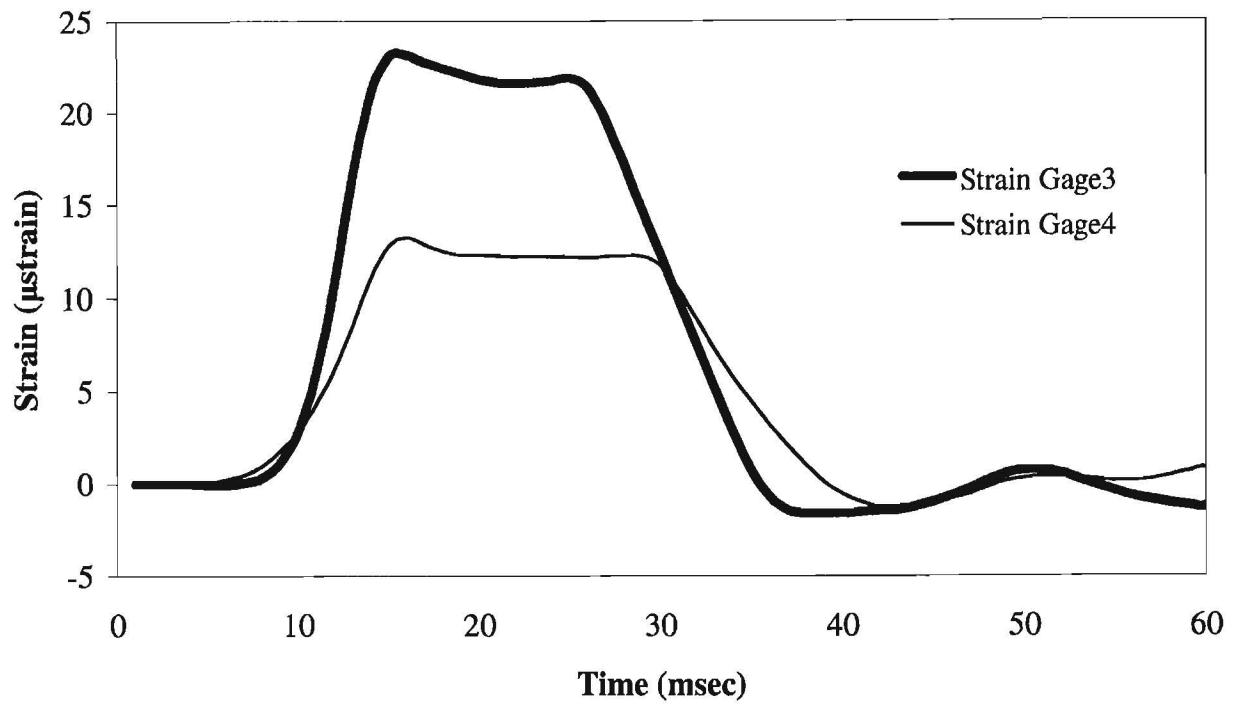


Figure 3.6 – Variations in Strain Time Histories along FWD Load Plate (Split Plate Assembly)

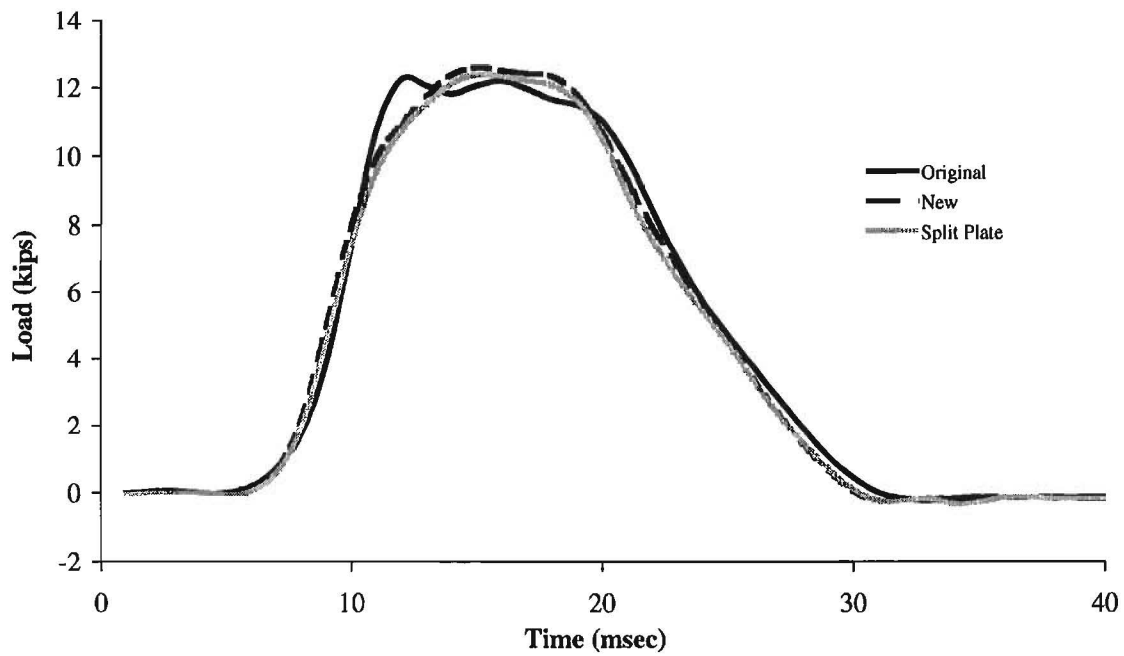


Figure 3.7 – Comparison of Load Time Histories Reported by FWD from Three Different Load Plates

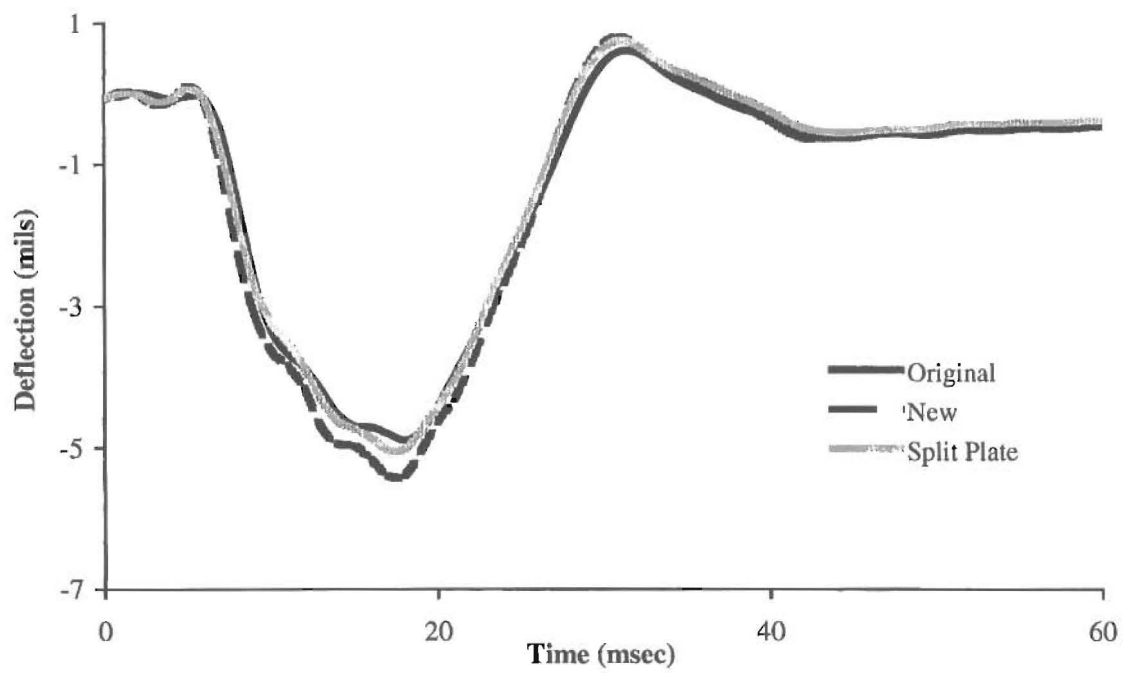


Figure 3.8 - Comparison of Deflection Time Histories Reported by FWD from Three Different Load Plates

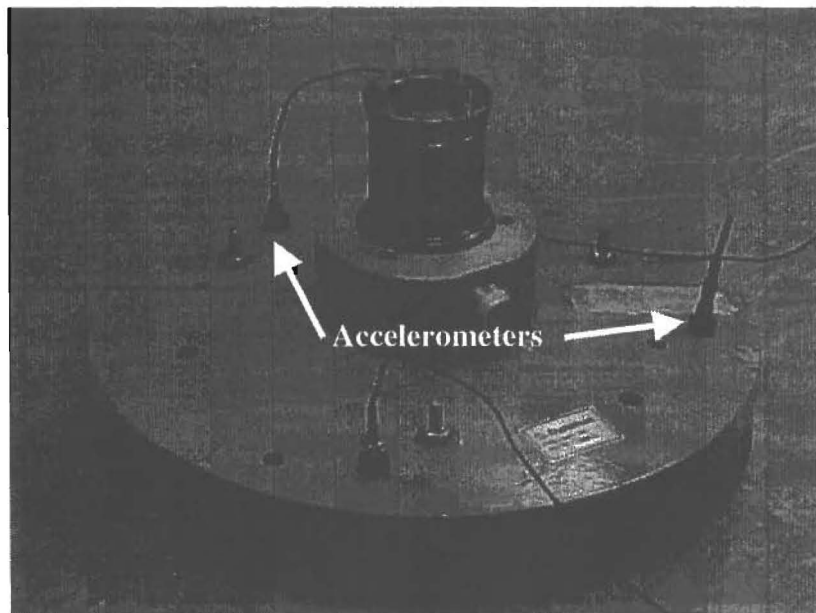


Figure 3.9- Typical Placement of Accelerometers on Load Plate

of the accelerometer has to be integrated twice. Mathematically this is a simple task. However, because of practical complications of this operation in the presence of noise in data, double integration should be avoided except for high quality accelerometers. As such, the accelerometers were used to compare relative motion between different components. The nominal sensitivity of the accelerometers used is 100 mV/g (i.e., 0.25 mV/in./sec² or 10 μV/mm/sec²).

Typical responses from the accelerometers are shown in Figure 3.10. The motion of the plate measured at three locations is usually reasonably similar. These measurements were carried out throughout this study and are reported in the next chapter.

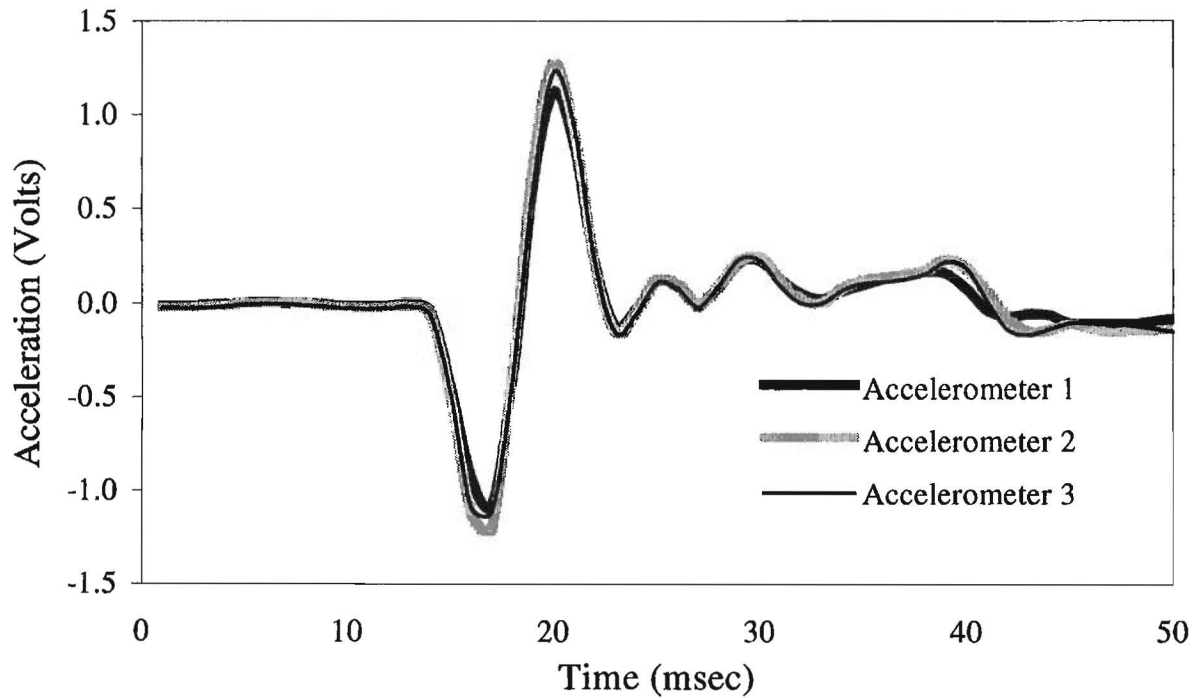


Figure 3.10 – Typical Motion of Load Plate

Chapter 4

Evaluation of Plates on Rutted and Inclined Pavement

Introduction

The behavior of the two types of load plate assemblies on a smooth surface was examined in the previous chapter. However, this type of surface characteristic may not be often found in real world testing. A more realistic scenario would be one where the surface is either worn, bumpy, cracked or is at an inclination. The responses of the load cell, load plate, and the deflection directly under the load were evaluated in this study for two plate types and the results are reported in this chapter.

Preparation of Test Slabs

To simulate rutted and sloped pavements, three slabs were poured from a single batch of concrete to maintain common material characteristics. The three slabs were 3 ft (0.9 m) by 6 ft (1.8 m) by 6 in. (0.15 m) thick.

The control slab, as shown in Figure 4.1, was built to simulate a flat and level surface. The second slab was built with a 10-15 degree inclination while the third slab had a rut running down its middle. The rut, which was 0.5 in. (12 mm) deep, was 18 in. (0.45 m) wide on one side which gradually widens to 20 in. (0.5 m) on the other side. As shown in Figure 4.1, three points were tested on each slab.

To conveniently test these slabs, an FWD loading mechanism was obtained from TxDOT (see Figure 4.2). The loading mechanism was retrofitted into an undercarriage that supported the loading mechanism, its control box and the batteries used to run the hydraulic motor, the FWD processor and the control box.

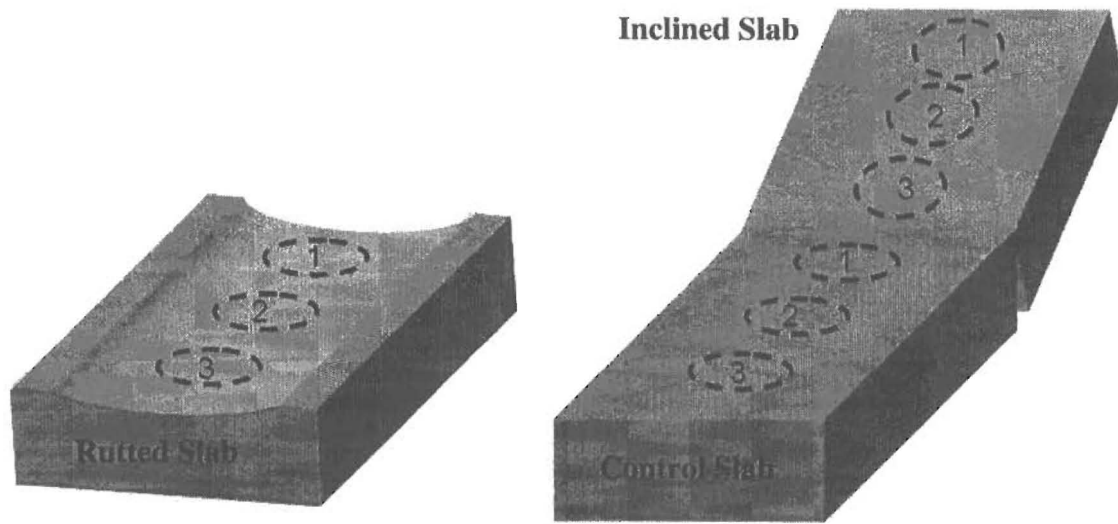


Figure 4.1 - Layout of concrete slabs Used for Evaluating Load Plates

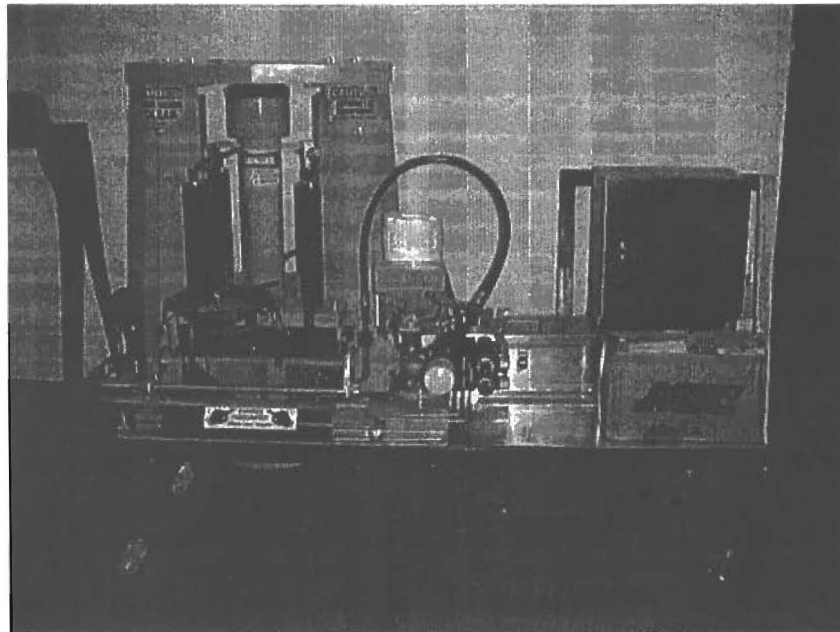


Figure 4.2 - FWD Loading Assembly and Control Box on Undercarriage

Description of Experiments

The testing began by selecting the test points on each slab. The center of each slab as well as 12 in. (0.3 m) from each of its edges was tested. The temperature of the slabs was monitored to ensure that there were no drastic changes during the entire testing process.

At first, the control slab was tested to obtain reference information. Although an undercarriage was developed, the maneuvering of the loading mechanism is still somewhat cumbersome because it is a heavy piece of machinery. The positioning was done extremely carefully to avoid any accidental tip over and to ensure that exactly the same location was tested with both plate assemblies. Once in place, the following steps were carried out:

- 1) Measure slab temperature
- 2) Perform FWD tests
 - a) Drop load six times at four nominal load levels of 6 kip (27 KN), 9 kip (40 KN), 12 kip (53 KN) and 15 kip (67 KN). Record peak loads and peak deflections for all the drops and record deflection time history for the last drop at each load level.
 - b) After the second drop on drop height 2, raise the load plate and place pressure sensitive film under it. Lower the plate back and record a single drop at Height 2 on the film. Remove the film and continue with the remaining drops.
 - c) Lift load plate, maneuver to the next test location, repeat Steps a and b.

The above process was repeated for the other two slabs for both plate assemblies. The detailed results are included in appendices B and C for a thorough inspection. Results of their analysis are presented in the next section.

Test Results

Level Slab

Figure 4.3 contains typical load and deflection time histories measured with the FWD at the center (Point 2 in Figure 4.1) for the level slab. The load pulses are generally similar with the deflections from the loads applied with the split plate being slightly larger. This finding is in concurrence with the Boddapati et al. (1994) numerical results summarized in Chapter 2. The magnitude of the deflections appears to be larger than expected for a six-inch thick PCC slab because it is not in full contact with the sub-base.

The variations in deflection with the measured load for all experiments at all three points are summarized in Figure 4.4. For Test Point 1, the results from the two plates are fairly similar. However, for Test Points 2 and 3, the deflections measured with the split plates are typically about 10% larger for a given load.

The distribution of the pressure under the FWD plate measured using pressure-sensitive film is shown in Figure 4.5. The distribution of stress under the plate is similar for both plates at each point. Based on the careful inspection of the films, the pressure exerted to the pavement, especially at higher loads, are slightly greater for the split plate. At Test Point 1 for both solid and split plates an area with no appreciable contact pressure is apparent. This lack of contact can be most likely attributed to the imperfections in finishing the slab.

Typical outputs from one of the accelerometers mounted on the two plates are compared in Figure 4.6. The accelerometers provide more or less similar behaviors as well with those measured on the split plate being slightly greater especially at the higher pressures. Based on the data presented here as well as the detailed results from all cases, it can be concluded that both plates provide similar contact pressures and loads for intact level pavements. However, the deflections measured directly under the load are slightly larger with the split plate.

Inclined Slab

The three test points used on the inclined slab are marked in Figure 4.1. In this study, Test Point 1 corresponds to a down-slope test, while Test Points 2 and 3 correspond to up-slope tests. Figure 4.7 contains typical load and deflection time histories measured at Test Point 2. The load pulses are again similar with the deflections from the split plate being larger.

The variations in deflection with the measured load for all experiments at all three points are summarized in Figure 4.8. For Test Point 1, the results from the two plates are fairly similar. However, for Test Points 2 and 3, the deflections measured with the split plates are significantly greater. The distribution of pressure under the plate may shed some light to this behavior.

The distribution of the pressure under the FWD is shown in Figure 4.9. For Test Point 1, the distribution of the stress is somewhat different. Along the outer ream, the pressures are greater for the split plate; whereas near the center the solid plate carries slightly higher pressure. For Test Point 2, the outer ream of the split plate by far carries higher pressures with the center of plates carrying similar loads.

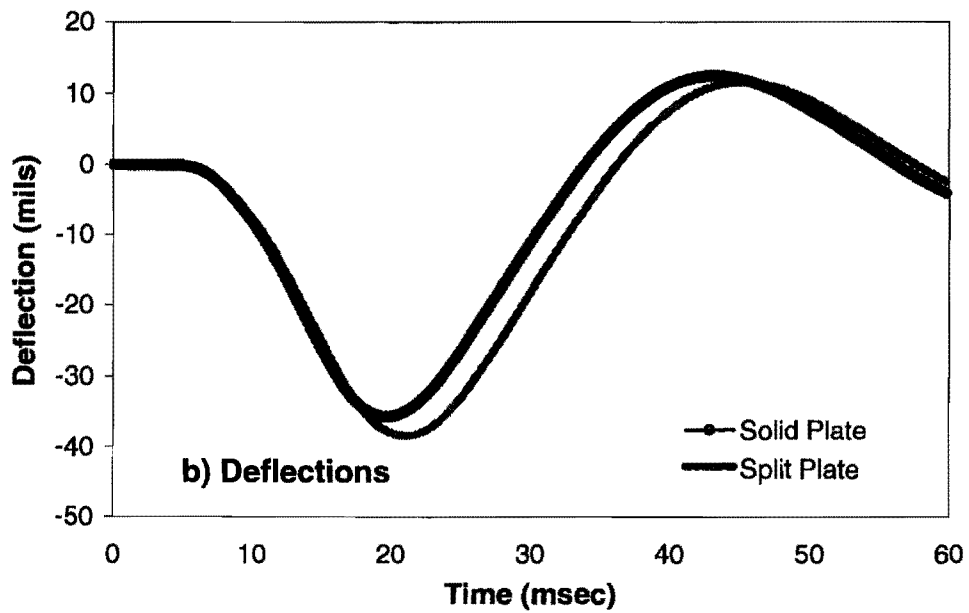
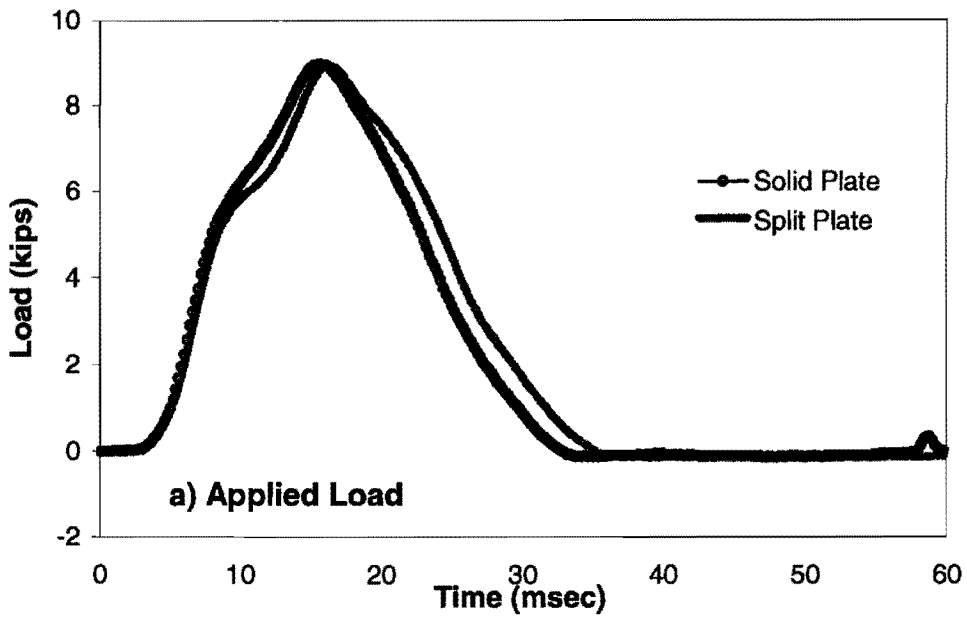


Figure 4.3 – Typical Load and Deflection Time Histories Measured on the Level Slab

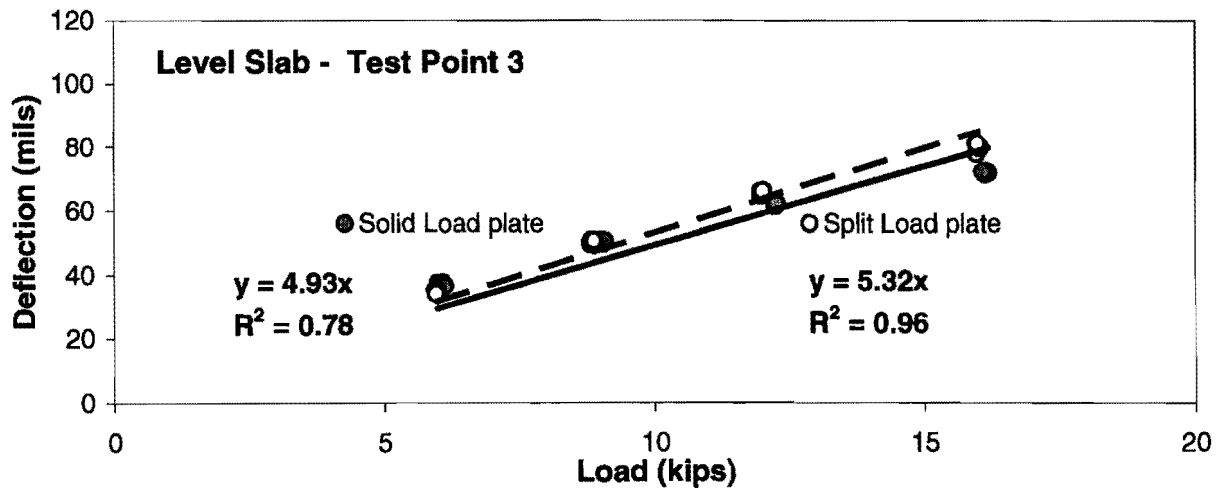
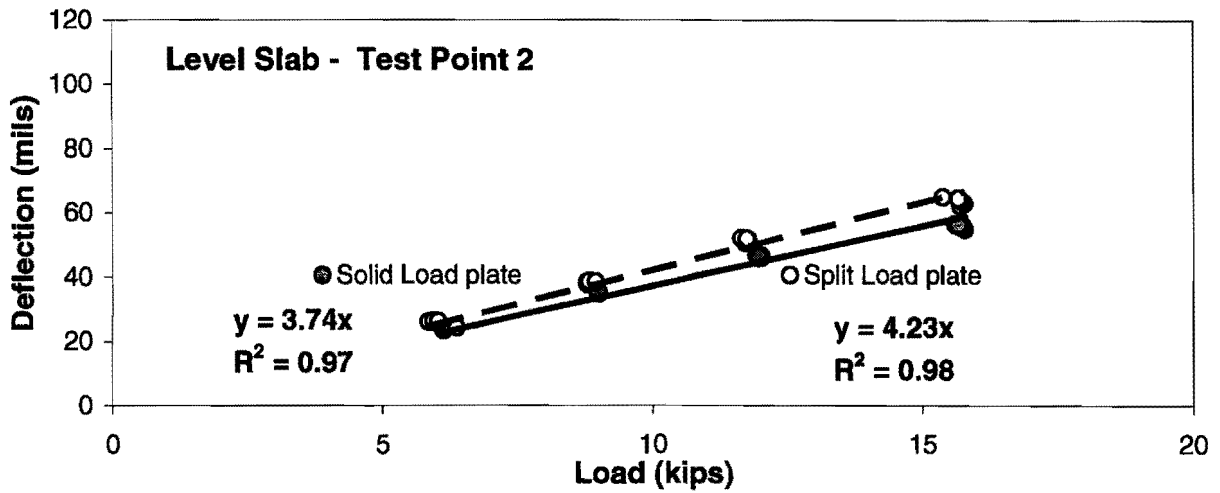
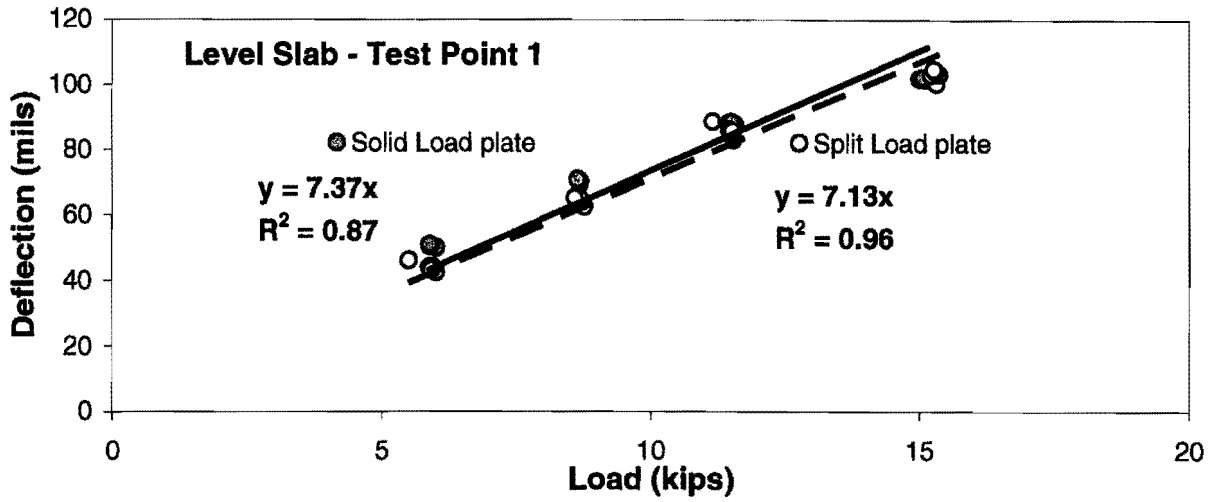
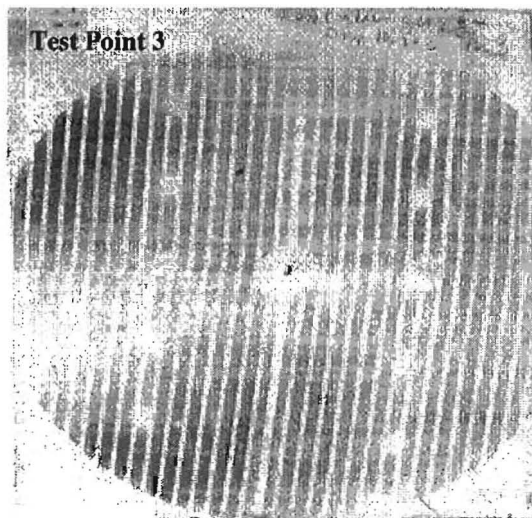
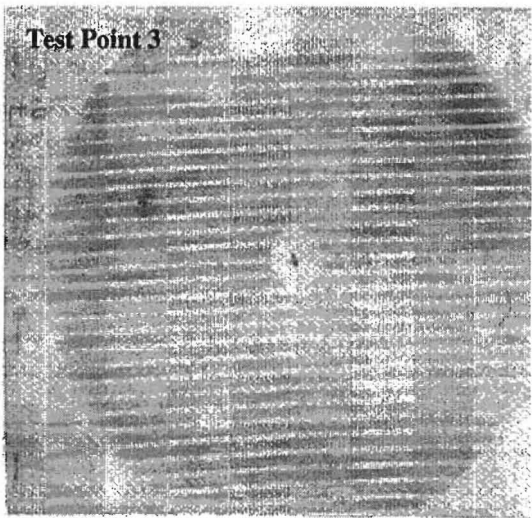
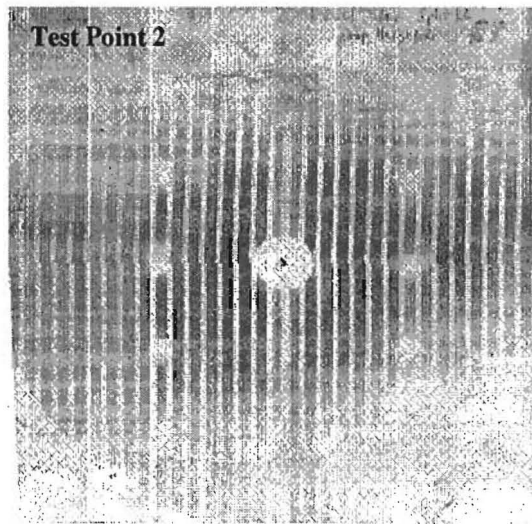
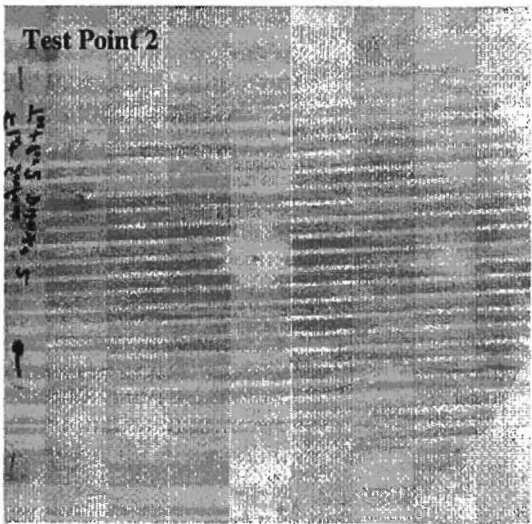
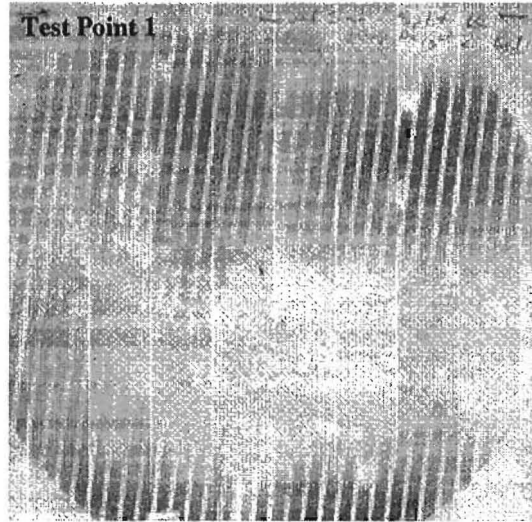
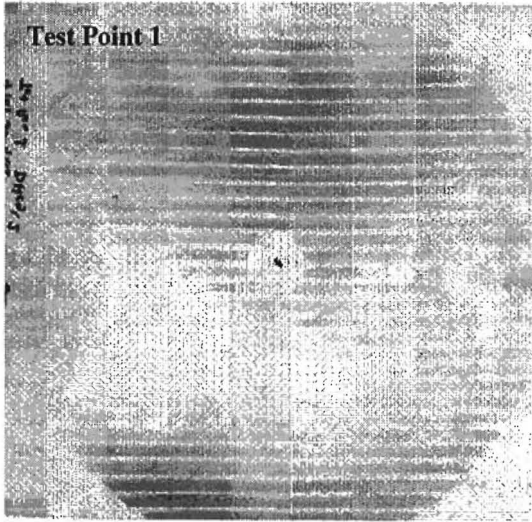


Figure 4.4 – Variations in Deflection with Load on Three Test Points Measured on the Level Slab



a) Solid Plate

b) Split Plate

Figure 4.5 – Variations in Contact Pressure on Three Test Points Measured on the Level Slab

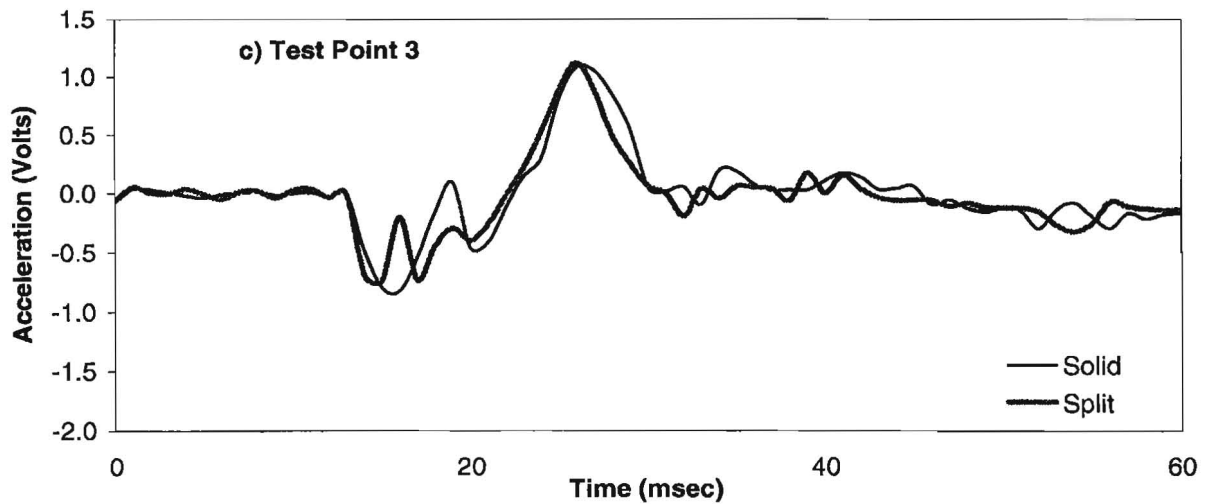
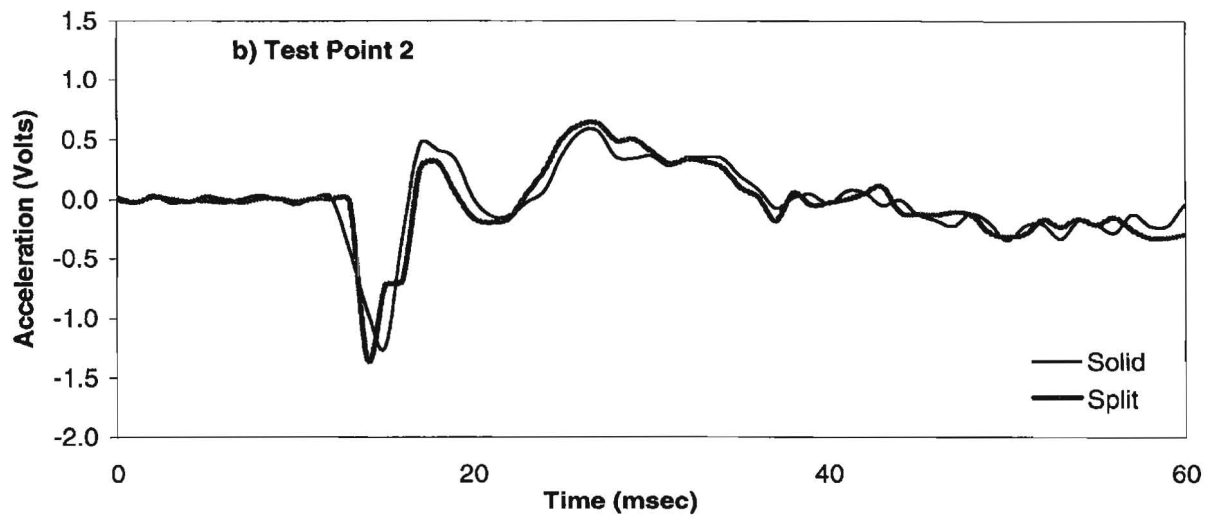
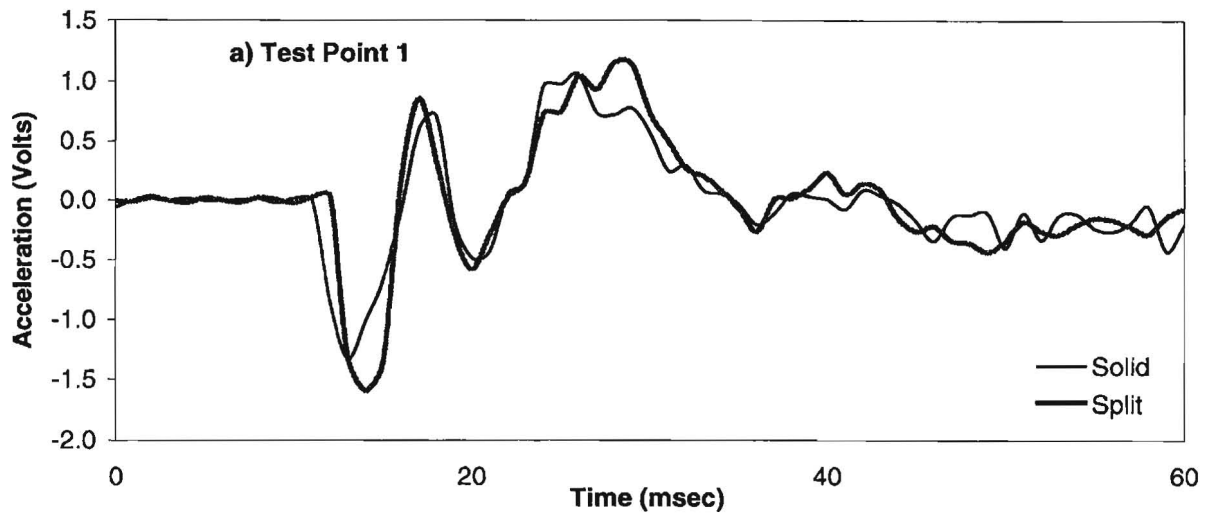


Figure 4.6 – Variations in Acceleration of the Plates on Three Test Points Measured on the Level Slab

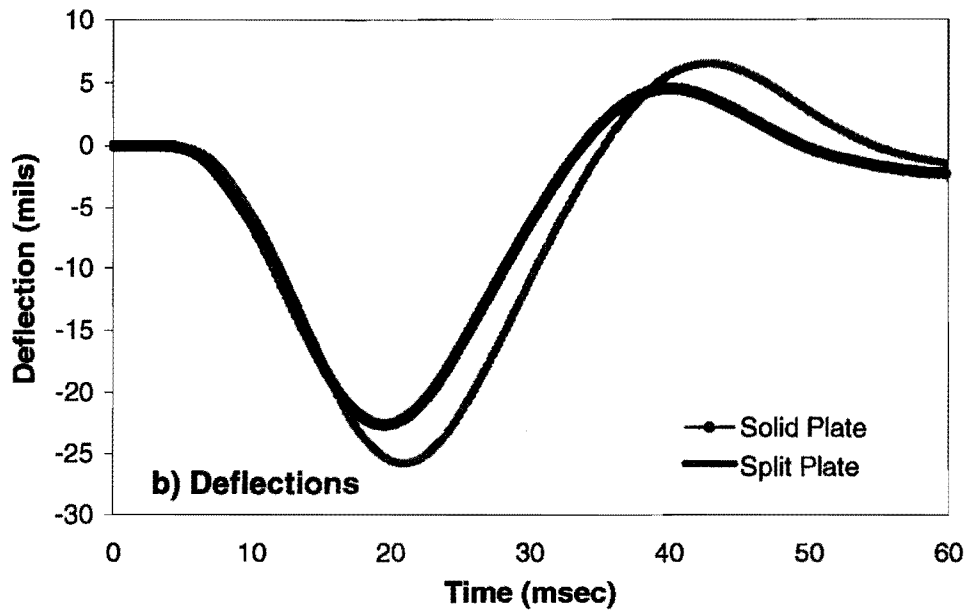
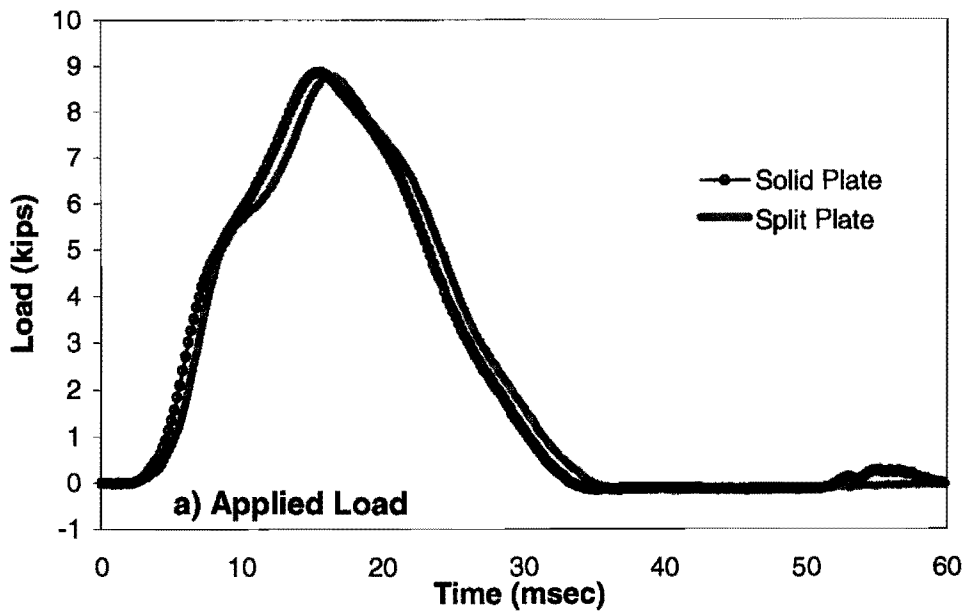


Figure 4.7 – Typical Load and Deflection Time Histories Measured on the Inclined Slab

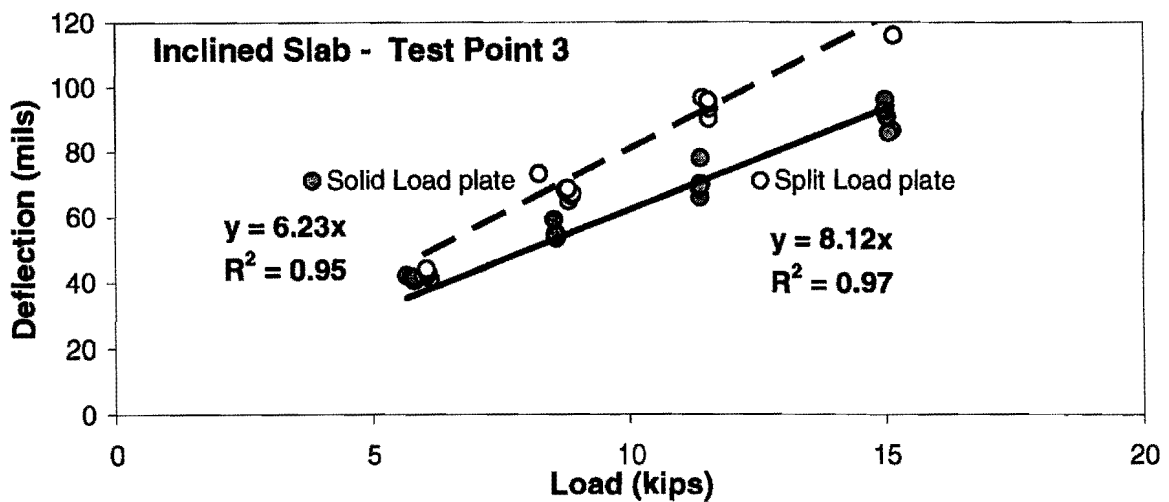
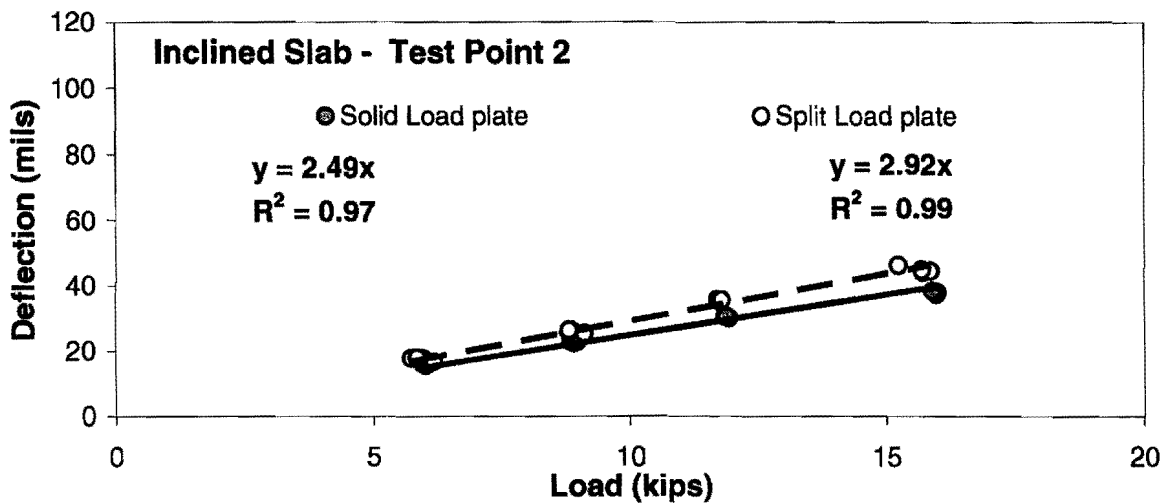
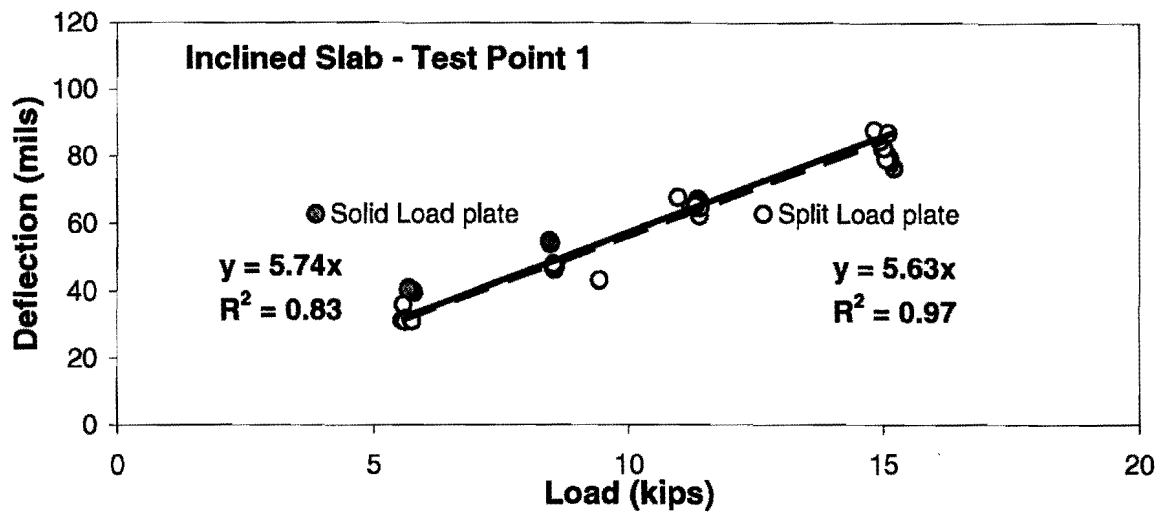


Figure 4.8 – Variations in Deflection with Load on Three Test Points Measured on the Inclined Slab

At Test Point 3, the behavior described for Test Point 2 is apparent but the pressure exerted to the pavement by the outer ream of the split plate is by far more exaggerated.

Typical outputs from one of the accelerometers mounted on the two plates are compared in Figure 4.10. The accelerometer in line with the FWD measure greater acceleration on the split plate, whereas the other two accelerometers 120 degrees away in each direction from Accelerometer 1 measure less acceleration on the split plate.

From our study on inclined surfaces, it can be concluded that the load cell measure similar time histories for the load cell under both plates. However, the deflections are typically greater for the split-plate since the split plate is able to exert more energy into the pavement as compared to the solid plate.

Rutted Slab

The three test points used on the rutted slab are marked in Figure 4.1. As indicated before, the depth of rut was about 0.5 in. (12 mm) but the width of the rutted area tapered, with Test Point 1 being on a “wide” rut and Test Point 3 being on a “narrow” rut. Figure 4.11 contains typical load and deflection time histories measured at Test Point 2. The load and the deflection time histories are somewhat different.

The variations in deflection with the measured load for all experiments at all three points are summarized in Figure 4.12. For Test Point 1 (“wide rut”), the deflections measured with the split plate are greater than those from the solid plate. However, for Test Points 2 and 3 the deflection-load relationships are fairly similar.

The distribution of the pressure under the FWD is shown in Figure 4.13. For the solid plate, the stress distribution becomes more concentrated around the edges as the rut becomes narrower. The central portion of the plate is hardly in contact with the pavement. On the other hand, for the split plate, both the central portion of the plate and the edges are in contact with the plate. Still a significant area of the plate is not in contact with the pavement.

As can be observed on all the pressure film imprints presented in Figures 4.5, 4.9, and 4.13, the contact areas are not completely circular because the film is not wide enough to encompass the entire load plate diameter.

Typical outputs from one of the accelerometers mounted on the two plates are compared in Figure 4.14. The accelerometers mounted on the split plate typically demonstrated much smaller values as compared to the solid plates. This demonstrates that the FWDs equipped with split plates may work more smoothly and last longer if routinely used on damaged pavements.

The results from the tests on the rutted pavements should be used with caution because even during our tests very small misalignment would result in significantly different results. If at all possible, it may be a good practice not to test rutted areas with the FWD to lengthen the life of the device and to minimize damage to the system.

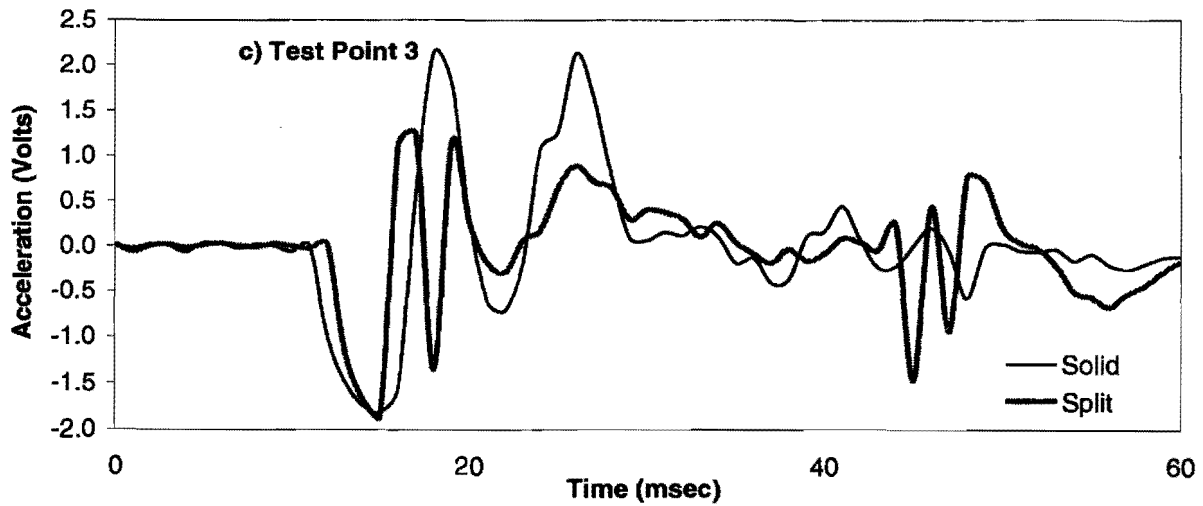
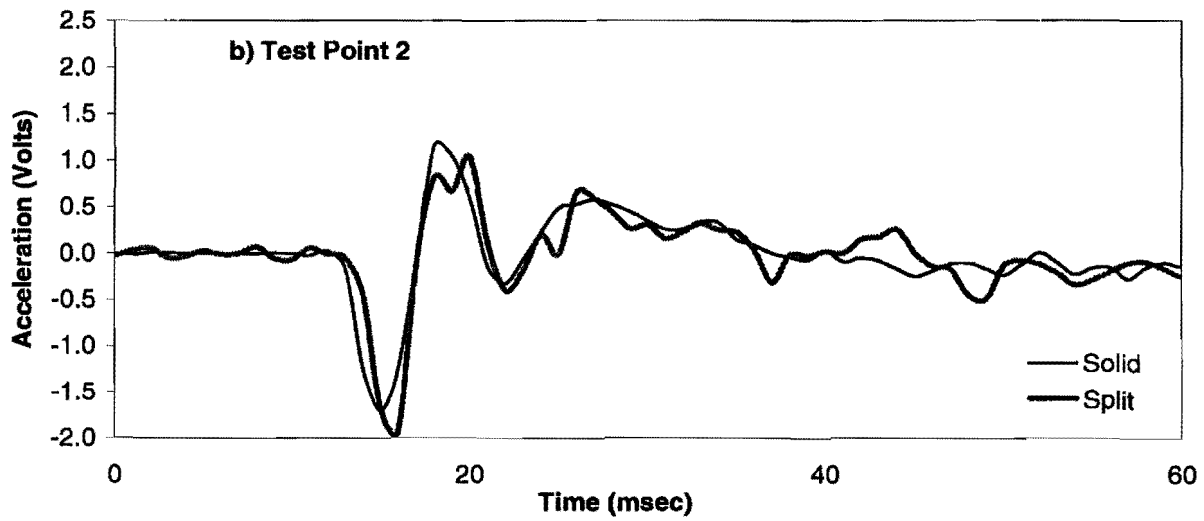
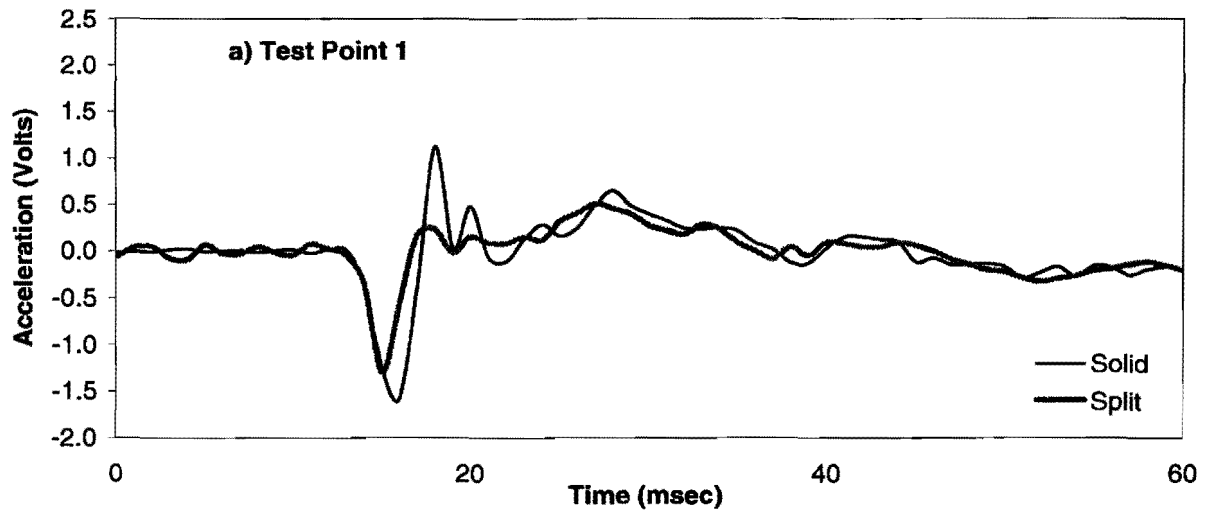


Figure 4.10 – Variations in Acceleration of the Plates on Three Test Points Measured on the Inclined Slab

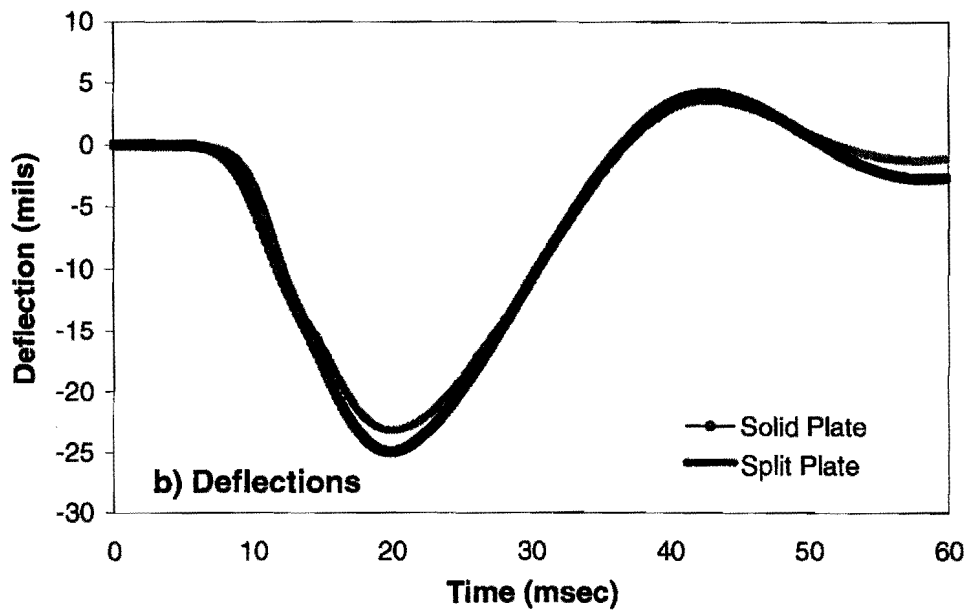
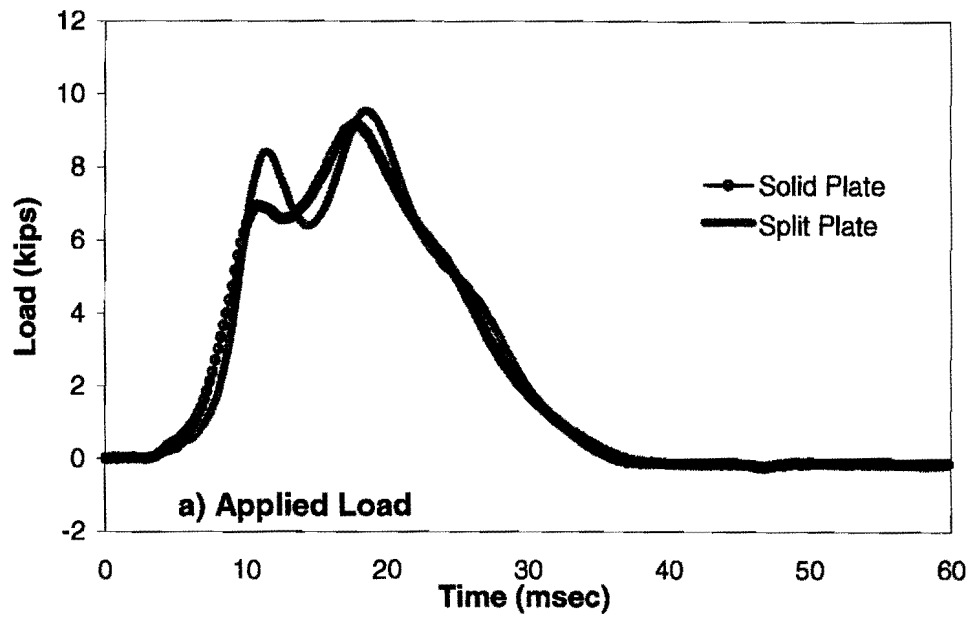


Figure 4.11 – Typical Load and Deflection Time Histories Measured on the Rutted Slab

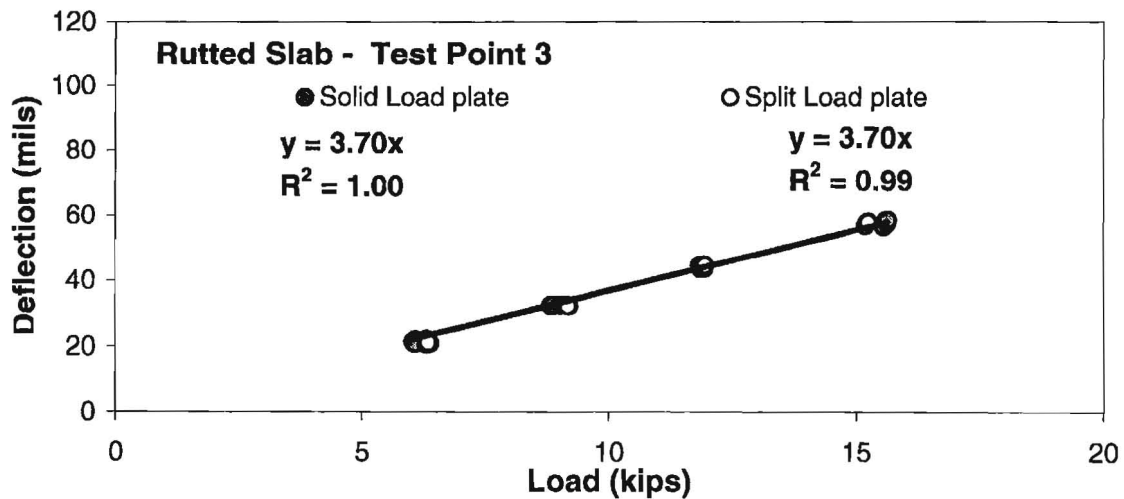
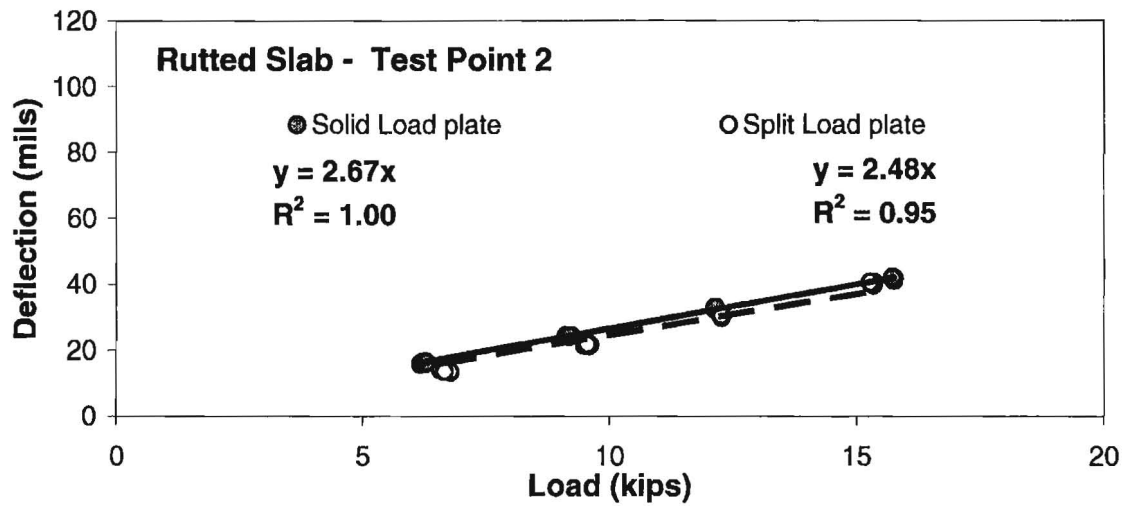
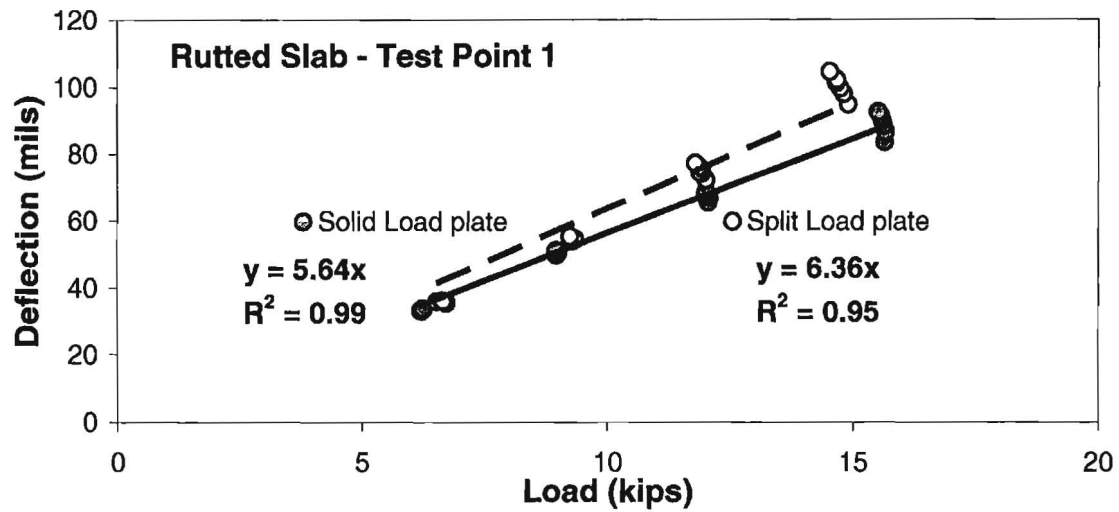
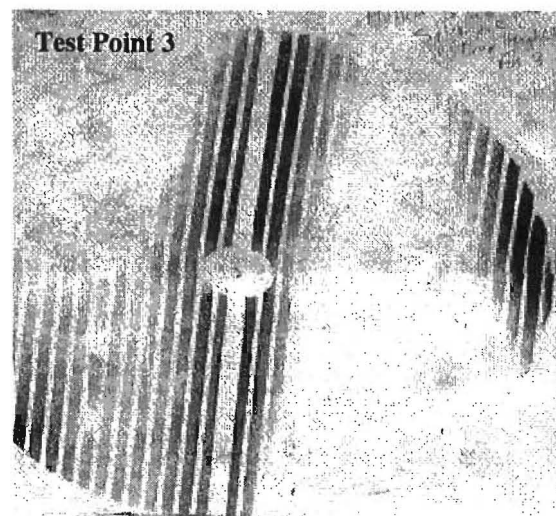
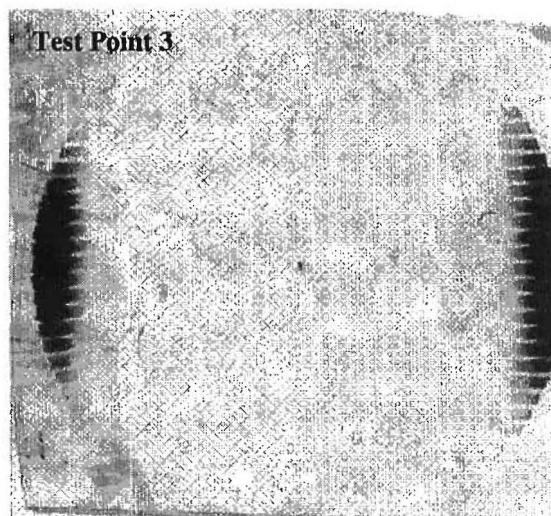
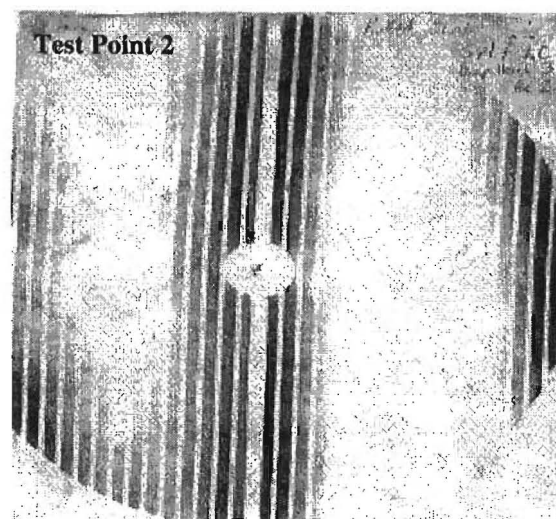
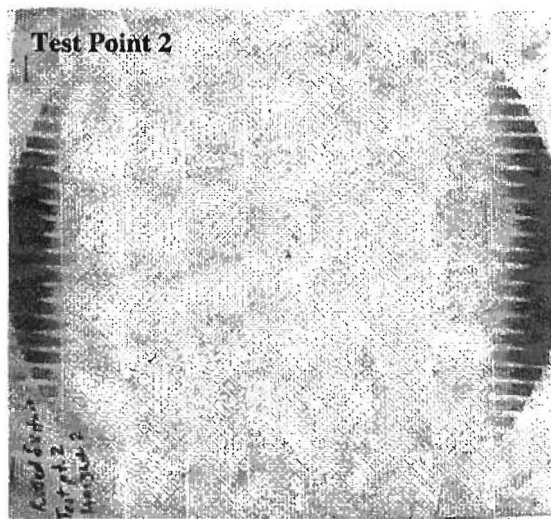
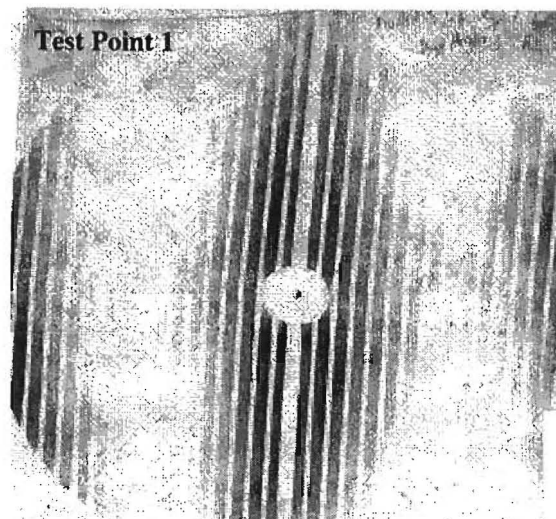
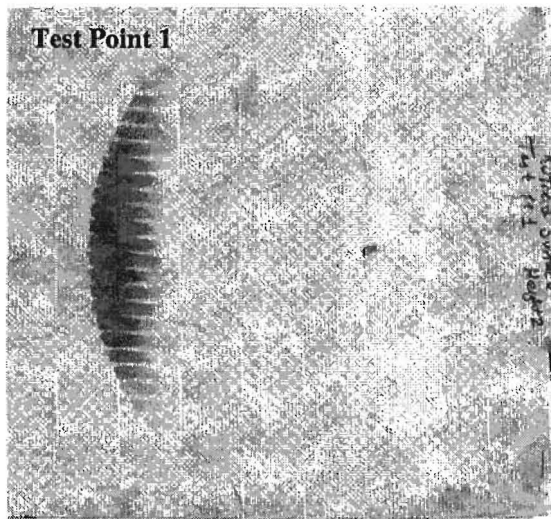


Figure 4.12 – Variations in Deflection with Load on Three Test Points Measured on the Rutted Slab



a) solid plate

b) split plate

Figure 4.13 – Variations in Contact Pressure on Three Test Points Measured on the Rutted Slab

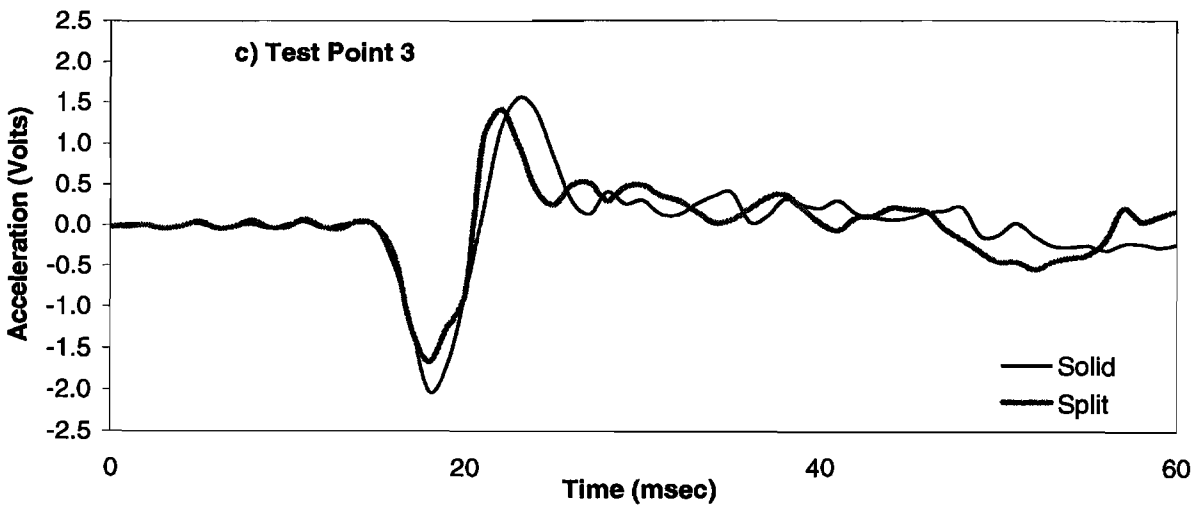
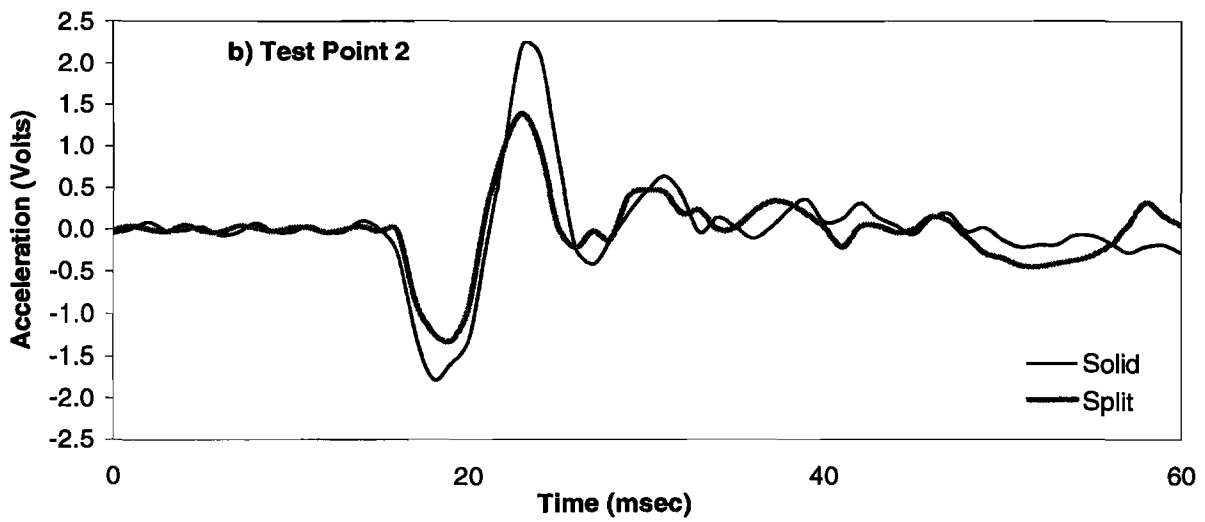
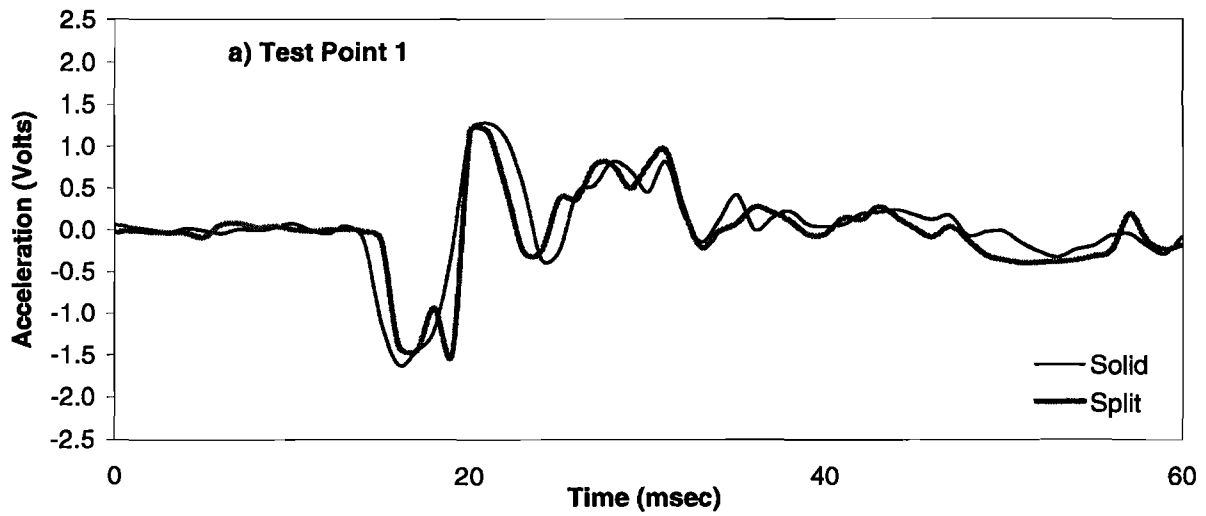


Figure 4.14 – Variations in Acceleration of the Plates on Three Test Points Measured on the Rutted Slab

Chapter 5

Closure

Summary

Currently, all TxDOT FWDs operate with a solid load plate. Several experimental and analytical studies have shown that such a configuration may result in a non-uniform load distribution under a rutted or weak flexible pavement. The FWD vendor currently offers a split plate design that may improve the load distribution on rutted or weak pavements. A non-uniform load distribution may significantly affect the central deflection measured on a weaker pavement structure. Since more than 50% of Texas roadways are farm-to-market structures, this matter is of utmost importance.

The primary objective of this report is to provide information about the behavior of FWDs under solid and split plates. This was achieved by a thorough review of the literature, and a comprehensive small-scale and full-scale field tests. The results are reported herein.

Conclusions

The behaviors of solid and split plates were thoroughly evaluated in this study. It seems that the falling weight deflectometers equipped with split plates impart more uniform load to the pavement. The split plate in general improved the performance of the FWD. However, the deflections measured with the two plates are different. As such, should TxDOT decide to utilize split load plates, a means of adjusting the deflections measured with the new configuration to those historically measured with the solid plate should be devised.

References

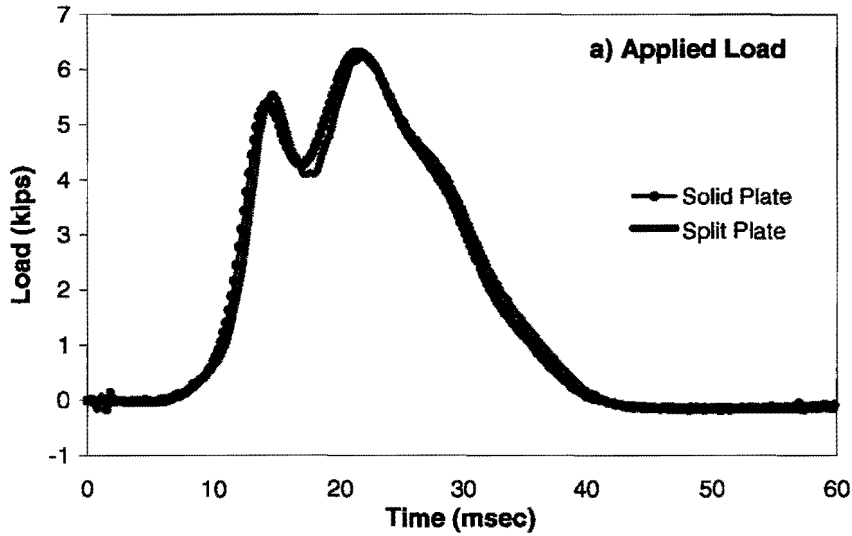
1. Boddapati, K.M., and Nazarian, S. (1994), "Effects of Pavement Falling Weight Deflectometer Interaction on Measured Pavement Response," *Nondestructive Testing of Pavements and Backcalculation of Moduli (Second Volume)*, ASTM STP 1198, American Society of Testing and Materials Philadelphia, pp. 326-340.
2. Rocha S., Tandon V. and Nazarian S. (2001), "Reproducibility of Texas Department of Transportation Falling Weight Deflectometer Fleet," Research Report No. 1784-1, Texas Department of Transportation, Austin, Texas.
3. Rocha S., Tandon V. and Nazarian S. (2002), "Evaluate Reproducibility of TxDOT FWD fleet and Recommend Improvements to FWD Calibration Procedure," Research Report No. 1784-2, Texas Department of Transportation, Austin, Texas.
4. Tandon, V. (1990), "Development of an Absolute Calibration System for Nondestructive Testing Devices," Master of Science Thesis, Department of Civil Engineering, The University of Texas at El Paso.
5. Tandon, V. and Nazarian, S. (2000), "Calibration Procedures for Seismic and Deflection-Based Devices," Report No. TX-00 2984-2F, Texas Department of Transportation, Texas.
6. Touma, B.E., Croveti, J.A., and Shahin, M.Y. (1991), "Effects of Various Load Distributions of Backcalculated Moduli Values in Flexible Pavements," TRR No. 1293, Transportation Research Board, National Research Council, Washington, D.C.

Appendix A

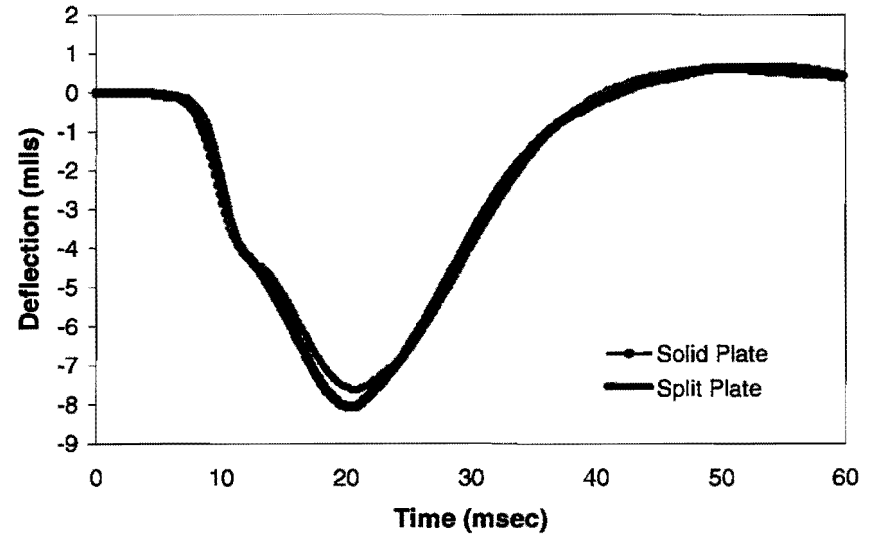
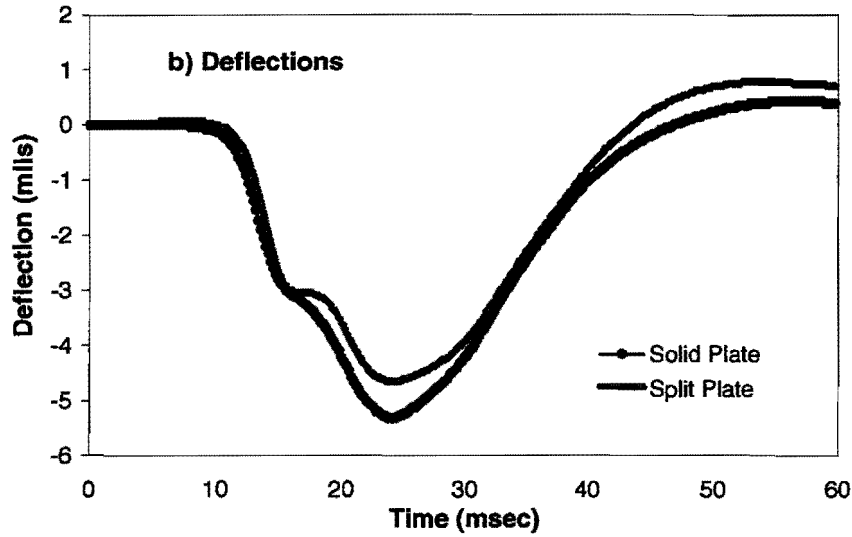
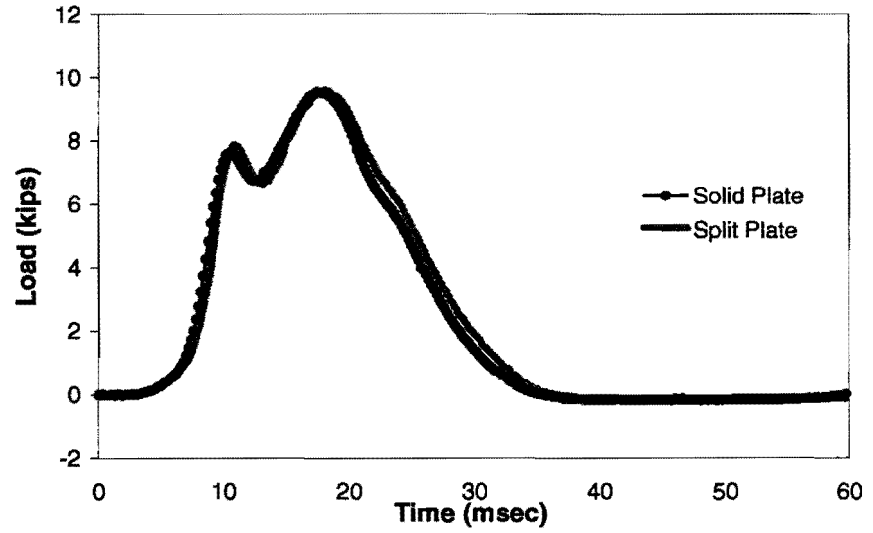
Complete Load and Deflection Data Solid and Split Plates on TTI Test Sites

Load and Deflection data from TTI Rigid Site

Drop 2 - Height 1

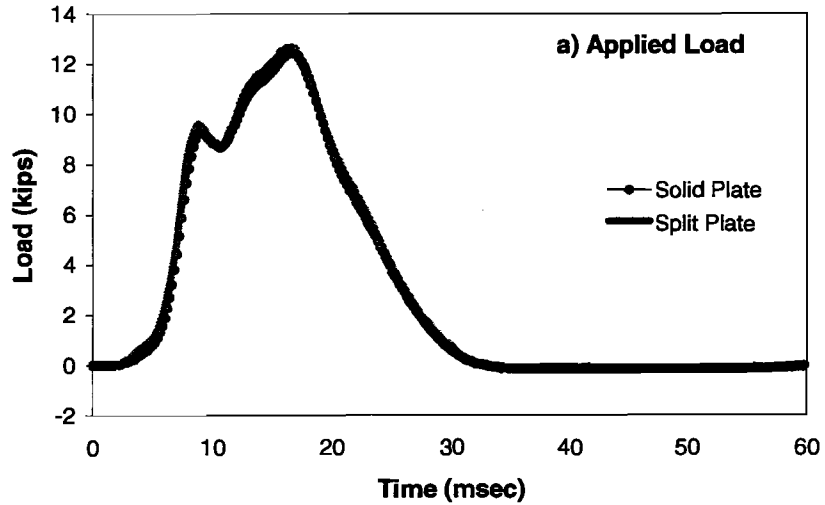


Drop 2 - Height 2

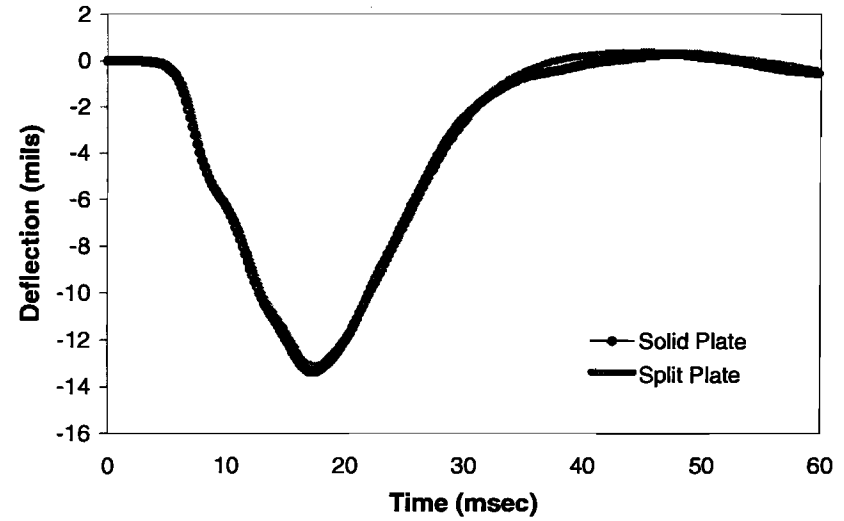
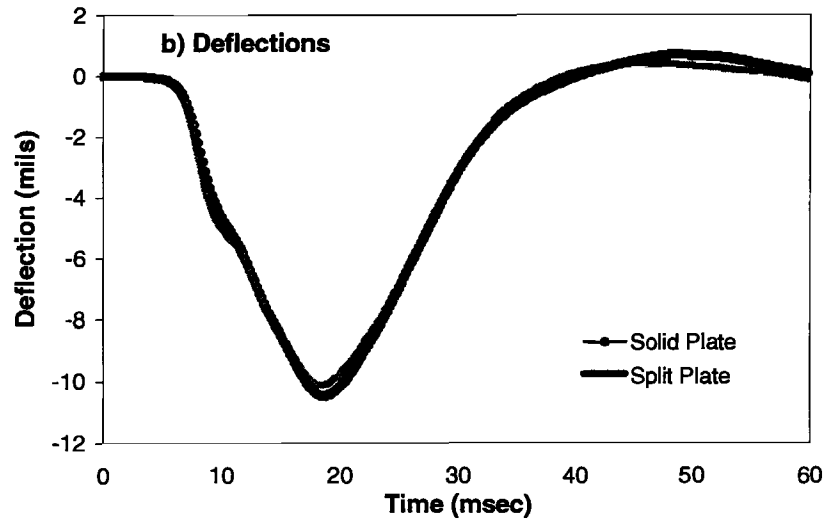
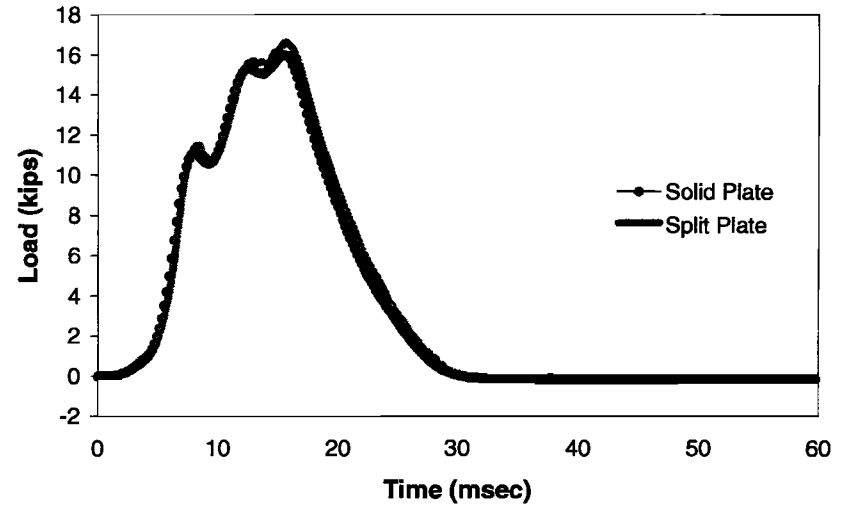


Load and Deflection data from TTI Rigid Site

Drop2 - Height 3



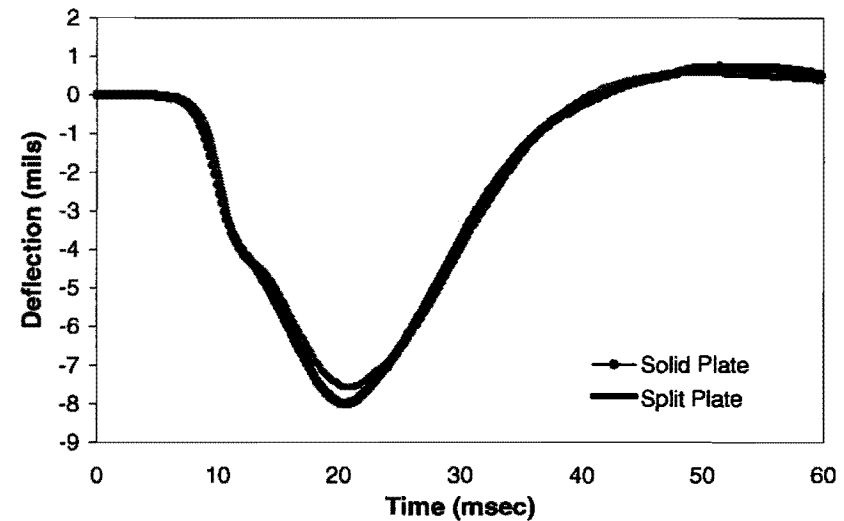
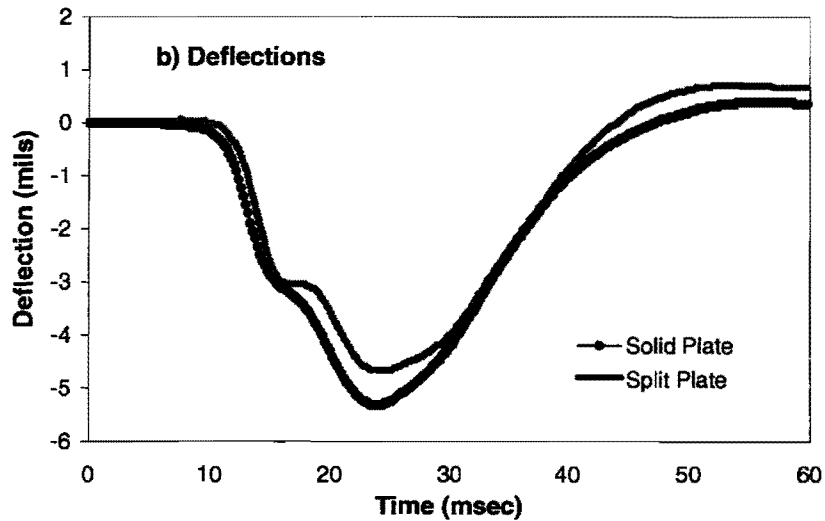
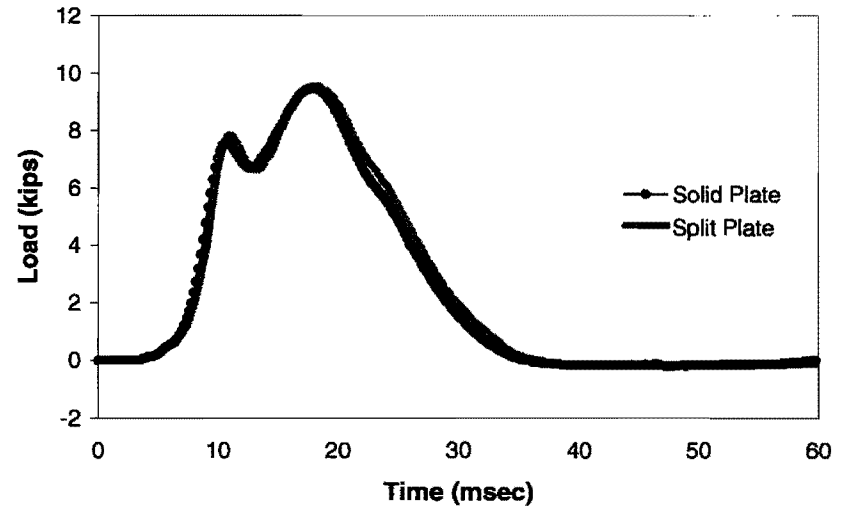
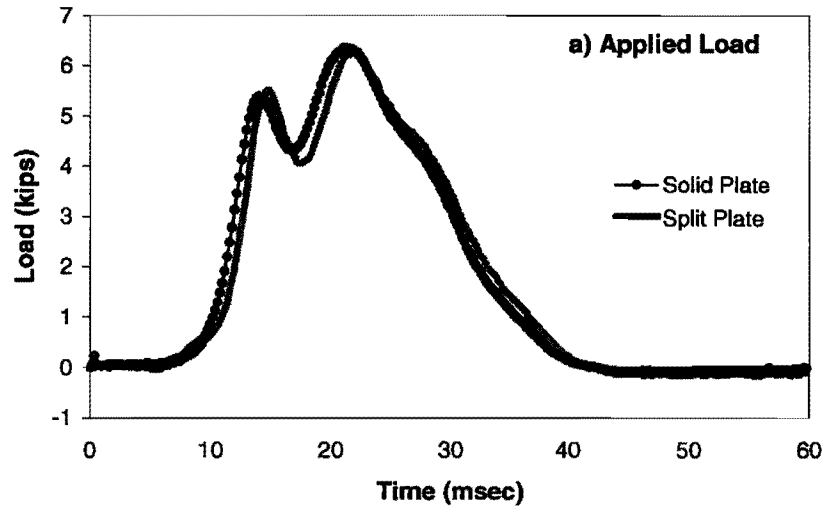
Drop2 - Height 4



Load and Deflection data from TTI Rigid Site

Drop4 - Height 1

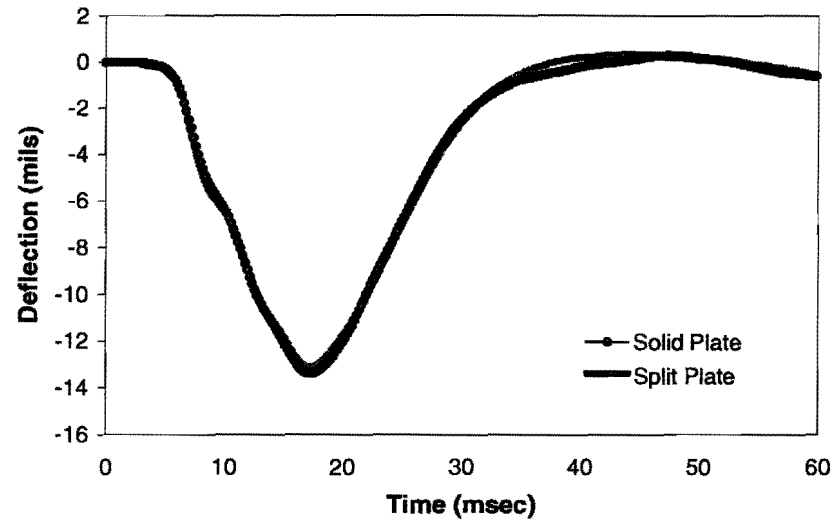
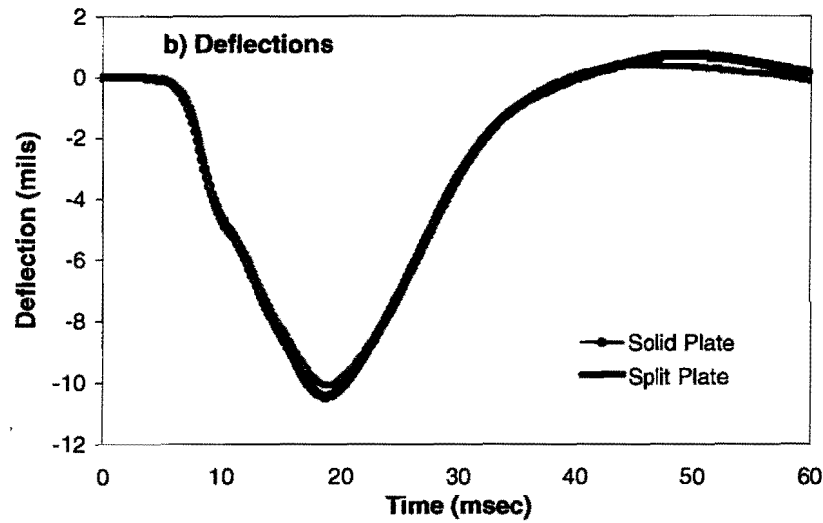
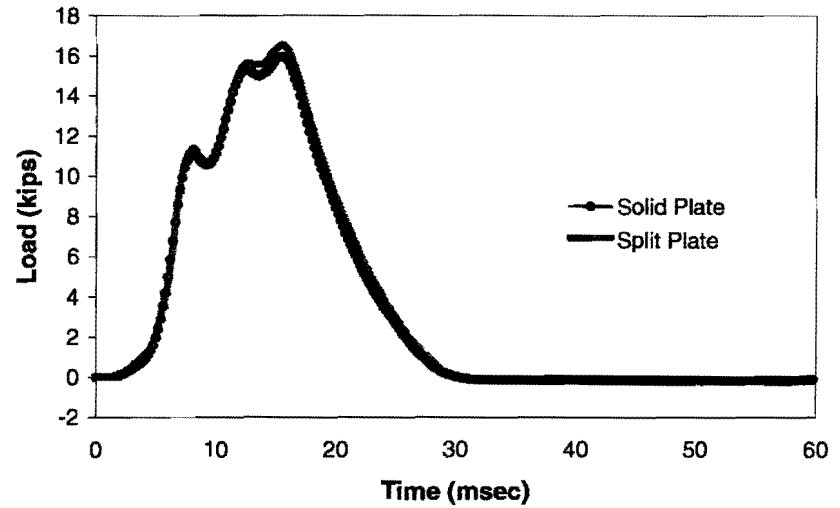
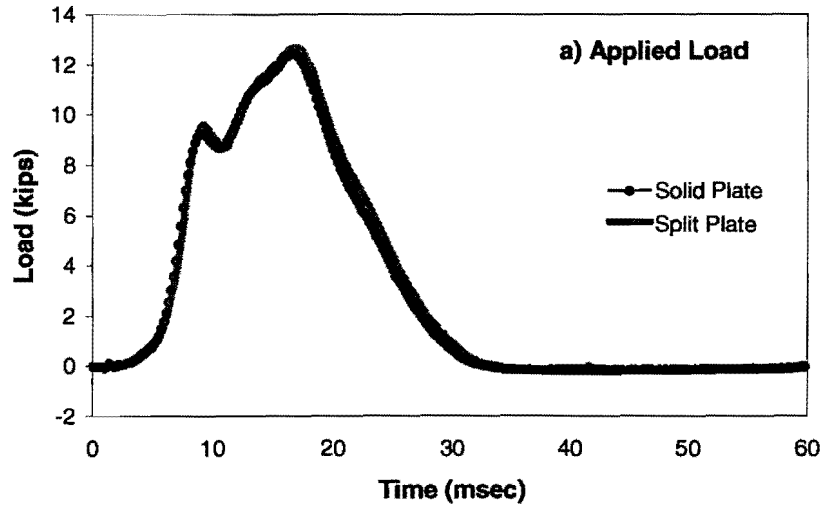
Drop4 - Height 2



Load and Deflection data from TTI Rigid Site

Drop 4 - Height 3

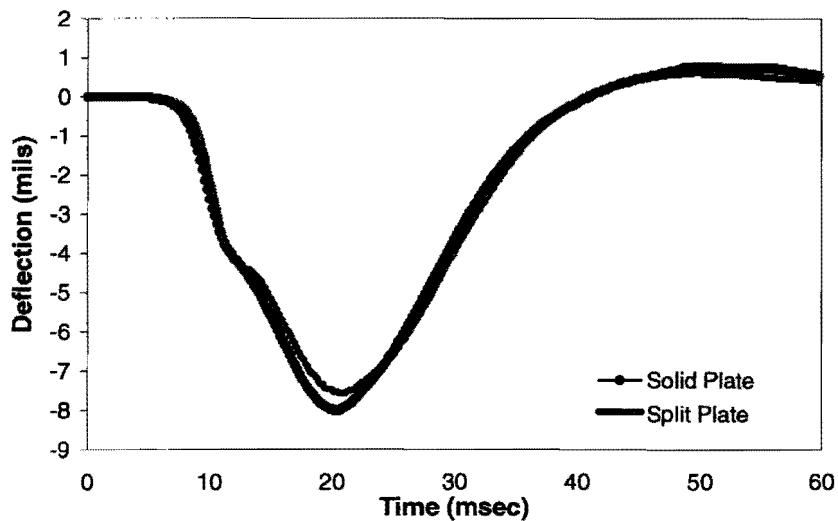
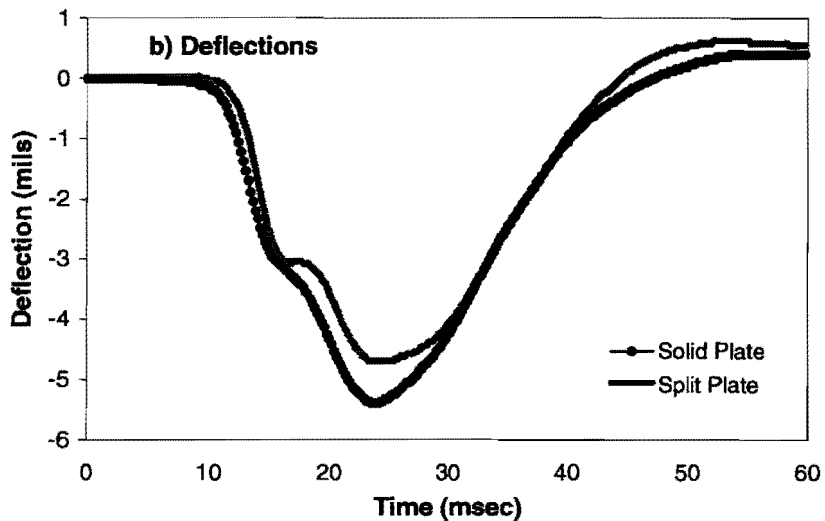
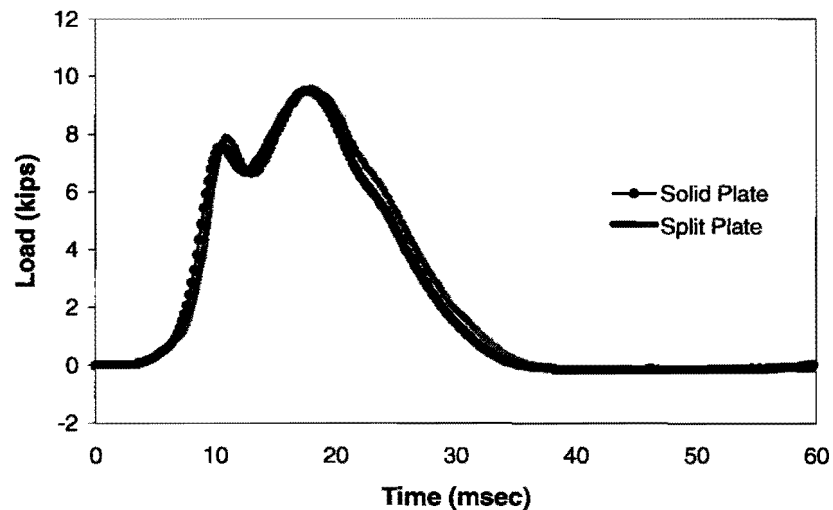
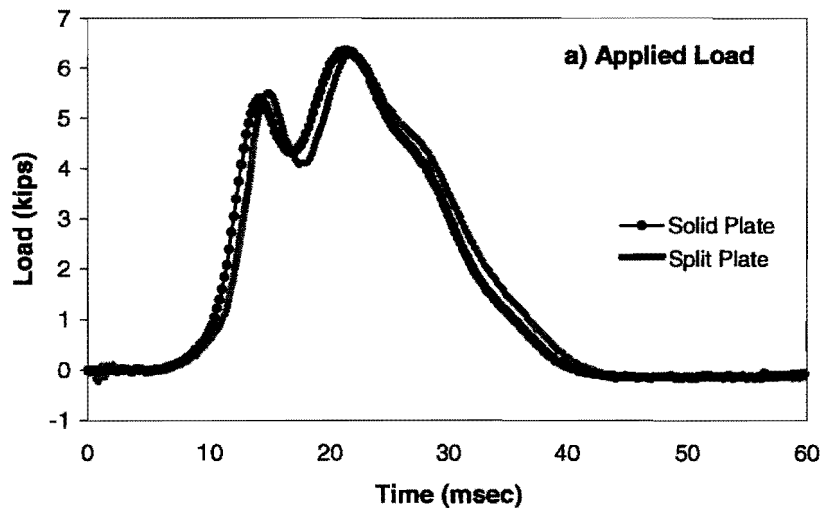
Drop 4 - Height 4



Load and Deflection data from TTI Rigid Site

Drop 6 - Height 1

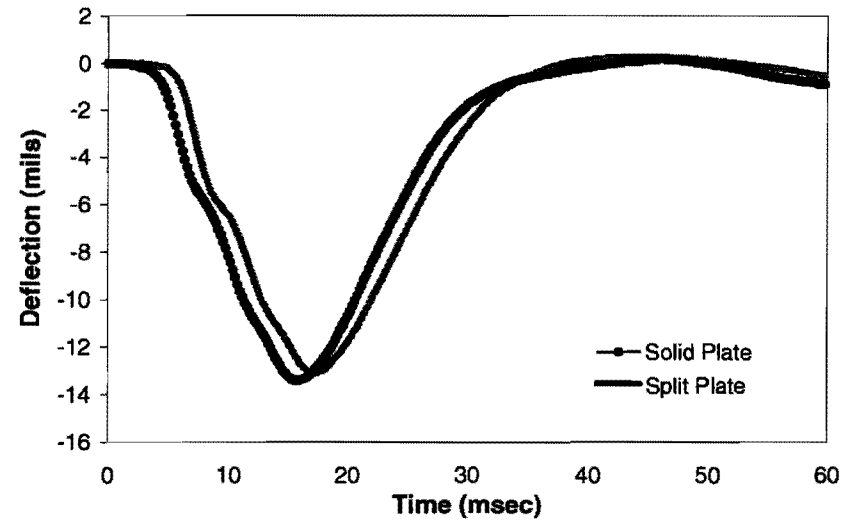
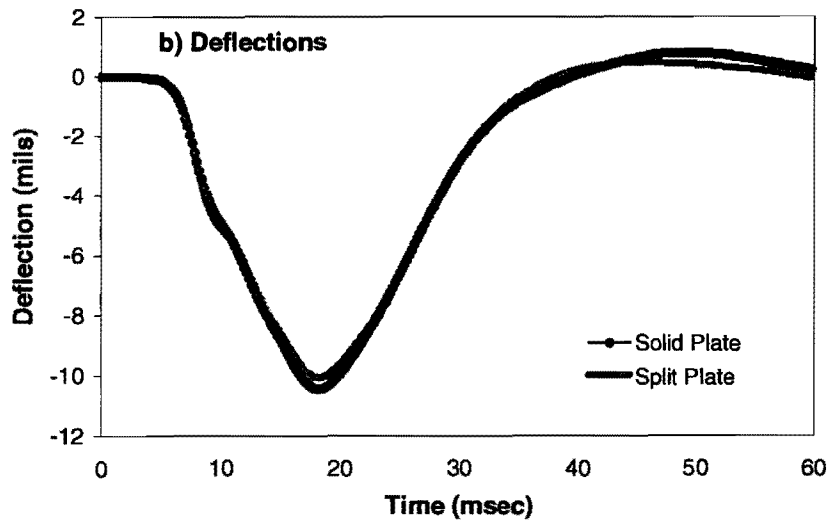
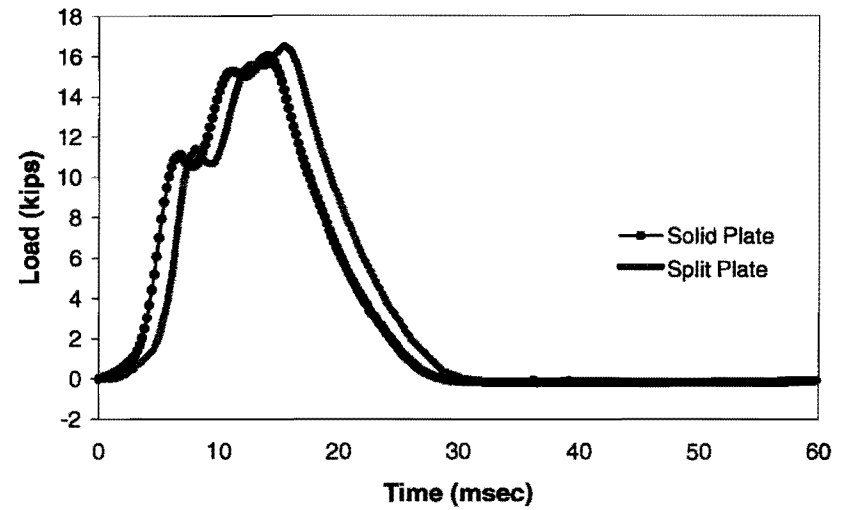
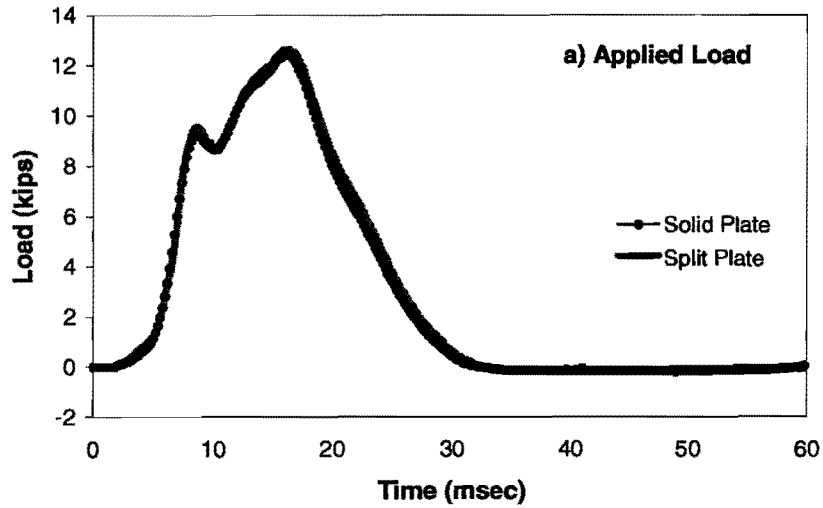
Drop 6 - Height 2



Load and Deflection data from TTI Rigid Site

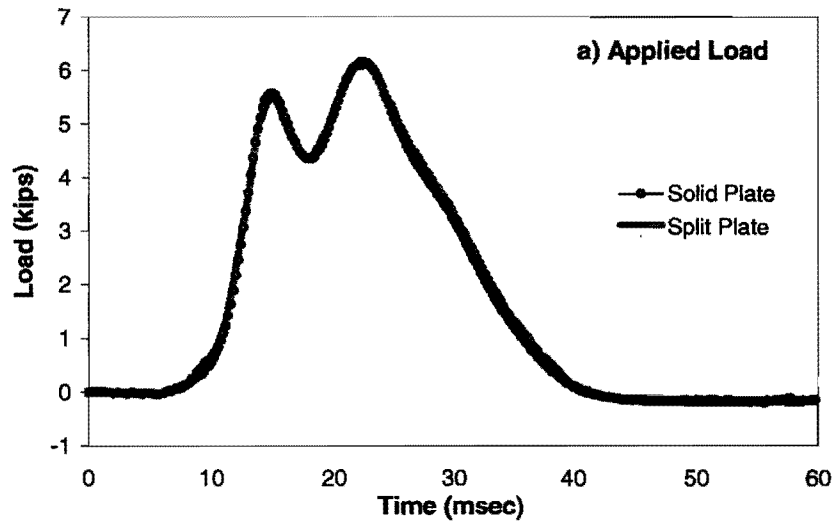
Drop 6 - Height 3

Drop 6 - Height 4

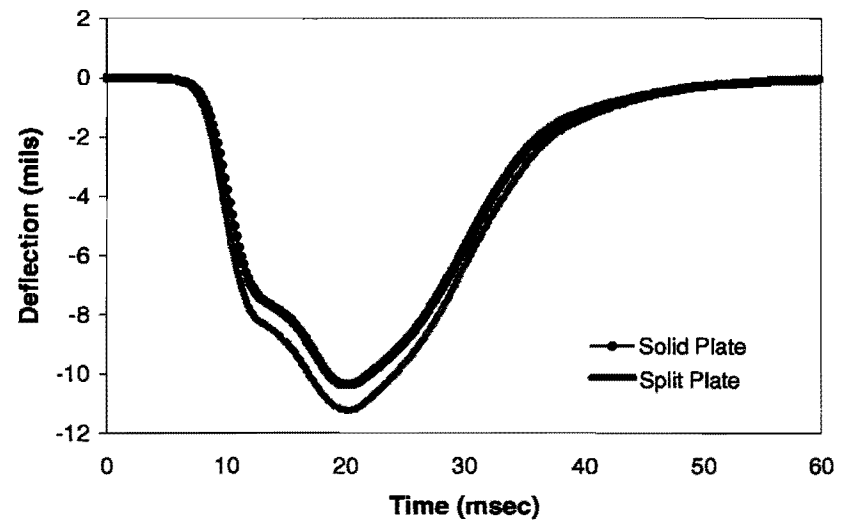
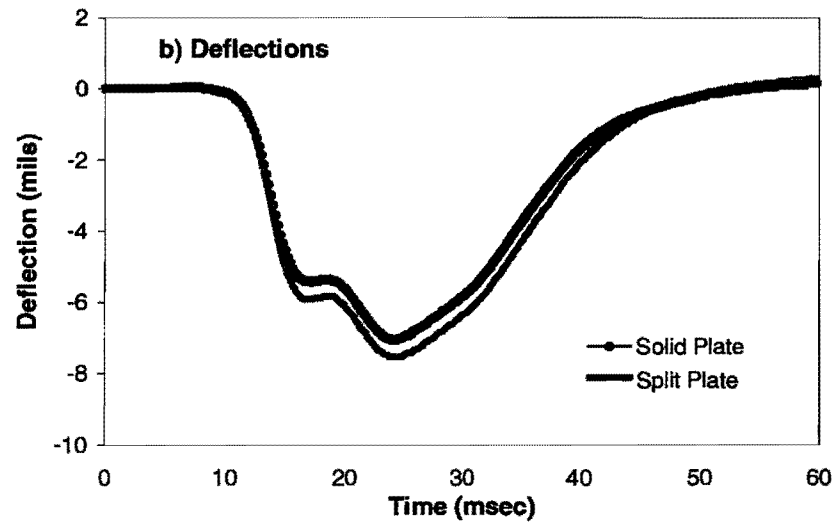
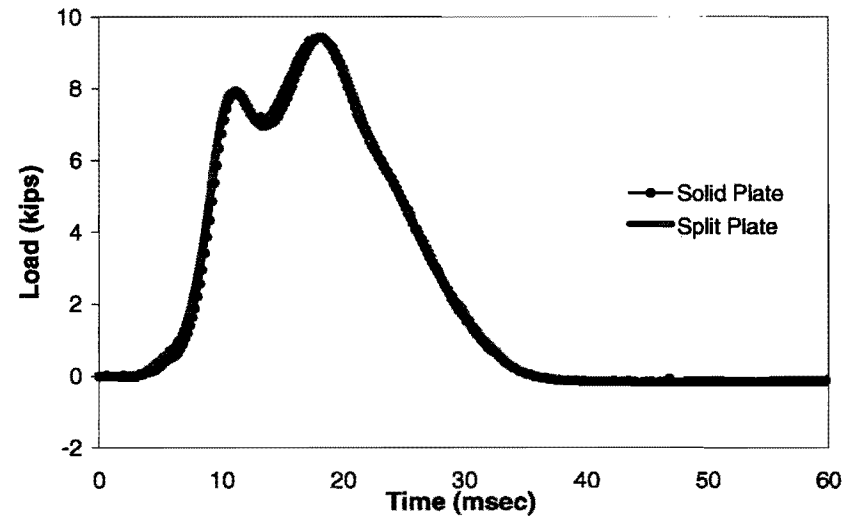


Load and Deflection data from TTI Strong Flexible Site

Drop 2 - Height 1

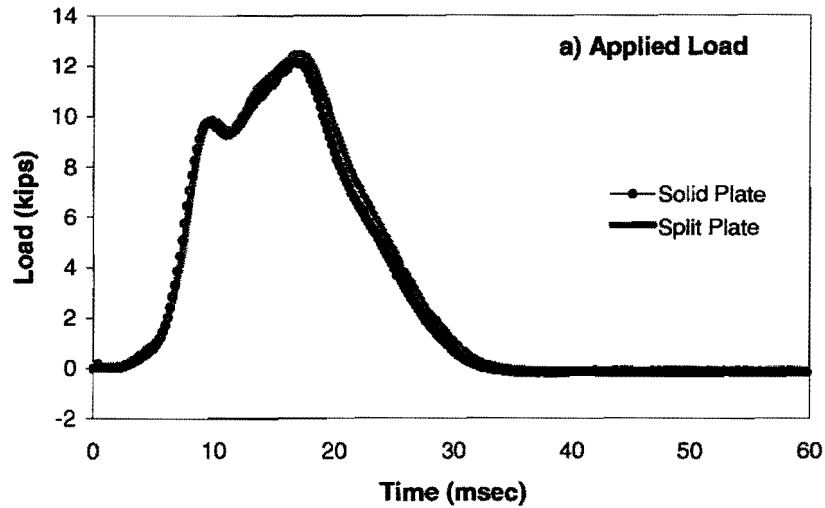


Drop 2 - Height 2

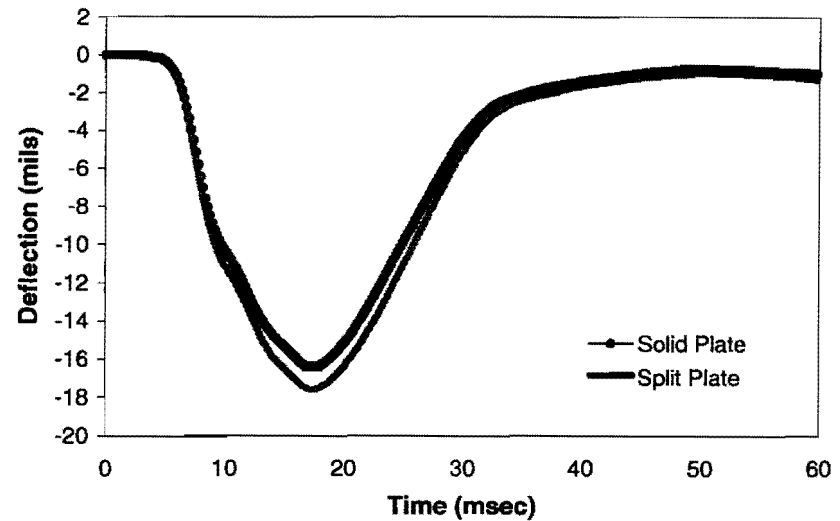
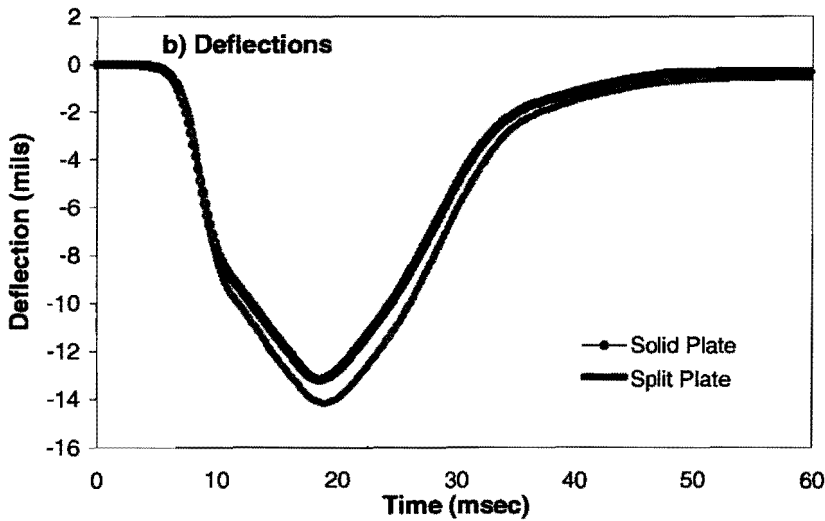
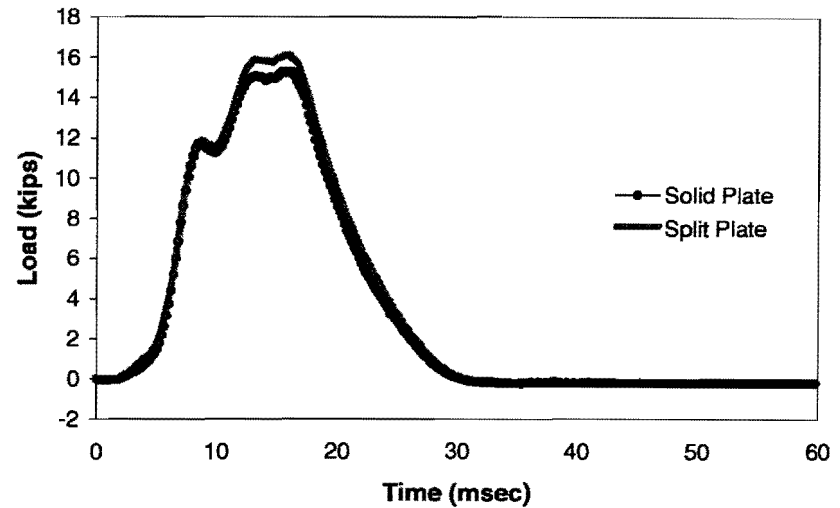


Load and Deflection data from TTI Strong Flexible Site

Drop2 - Height 3

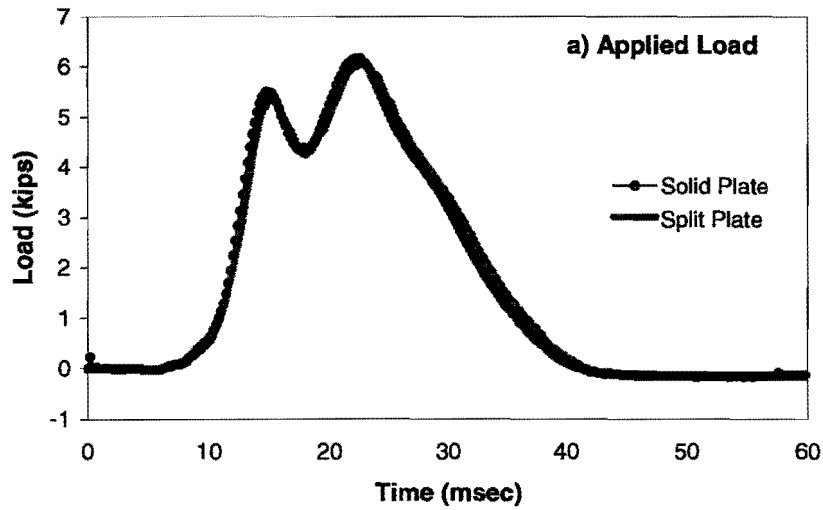


Drop2 - Height 4

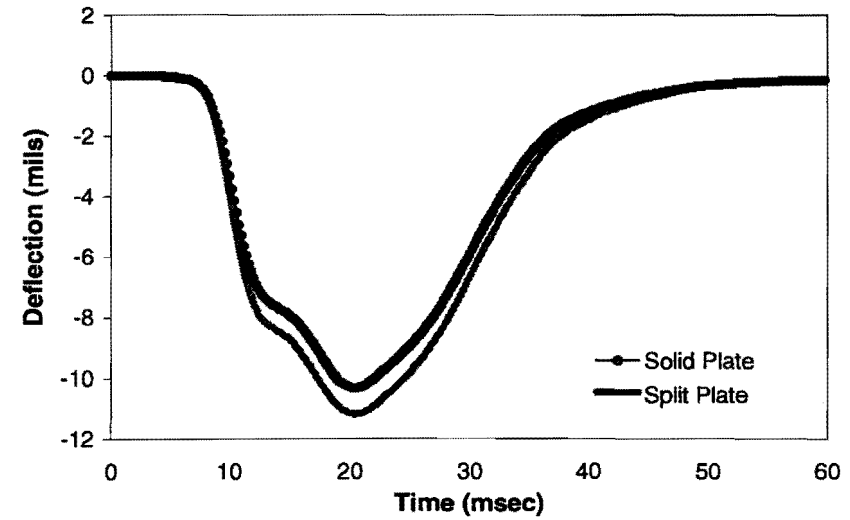
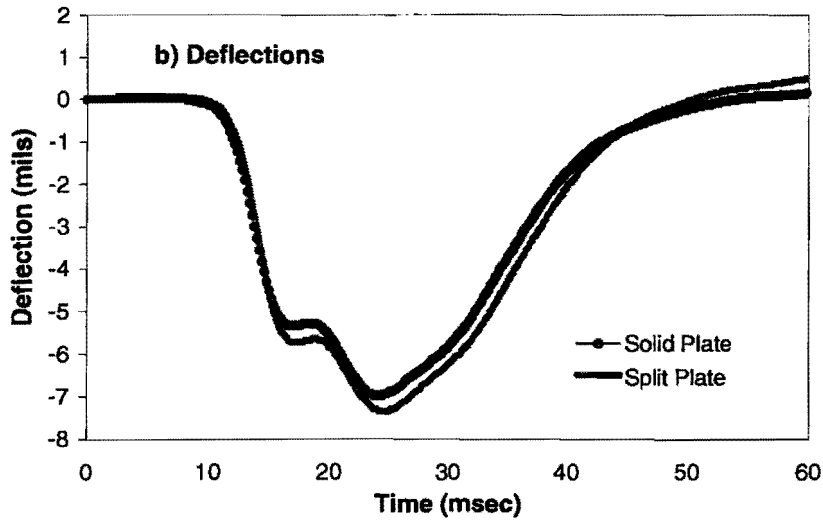
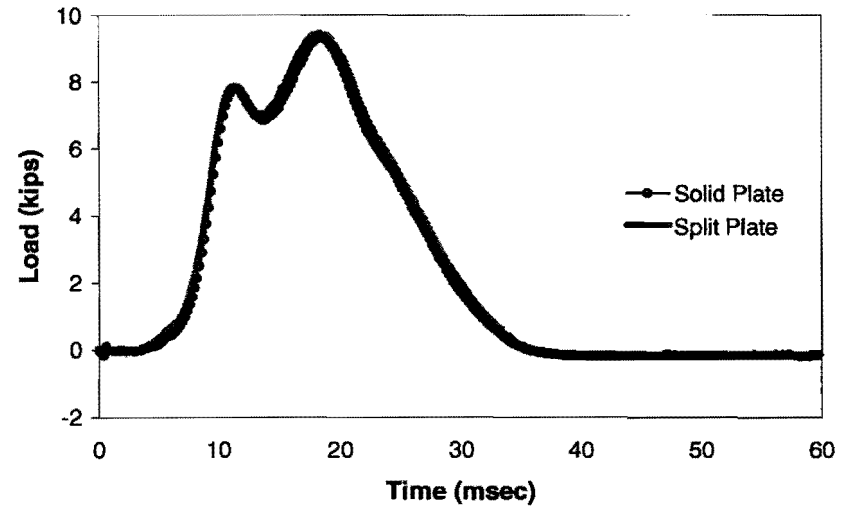


Load and Deflection data from TTI Strong Flexible Site

Drop4 - Height 1

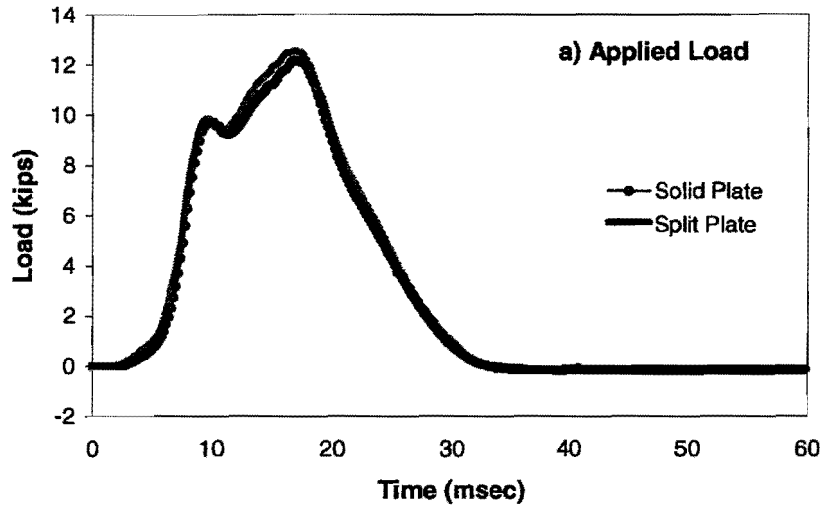


Drop4 - Height 2

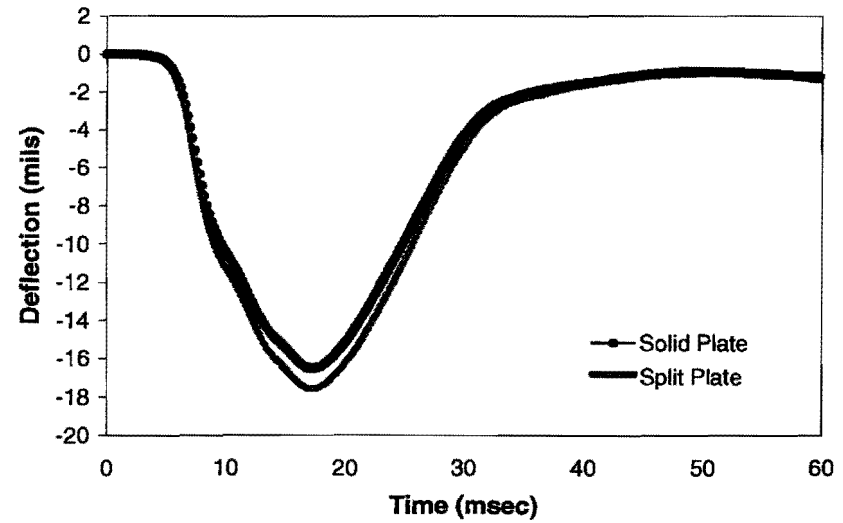
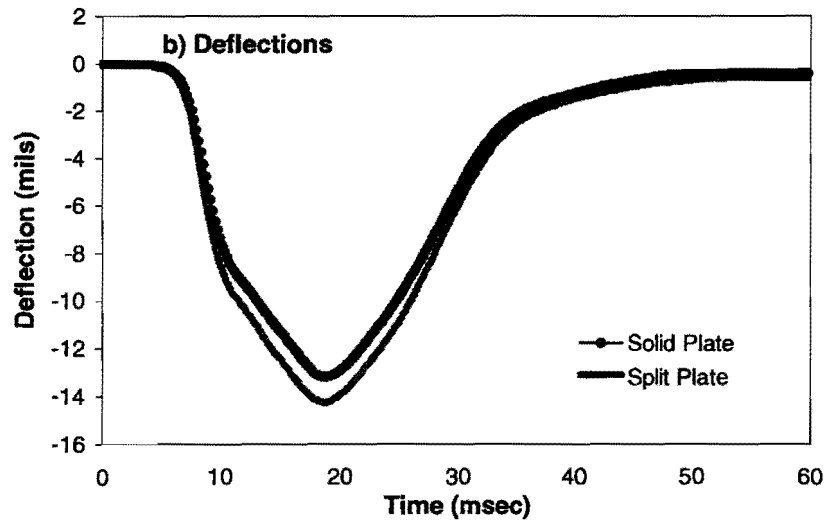
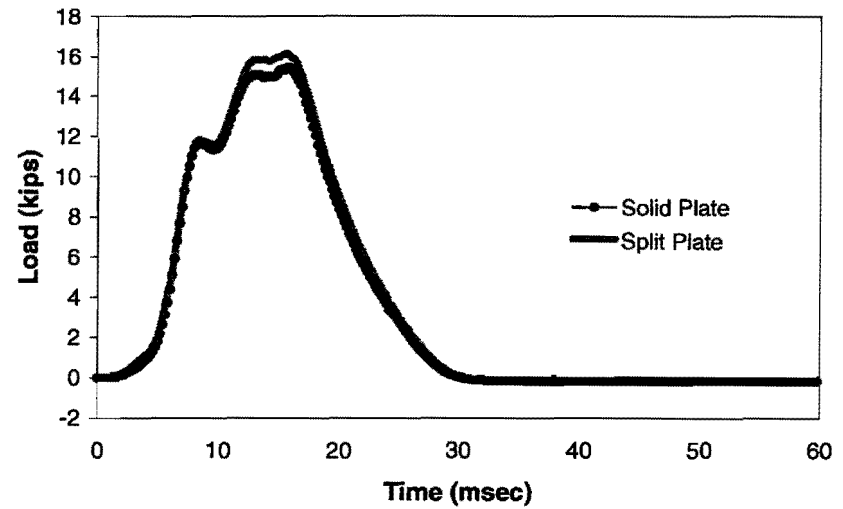


Load and Deflection data from TTI Strong Flexible Site

Drop 4 - Height 3

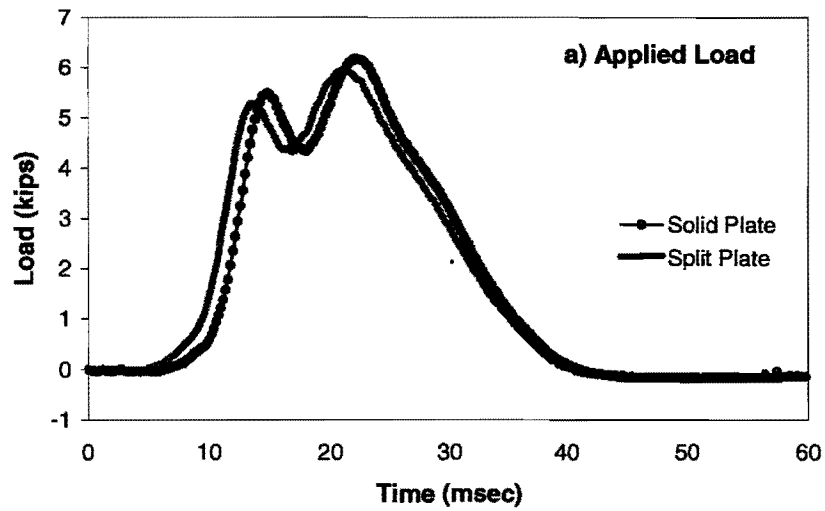


Drop 4 - Height 4

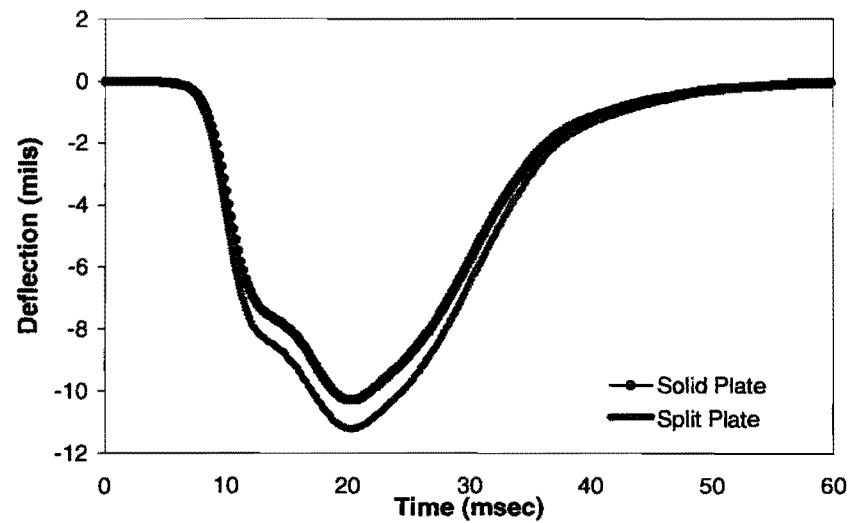
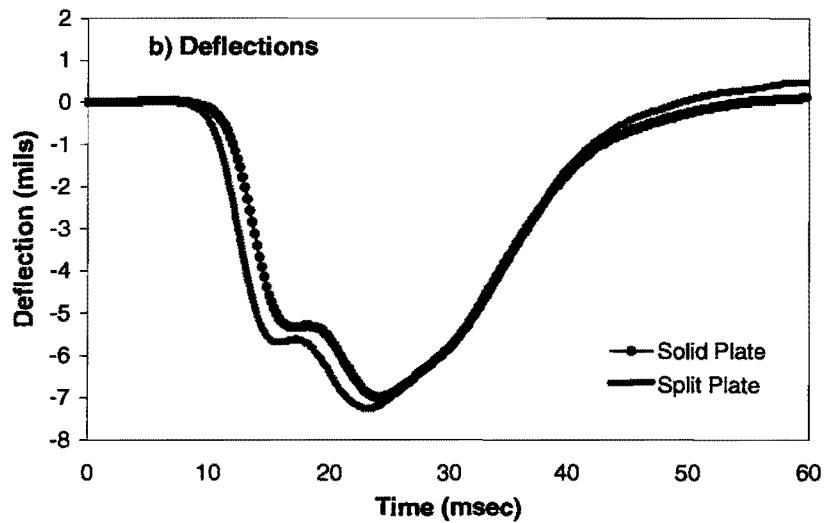
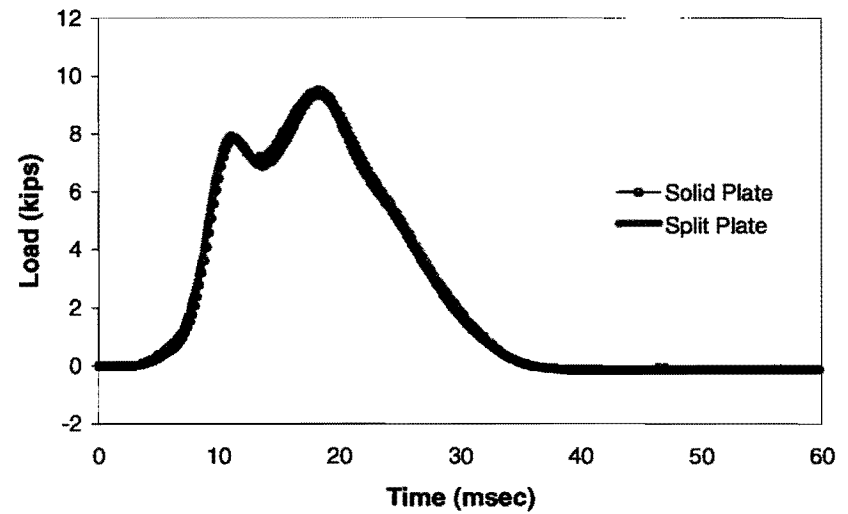


Load and Deflection data from TTI Strong Flexible Site

Drop 6 - Height 1

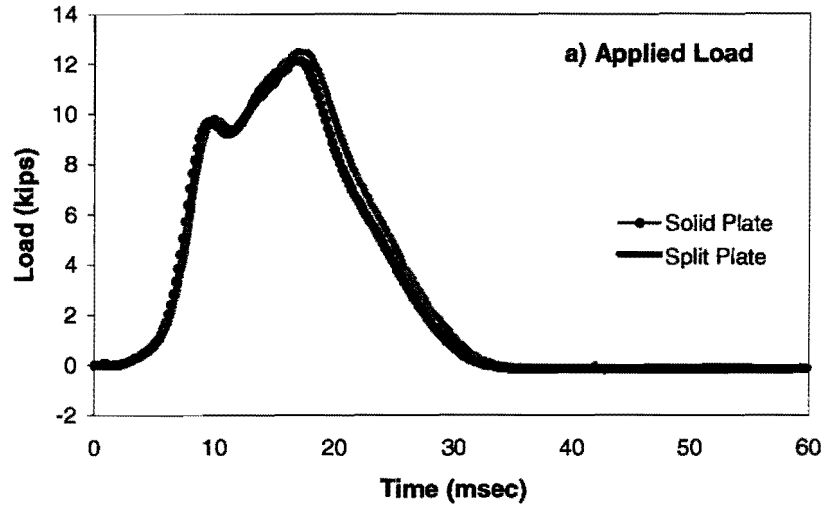


Drop 6 - Height 2

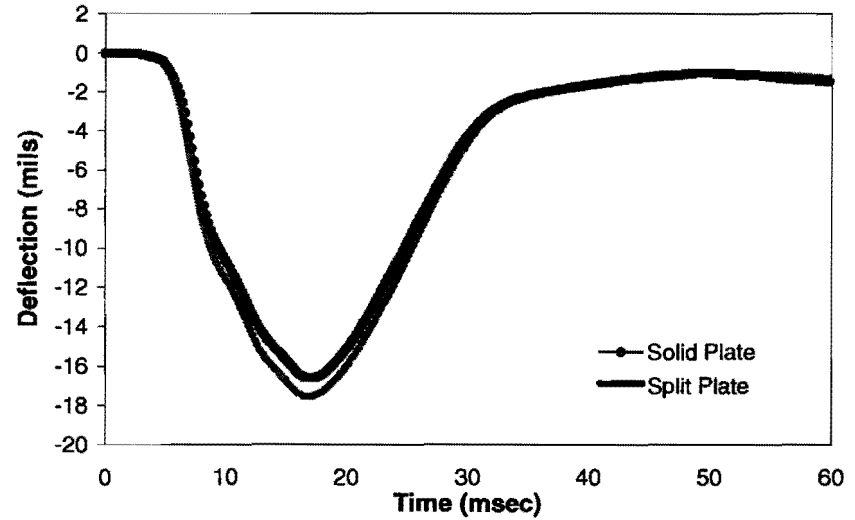
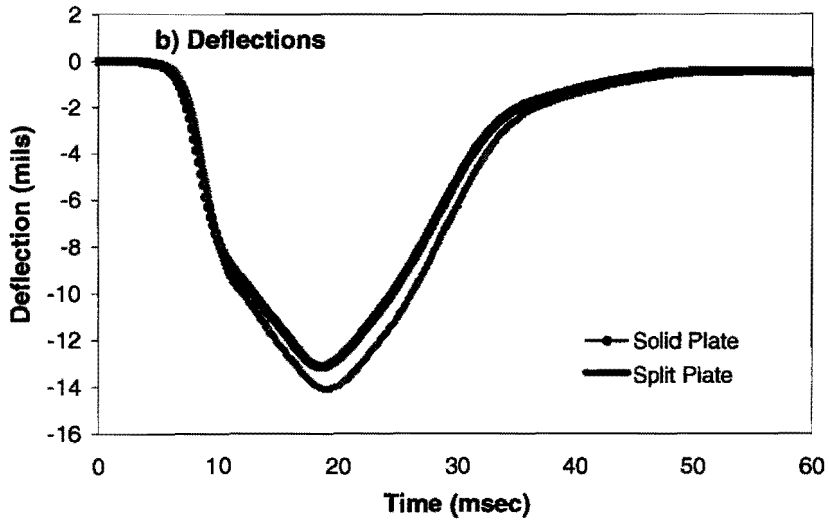
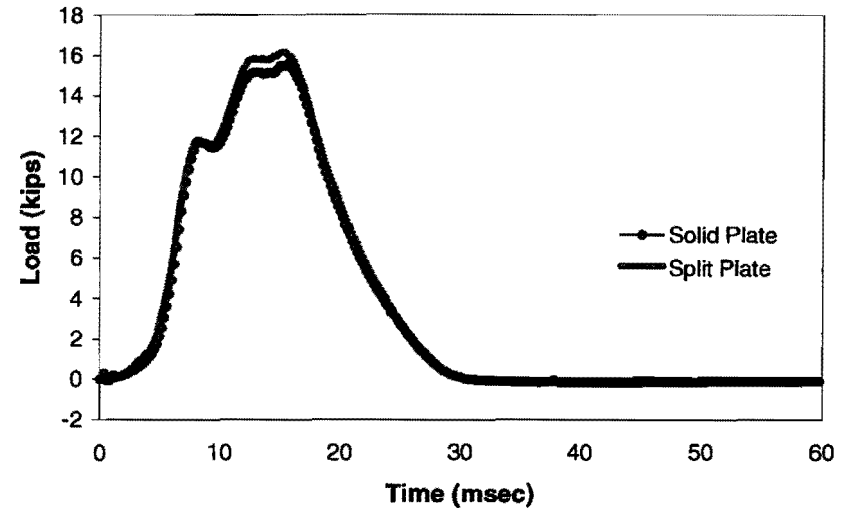


Load and Deflection data from TTI Strong Flexible Site

Drop 6 - Height 3

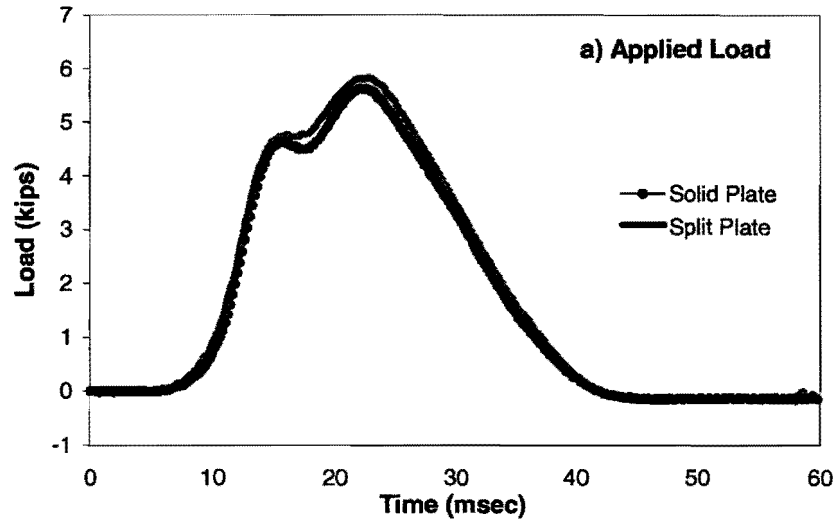


Drop 6 - Height 4

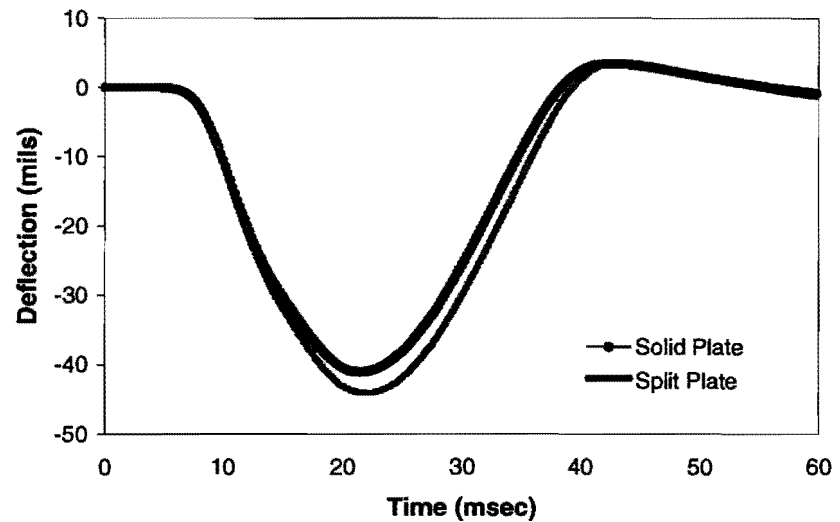
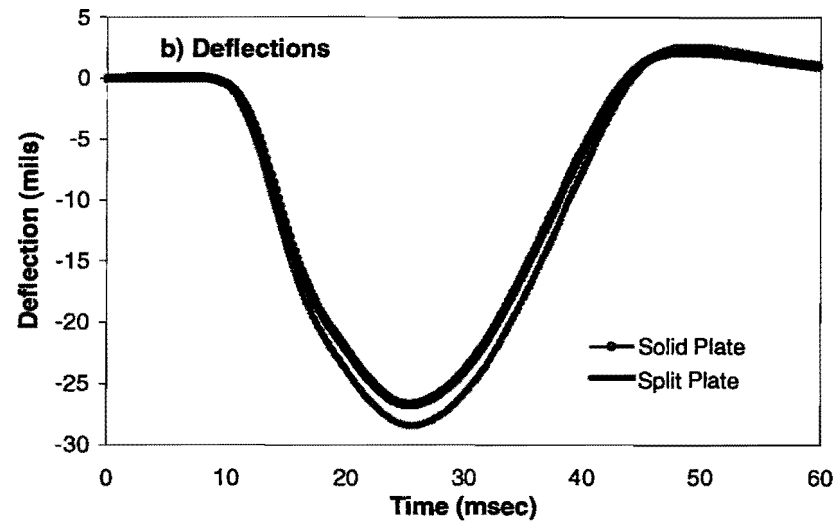
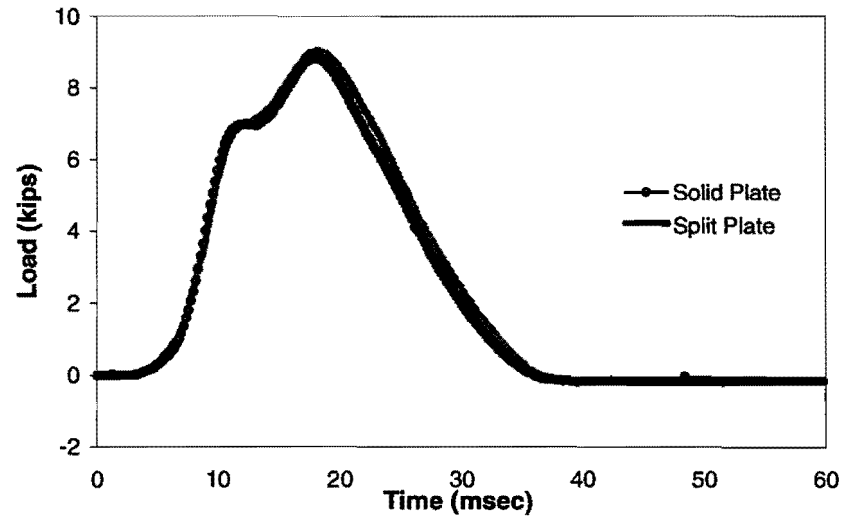


Load and Deflection data from TTI Weak Flexible Site

Drop 2 - Height 1

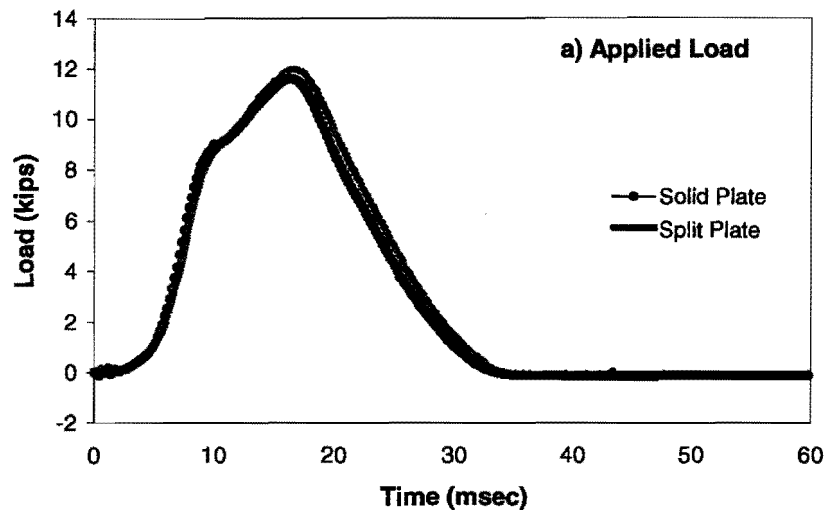


Drop 2 - Height 2

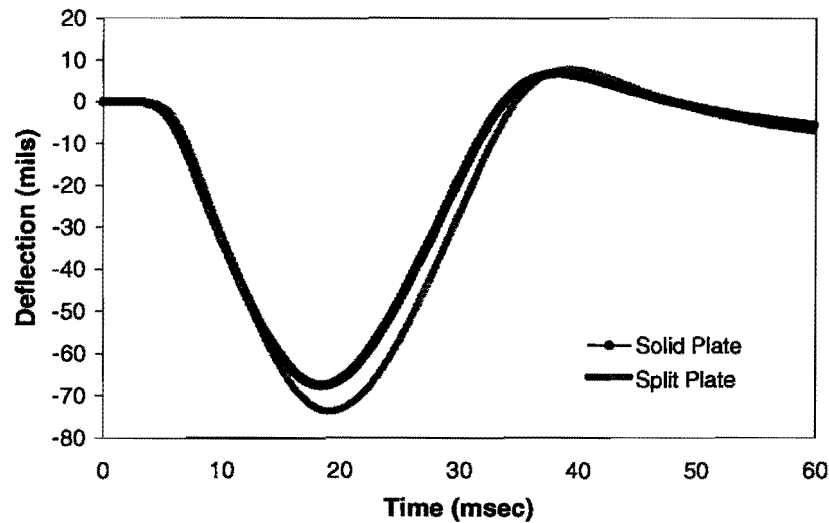
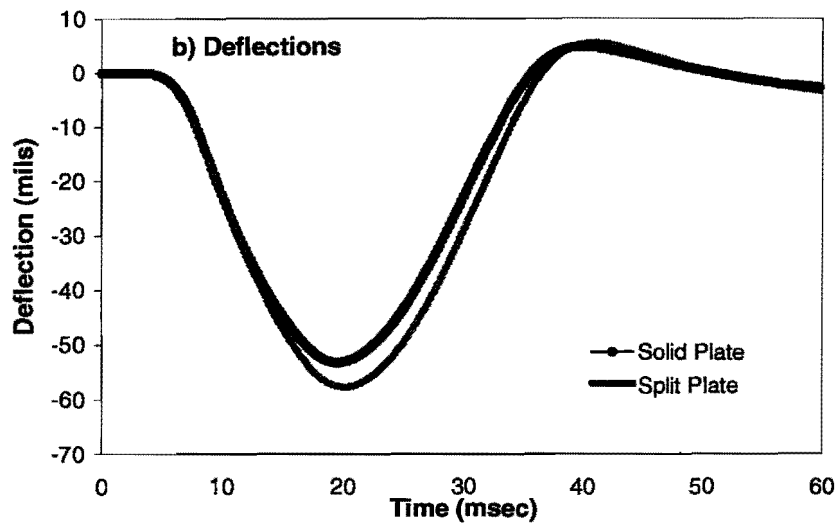
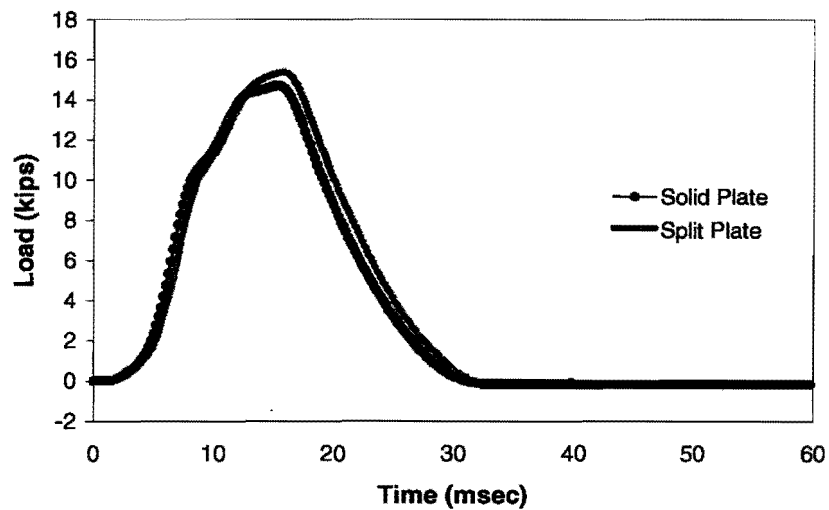


Load and Deflection data from TTI Weak Flexible Site

Drop2 - Height 3

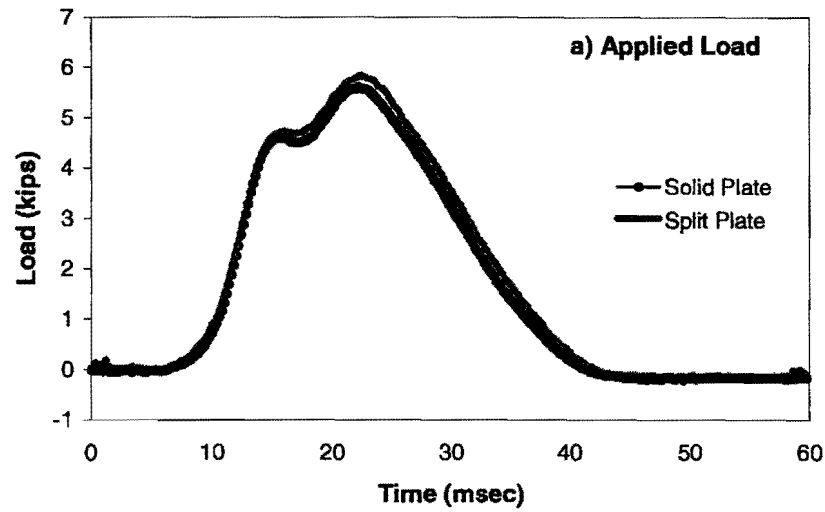


Drop2 - Height 4

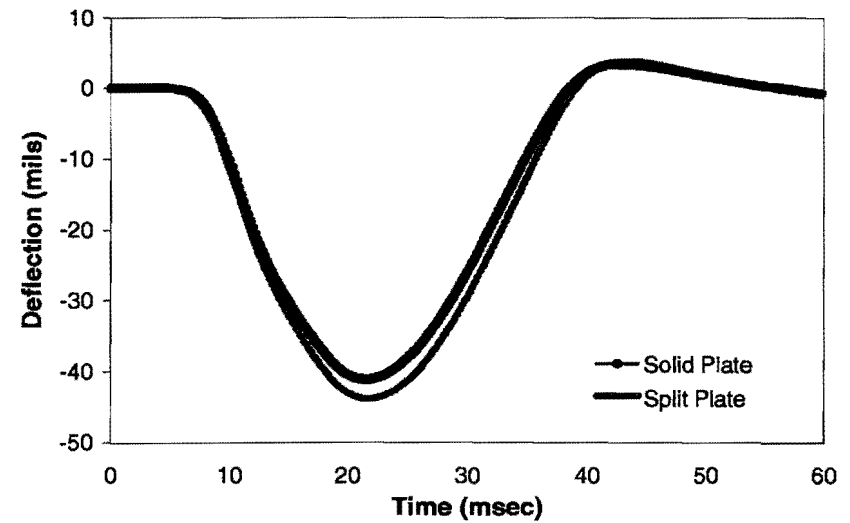
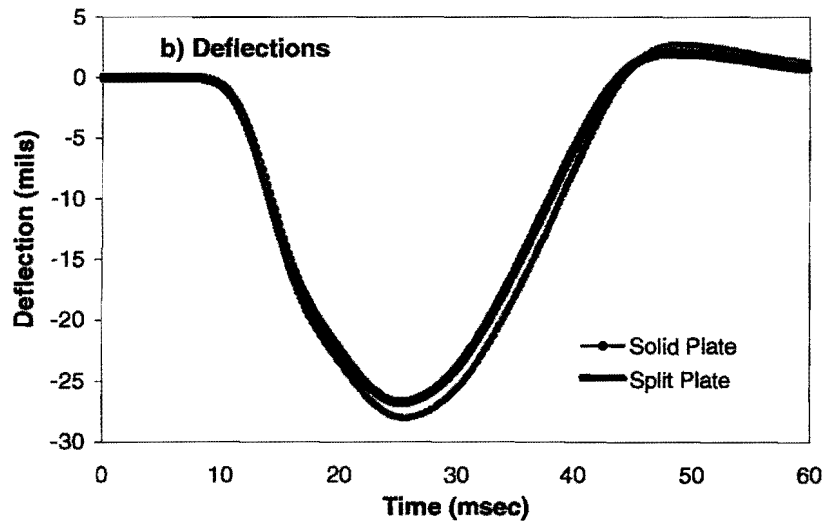
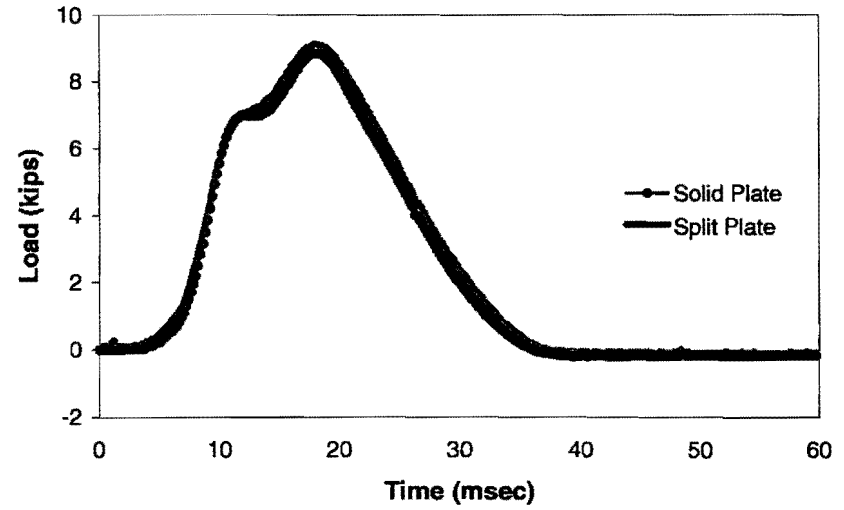


Load and Deflection data from TTI Weak Flexible Site

Drop4 - Height 1

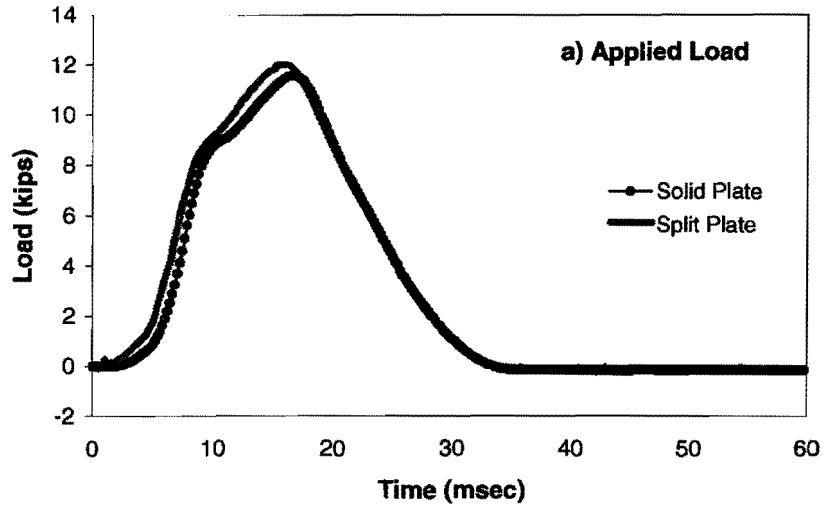


Drop4 - Height 2

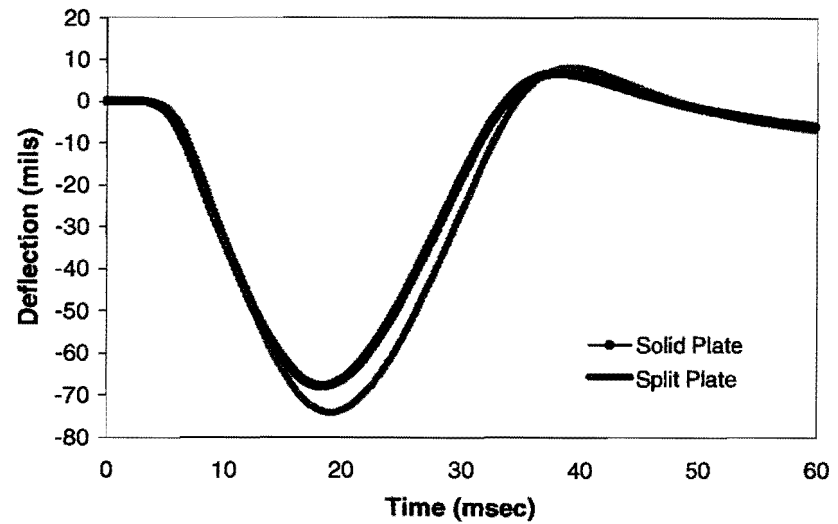
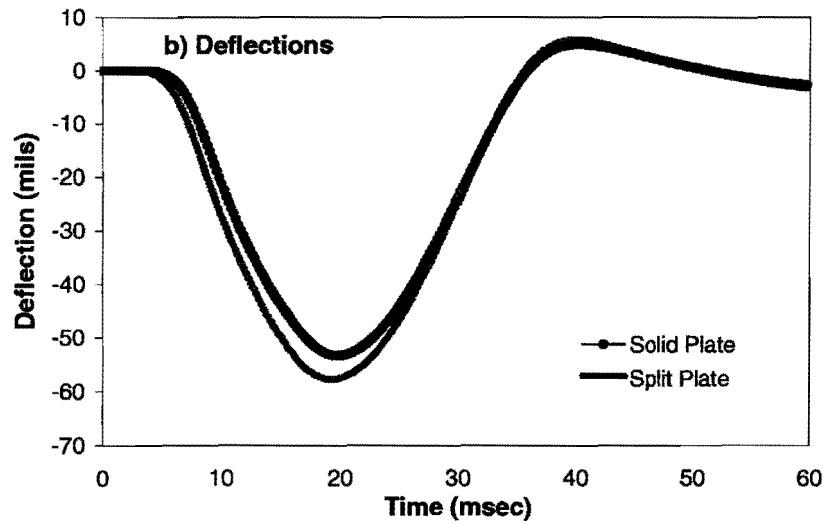
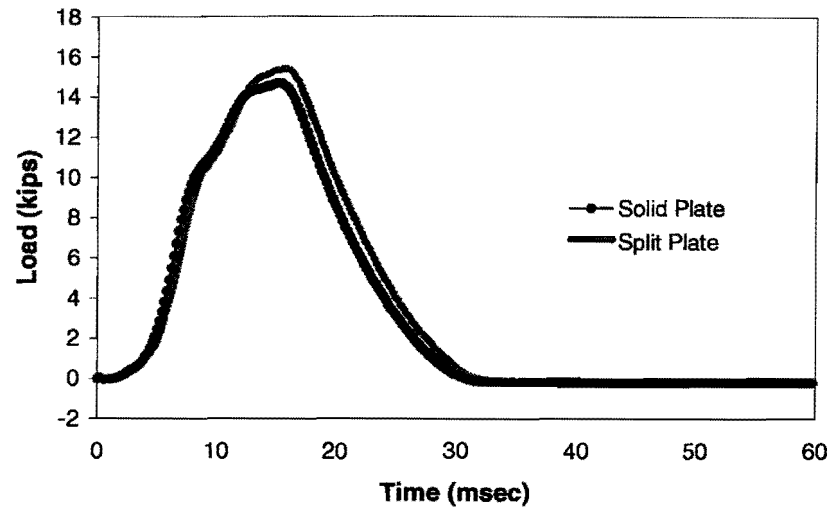


Load and Deflection data from TTI Weak Flexible Site

Drop 4 - Height 3

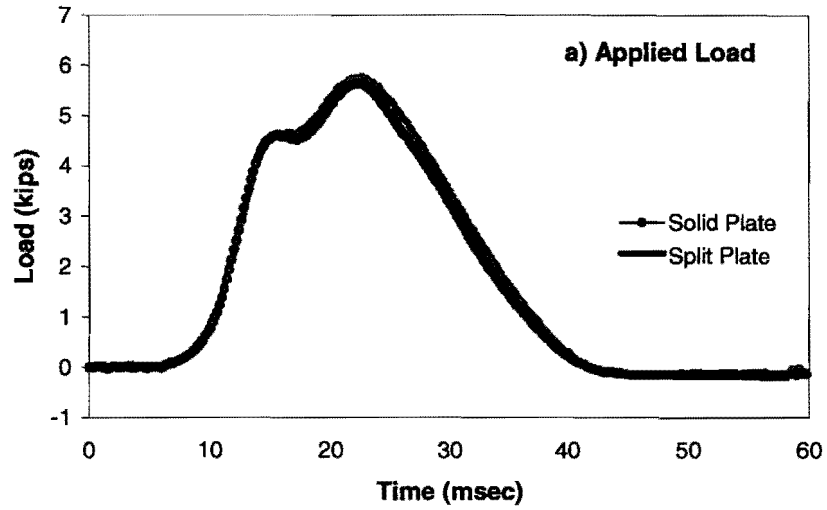


Drop 4 - Height 4

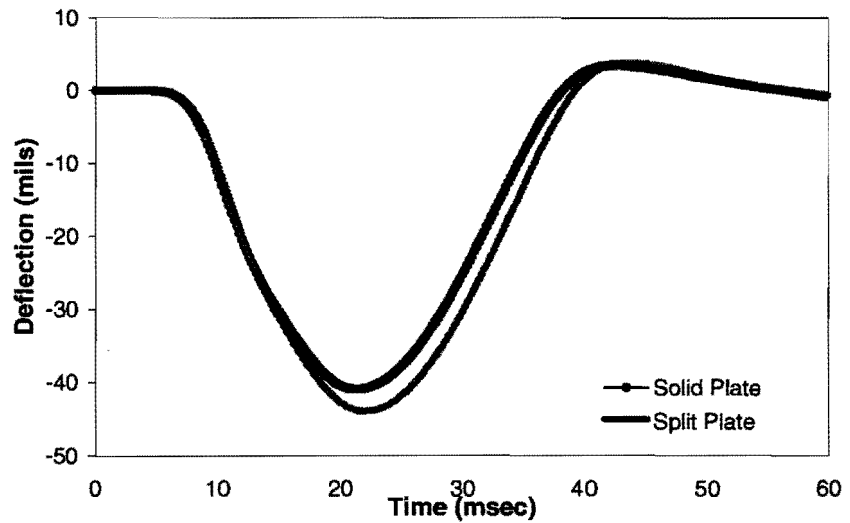
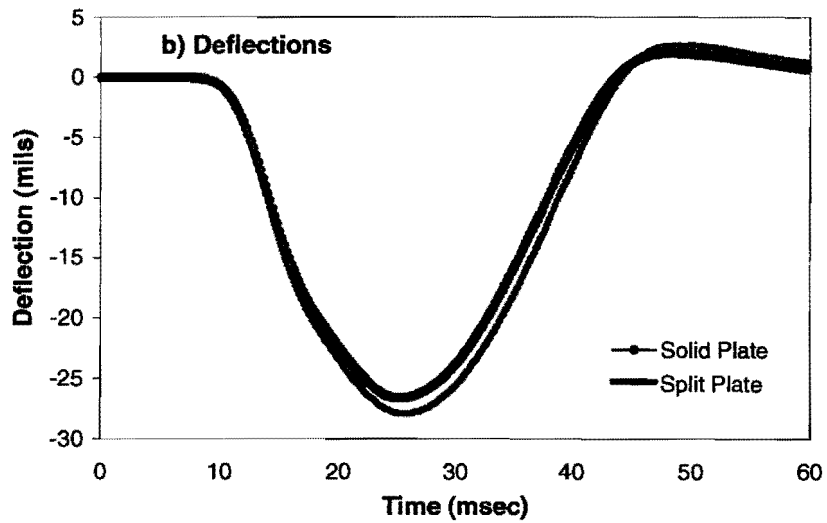
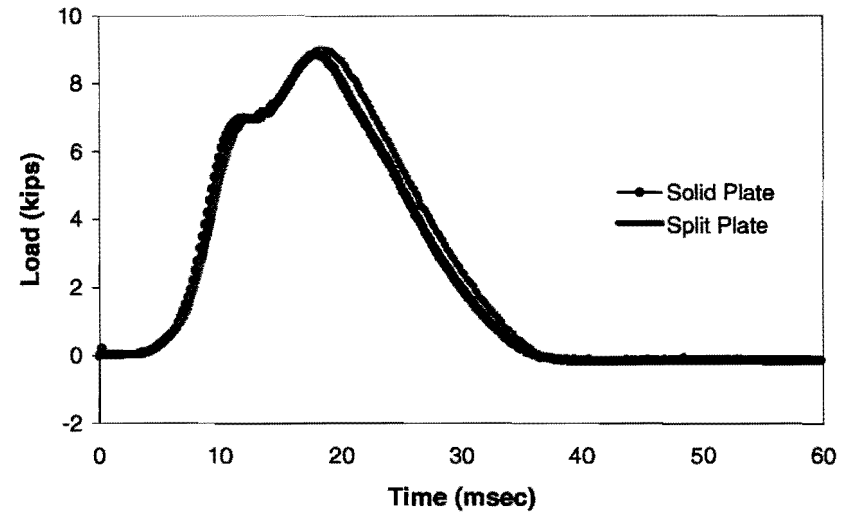


Load and Deflection data from TTI Weak Flexible Site

Drop 6 - Height 1



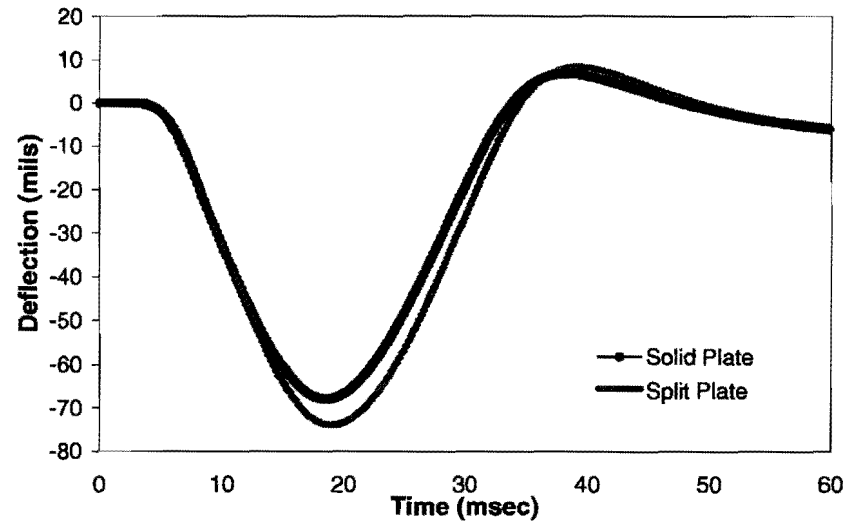
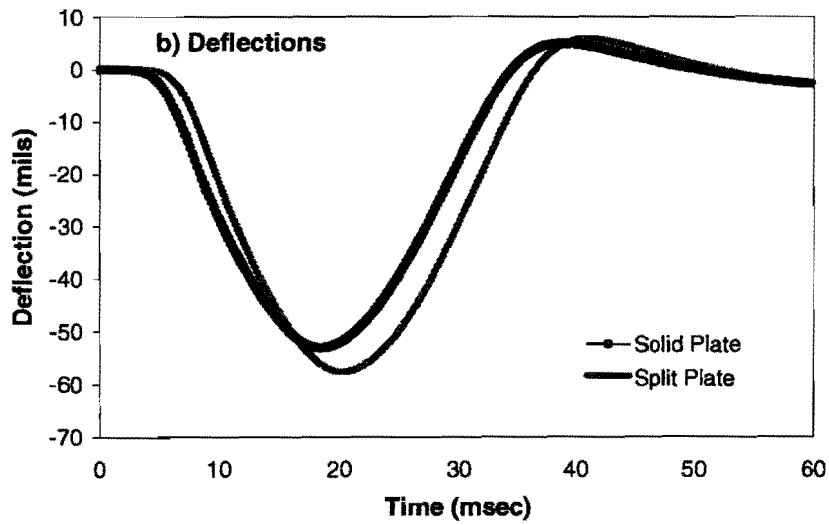
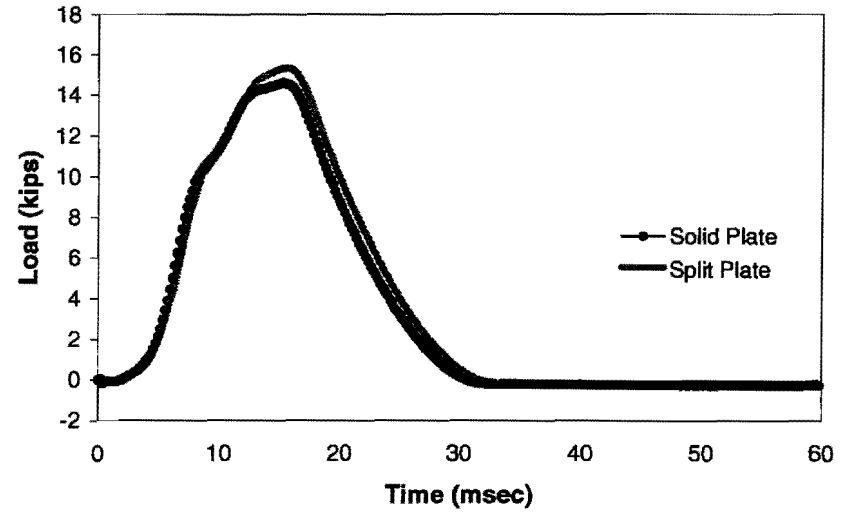
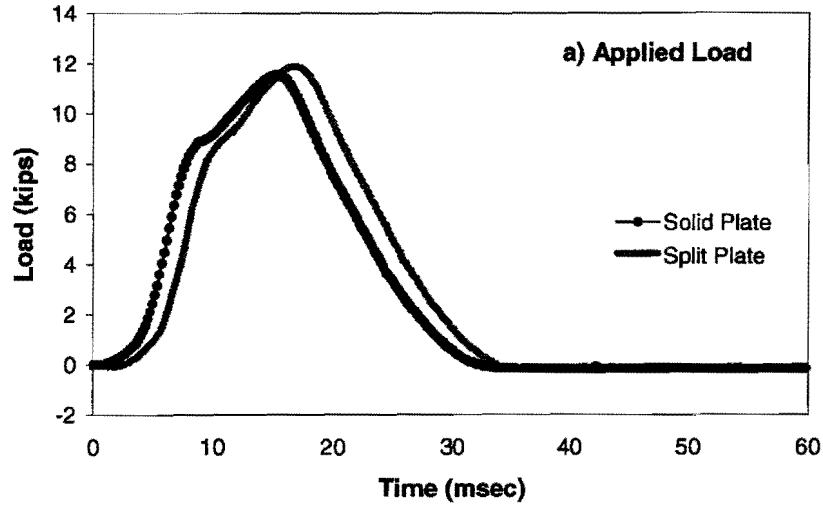
Drop 6 - Height 2



Load and Deflection data from TTI Weak Flexible Site

Drop 6 - Height 3

Drop 6 - Height 4

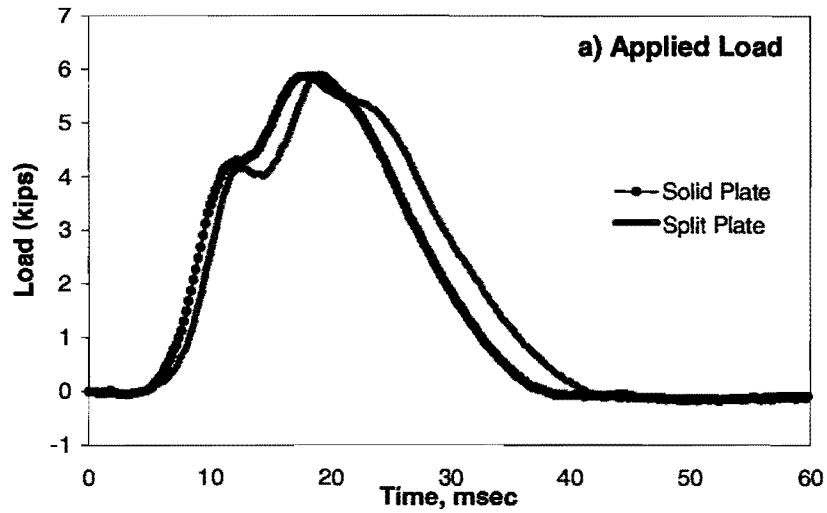


Appendix B

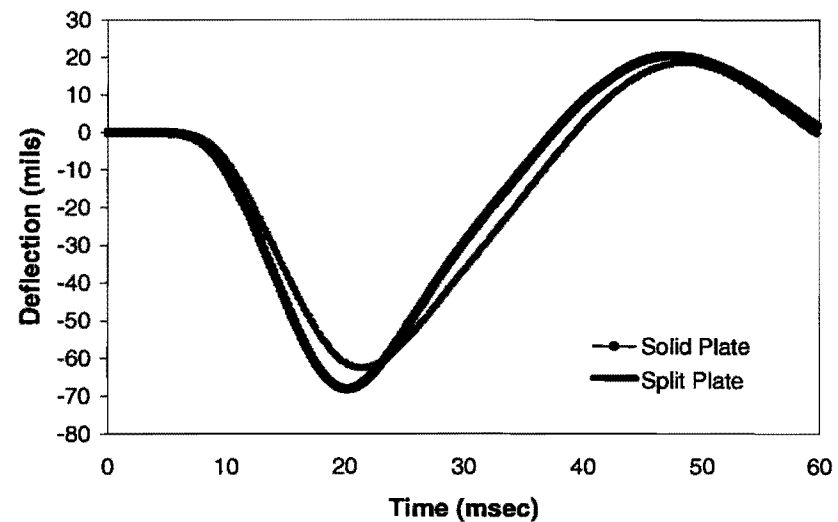
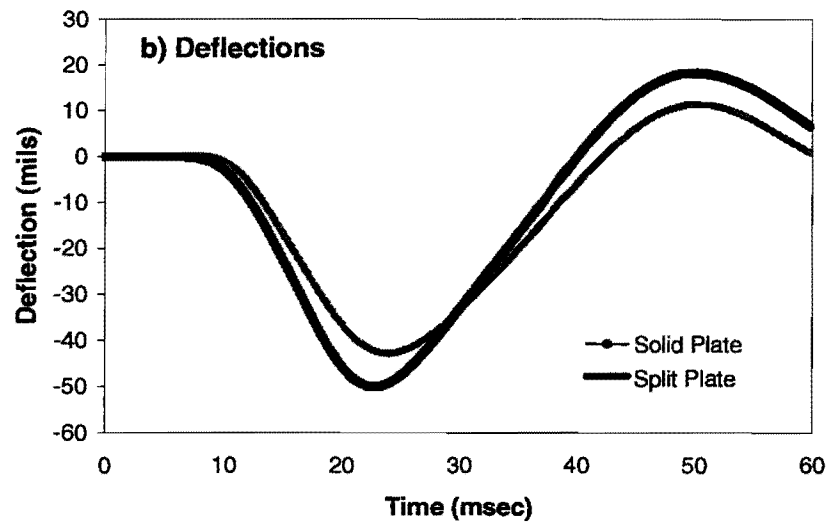
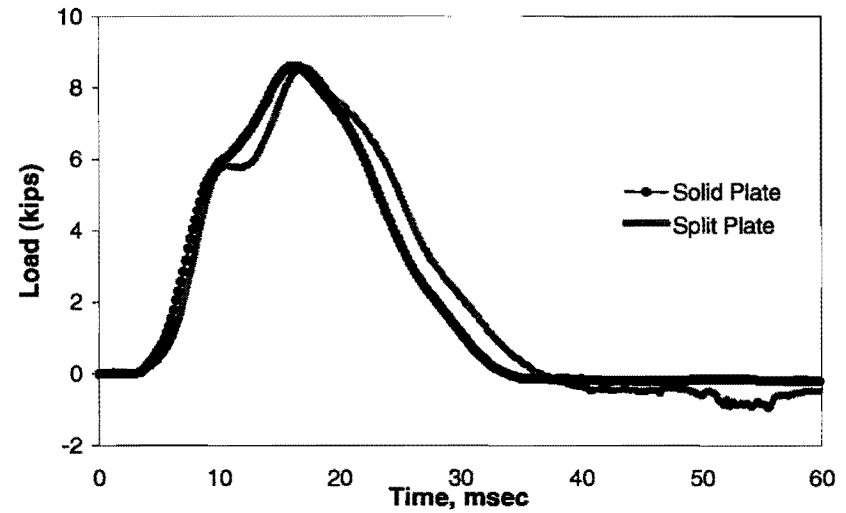
Complete Load and Deflection Data Solid and Split Plates on UTEP Test Slabs

Load and Deflection data from UTEP Test Slabs – Level

Test Point 1 - Height 1

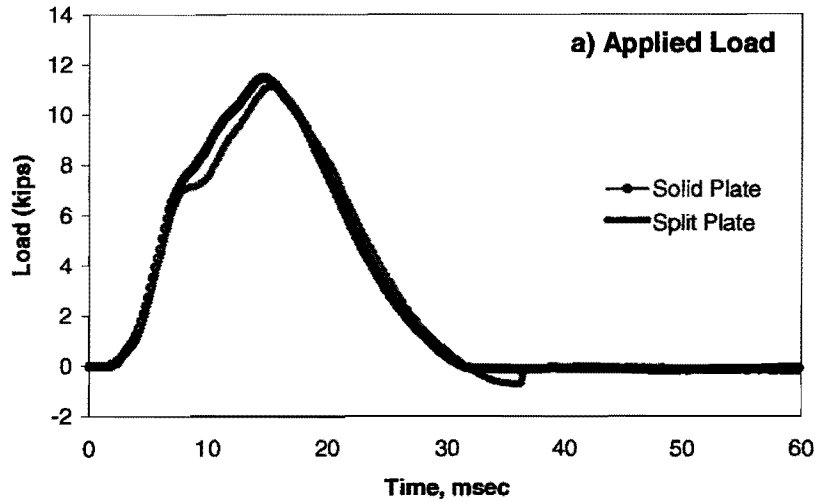


Test Point 1 - Height 2

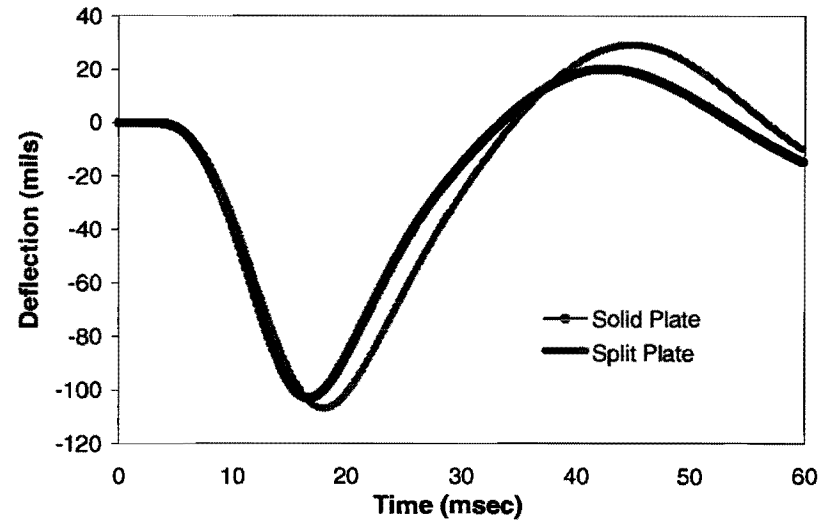
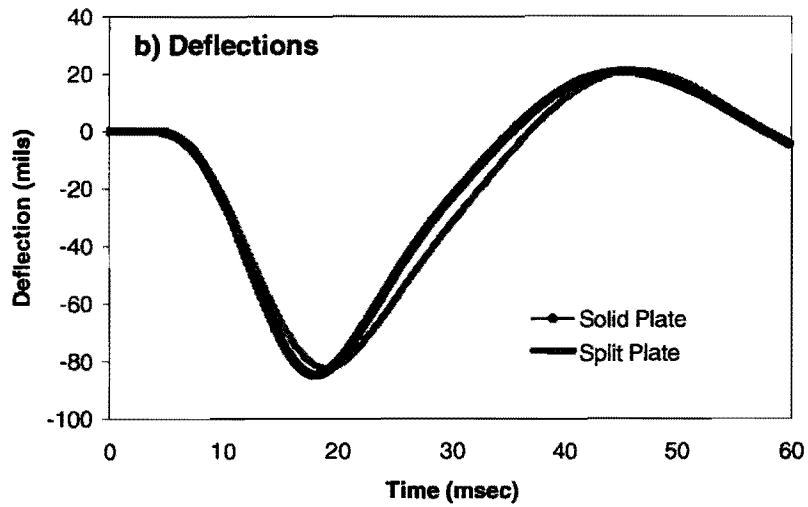
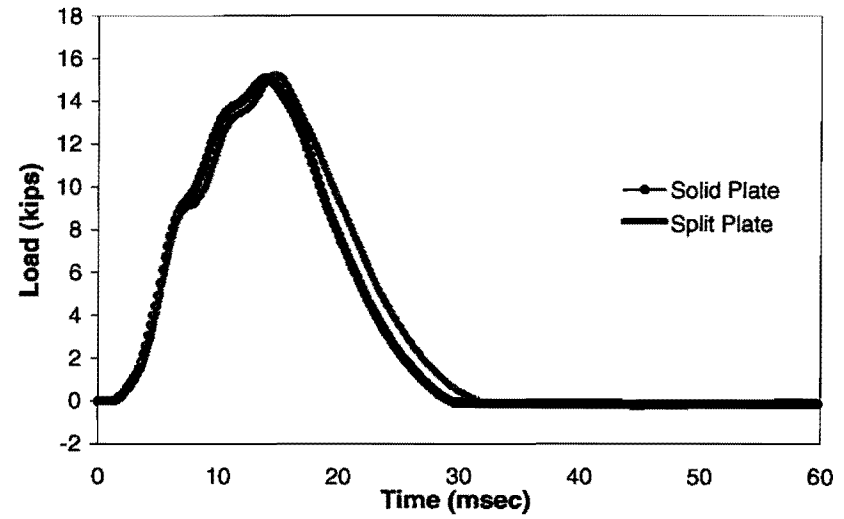


Load and Deflection data from UTEP Test Slabs – Level

Test Point 1 - Height 3

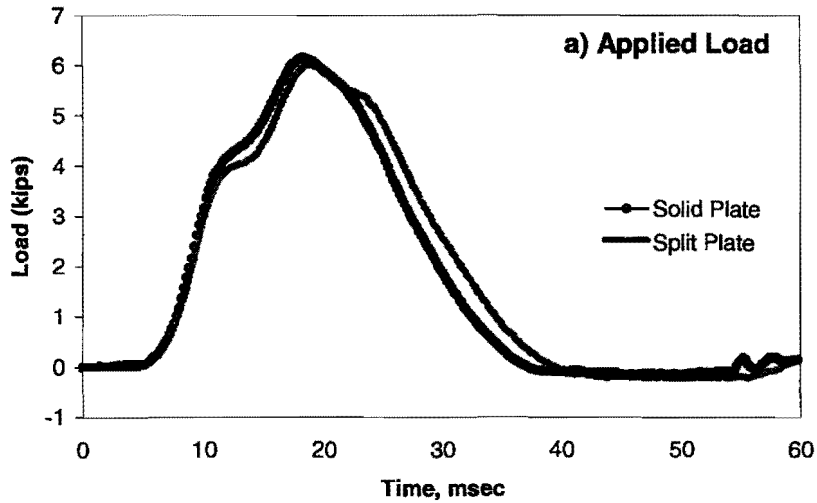


Test Point 1 - Height 4

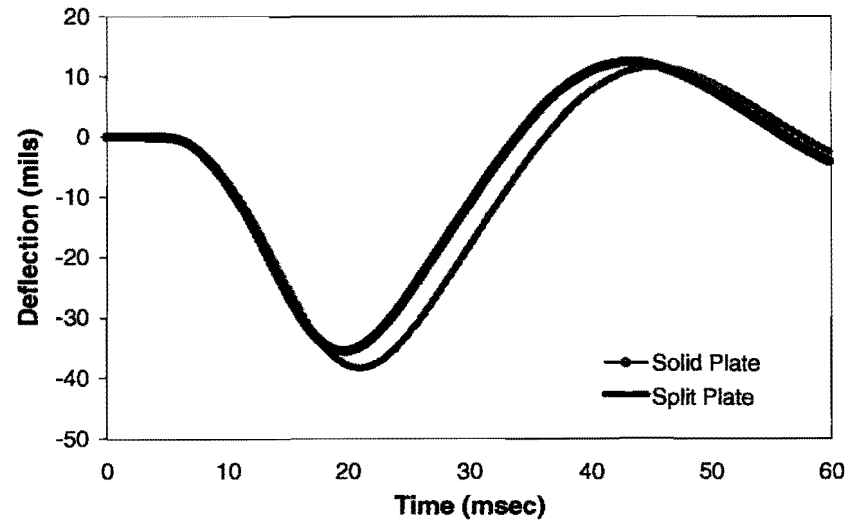
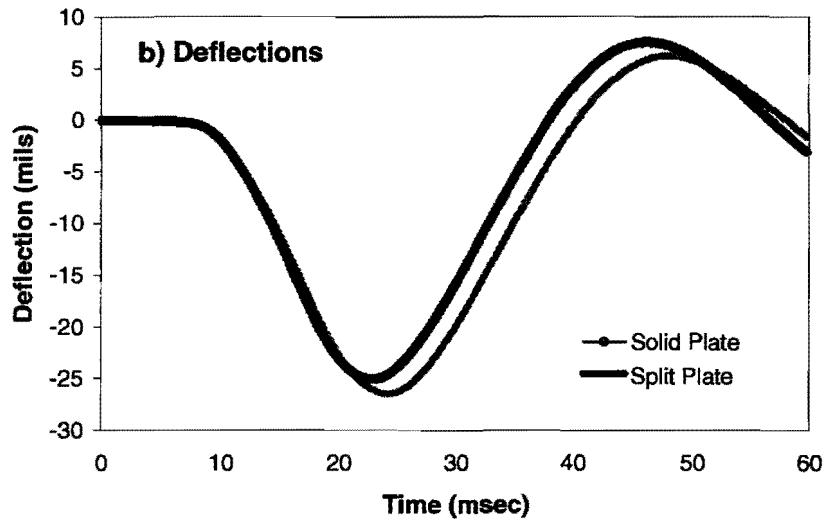
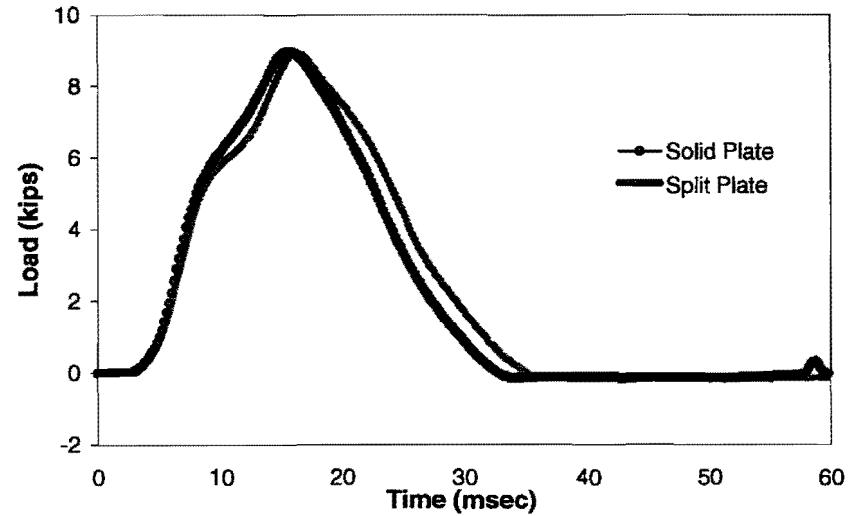


Load and Deflection data from UTEP Test Slabs – Level

Test Point 2 - Height 1

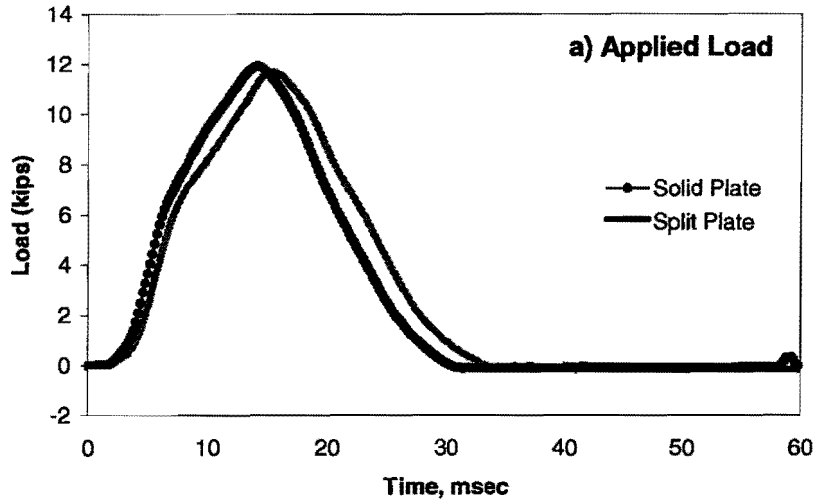


Test Point 2 - Height 2

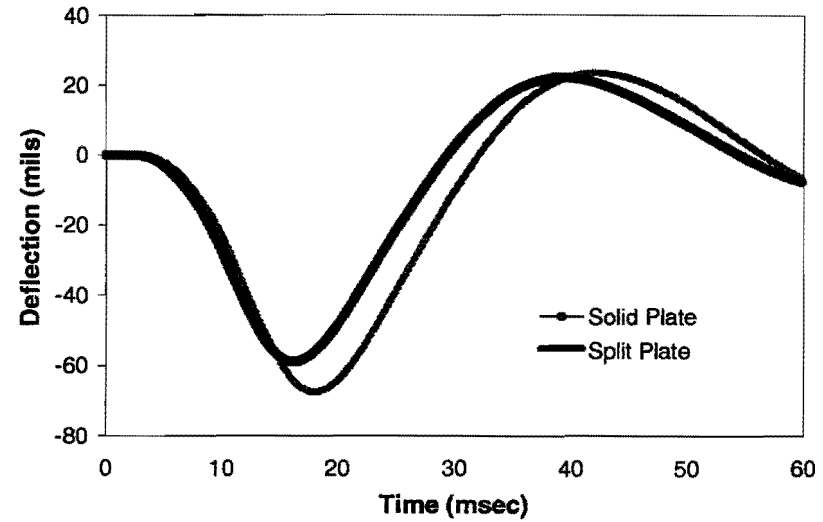
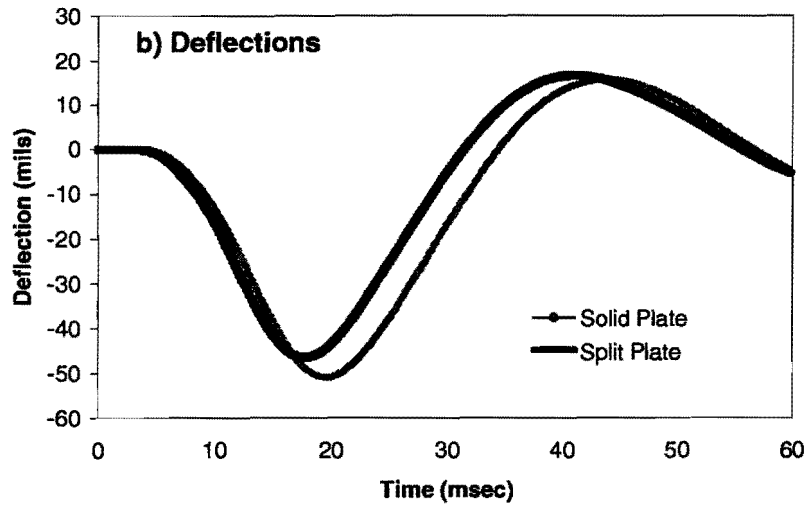
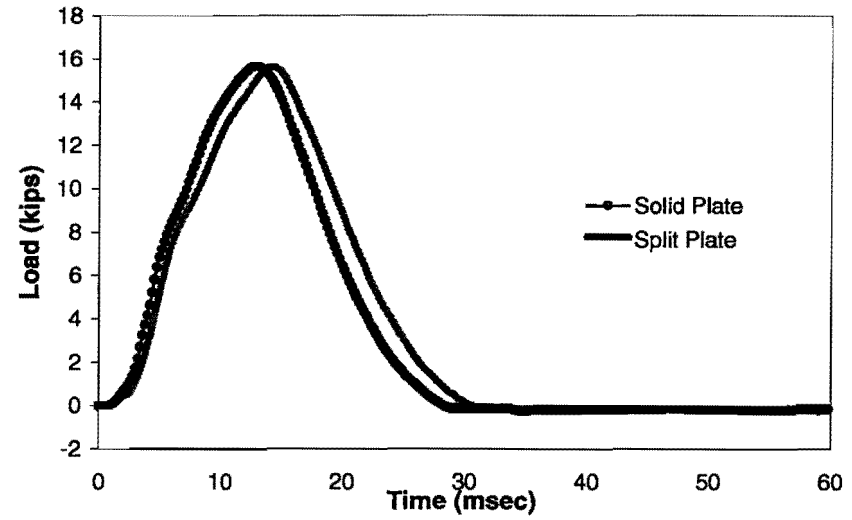


Load and Deflection data from UTEP Test Slabs – Level

Test Point 2 - Height 3

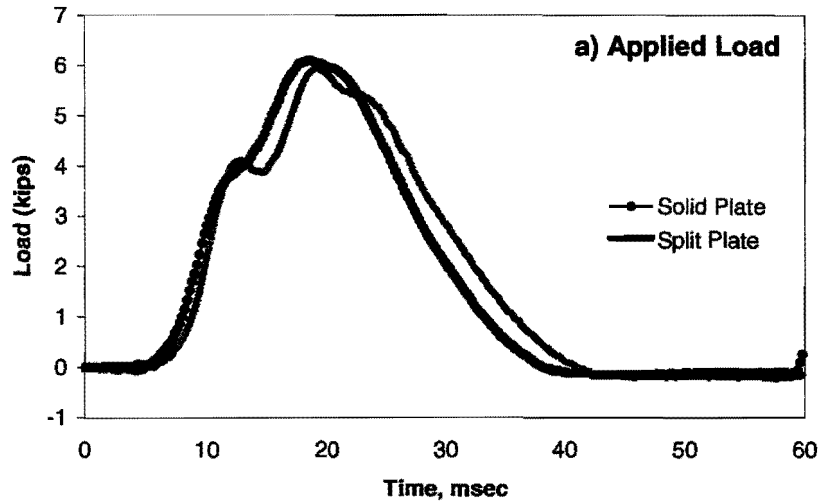


Test Point 2 - Height 4

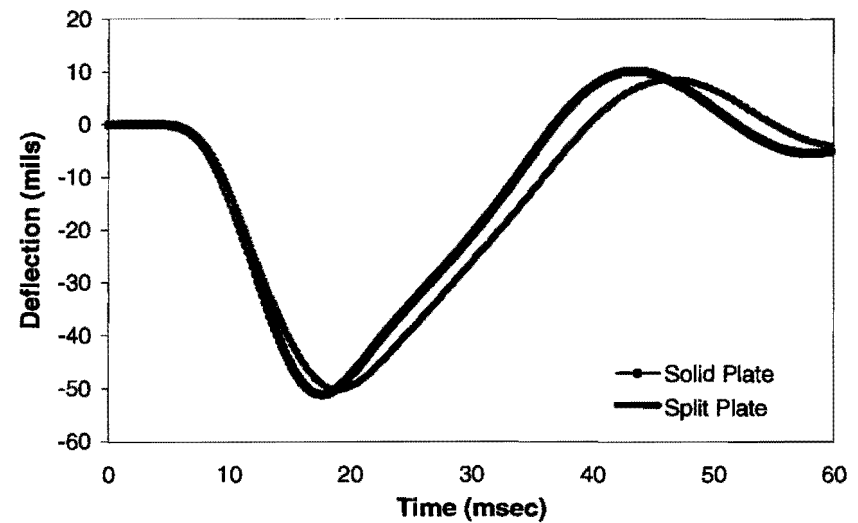
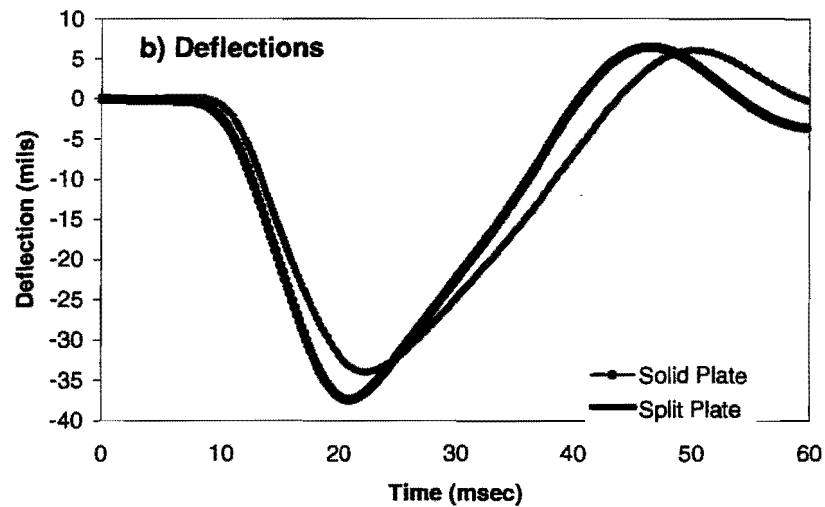
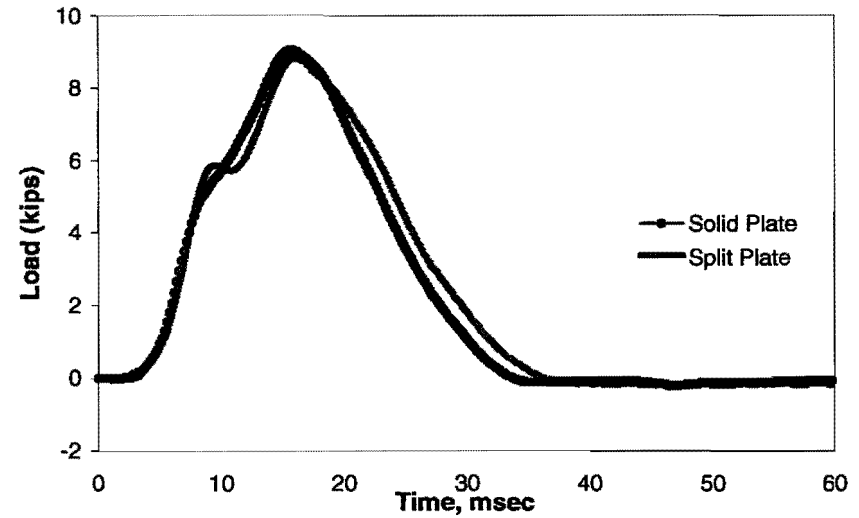


Load and Deflection data from UTEP Test Slabs – Level

Test Point 3 - Height 1

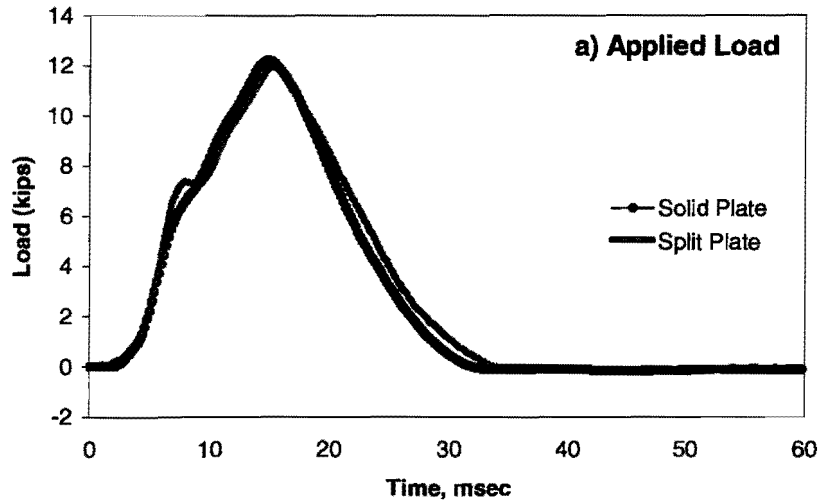


Test Point 3 - Height 2

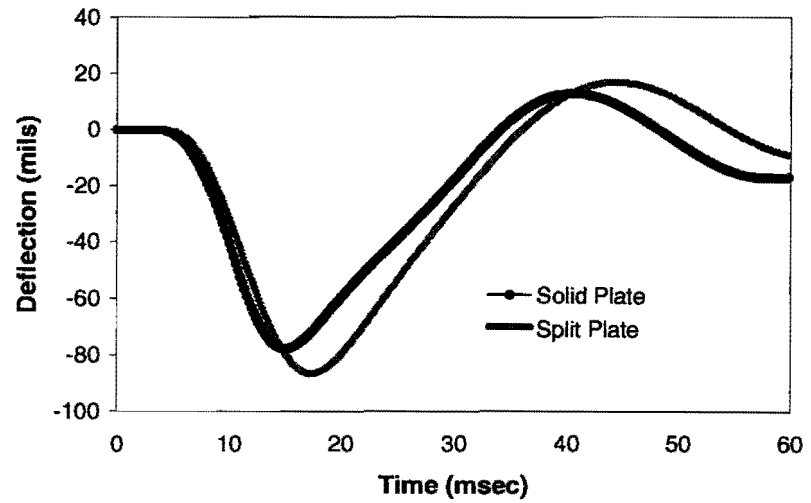
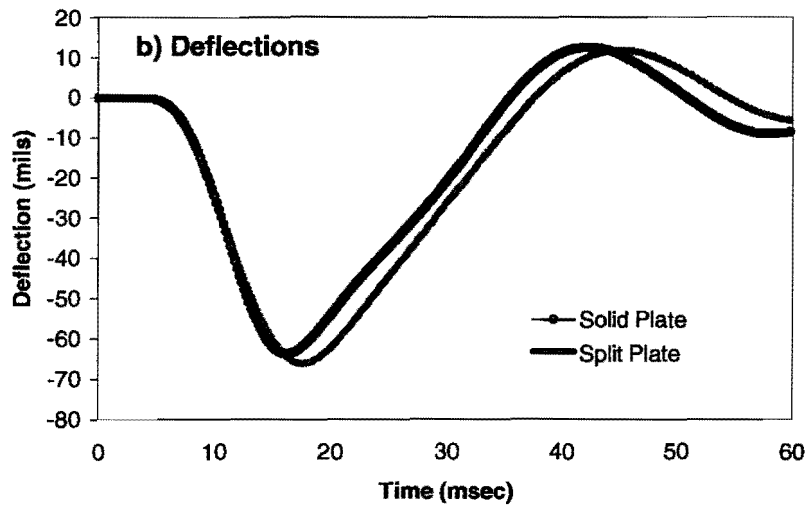
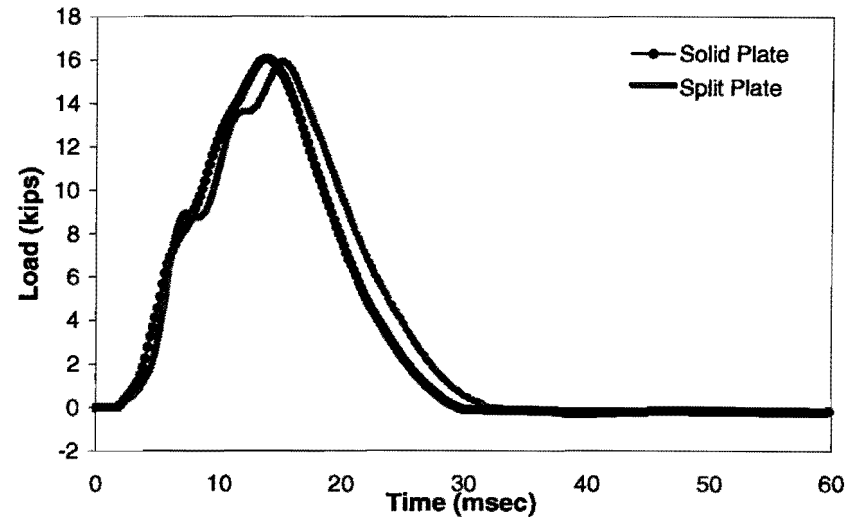


Load and Deflection data from UTEP Test Slabs – Level

Test Point - Height 3

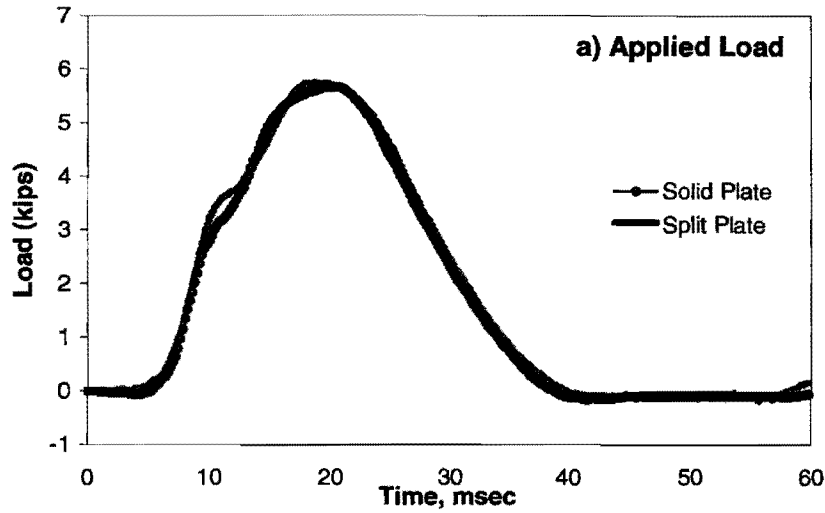


Test Point 3 - Height 4

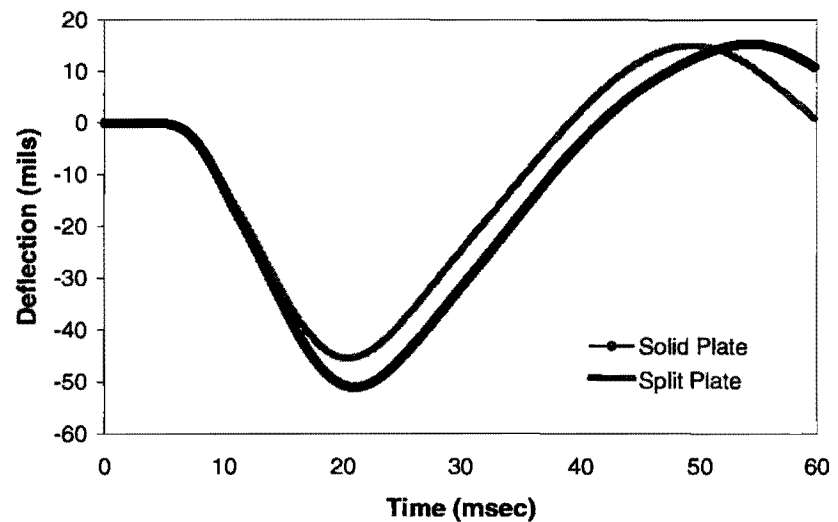
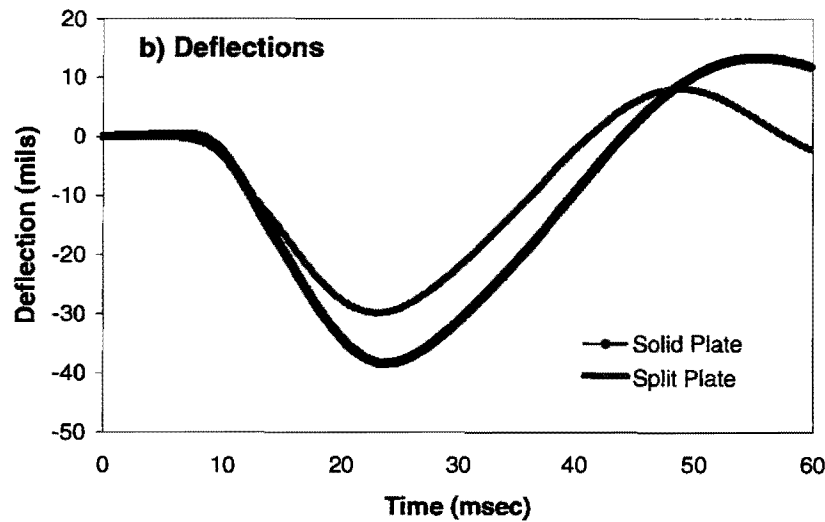
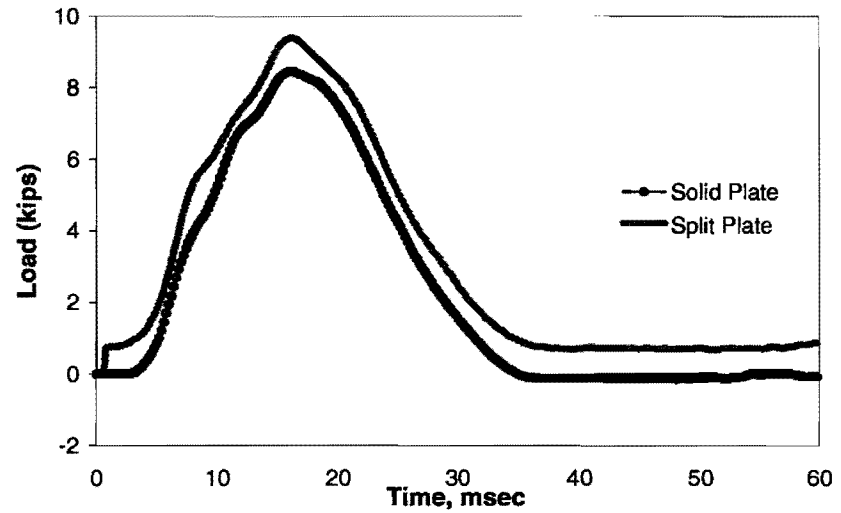


Load and Deflection data from UTEP Test Slabs – Inclined

Test Point 1 - Height 1

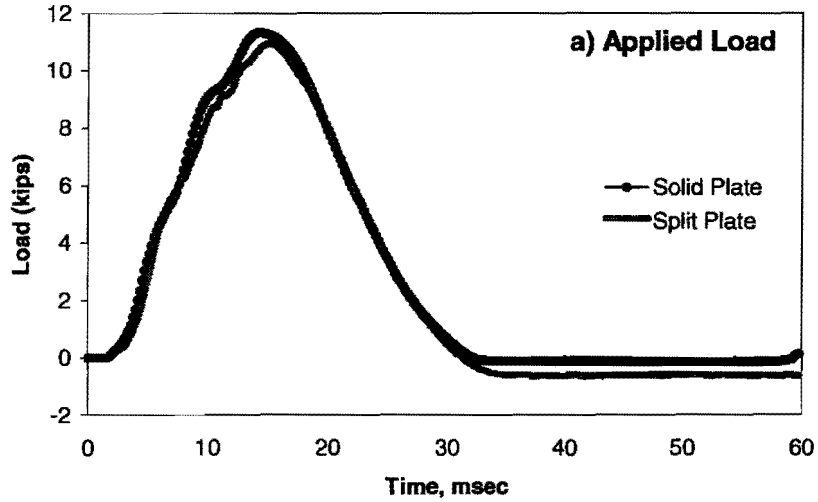


Test Point 1 - Height 2

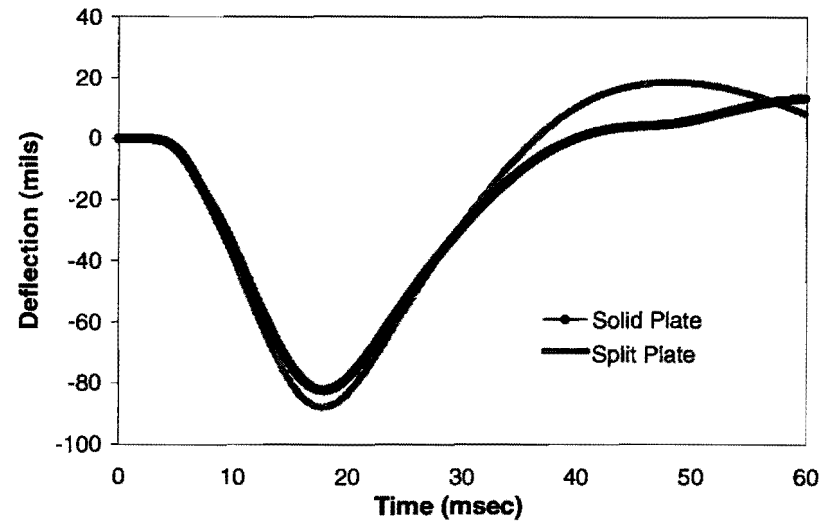
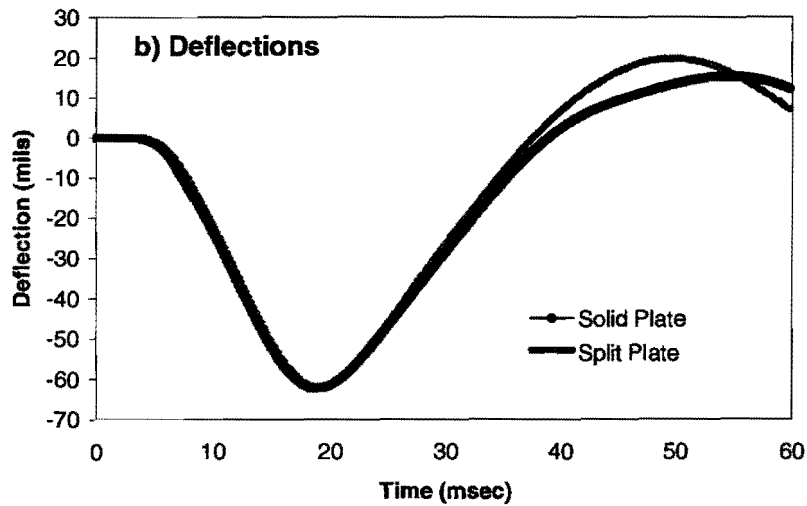
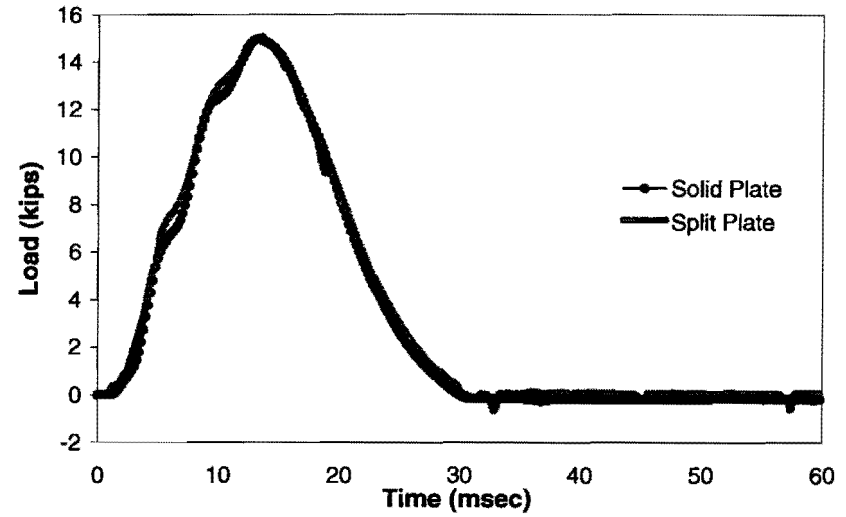


Load and Deflection data from UTEP Test Slabs – Inclined

Test Point 1 - Height 3

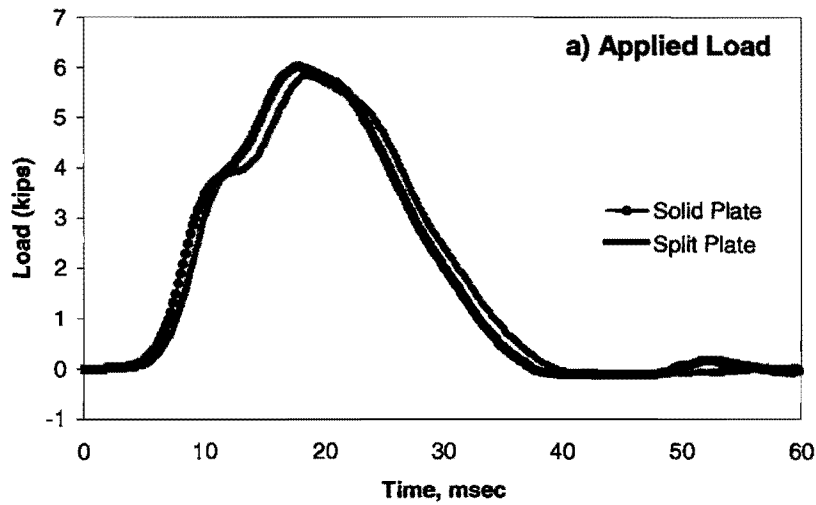


Test Point 1 - Height 4

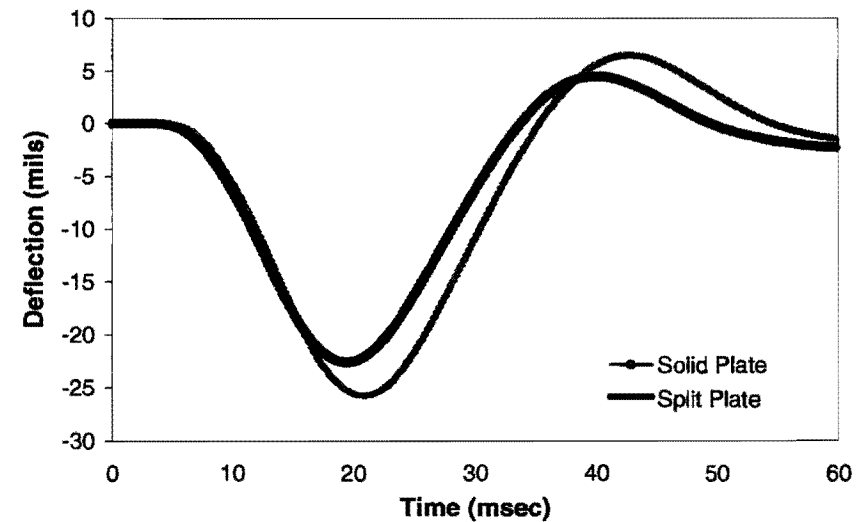
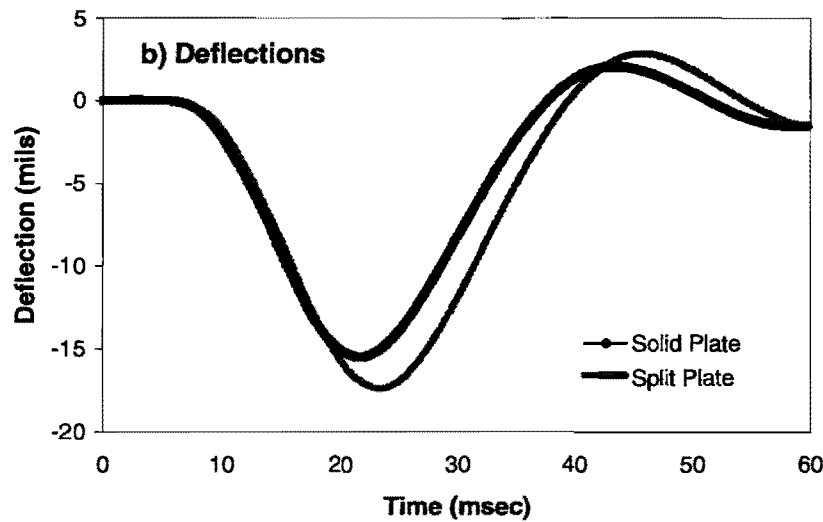
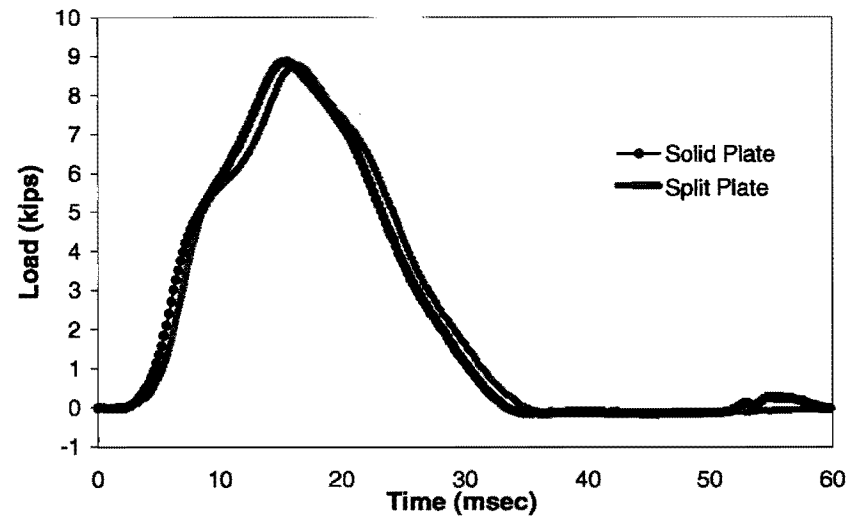


Load and Deflection data from UTEP Test Slabs – Inclined

Test Point 2 - Height 1

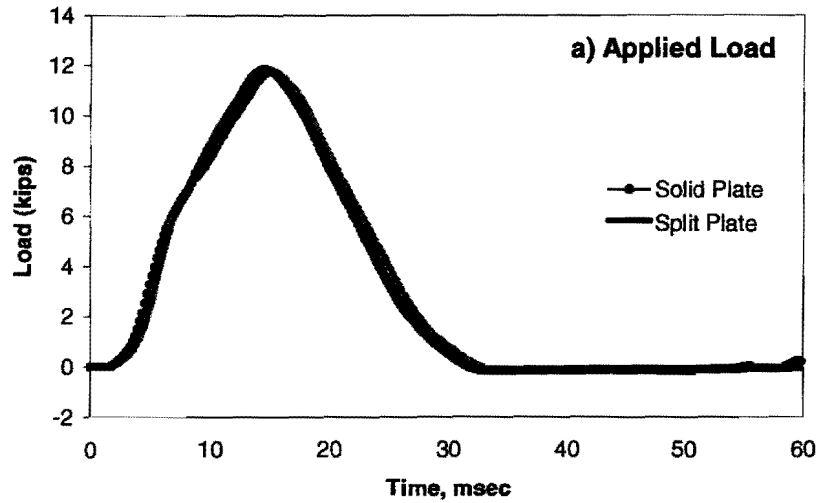


Test Point 2 - Height 2

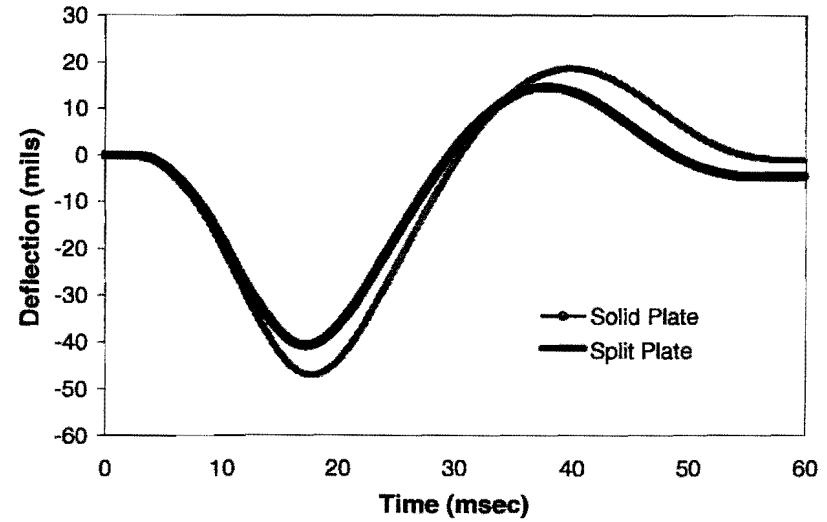
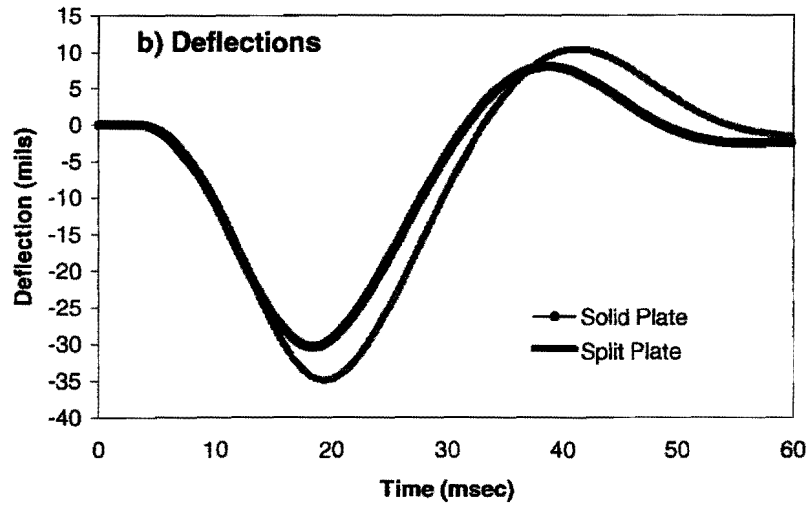
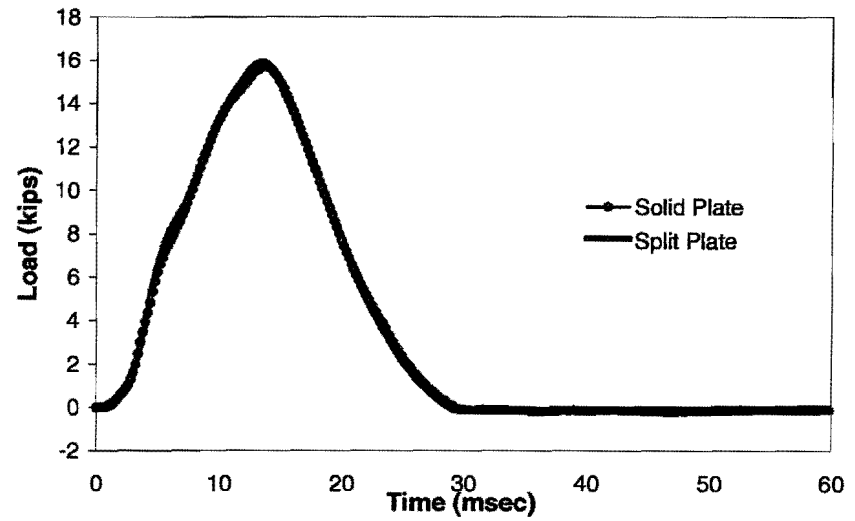


Load and Deflection data from UTEP Test Slabs – Inclined

Test Point 2 - Height 3

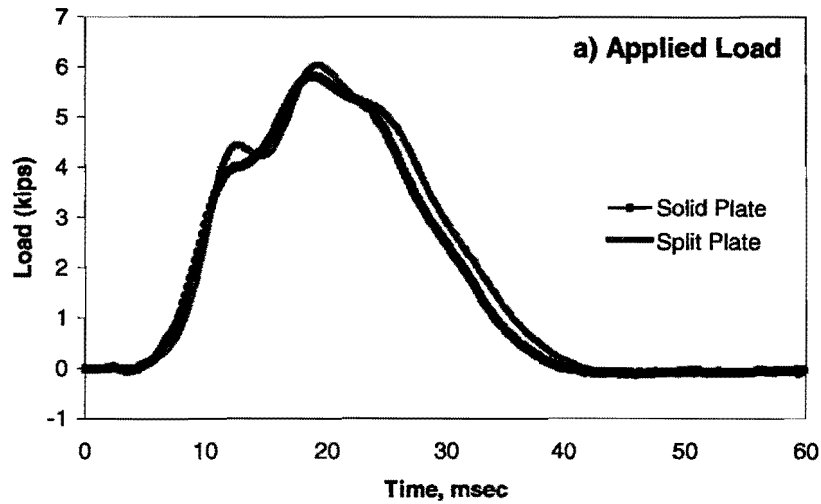


Test Point 2 - Height 4

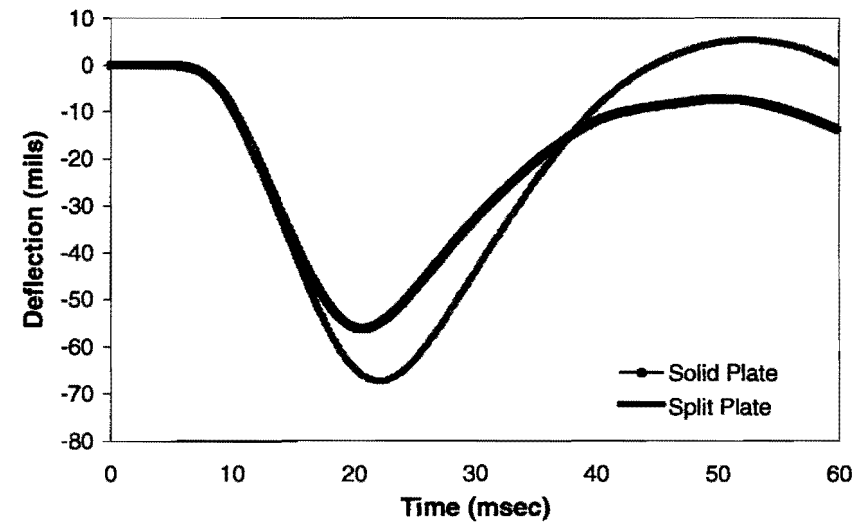
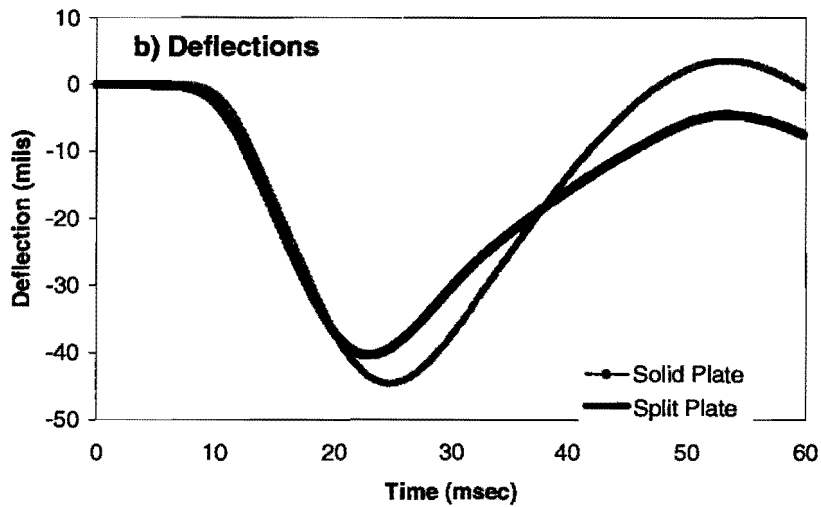
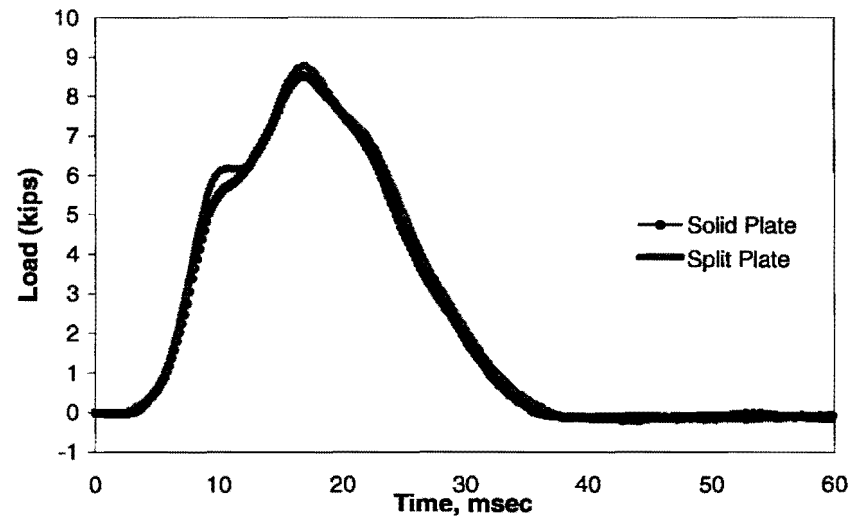


Load and Deflection data from UTEP Test Slabs – Inclined

Test Point 3 - Height 1

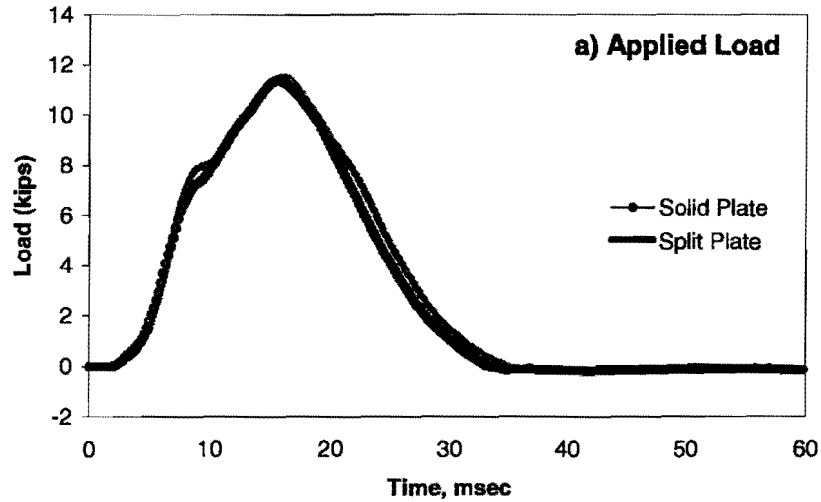


Test Point 3 - Height 2

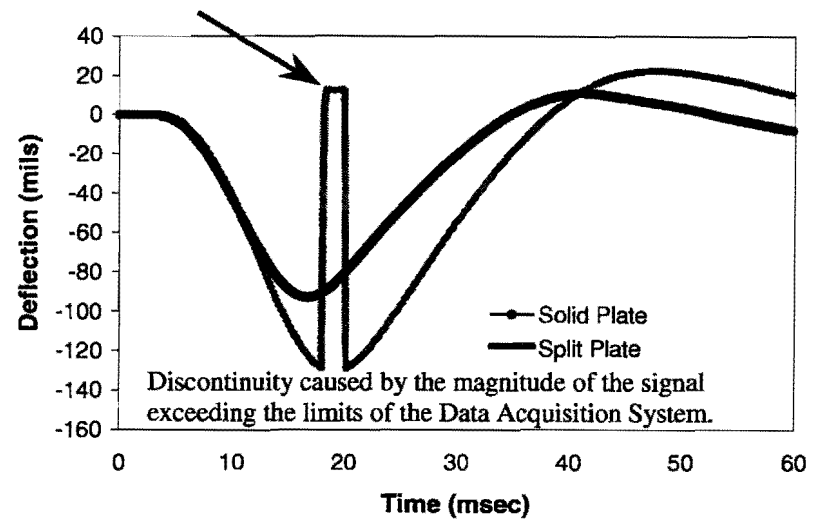
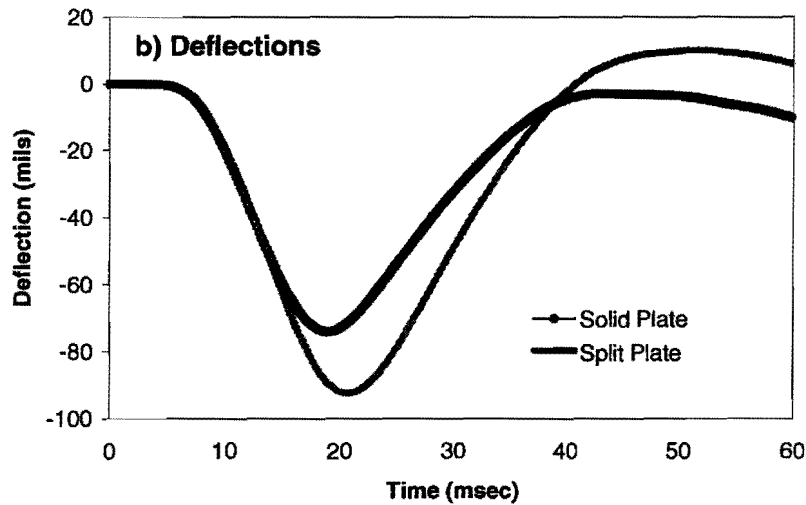
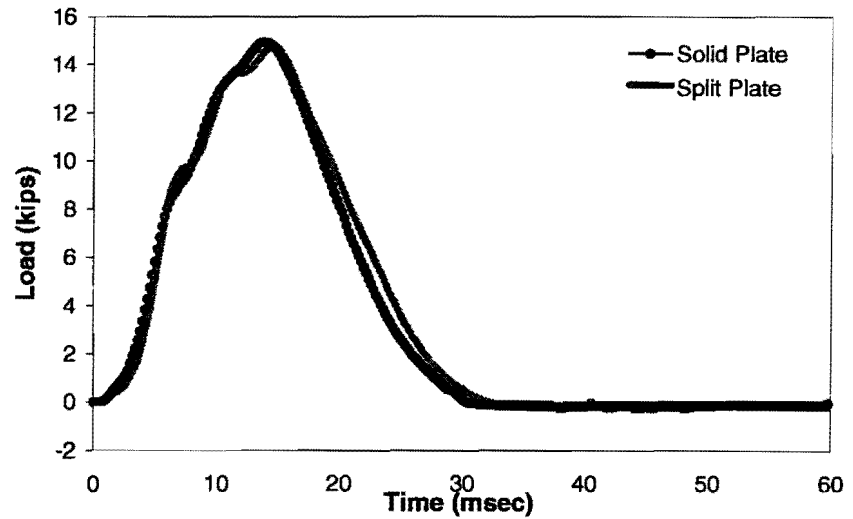


Load and Deflection data from UTEP Test Slabs – Inclined

Test Point - Height 3

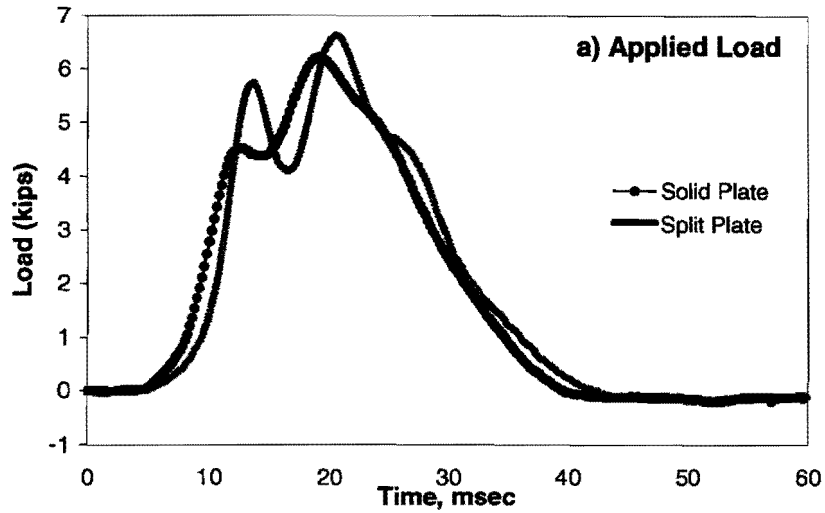


Test Point 3 - Height 4

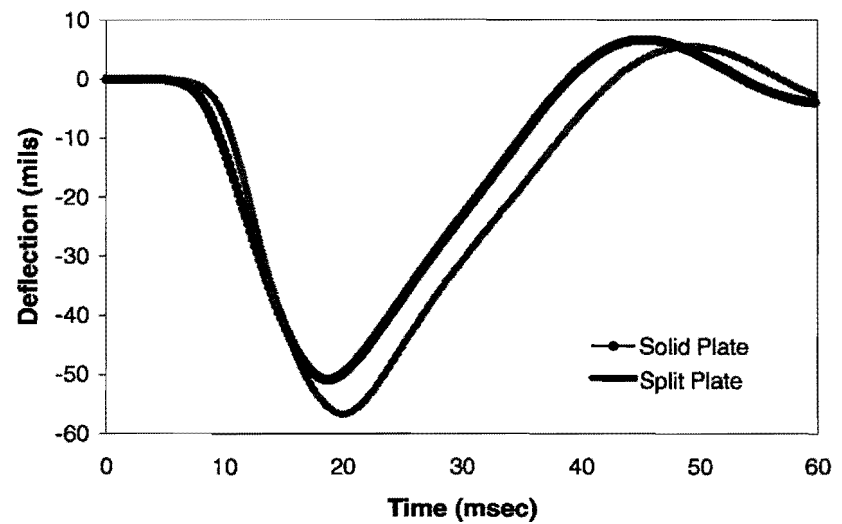
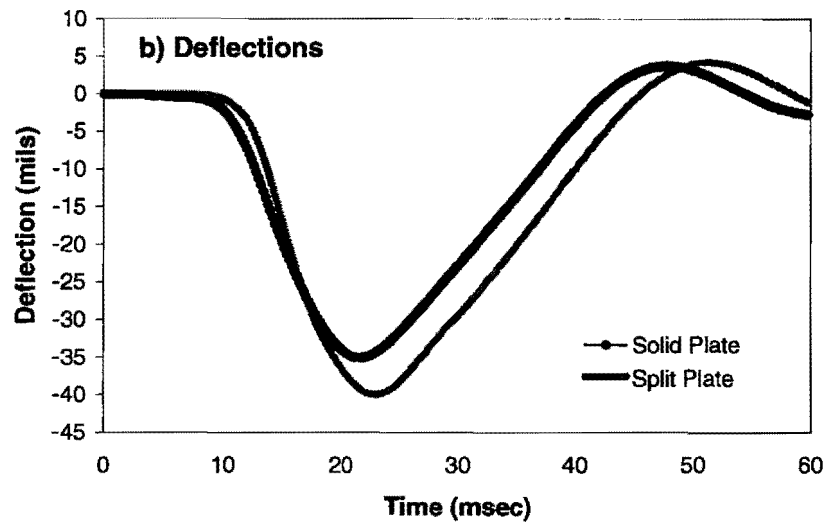
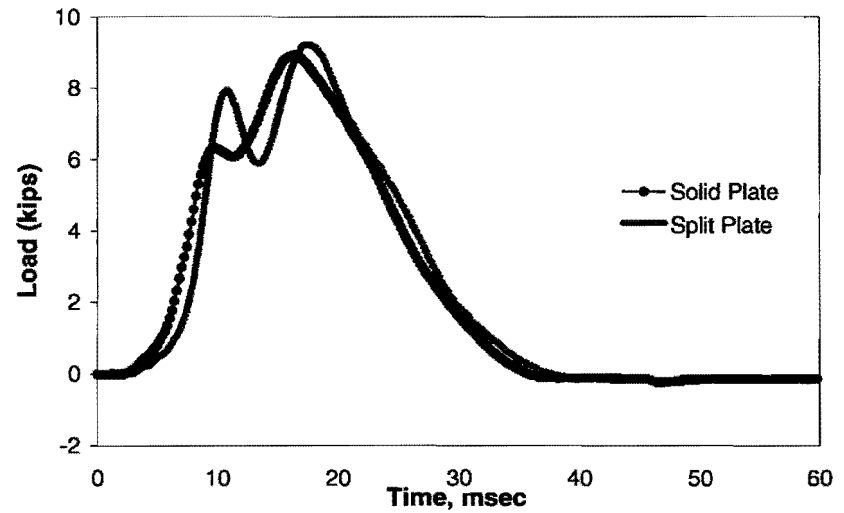


Load and Deflection data from UTEP Test Slabs – Rutted

Test Point 1 - Height 1

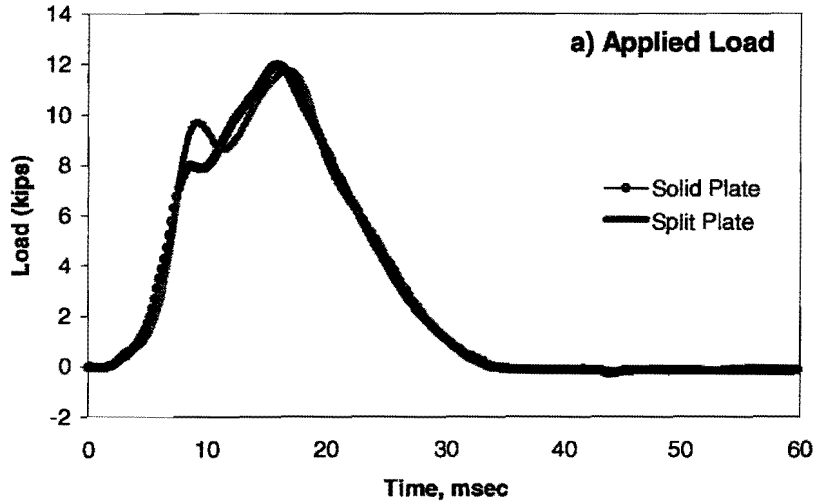


Test Point 1 - Height 2

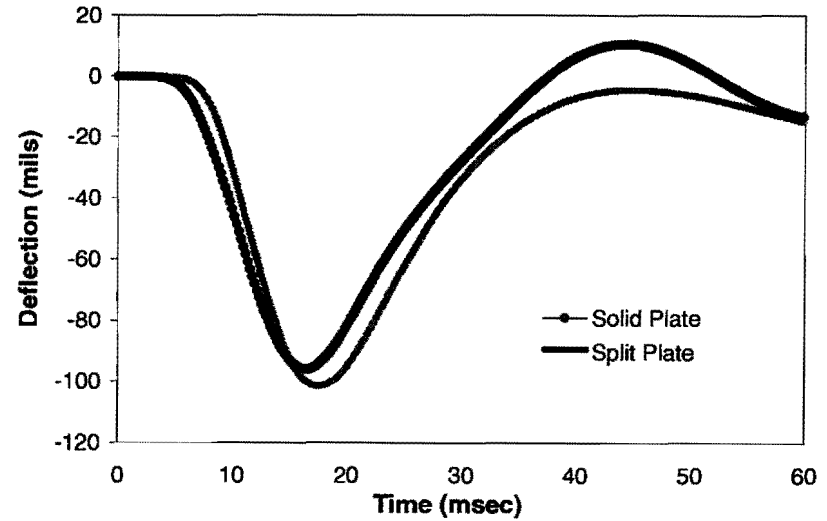
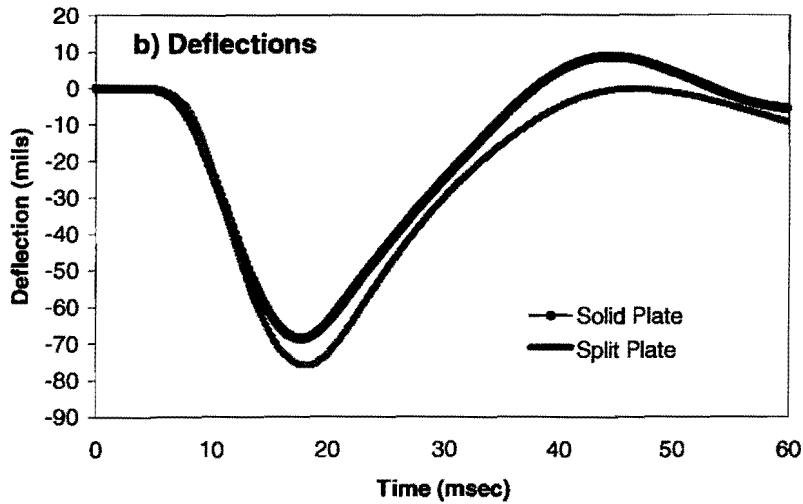
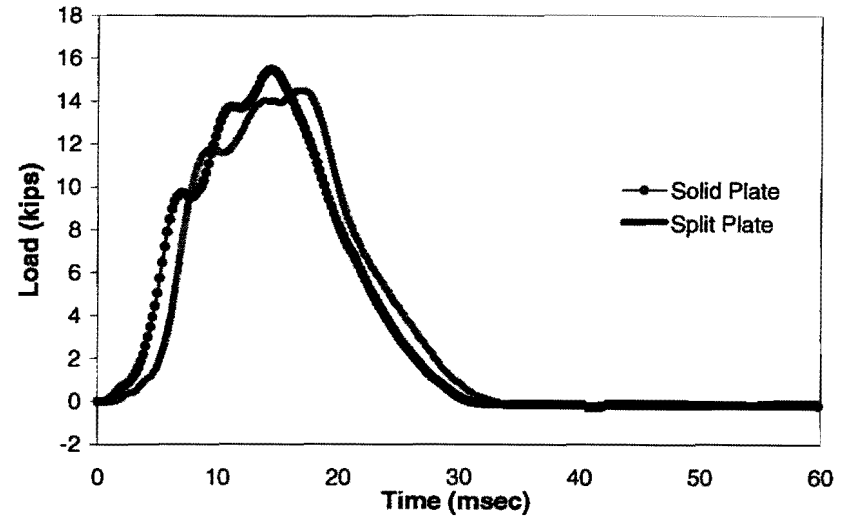


Load and Deflection data from UTEP Test Slabs – Rutted

Test Point 1 - Height 3

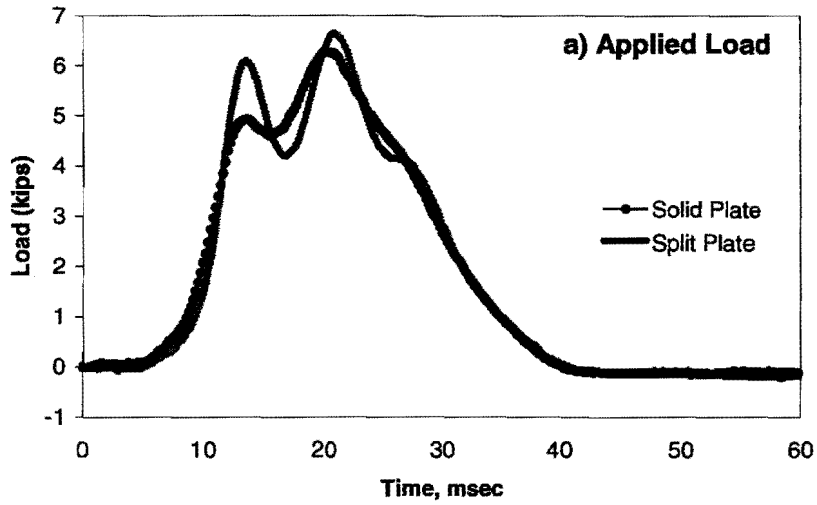


Test Point 1 - Height 4

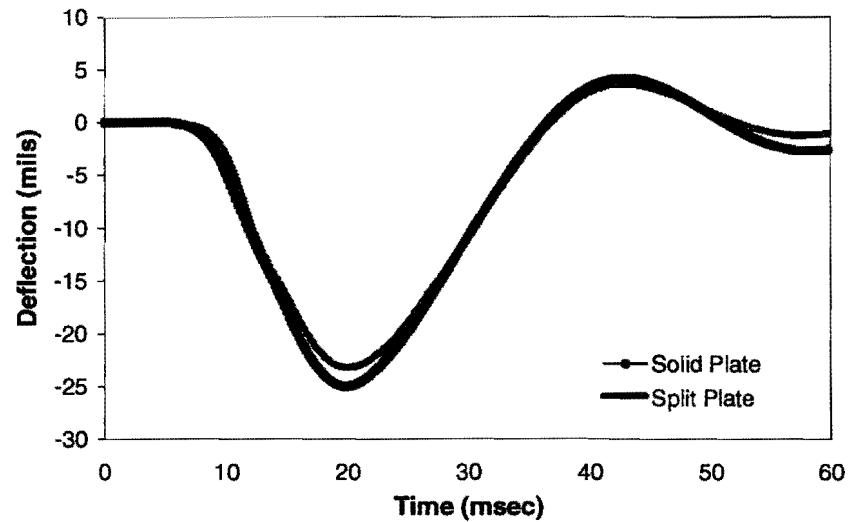
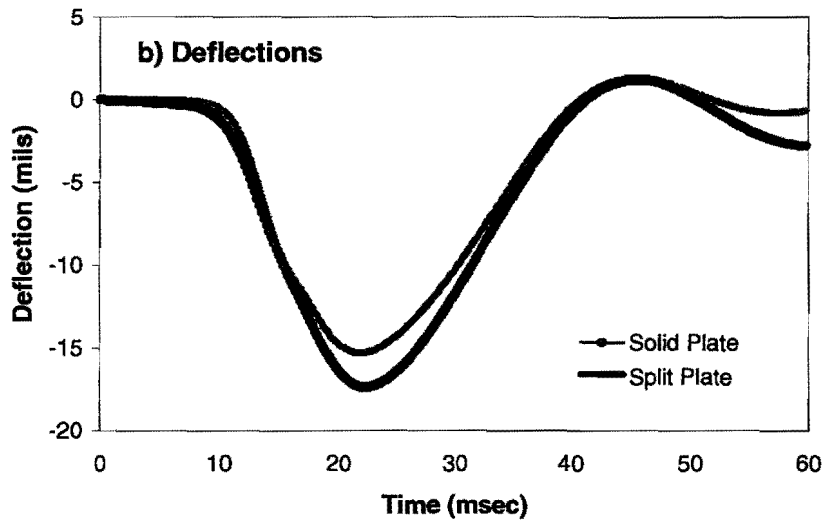
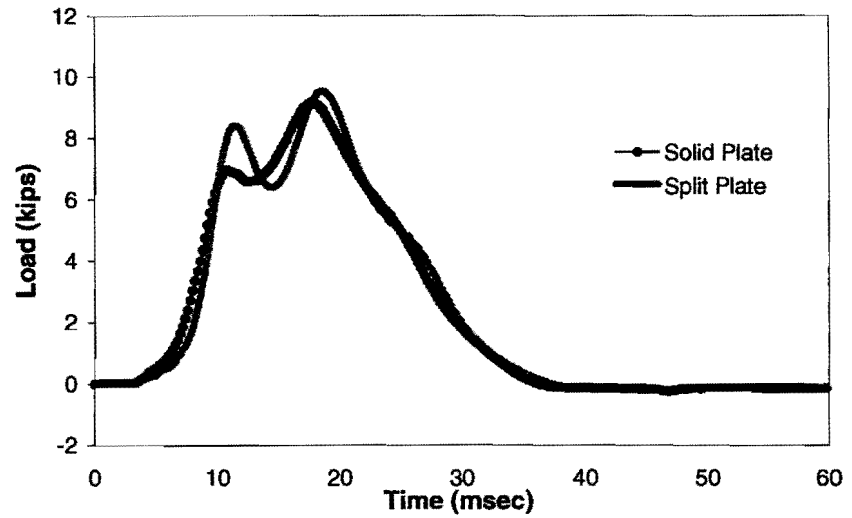


Load and Deflection data from UTEP Test Slabs – Rutted

Test Point 2 - Height 1

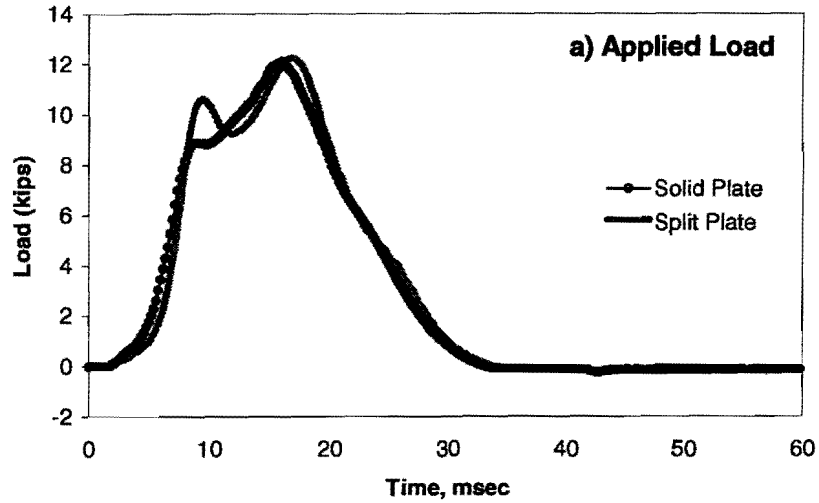


Test Point 2 - Height 2

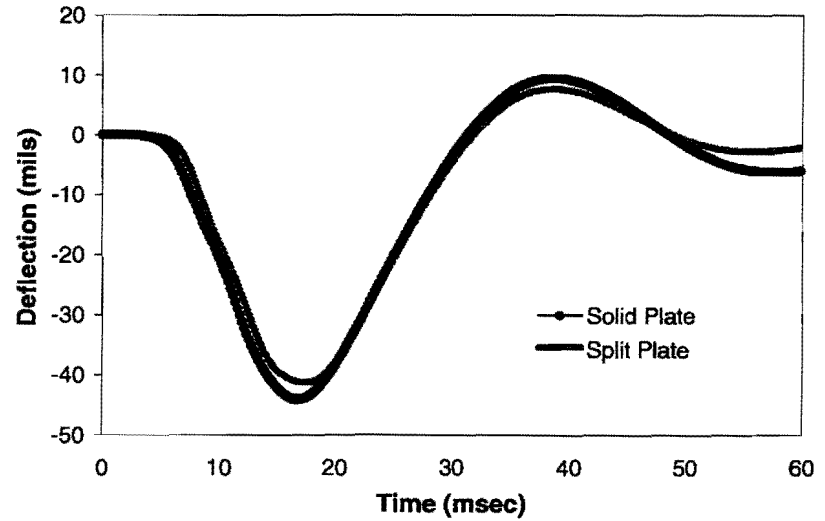
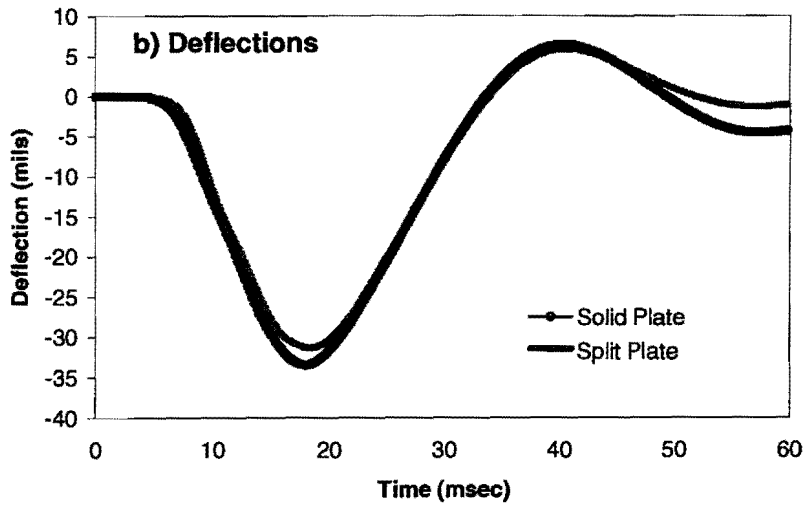
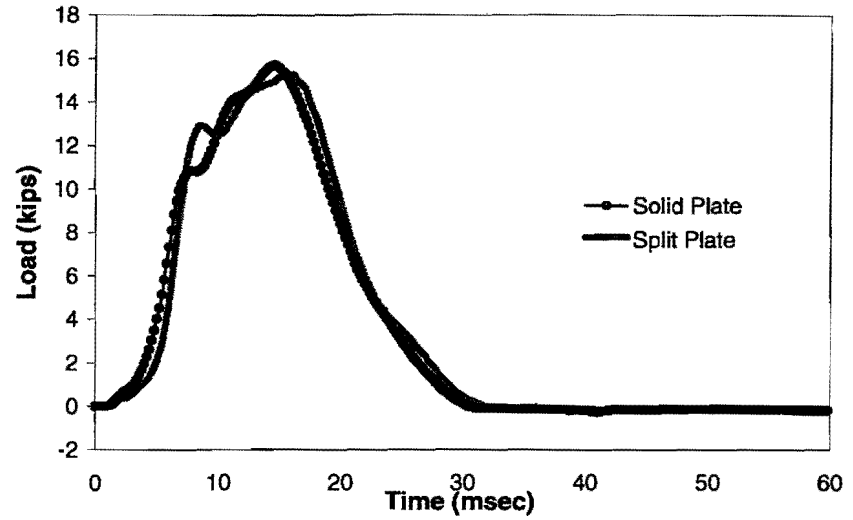


Load and Deflection data from UTEP Test Slabs – Rutted

Test Point 2 - Height 3

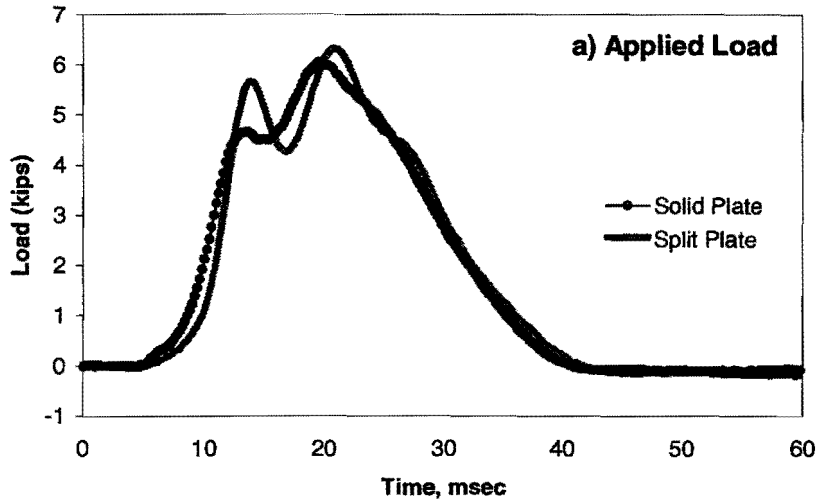


Test Point 2 - Height 4

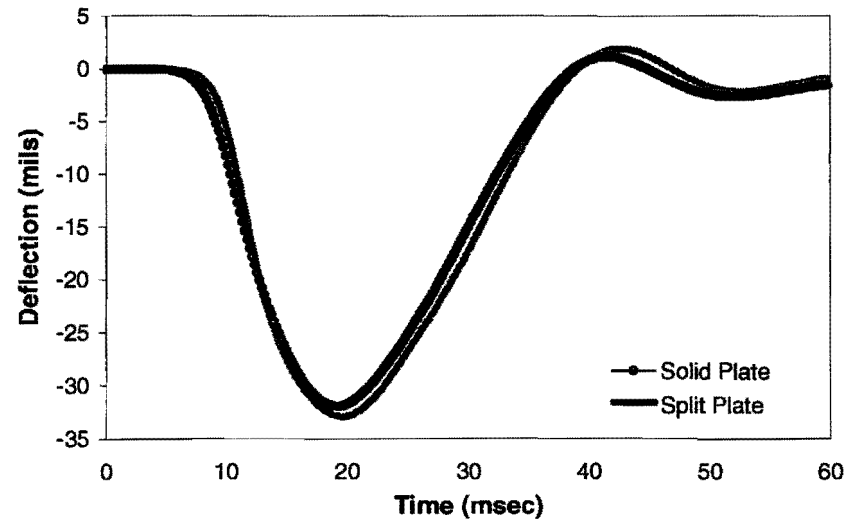
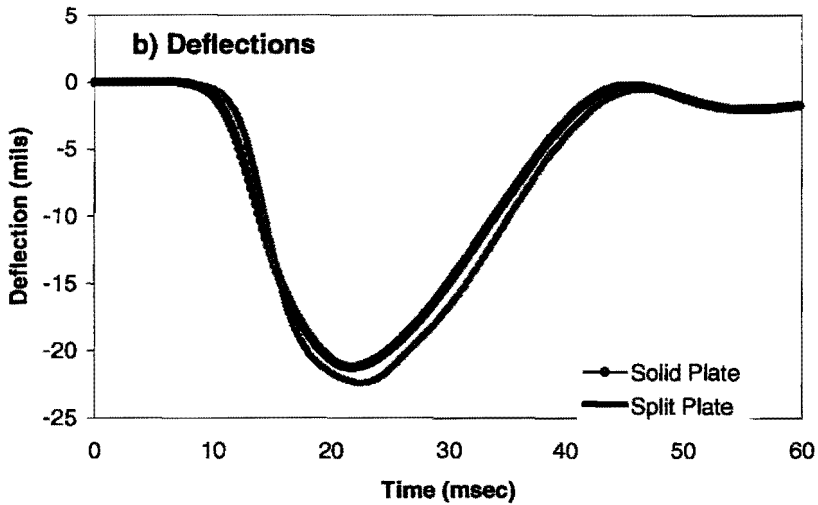
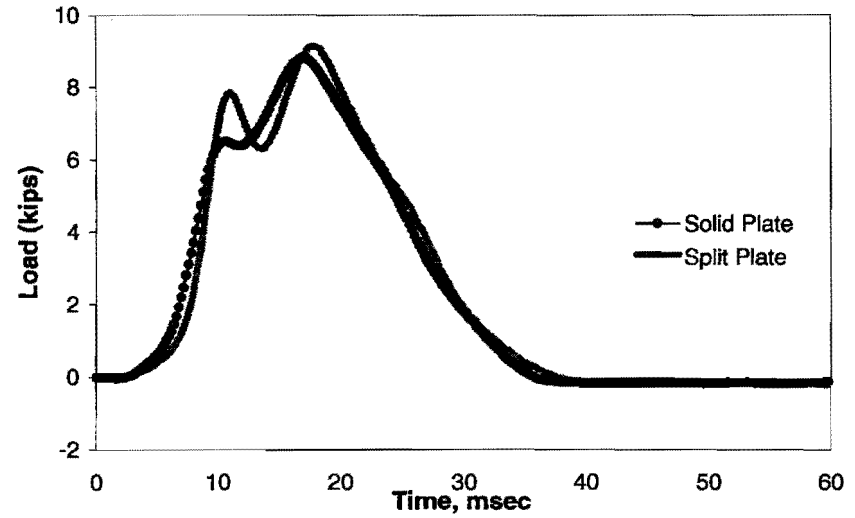


Load and Deflection data from UTEP Test Slabs – Rutted

Test Point 3 - Height 1



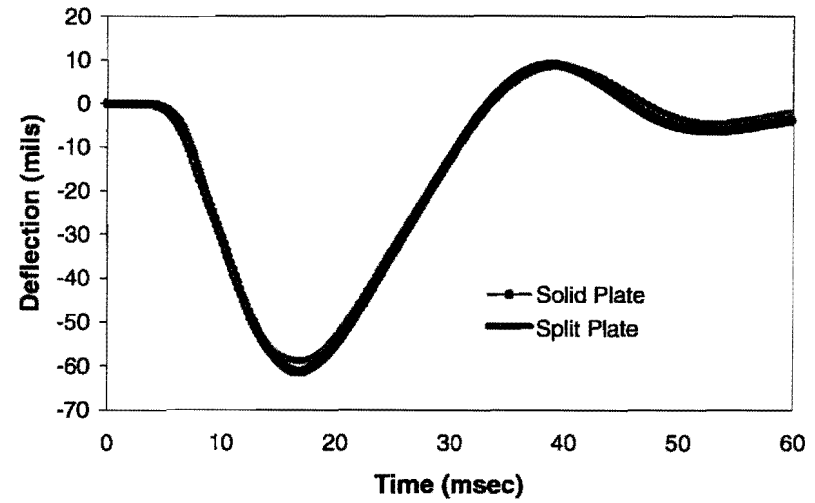
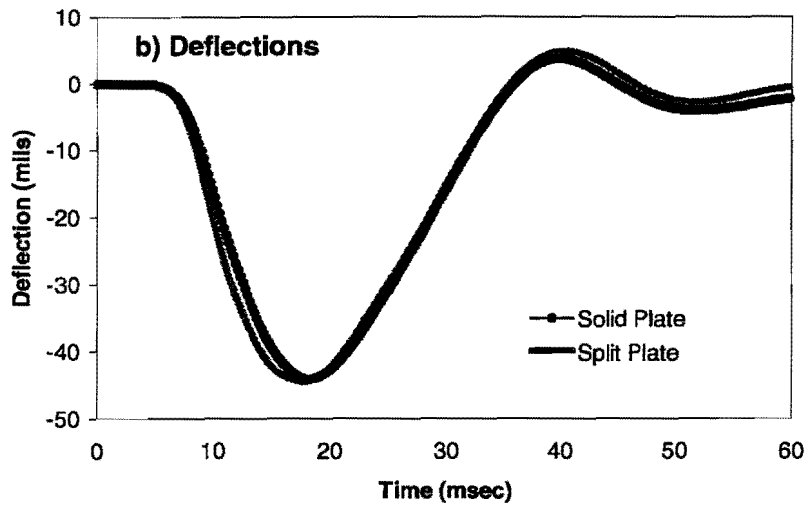
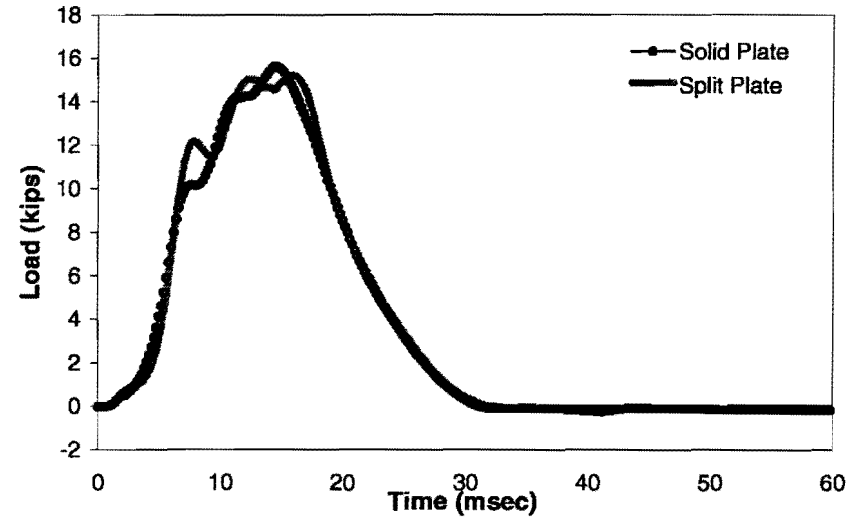
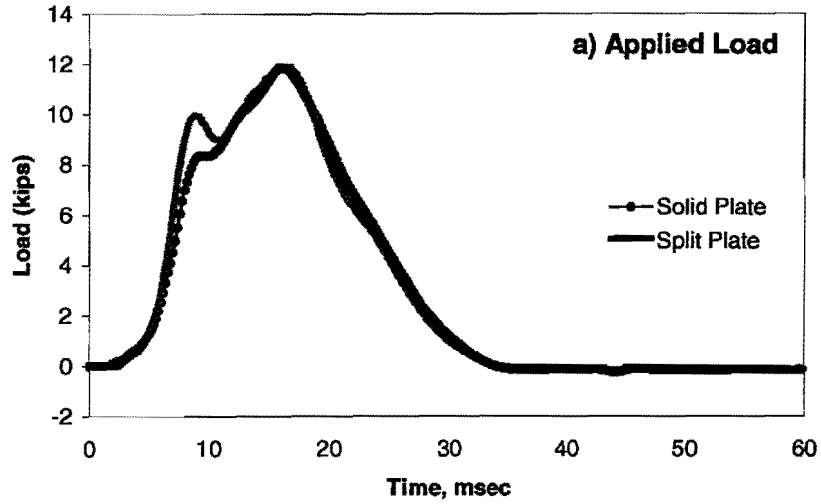
Test Point 3 - Height 2



Load and Deflection data from UTEP Test Slabs – Rutted

Test Point - Height 3

Test Point 3 - Height 4



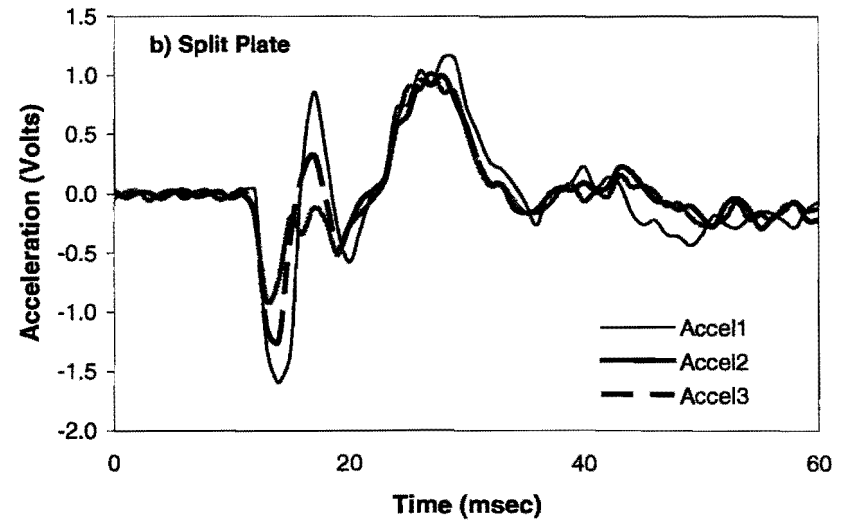
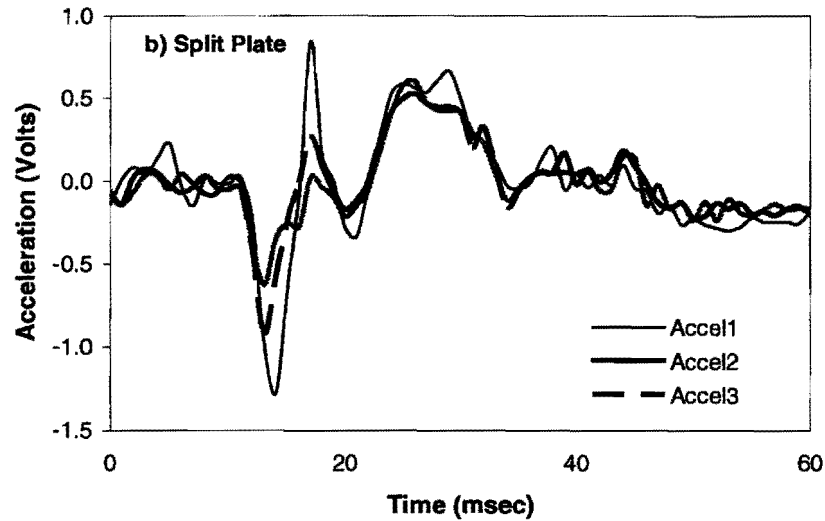
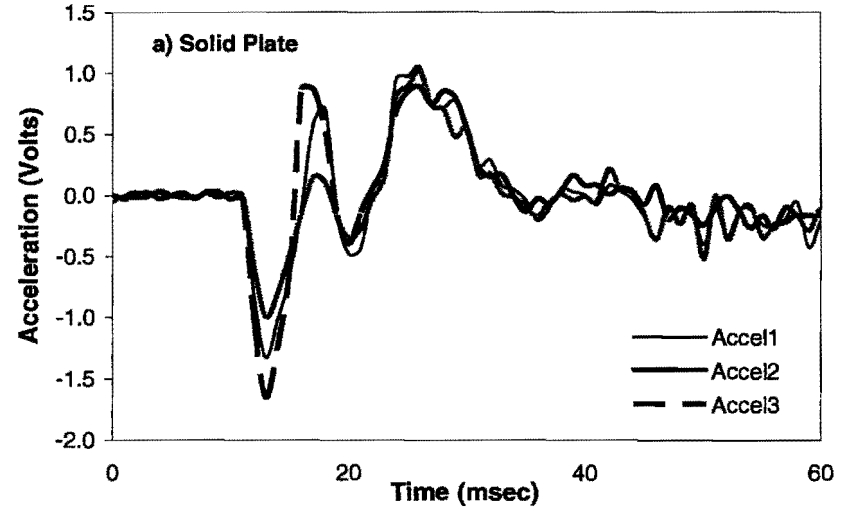
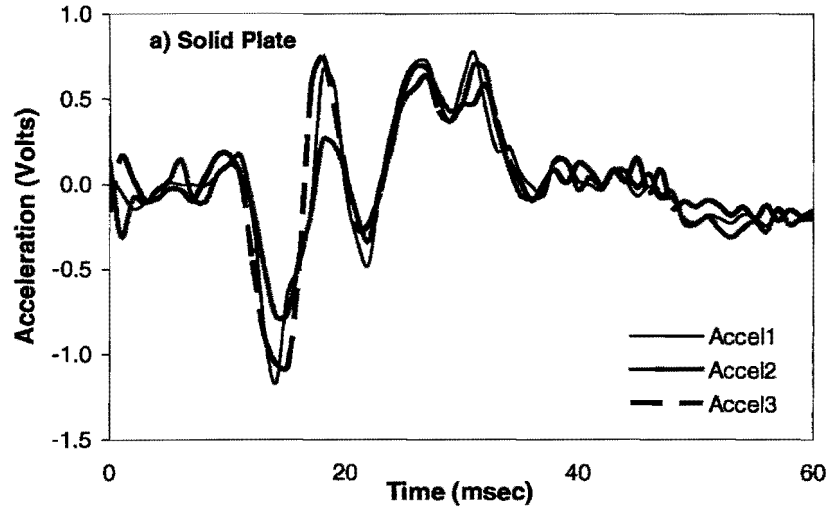
Appendix C

Complete Load Plate Motion Data Solid and Split Plates on UTEP Test Slabs

Load Plate Motion data from UTEP Test Slabs – Level

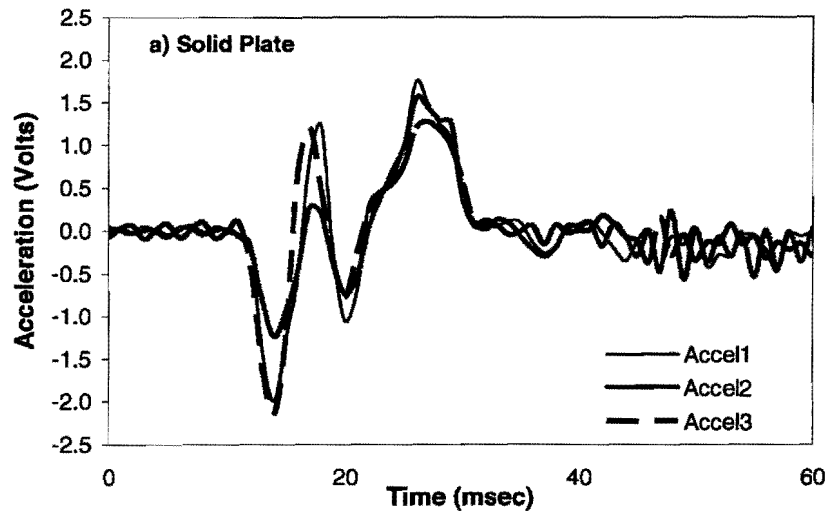
Test Point 1 - Height 1

Test Point 1 - Height 2

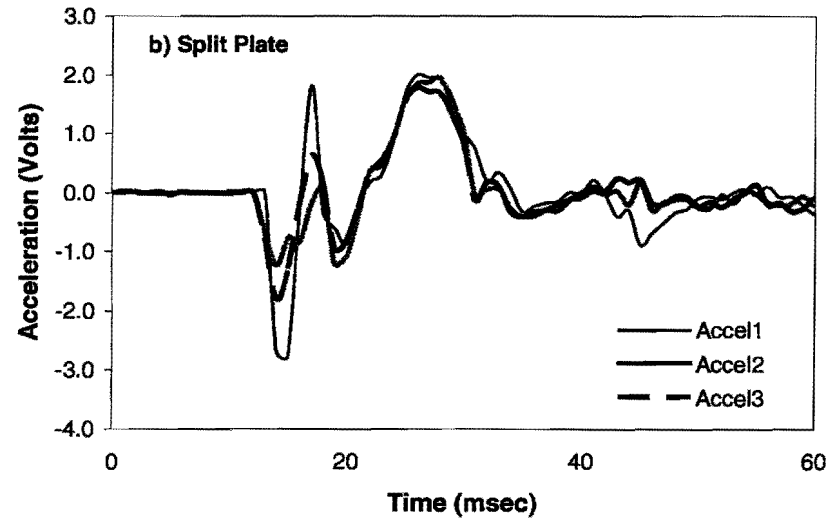
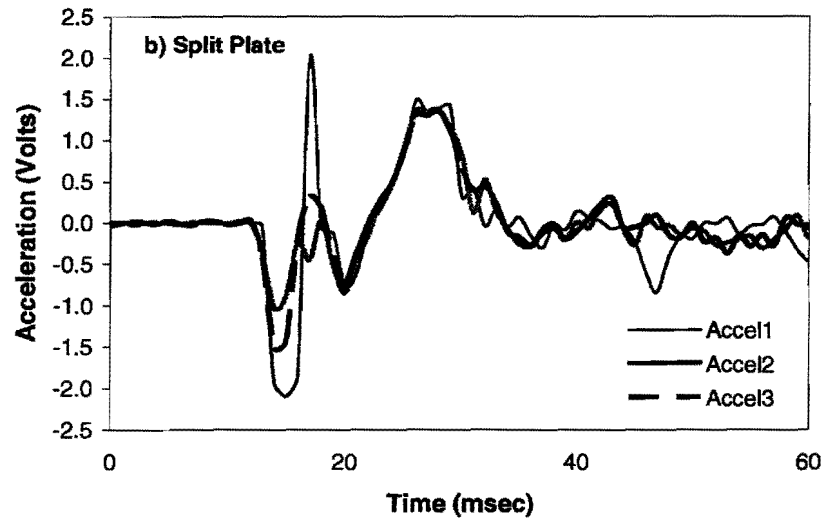
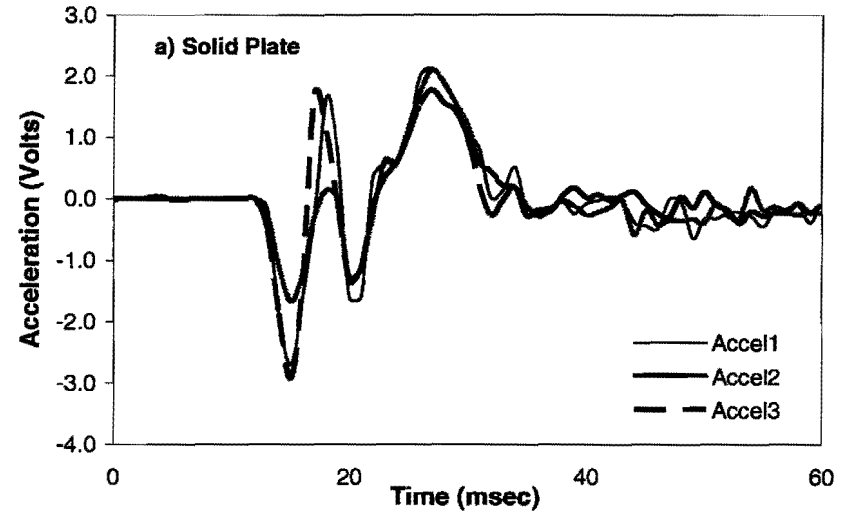


Load Plate Motion data from UTEP Test Slabs – Level

Test Point 1 - Height 3



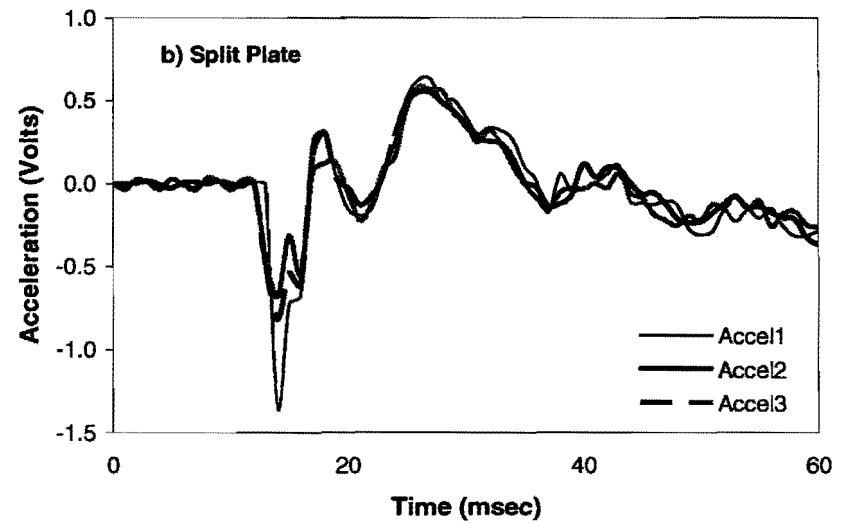
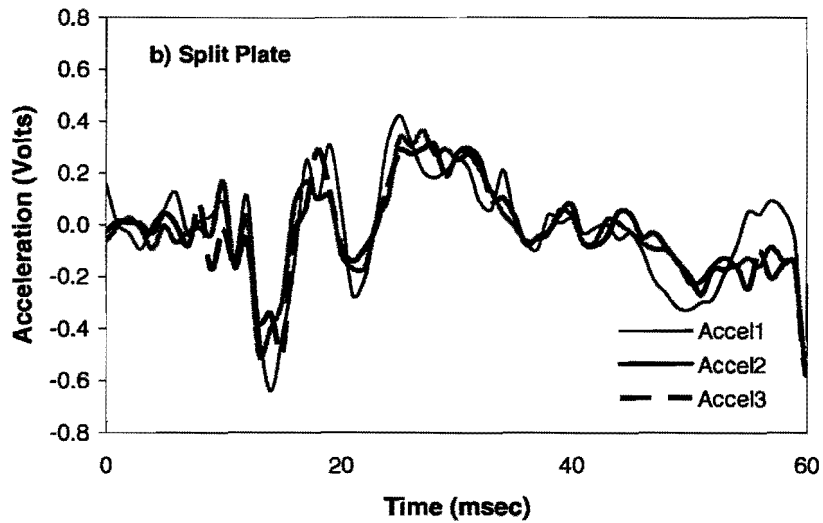
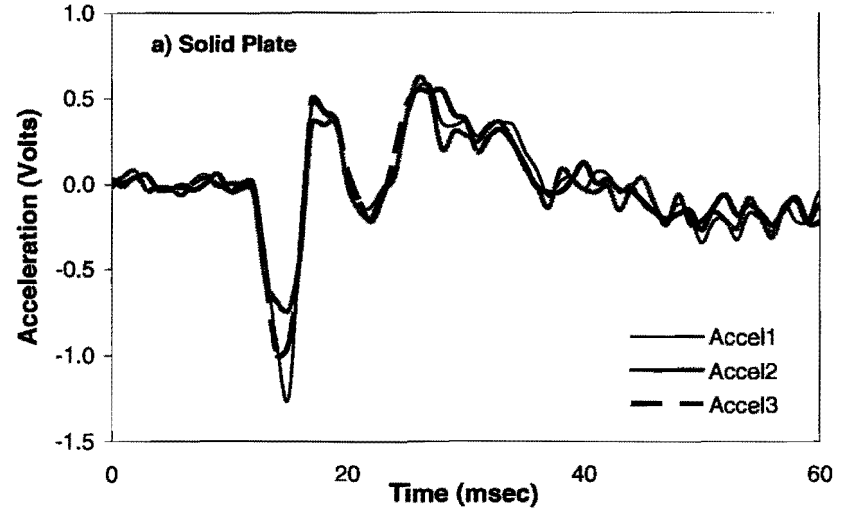
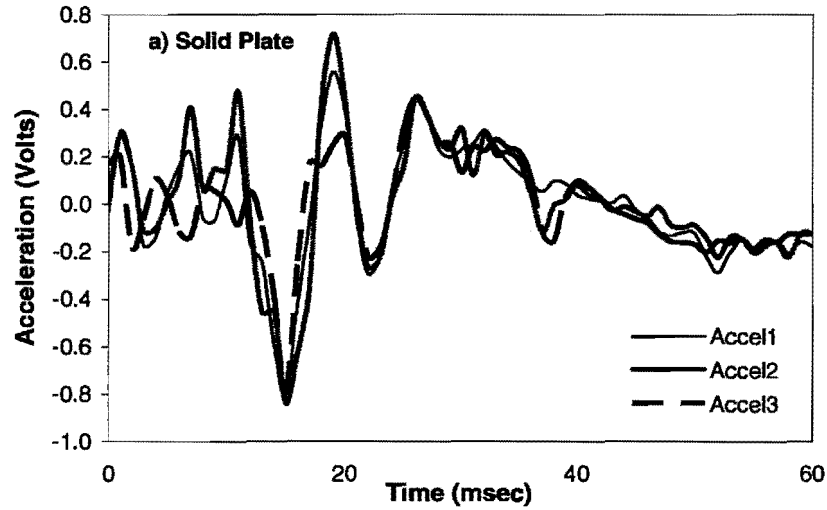
Test Point 1 - Height 4



Load Plate Motion data from UTEP Test Slabs – Level

Test Point 2 - Height 1

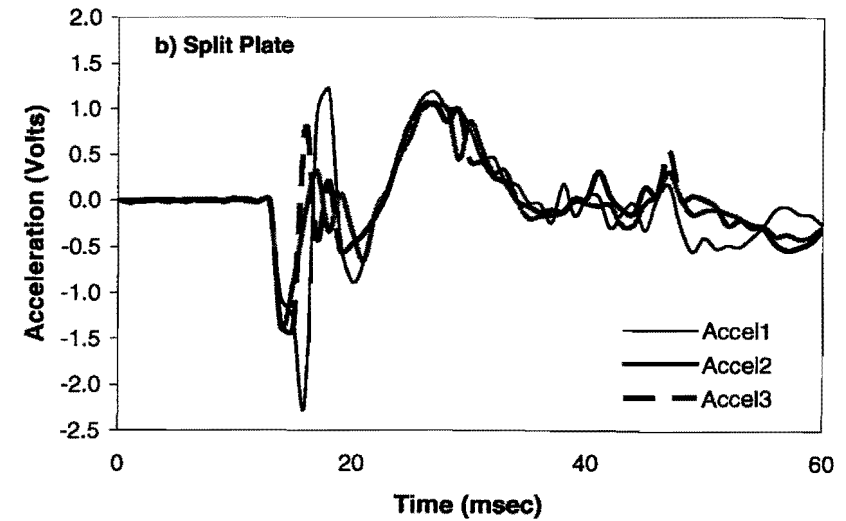
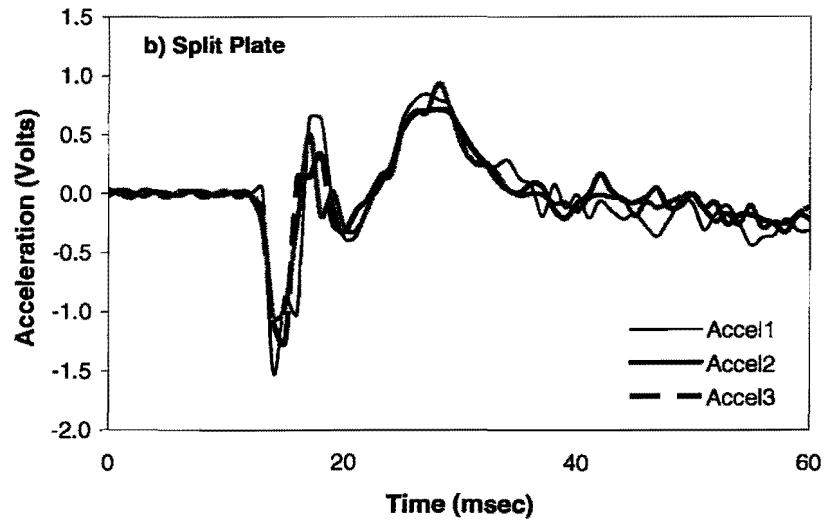
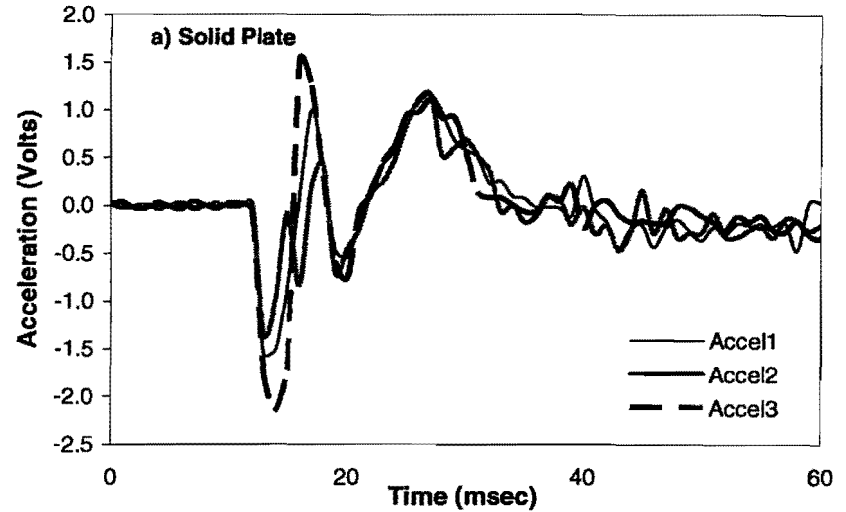
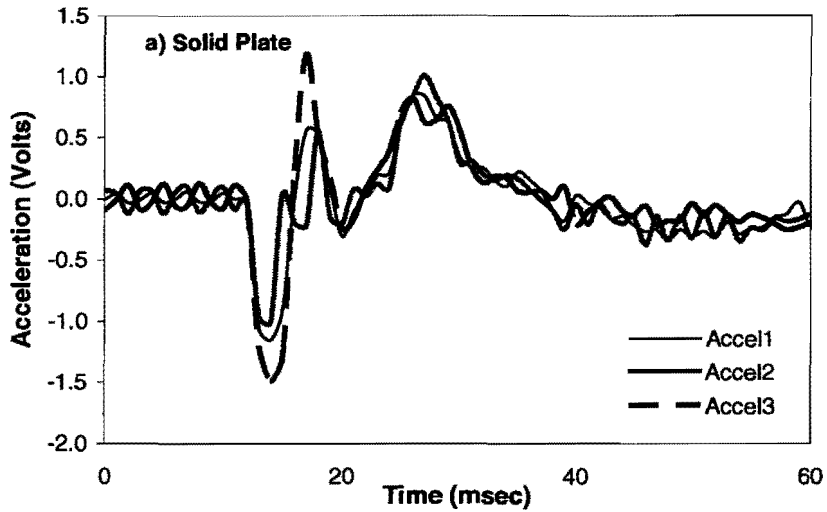
Test Point 2 - Height 2



Load Plate Motion data from UTEP Test Slabs – Level

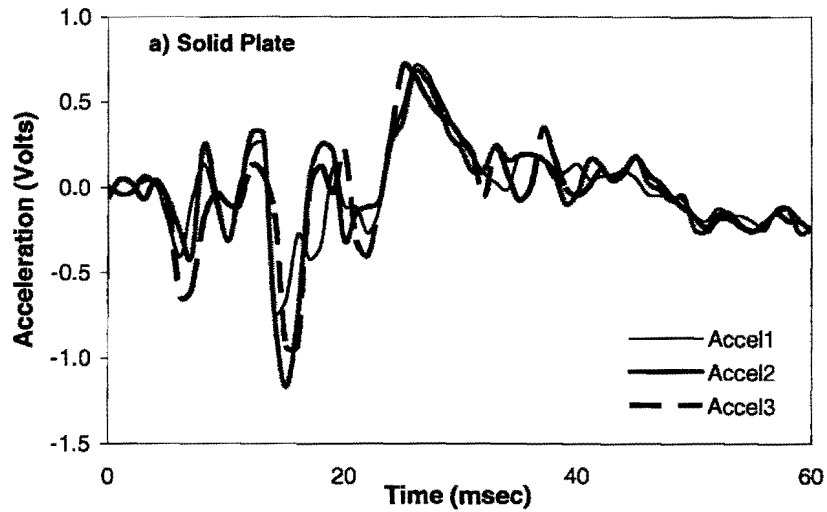
Test Point 2 - Height 3

Test Point 2 - Height 4

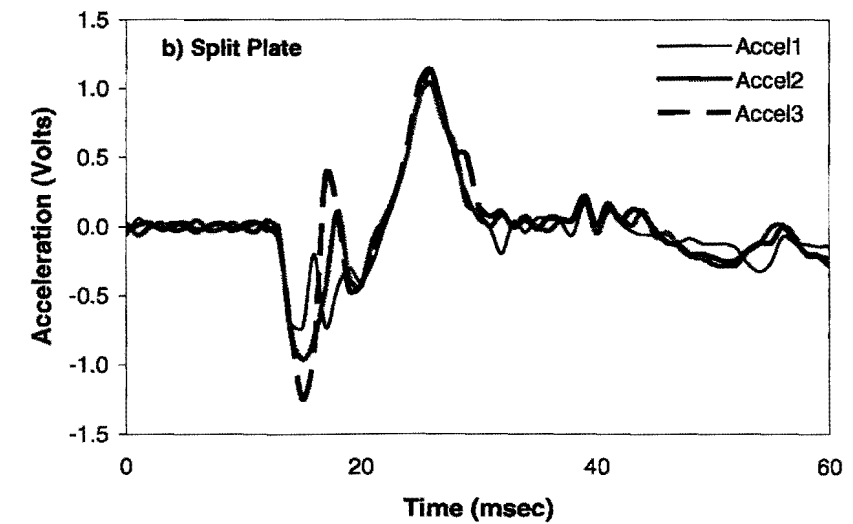
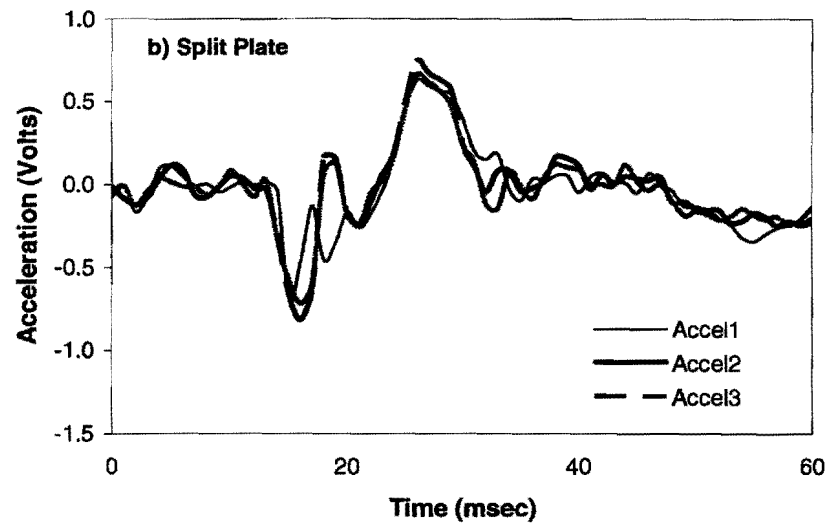
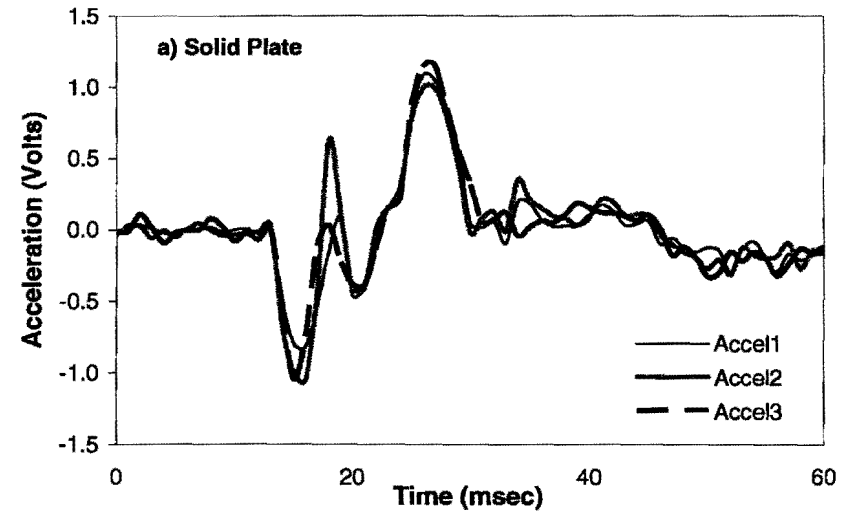


Load Plate Motion data from UTEP Test Slabs – Level

Test Point 3 - Height 1

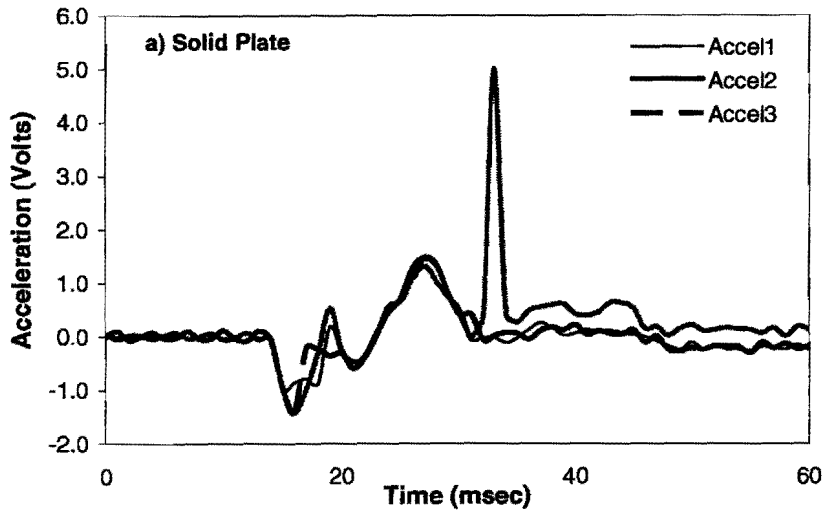


Test Point 3 - Height 2

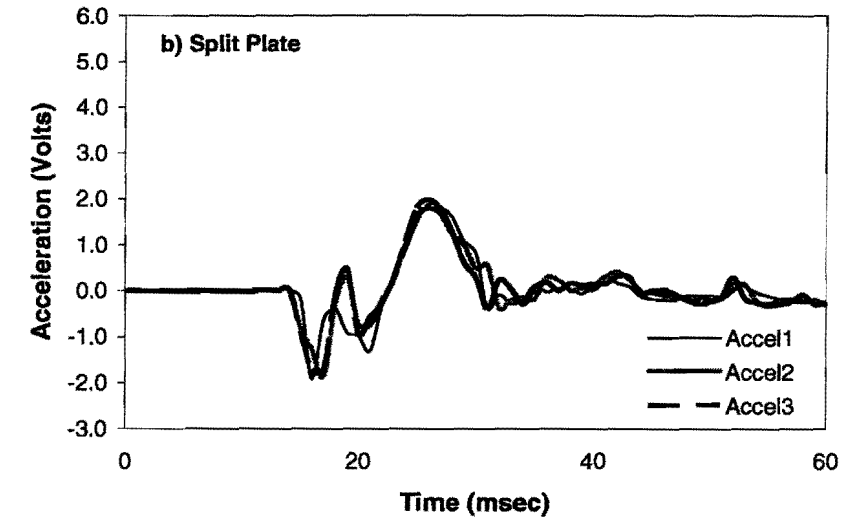
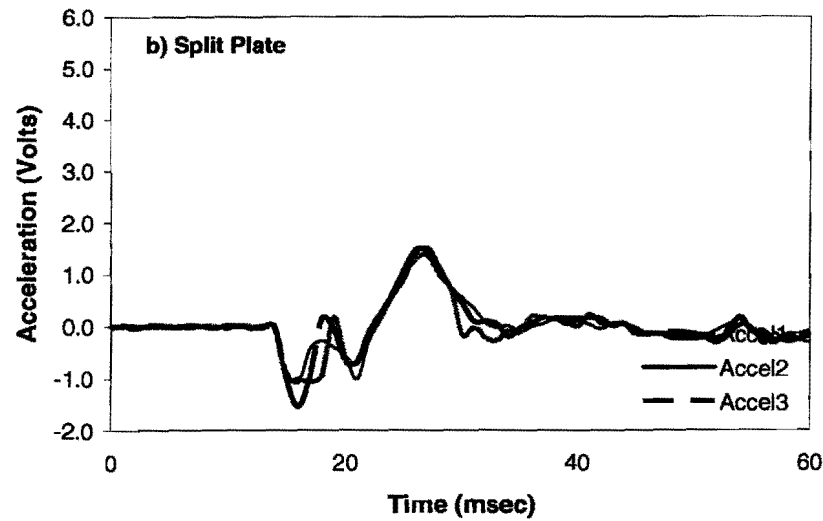
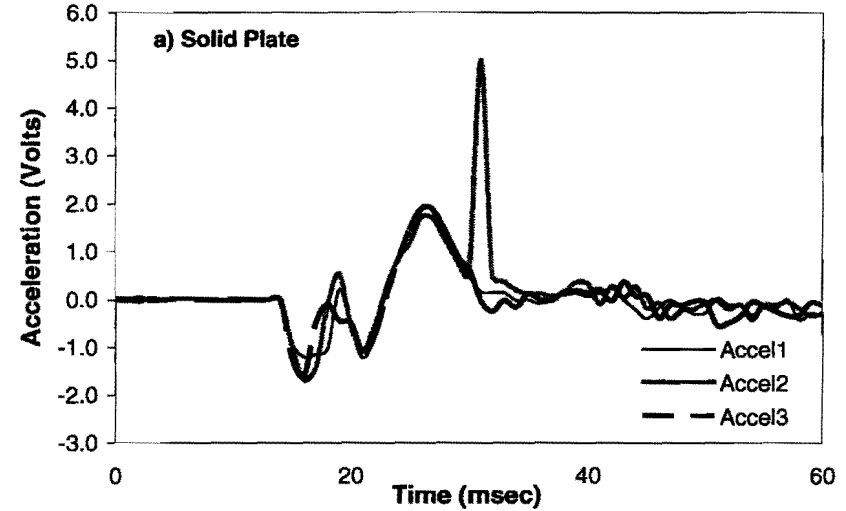


Load Plate Motion data from UTEP Test Slabs – Level

Test Point 3 - Height 3

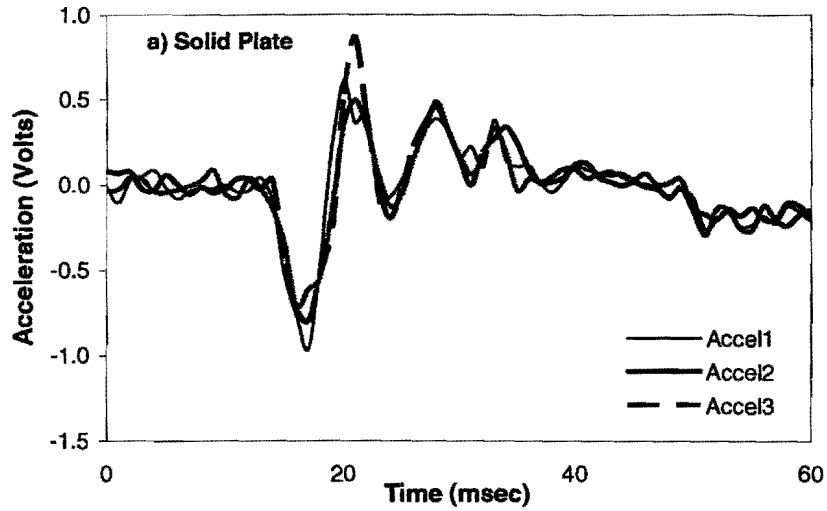


Test Point 3 - Height 4

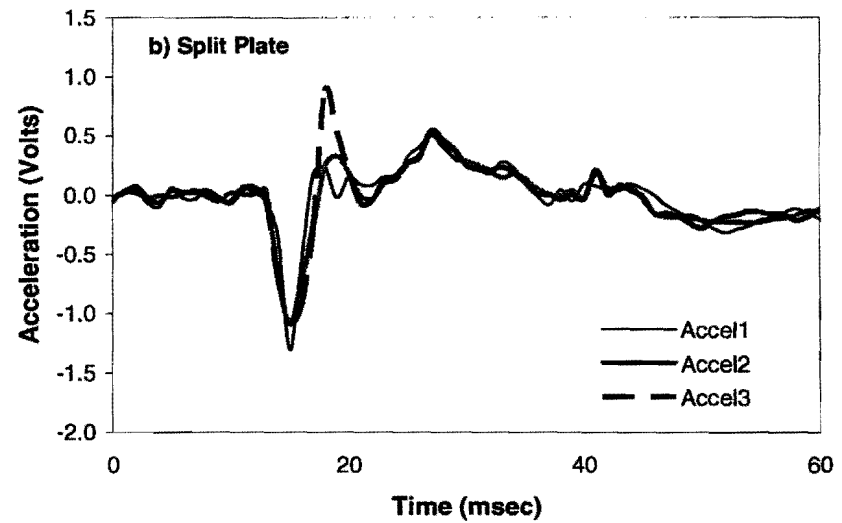
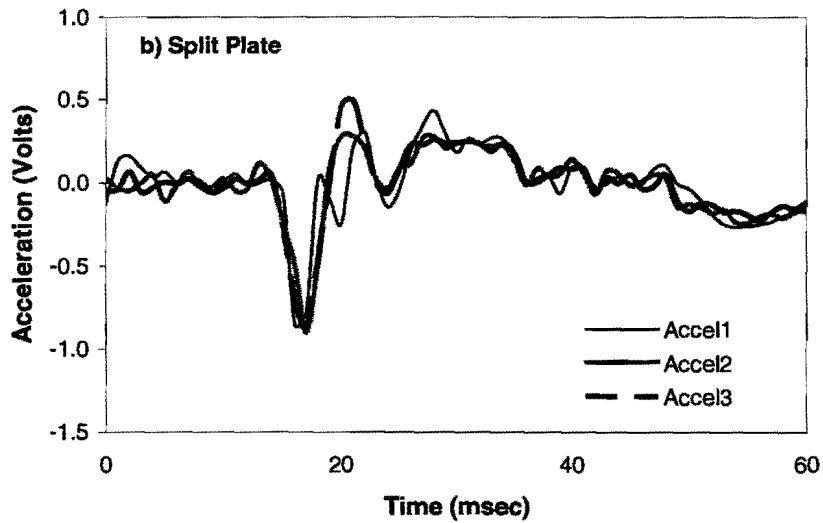
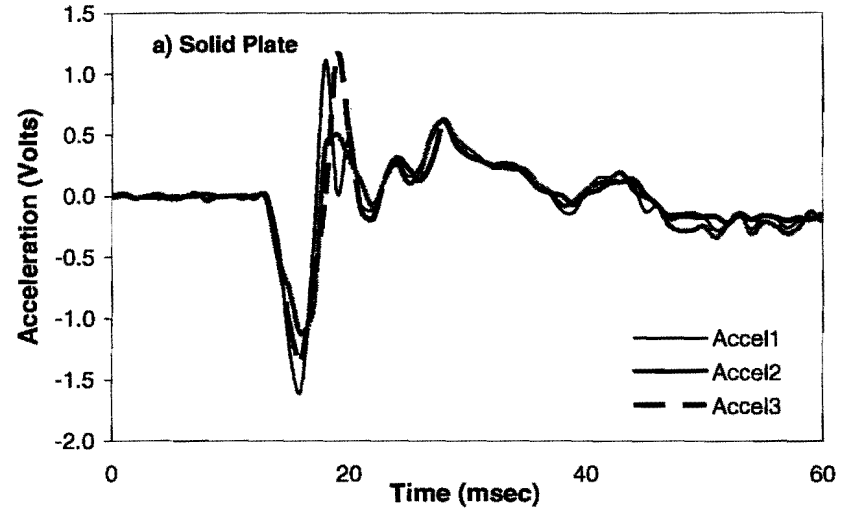


Load Plate Motion data from UTEP Test Slabs – Inclined

Test Point 1 - Height 1

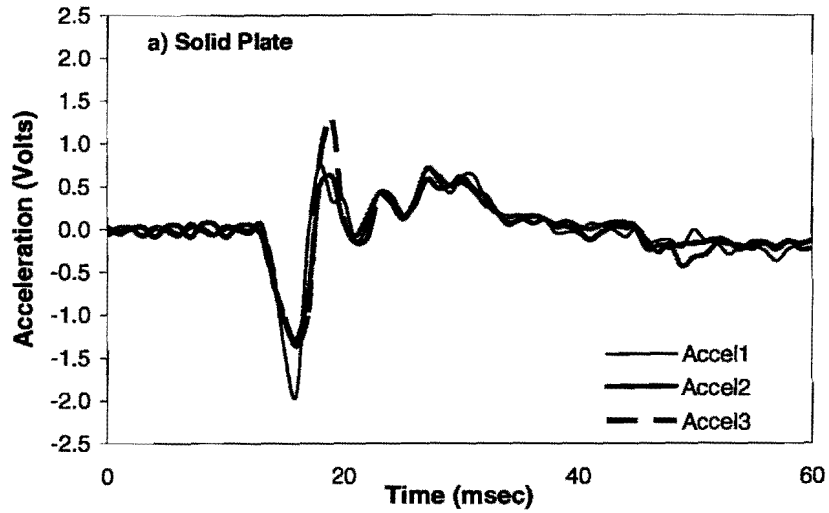


Test Point 1 - Height 2

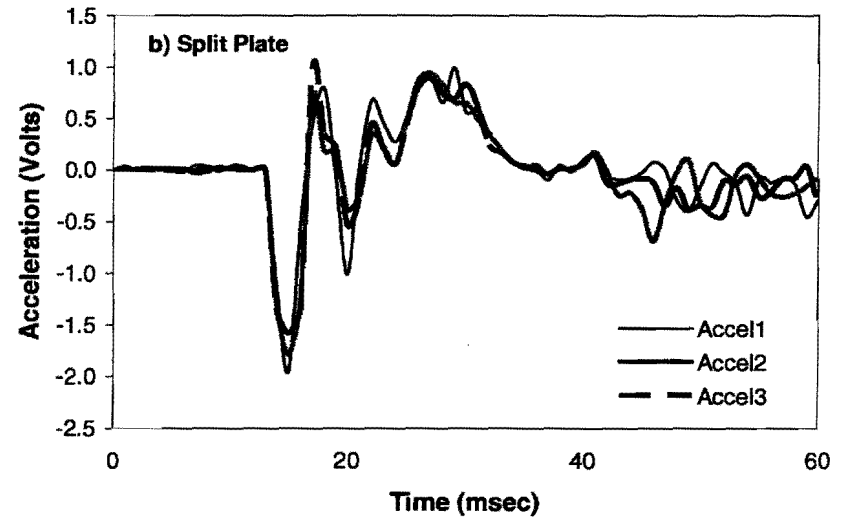
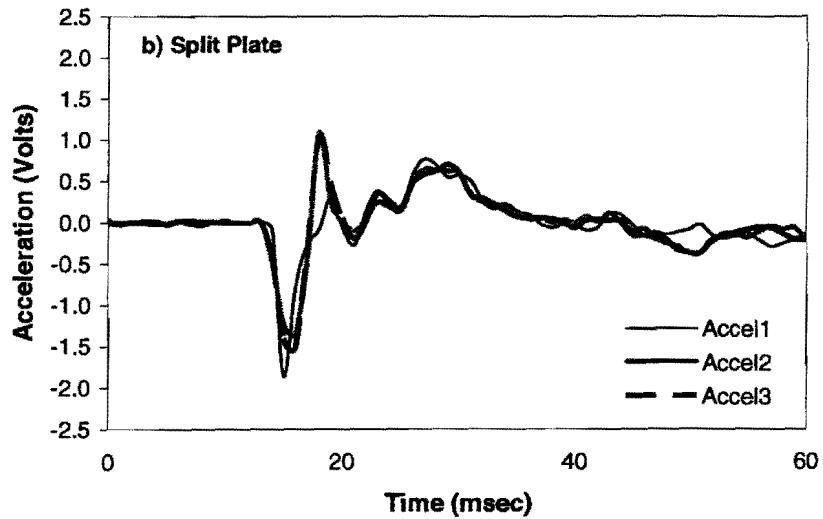
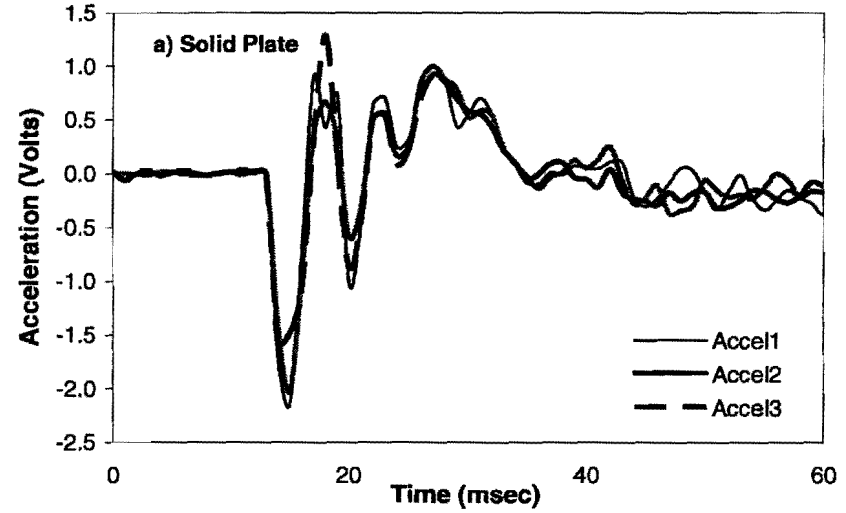


Load Plate Motion data from UTEP Test Slabs – Inclined

Test Point 1 - Height 3

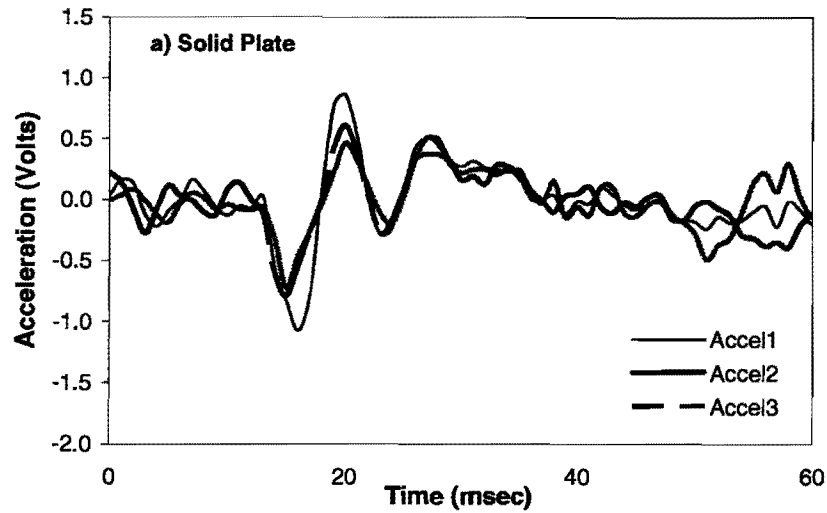


Test Point 1 - Height 4

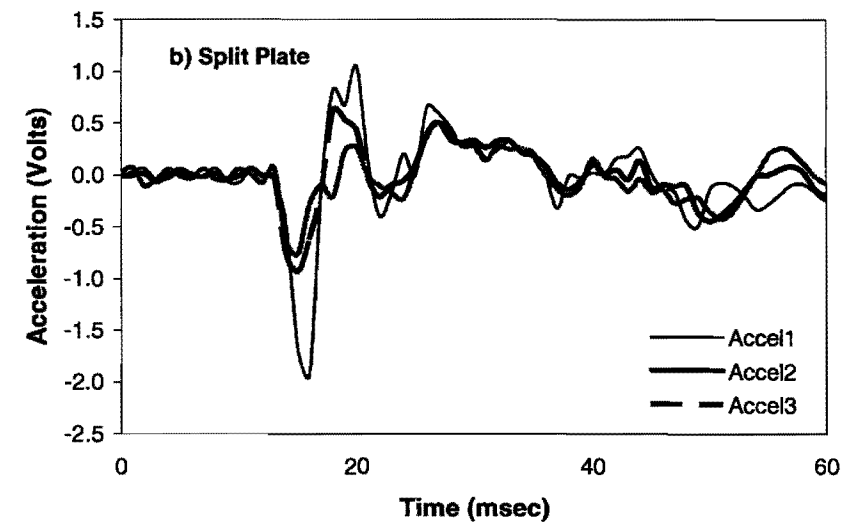
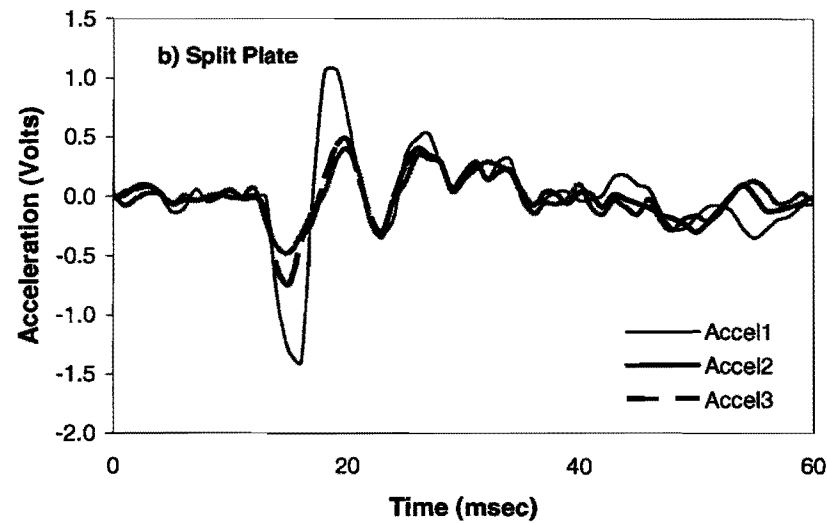
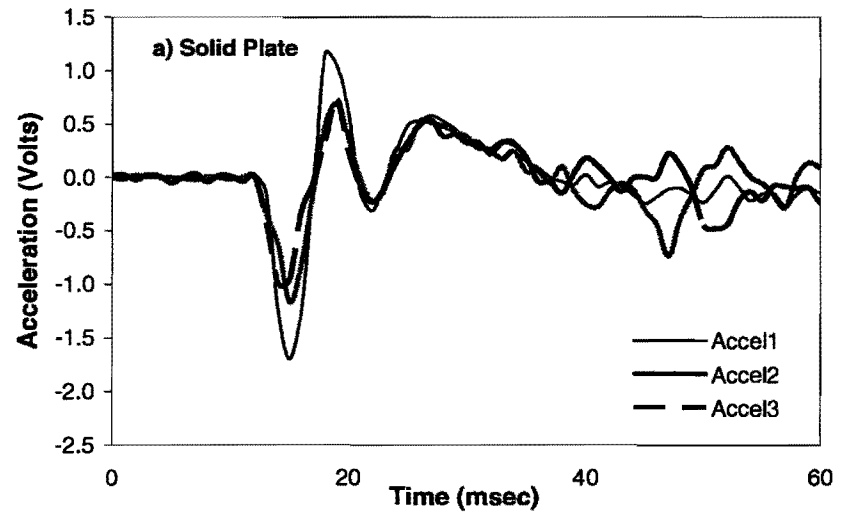


Load Plate Motion data from UTEP Test Slabs – Inclined

Test Point 2 - Height 1



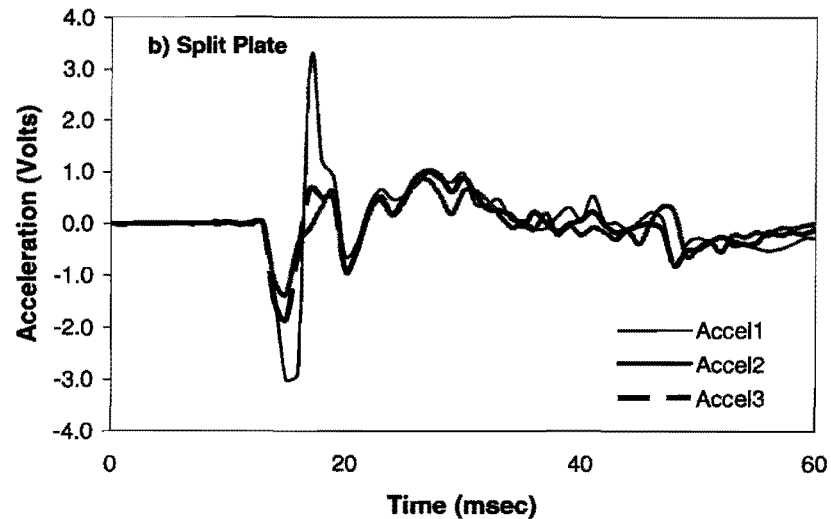
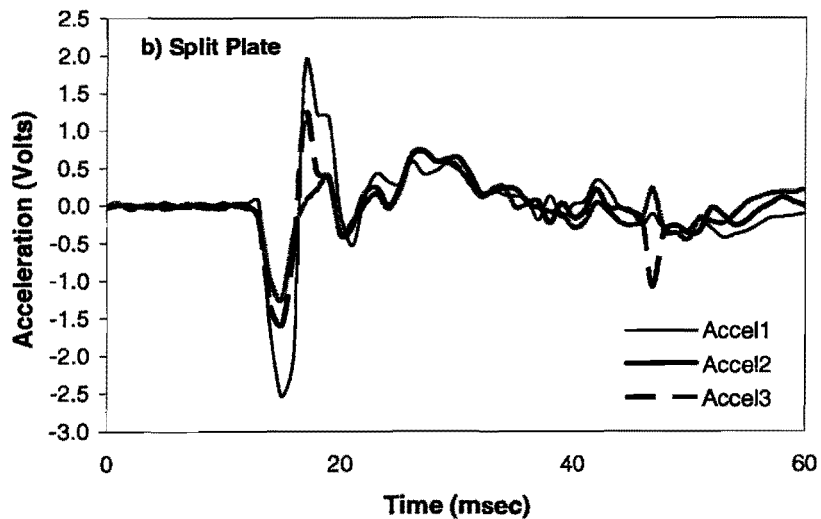
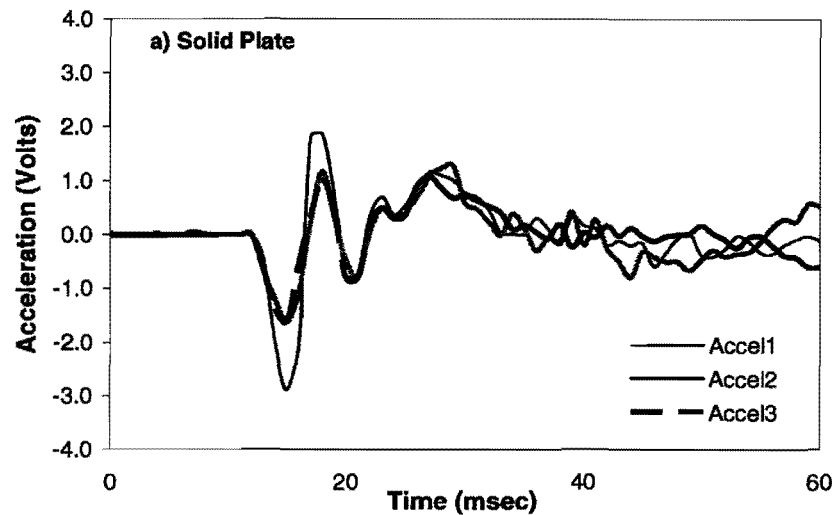
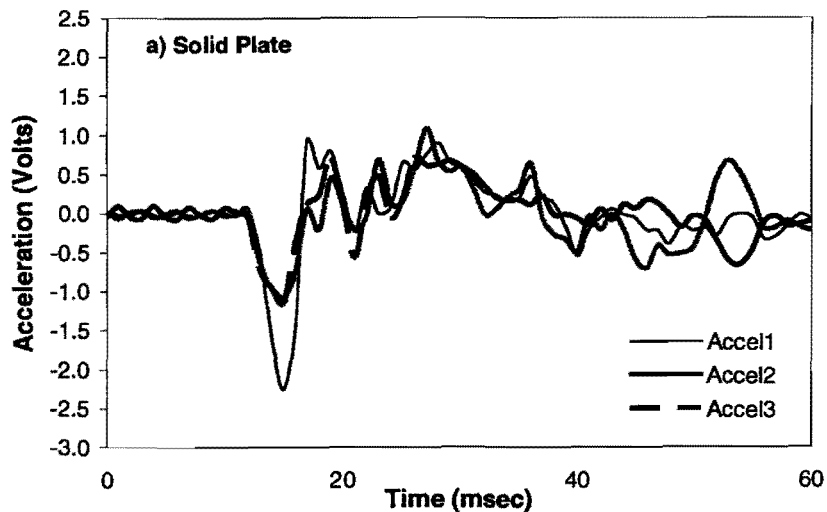
Test Point 2 - Height 2



Load Plate Motion data from UTEP Test Slabs – Inclined

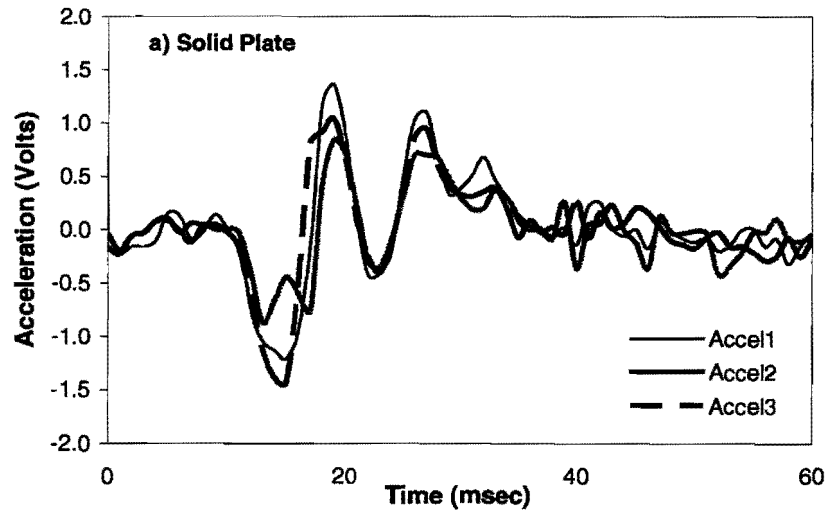
Test Point 2 - Height 3

Test Point 2 - Height 4

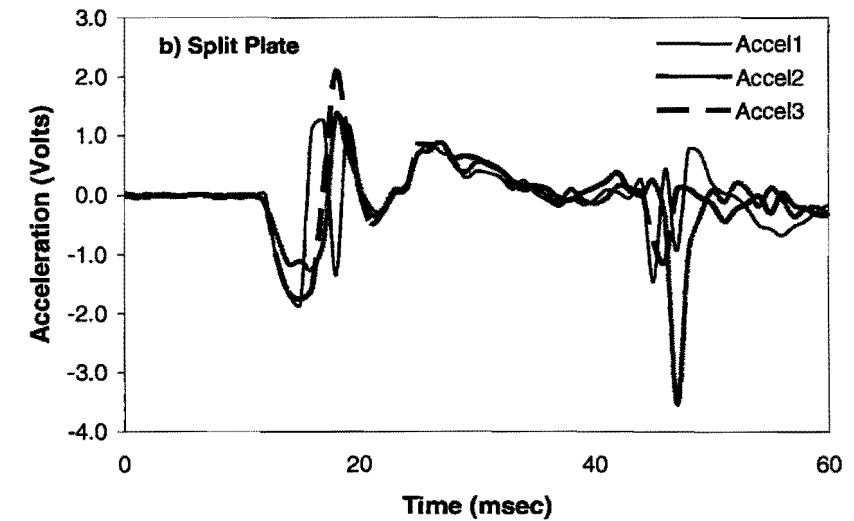
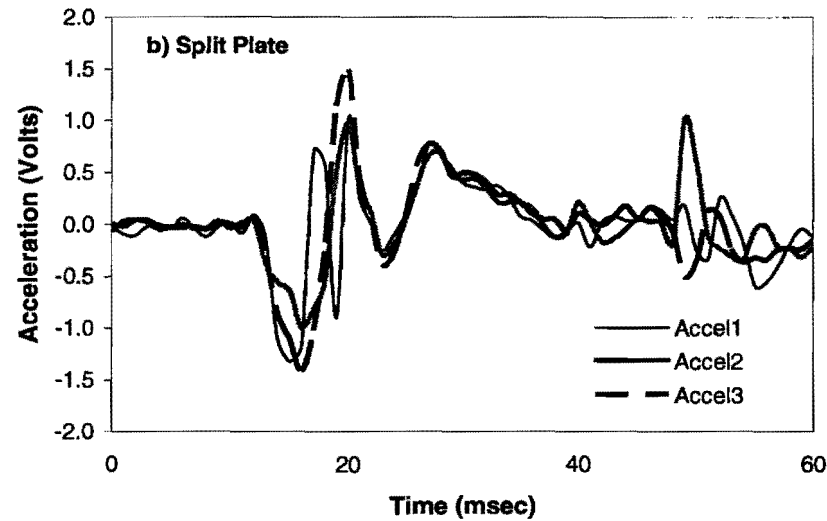
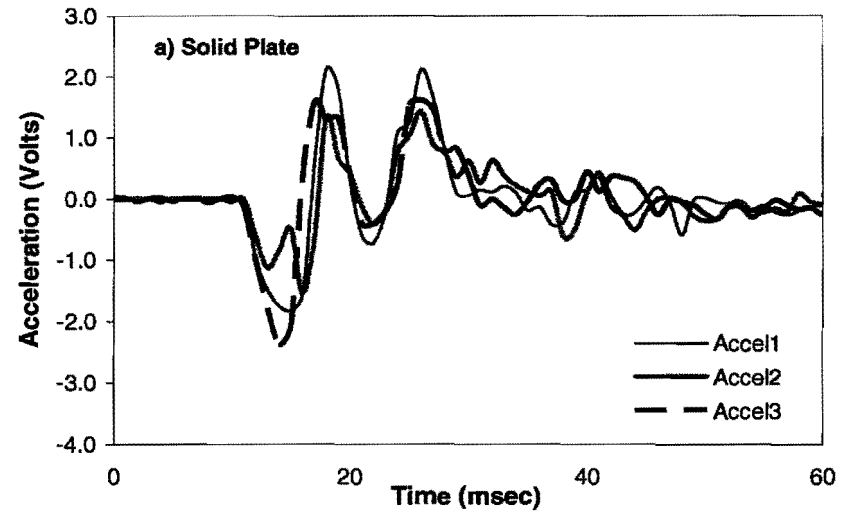


Load Plate Motion data from UTEP Test Slabs – Inclined

Test Point 3 - Height 1

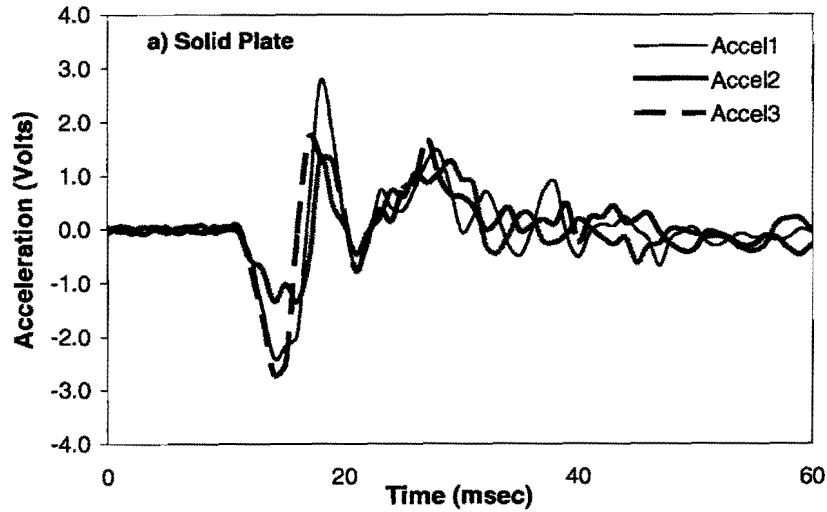


Test Point 3 - Height 2

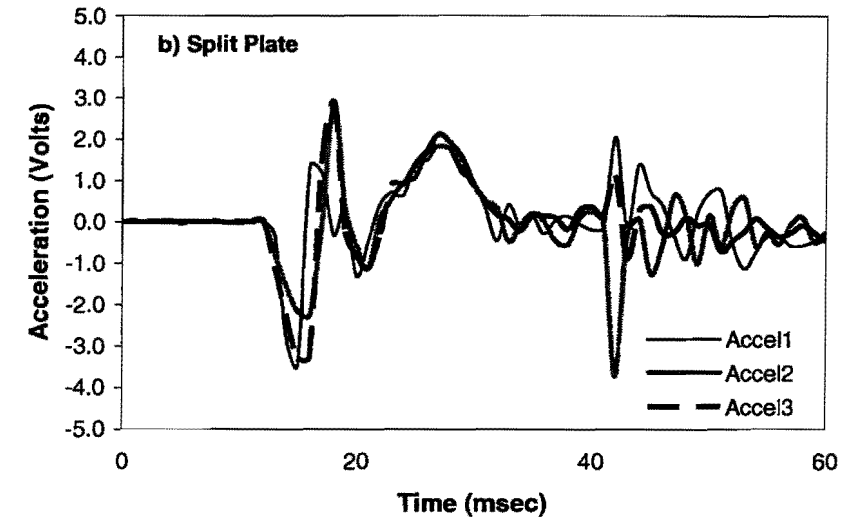
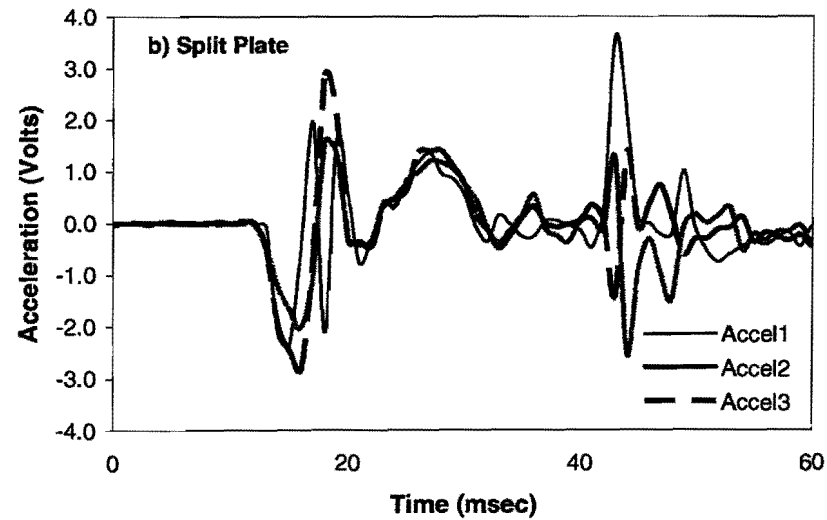
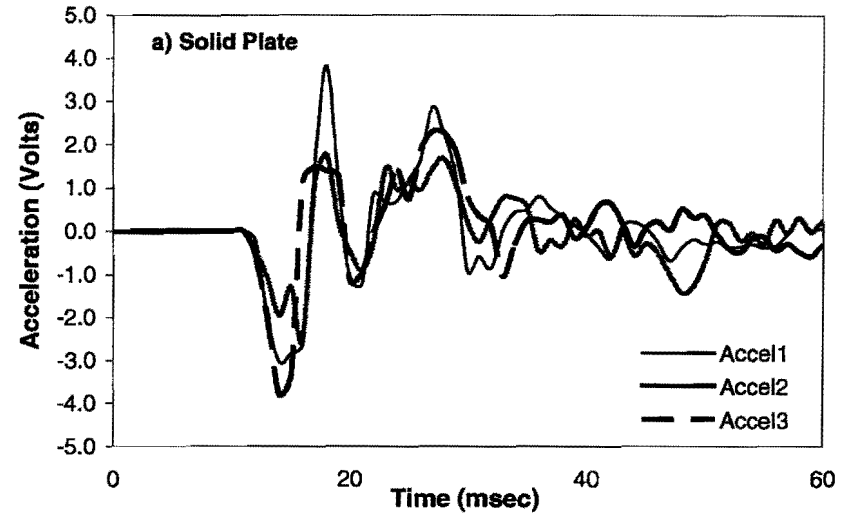


Load Plate Motion data from UTEP Test Slabs – Inclined

Test Point 3 - Height 3

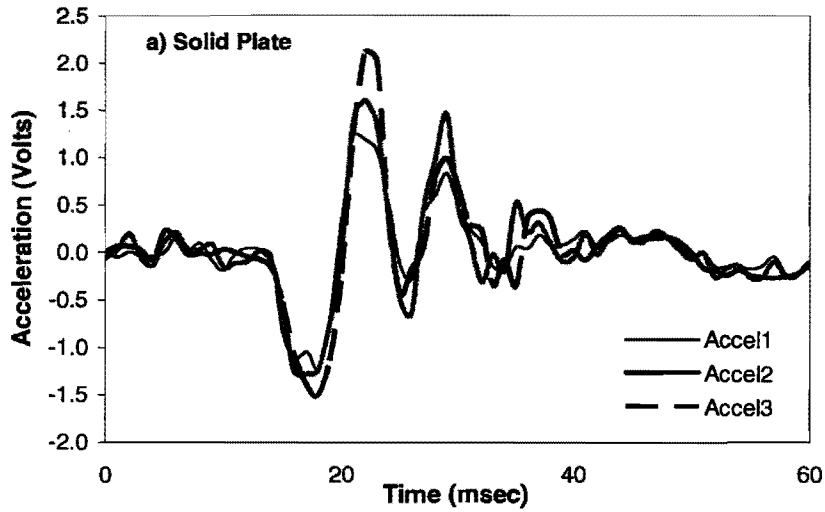


Test Point 3 - Height 4

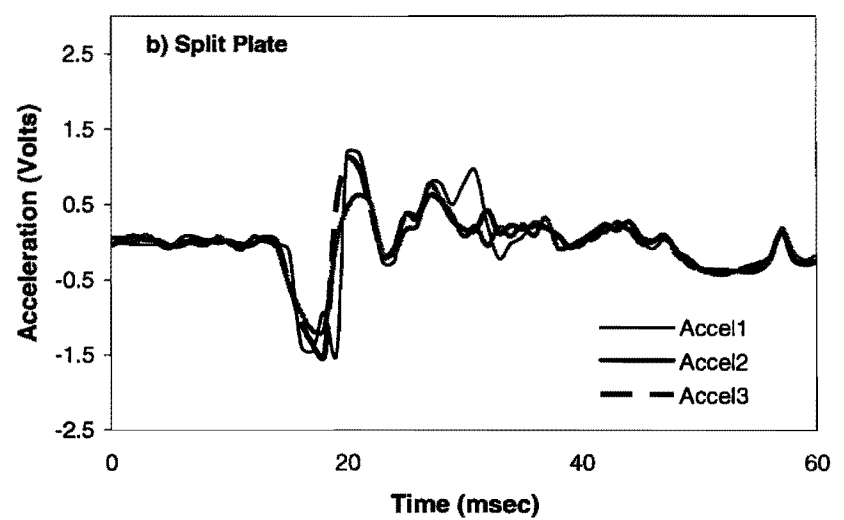
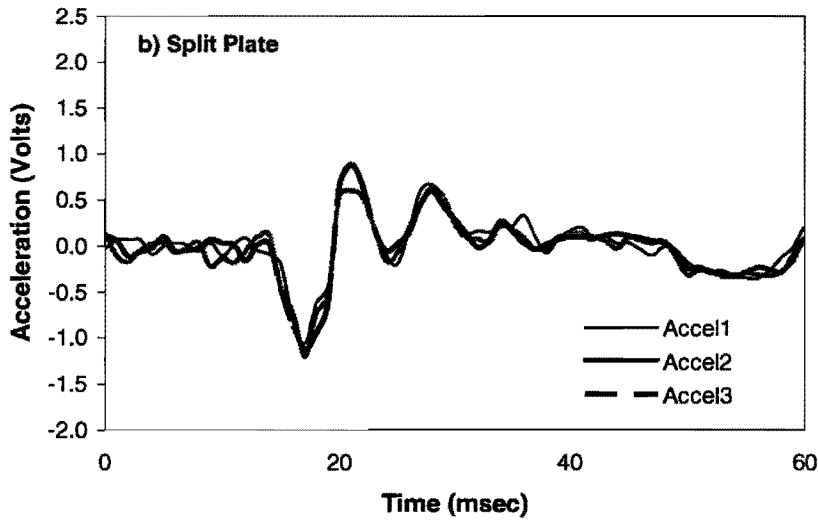
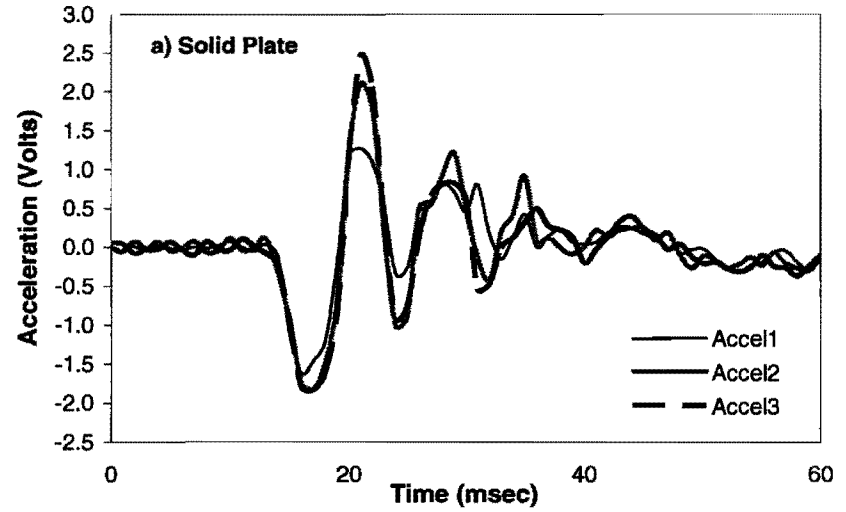


Load Plate Motion data from UTEP Test Slabs – Rutted

Test Point 1 - Height 1

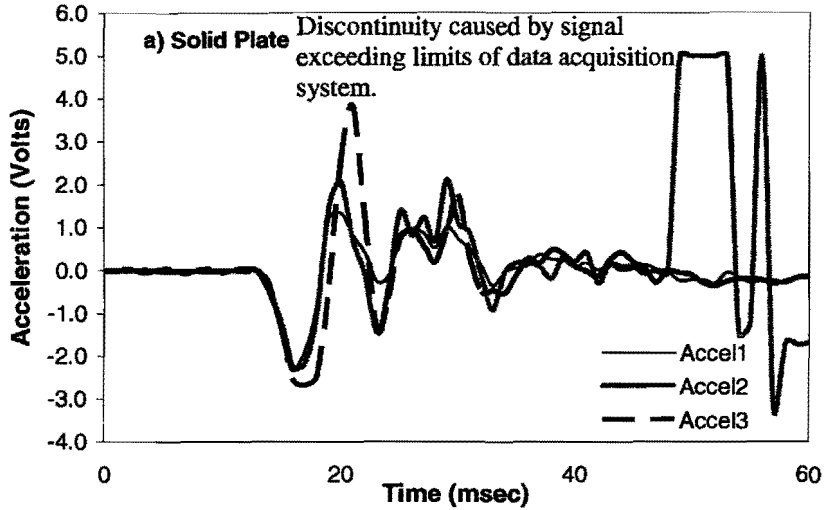


Test Point 1 - Height 2

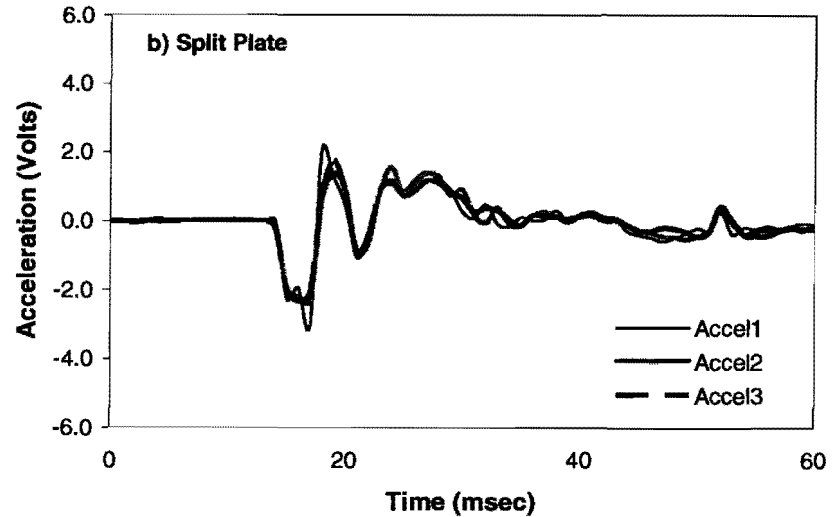
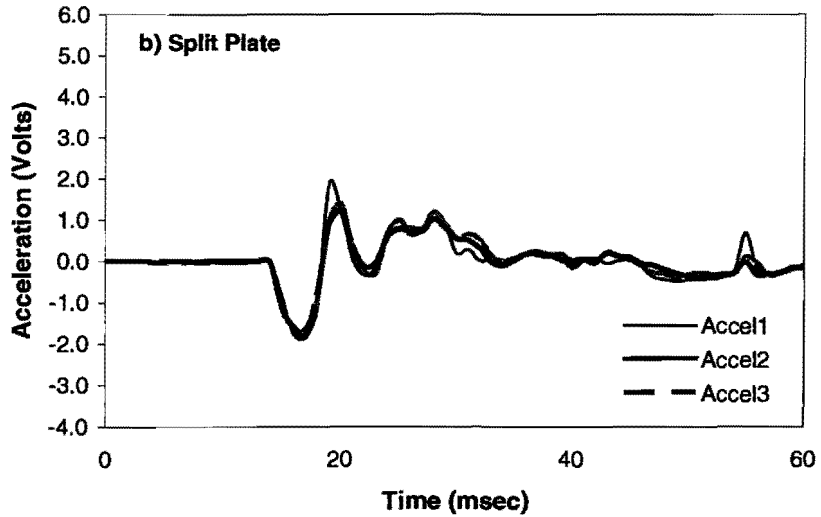
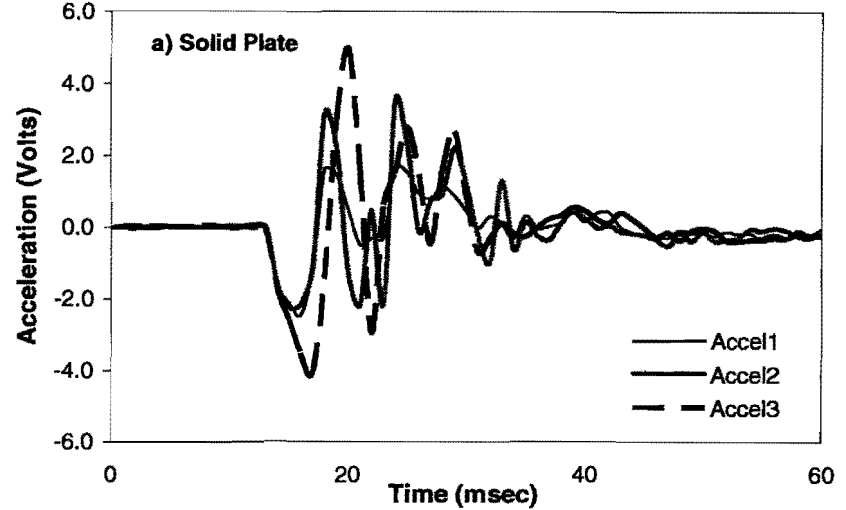


Load Plate Motion data from UTEP Test Slabs – Rutted

Test Point 1 - Height 3

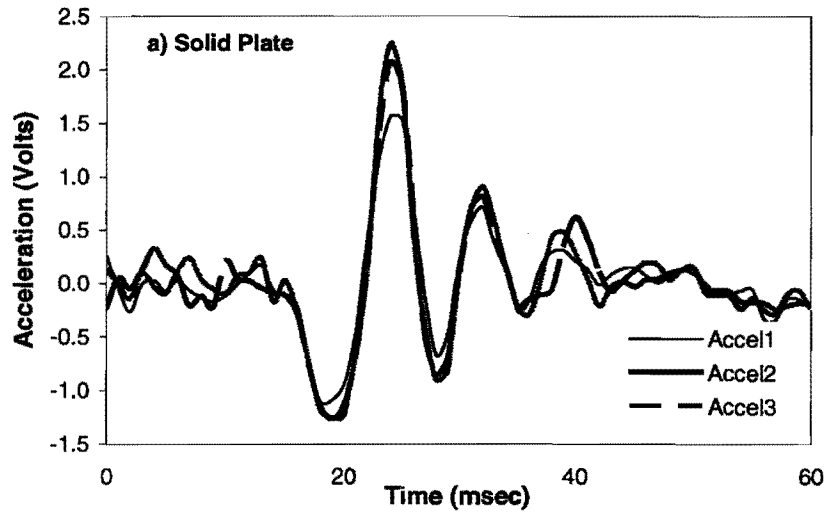


Test Point 1 - Height 4

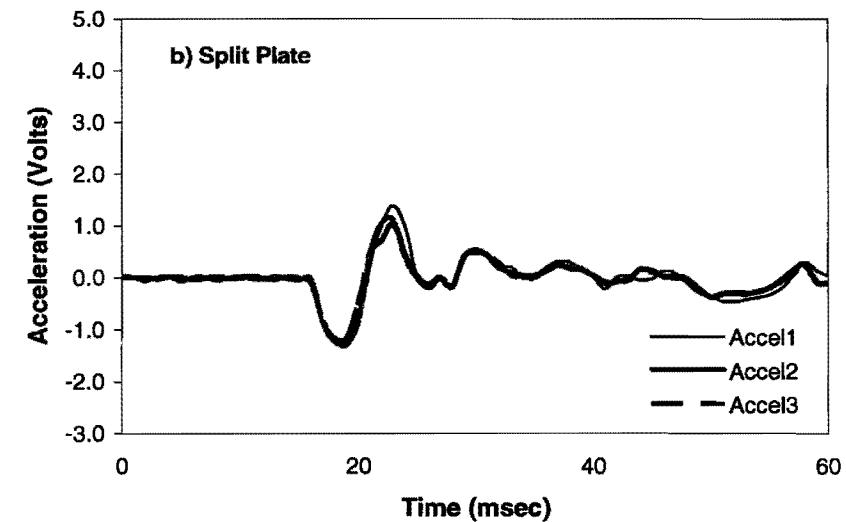
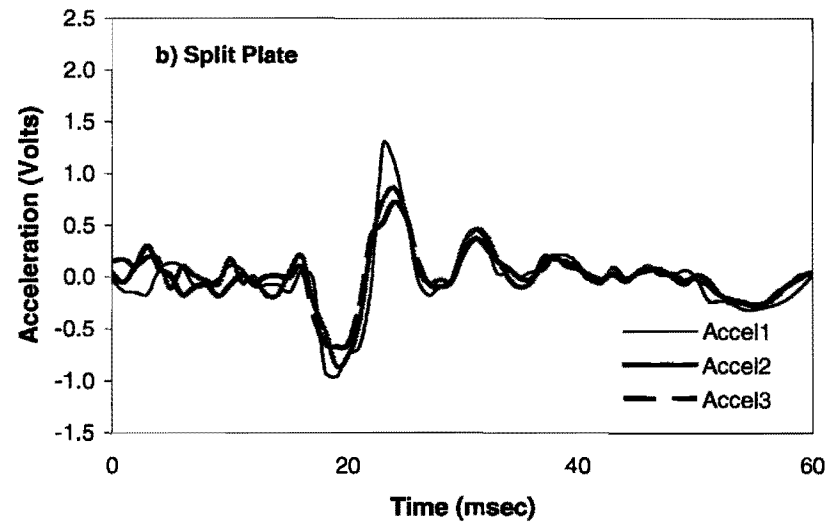
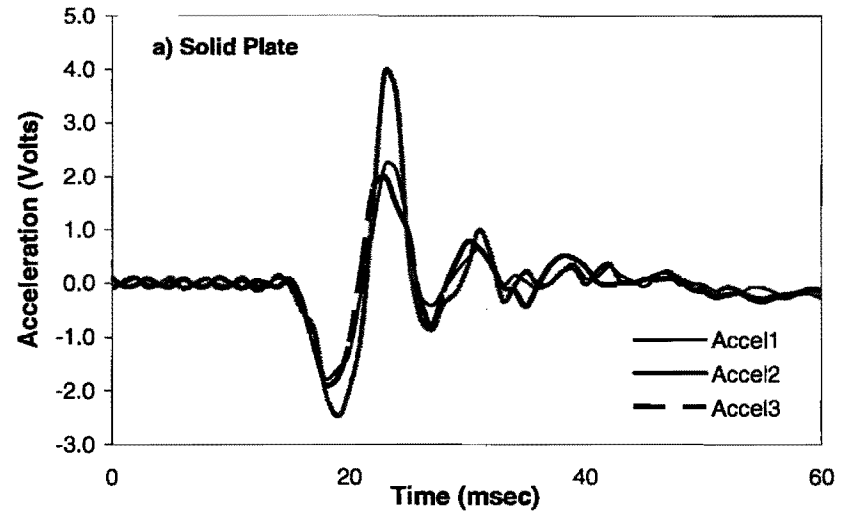


Load Plate Motion data from UTEP Test Slabs – Rutted

Test Point 2 - Height 1

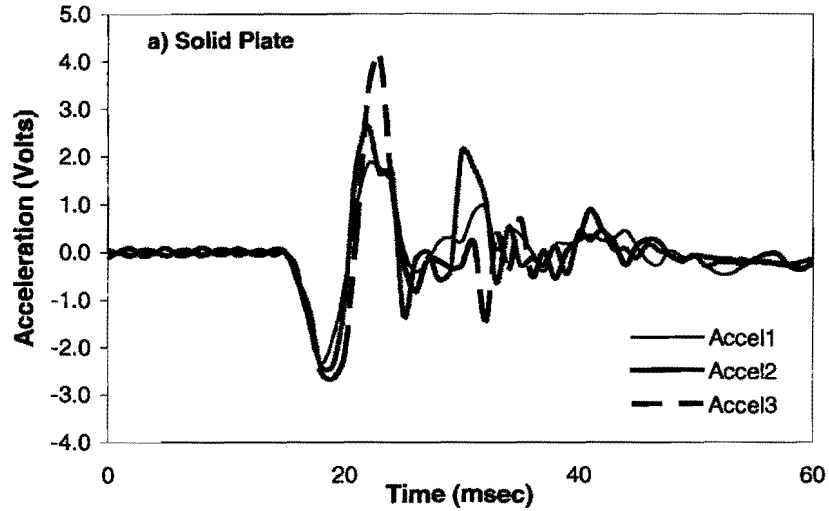


Test Point 2 - Height 2

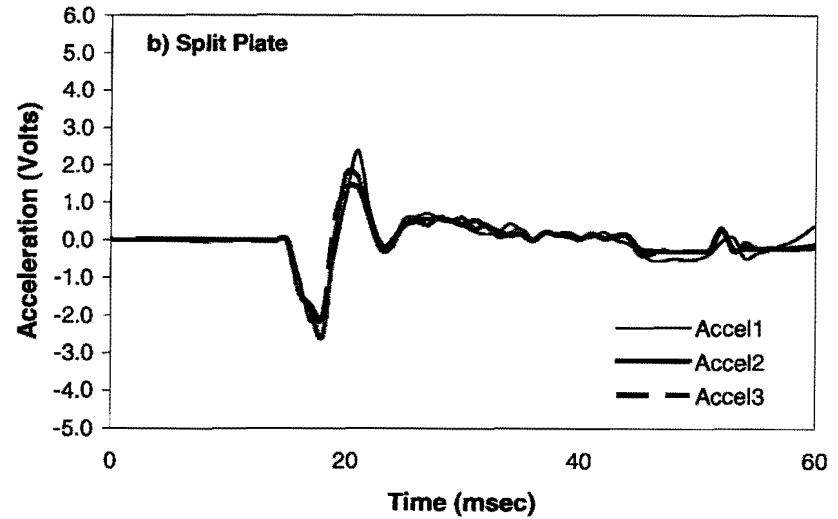
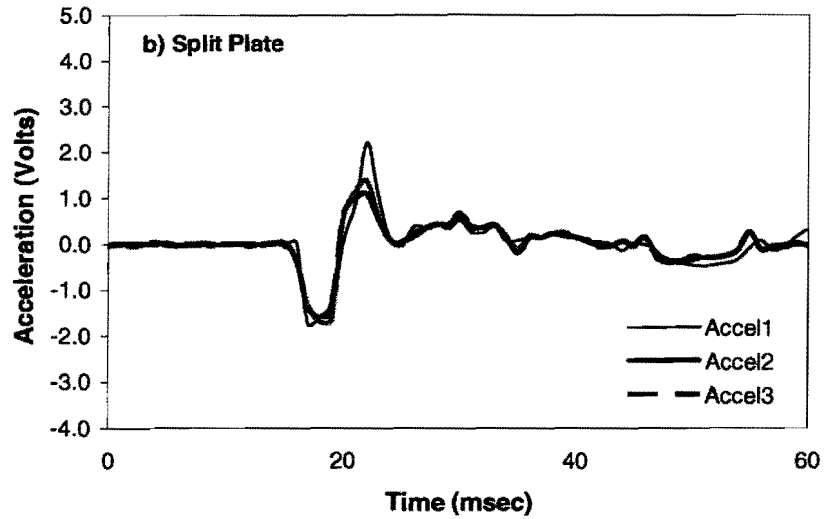
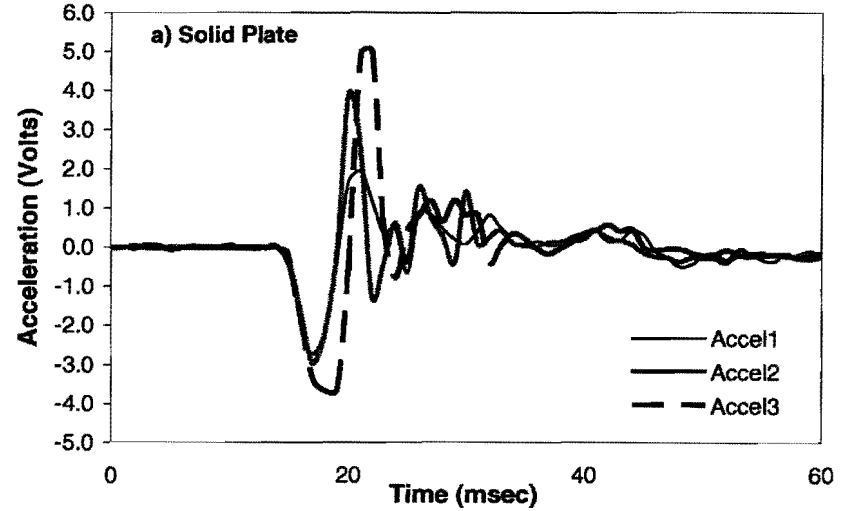


Load Plate Motion data from UTEP Test Slabs – Rutted

Test Point 2 - Height 3



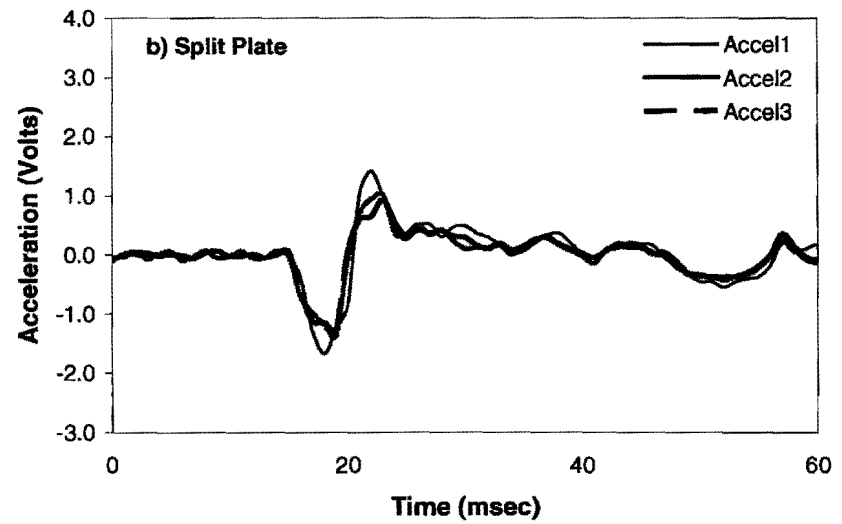
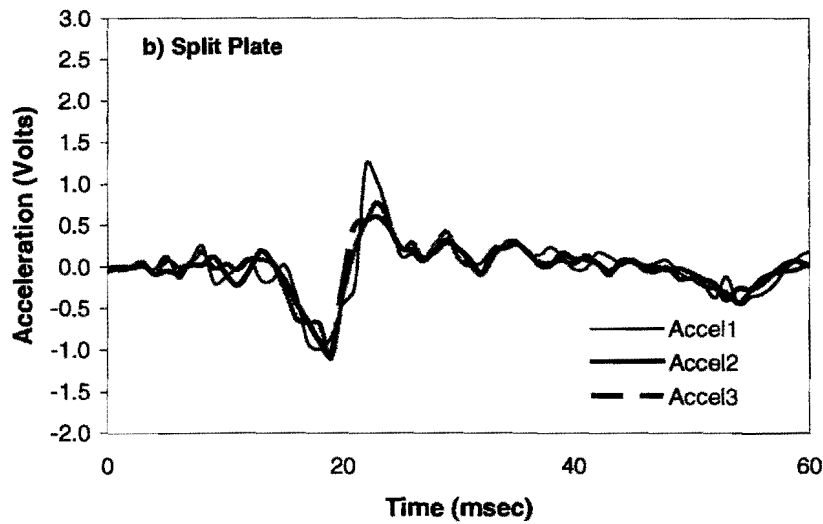
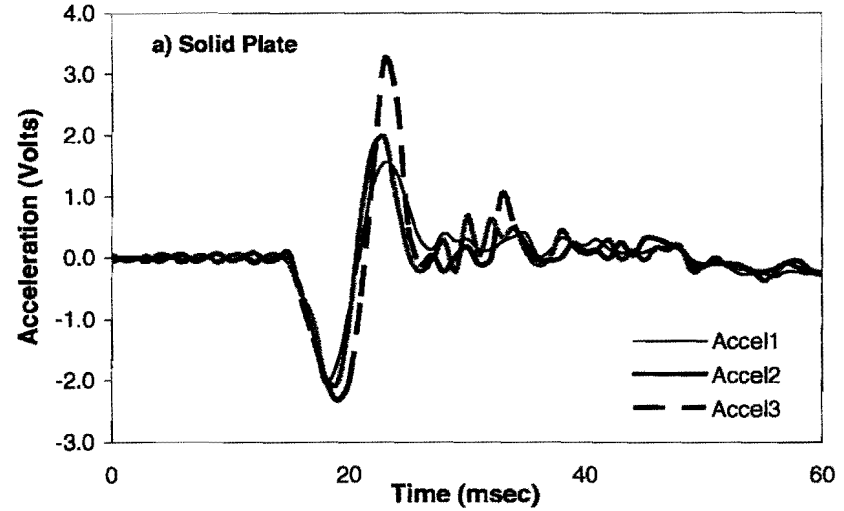
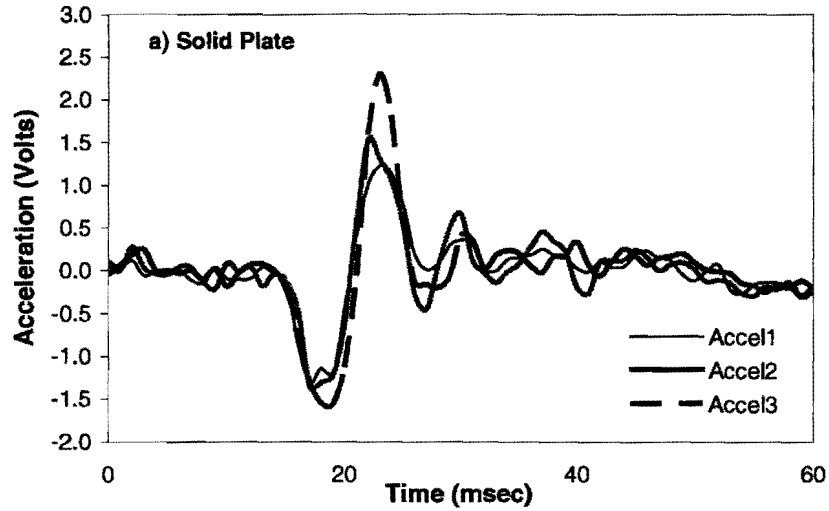
Test Point 2 - Height 4



Load Plate Motion data from UTEP Test Slabs – Rutted

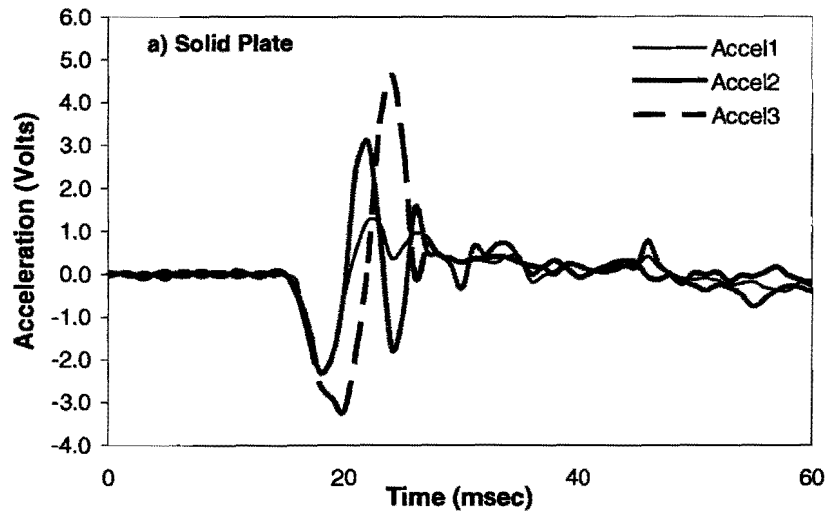
Test Point 3 - Height 1

Test Point 3 - Height 2



Load Plate Motion data from UTEP Test Slabs – Rutted

Test Point 3 - Height 3



Test Point 3 - Height 4

